TTI: 0-6839

Texas A&M
Transportation
Institute

Pavement Designs for the Energy Development Areas with Heavy Loads—Part I: Flexible Pavements and Part II: Rigid Pavements

Technical Report 0-6839-R1

Cooperative Research Program

TEXAS A&M TRANSPORTATION INSTITUTE
COLLEGE STATION, TEXAS

in cooperation with the
Federal Highway Administration and the
Texas Department of Transportation
http://tti.tamu.edu/documents/0-6839-R1.pdf

Technical Report Documentation Page

1. Report No. FHWA/TX-18/0-6839-R1	2. Government Accession No.	3. Recipient's Catalog No.

4. Title and Subtitle
PAVEMENT DESIGNS FOR THE ENERGY DEVELOPMENT AREAS WITH HEAVY LOADS—PART I: FLEXIBLE PAVEMENTS AND PART II: RIGID PAVEMENTS

5. Report Date
Published: November 2018

6. Performing Organization Code

7. Author(s)
Jun Zhang, Soohyok Im, Issa Mahmoud, Dan Zollinger, and Fujie Zhou

8. Performing Organization Report No.
Report 0-6839-R1

9. Performing Organization Name and Address
Texas A&M Transportation Institute
The Texas A&M University System
College Station, Texas 77843-3135

10. Work Unit No. (TRAIS)

11. Contract or Grant No.
Project 0-6839

12. Sponsoring Agency Name and Address
Texas Department of Transportation
Research and Technology Implementation Office
125 E. 11th Street
Austin, Texas 78701-2483

13. Type of Report and Period Covered
Technical Report:
January 2015–February 2018

14. Sponsoring Agency Code

15. Supplementary Notes
Project performed in cooperation with the Texas Department of Transportation and the Federal Highway Administration.
Project Title: Designing Pavements to Support the Heavy Loads in the Energy Development Areas
URL: http://tti.tamu.edu/documents/0-6839-R1.pdf

16. Abstract

In recent years, rapid energy development in Texas has caused significant damage to many farm-to-market (FM) roads, which traditionally have a thin asphalt surface layer plus a stabilized base directly over the subgrade. These roadways were often rehabilitated with full depth reclamation (FDR) and often 2 to 3 percent cement was added to the pulverized existing materials. They performed well under normal traffic loads but failed dramatically under the energy sector truck loads. There is an urgent need to repair many of these badly damaged roadways in all energy development areas. The main objectives of this project were to 1) determine traffic conditions (in terms of actual axle load level) for pavement designs in the energy development areas, 2) develop materials options for handling the early trafficking requirement, and 3) recommend improved pavement designs for overloaded vehicles.

Researchers first reviewed and analyzed all the traffic data collected by the permanent weigh-in motion stations around Texas, and identified 17 stations with adequate traffic records for developing traffic loading spectra for pavement designs. Researchers found that the energy development areas have much heavier trucks than the non-energy development areas; through comparison with regular equivalent single axle load, researchers conclude overloading traffic caused much damage to pavements. Researchers also surveyed field performance of FDR test sections with asphalt stabilization and some roller compacted concrete pavements. Overall, most FDR test sections performed well; and only one section had a few cracks. Guidance for selecting optimal rehabilitation options and associated materials and their mechanical properties required by pavement designs were then recommended. Following TxDOT's pavement design methods, researchers developed pavement design catalogs and material options to support heavy loads in the energy development areas. Additionally, huge efforts were made to assist the Corpus Christi District in designing the intersection between US 281 and SH 123. Researchers highly recommend that the design catalog and the guidance for selecting optimal rehabilitation options and associated materials be implemented to make pavements last longer and have better performance. Also, the construction of the intersection between US 281 and SH 123 should be well documented for future performance evaluation.

17. Key Words
Overload, Load Spectrum, FDR, FWD, Concrete Pavement, Flexible Pavement, RCC

18. Distribution Statement
No restrictions. This document is available to the public through NTIS:
National Technical Information Service
Alexandria, Virginia
http://www.ntis.gov

19. Security Classif. (of this report) Unclassified	20. Security Classif. (of this page) Unclassified	21. No. of Pages 258	22. Price

Form DOT F 1700.7 (8-72) Reproduction of completed page authorized

PAVEMENT DESIGNS FOR THE ENERGY DEVELOPMENT AREAS WITH HEAVY LOADS—PART I: FLEXIBLE PAVEMENTS AND PART II: RIGID PAVEMENTS

by

Part I Authors:

Jun Zhang
Graduate Research Assistant
Texas A&M Transportation Institute

Soohyok Im
Associate Transportation Researcher
Texas A&M Transportation Institute

Fujie Zhou, Ph.D., P.E.
Research Engineer
Texas A&M Transportation Institute

Part II Authors:

Issa Mahmoud
Graduate Research Assistant
Texas A&M Transportation Institute

Dan Zollinger
Research Engineer
Texas A&M Transportation Institute

Report 0-6839-R1
Project 0-6839
Project Title: Designing Pavements to Support the Heavy Loads in the Energy Development Areas

Performed in cooperation with the
Texas Department of Transportation
and the
Federal Highway Administration

Published: November 2018

TEXAS A&M TRANSPORTATION INSTITUTE
College Station, Texas 77843-3135

DISCLAIMER

This research was performed in cooperation with the Texas Department of Transportation (TxDOT) and the Federal Highway Administration (FHWA). The contents of this report reflect the views of the authors, who are responsible for the facts and the accuracy of the data presented herein. The contents do not necessarily reflect the official view or policies of the FHWA or TxDOT. This report does not constitute a standard, specification, or regulation.

This report is not intended for construction, bidding, or permit purposes. The engineer in charge of the project was Fujie Zhou, P.E. (Texas #95969).

The United States Government and the State of Texas do not endorse products or manufacturers. Trade or manufacturers' names appear herein solely because they are considered essential to the object of this report.

ACKNOWLEDGMENTS

This project was conducted in cooperation with TxDOT and FHWA. The authors thank many personnel who contributed to the coordination and accomplishment of the work presented here. Special thanks are extended to Mr. Darrin Jensen for serving as the project manager. Many people volunteered their time to serve as project advisors, including:

- Miguel Arellano.
- Dar-Hao Chen.
- Hua Chen.
- Robert Moya III.
- Andy Naranjo.

TABLE OF CONTENTS

Page

List of Figures .... **ix**
List of Tables .... **xiv**

Part I: Flexible Pavements **1**
Chapter 1. Introduction **3**
  Background 3
  Challenges of Repairing Pavements for Energy Development Areas 3
  Rehabilitation Options for Repairing Damaged Pavements 4
  Research Objective 6
Chapter 2. Weigh-In-Motion Data Analysis and Traffic Input for Pavement Design **7**
  TxDOT Weigh-In-Motion Sensors 7
  WIM Data Analysis 14
  Comparison of ESAL Calculations from Traditional Method and Load Spectra 16
  Comparison of Traffic Volume and Loading for Energy and Non-Energy Areas 20
  Comparison of Predicted Performances from TxME with Use of WIM Traffic Data Inputs 22
Chapter 3. Flexible Pavement Rehabilitation Options **25**
  Introduction 25
  Guidance for Selecting Optimal Rehabilitation Options 25
  Laboratory Tests and Results for Stabilized Materials for FDR Option 33
Chapter 4. Field Projects with Implementation of FDR **43**
  SH 202 Project 48
  I-10 Project 52
  SH 7 Project 53
  FM 99 Project 55
Chapter 5. Pavement Design Catalogue for Pavements in Energy Development Areas **59**
  Introduction 59
  Objective 59
  Methodology for Developing Pavement Design Catalog 59
  Pavement Design Curves for 4-Layer Pavements 63
  Pavement Design Curves for 3-Layer Pavements 65
  Traffic Analysis 67
  Pavement Design Catalog Tables 68
Chapter 6. Conclusions and Recommendation **81**
  Conclusions 81
  Recommendation 82

Part II: Rigid Pavements **83**
Chapter 1. Analysis of Texas RCC Field Performance Data **85**
  Introduction 85
  Objective 86

Testing Plan 86
Sites 86
Field Research Summary 118
Conclusion/Recommendations 118
Chapter 2. Field Analysis of the Intersection of US 181/SH 123 in Karnes City, Texas 121
Introduction 121
Site Description 121
Current Site Condition 121
Testing/Data Collection Performed 122
Field Results/Findings 123
Laboratory Results/Findings 129
Summary 136
Chapter 3. Decision Tree Procedure for Suitable Alternative Selection 139
Introduction 139
Select Feasible Concrete Pavement Types 140
Select Suitable Concrete Pavement Types 143
Recommendations 148
Chapter 4. Rigid Pavement Design 151
Introduction 151
Rigid Pavement Design Methodology 151
Chapter 5. Traffic Analysis 157
Introduction 157
Traffic Computation Model 157
Estimating Design ESALs 162
Chapter 6. Design Methodology 167
Background to AASHTO and PCA Rigid Pavement Design 167
TxDOT Design Practices 169
Design Inputs for JPCP 170
Design Inputs for CRCP 180
Chapter 7. Economic Evaluation 187
Introduction 187
LCCA Procedure 187
LCCA Inputs for JPCP and CRCP 196
LCCA Example for JPCP and CRCP Alternatives 198
LCCA Inputs 199
LCCA Outputs 203
Appendix A. Method of Structural Assessment 209
Appendix B. Pioneer Site Photos, Plots, and Data (July 2015) 219
Appendix C. SEC Site Photos, Plots, and Data (July 2015) 223
Appendix D. SEC Site Photos, Plots, and Data (December 2015) 225
Appendix E. Bella Vista Site Photos, Plots, and Data (July 2015) 227
Appendix F. Bella Vista Site Photos, Plots, and Data (December 2015) 231
Appendix G. Solms Rd. Site Photos, Plots, and Data (December 2015) 237
References 241

LIST OF FIGURES

Page

Figure 1. Pavement Damage Caused by Overload Trucks in Energy Development Areas........... 3
Figure 2. Location of TxDOT Permanent Stations for Weigh-in-Motion Data Collection........... 8
Figure 3. Logical and Physical (Microsoft Access) Data Model of TPP WIM Data. 13
Figure 4. Physical Data Model of Permanent Stations GIS Data. 14
Figure 5. Load Spectrum Traffic Data Inputted in TxME. 15
Figure 6. ESALs Calculated from Truck Factors and TxME Load Spectra. 19
Figure 7. Comparison of AADTT for Interstate Highways. 21
Figure 8. Comparison of AADTT for US or State Highways. 21
Figure 9. Comparison of AADTT for FM Roads. 22
Figure 10. A Typical Pavement Structure.. 23
Figure 11. Total Rut Depths from TxME with Load Spectra Inputs. 23
Figure 12. AC Fatigue Cracking Area from TxME with Load Spectra Inputs............................ 24
Figure 13. Pavement Rehabilitation Alternative Selection and Design Process for Energy Sector Roads. 26
Figure 14. GPR Image Obtained on FM 99. 28
Figure 15. Example of FWD and DCP Survey Results. 28
Figure 16. Materials Collected from FM 99. 29
Figure 17. Stabilizer Selection Guidelines... 29
Figure 18. Three Different Cold Recycling Application Options... 31
Figure 19. Mix Design Process for Stabilized Materials. 32
Figure 20. Dynamic Modulus Testing of Asphalt Stabilized Material. 33
Figure 21. Samples Taken during the Moisture Conditioning and the IDT Test. 34
Figure 22. Test Pit on FM 906. 35
Figure 23. Pictures of Collected Soil Materials from FM 906. 35
Figure 24. Location of the FM 541 Project.. 37
Figure 25. Pavement Condition prior to Construction... 38
Figure 26. Comparison of All the IDT Test Results. 39
Figure 27. Dynamic Modulus Testing of Stabilized Materials (FDR). 40
Figure 28. Dynamic Modulus for FM 99: (a) 3-Day Curing, and (b) 7-Day Curing................... 41
Figure 29. Dynamic Modulus for FM 541 (3 Day Curing). 41
Figure 30. Dynamic Modulus for FM 541: (a) 3-Day Curing, and (b) 7-Day Curing................. 42
Figure 31. Location of FM 541. 43
Figure 32. Soil Map for PI. 44
Figure 33. Structural Damage Found and Layer Thicknesses Verified by GPR Test. 45
Figure 34. FWD Output from FM 541 Existing Pavement. 45
Figure 35. Pavement Design for FM 541... 46
Figure 36. Typical Construction Sequence. 47
Figure 37. FWD Test on FM 541 Section after Two Weeks after Construction. 48
Figure 38. Pictures of Pavement Surface and Rutting: (a) No Cracking, and (b) Rutting............ 48
Figure 39. Location of SH 202. 49
Figure 40. Soil Map for PI. 49
Figure 41. Example of GPR Test Results. 50

Figure 42. FWD Output from SH 202 Existing Pavement. 50
Figure 43. Construction Sequence on SH 202. 51
Figure 44. FWD Test Results on SH 202. 51
Figure 45. Pictures of Pavement Surface and Rutting: (a) No Cracking, and (b) Rutting. 52
Figure 46. Location of I-10. 52
Figure 47. FWD Test Results on I-10. 53
Figure 48. Pictures of Pavement Surface and Rutting: (a) No Cracking, and (b) Rutting. 53
Figure 49. Location of SH 7. 54
Figure 50. FWD Test Results on SH 7. 55
Figure 51. Condition of FM 99 prior to Rehabilitation. 56
Figure 52. Location of FM 99. 56
Figure 53. Pictures of Pavement Surface and Rutting: (a) Cracking and (b) Rutting. 57
Figure 54. (a) 4-Layer Pavement Structure for Rehabilitation, and (b) 3-Layer Pavement Structure for Rehabilitation. 61
Figure 55. Pavement Design Curves for FDR with Asphalt Stabilization and Surface Treatments: (a) FPS Curves and (b) Triaxial Check. 65
Figure 56. 3-Layer Design Curves for 4-in. AC Surface. 67
Figure 57. ATHWLD for 20-Year ESAL Level. 68
Figure 58. Comparison of Pavement Sections Using Table 4 for 2 Million ESAL, Soft Subgrade, and 8 In. of FDR. 70
Figure 59. Comparison of Pavement Sections Using Table 4 for 80 Wells in Permian Basin with Stiff Subgrade and Medium Stiffness FDR. 72
Figure 60. Four Layers: TxME Results for Subgrade Modulus 10 ksi and 3.0 Million ESAL. 77
Figure 61. Four Layers: TxME Results for Subgrade Modulus 10 ksi and 5.0 Million ESAL. 77
Figure 62. Three Layers: TxME Results for Subgrade Modulus 10 ksi and 3.0 Million ESAL. 78
Figure 63. Three Layers: TxME Results for Subgrade Modulus 10 ksi and 5.0 Million ESAL. 79
Figure 64. Map of Pioneer National Resources USA. 87
Figure 65. Pioneer Site Layout. 88
Figure 66. Pioneer Site Layout with Captions. 88
Figure 67. Pioneer Site Layout with Traffic Routes. 89
Figure 68. Pioneer FWD Testing Locations. 90
Figure 69. Pioneer Infiltration Testing Locations. 91
Figure 70. Pioneer Distress Locations. 92
Figure 71. Pioneer Distress Locations with Captions. 92
Figure 72. Pioneer Effective Thickness Chart. 93
Figure 73. Pioneer k-Value Chart. 94
Figure 74. Pioneer Load-Transfer Efficiency Chart. 94
Figure 75. Map of SEC Energy Products and Services. 95
Figure 76. Heavy Duty Industrial Fork Lift. 96
Figure 77. SEC Building/Site Layout. 96
Figure 78. SEC Pavement Types Layout. 97
Figure 79. SEC Major Traffic Routes. 97

Figure 80. SEC July 2015 FWD Testing Positions Layout (App C and D Figures). 99
Figure 81. SEC Longitudinal Joint Further Examined. 100
Figure 82. SEC Effective Thickness (July 2015).. 101
Figure 83. SEC Effective Thickness (December 2015).. 101
Figure 84. SEC k-Value (July 2015).. 102
Figure 85. SEC k-Value (December 2015).. 102
Figure 86. SEC Load-Transfer Efficiency (July 2015)... 103
Figure 87. SEC Load-transfer Efficiency (December 2015). 103
Figure 88. Map of Bella Vista Community. 104
Figure 89. Bella Vista Site Layout with Testing Layout. 105
Figure 90. Bella Vista Effective Thickness for Site 1. 106
Figure 91. Bella Vista Effective Thickness for Site 2—Stabilized. 107
Figure 92. Bella Vista Effective Thickness for Site 2—Unstabilized. 107
Figure 93. Bella Vista k-Value for Site 1. 108
Figure 94. Bella Vista k-Value for Site 2—Stabilized. 108
Figure 95. Bella Vista k-Value for Site 2—Unstabilized. 109
Figure 96. Bella Vista Load Transfer Efficiency for Site 1. 109
Figure 97. Bella Vista Load Transfer Efficiency for Site 2—Stabilized. 110
Figure 98. Bella Vista Load Transfer Efficiency for Site 2—Unstabilized. 110
Figure 99. Map of Solms Rd. 111
Figure 100. Solms Rd.—FWD Testing Patterns... 112
Figure 101. Solms Rd. Effective Thickness... 113
Figure 102. Solms Rd. Effective Thickness... 113
Figure 103. Solms Rd. k-Value... 114
Figure 104. Solms Rd. k-Value... 114
Figure 105. Solms Rd. Load Transfer Efficiency. 115
Figure 106. Solms Rd. Load Transfer Efficiency. 115
Figure 107. Map of Location near Brownwood, Texas. 116
Figure 108. Effective Thickness—Brownwood Rest Area RCC... 117
Figure 109. Effective μ Brownwood Rest Area RCC. 117
Figure 110. LTE Brownwood Rest Area. 118
Figure 111. Alligator Cracking Distress Located on SH 123, Approach Lane toward US 181.. 123
Figure 112. US 181 Intersection Breakdown Layout. 124
Figure 113. FWD Deflection Data of Sensor at Load Plate Center Plot. 126
Figure 114. US 181/SH 123 Core and DCP Locations... 127
Figure 115. Core Location 4 Existing Material Samples.. 128
Figure 116. Moisture-Density Relation for Base Materials Only.. 130
Figure 117. Moisture-Density Relation for Base Materials+6 Percent Cement. 130
Figure 118. Moisture-Density Relation Subgrade Materials Only—Depth between 2 and 3 ft. 131
Figure 119. Moisture-Density Relation Subgrade Materials Only—Depth < 2 ft...................... 132
Figure 120. Moisture-Density Relation Subgrade Materials Only—Depth > 3 ft...................... 132
Figure 121. Moisture-Density Relation Subgrade+ 4 Percent Lime. 133
Figure 122. Relationship of pH with Lime Percent Change. 134
Figure 123. Capillarity Testing Results for Subgrade and Base Material Samples................... 136

Figure 124. Preconstruction or Pre-overlay Treatment Selection. 145
Figure 125. Long-Term Concrete Pavement Design Selection. 147
Figure 126. k-value Relationships with Other Soil Support Values (*8*). 153
Figure 127. Maximum Stresses due to Curling and Warping. 154
Figure 128. Load Distribution Model Used for a Given Axle Type. 157
Figure 129. The Cumulative Fraction of the Traffic. 160
Figure 130. Overview of Enhanced Punchout Model. 181
Figure 131. Schematic of Combination for Possibility of Punchouts. 182
Figure 132. Formation of Deep Delamination. 184
Figure 133. Establish Strategies and Activity Timing. 189
Figure 134. Expenditures throughout the Analysis Period. 193
Figure 135. Risk Analysis Approach. 195
Figure 136. Agency and User Cost for All Alternatives. 204
Figure 137. Probability Distribution of Agency Costs—Rural New Construction. 205
Figure 138. Probability Distribution of User Costs—Rural New Construction. 206
Figure 139. Cumulative Probability Distribution of Agency Costs—Rural New Overlay. 206
Figure 140. Cumulative Probability Distribution of User Costs—Rural New Overlay. 207
Figure 141. Variation of Deflection Basin Area with P (). 210
Figure 142. Stress Pattern of Unbonded and Partially-Bonded Transformed Section of a Concrete Slab (*20*). 212
Figure 143. Relationship between Backcalculated Values of μ and Degree of Bond (*20*). 214
Figure 144. Pioneer Slab Tested. 219
Figure 145. Location 3 and 4 (Joint Separation and Faulting). 219
Figure 146. Pioneer Cracked Slab (Repair/Sealed with Asphalt). 220
Figure 147. Major Blow-Up Located in the Center of the Property. 220
Figure 148. Pioneer Locations 16 and 17 (Major Blow-Up). 221
Figure 149. SEC Testing Location 7-12 (July 2015). 223
Figure 150. SEC Testing Locations 13-22 (July 2015). 223
Figure 151. SEC Testing Locations 7-16 (December 2015). 225
Figure 152. Construction Joint from Transverse to Longitudinal (December 2015). 225
Figure 153. Longitudinal Joint Separation. 227
Figure 154. Bella Vista Longitudinal Joint Separation (July 2015). 228
Figure 155. Bella Vista Paving Operation (July 2015). 228
Figure 156. Bella Vista Finishing Operation. 229
Figure 157. Bella Vista Testing Locations (1-16). 231
Figure 158. Bella Vista Transverse Joint Tested. 231
Figure 159. Bella Vista Longitudinal Joint (Separation Present) (December 2015). 232
Figure 160. Bella Vista Section—Stabilized Subgrade. 233
Figure 161. Bella Vista Site (Different Base Type). 233
Figure 162. Bella Vista New Joint Filling with Dirt. 234
Figure 163. Bella Vista—Older Joint Already Compressed with Dirt Present. 234
Figure 164. Bella Vista Natural Subgrade. 235
Figure 165. Solms Rd. Testing Paths/Lines Layout. 237
Figure 166. Solms Rd. Longitudinal Joint Spalling and Repair (along with Repair Material Failure). 237
Figure 167. Solms Rd. (Run 2) Testing along Edges/Corners. 238

Figure 168. Solms Rd. Patching of Longitudinal Cracking. 239
Figure 169. Solms Rd. Slab Heave and Failure/Crack Tested. 239

LIST OF TABLES

Page

Table 1. Permanent Stations of Type WIM and WIM/Piezo in Permanent Stations GIS File. 7
Table 2. 2012 WIM Data Set: Number of Records by Station ID. 9
Table 3. Texas Vehicle Classification Scheme (*1*). 12
Table 4. WIM Stations Selected for Data Analysis. 16
Table 5. Inputs for ESAL Calculations. 18
Table 6. Comparison of ESALs Calculated from Truck Factor and TxME Load Spectra. 19
Table 7. Summary of All the 19 WIM Data Sets. 20
Table 8. Summary of Predicted Pavement Performances Using Load Spectra Inputs. 23
Table 9. Failure Mode and Type of Distress. 27
Table 10. IDT Results from Foamed Asphalt Samples from FM 99. 34
Table 11. Aggregate Gradations for Existing Base and New Base. 36
Table 12. OMC and Dry Density for Two Aggregate Combinations. 36
Table 13. Evaluated Stabilization Designs. 36
Table 14. IDT Test Results on Stabilization Designs. 37
Table 15. IDT Results from Foamed Asphalt Samples from FM 541. 38
Table 16. Traffic Inputs for FM 541 in FPS Design. 46
Table 17. Pavement Material Properties for FPS21 Pavement Design. 62
Table 18. ESALs per Well during Development and Operation for Different Texas Formations (5). 68
Table 19. Pavement Design Catalog for 4-Layer (Surface, Flex Base, FDR, Subgrade) Pavement. Numbers in Table Are Flex Base Thickness in Inches. 71
Table 20. Pavement Design Catalog for 3-Layer (Surface, FDR, Subgrade) Pavement. Numbers in Table Are Flex Base Thickness in Inches. 73
Table 20. Pavement Design Catalog for 3-Layer (Surface, FDR, Subgrade) Pavement. Numbers in Table Are Flex Base Thickness in Inches (continued). 74
Table 21. 4-Layer Designs Selected for Demonstration of TxME Results. 76
Table 22. 3-Layer Designs Selected for Demonstration of TxME Results. 76
Table 23. FWD R1 Sensor Deflection Data. 124
Table 24. FWD Calculated Subgrade Modulus. 125
Table 25. FWD Calculated Base Layer Modulus. 125
Table 26. FWD Calculated Surface Layer Modulus. 125
Table 27. DCP Calculated Parameters. 128
Table 28. Materials Tested and Their OMC and Maximum Dry Density. 129
Table 29. pH Measurements for Subgrade Materials—at Depth < 3 ft. 133
Table 30. pH Measurements for Subgrade Materials—at Depth > 3 ft. 134
Table 31. Average Corrected Stress Measurements Different Cement Percent. 135
Table 32. Average Compressive Strength Measurement for 4 Percent Lime Stabilized Subgrade Samples. 135
Table 33. Types of Concrete Pavement. 140
Table 34. Secondary Factors to Prioritize between Design Options. 148
Table 35. PCA/ACI Truck Load Categories (SA). 160

Table 36. Number and Percent (%AT) of Different Axles per Truck. 161
Table 37. AASHTO-Typical Friction Coefficient of Stabilized Base/Subbase Materials. 164
Table 38. AASHTO Guidelines Development and Limitations. 168
Table 39. Truck Traffic Classification Group Description and Distribution. 171
Table 40. Dimensionless Stress Coefficients—Free Edge. 173
Table 41. Design Calculation Inputs. 179
Table 42. Framework of MRR Strategies. 190
Table 43. LCCA Inputs. 198
Table 44. Alternative 1—Framework of MMR Activities for 60 Years. 200
Table 45. Alternative 2—Framework of MMR Activities for 60 Years. 200
Table 46. Alternative 3—Framework of MMR Activities for 60 Years. 201
Table 47. Alternative 4—Framework of MMR Activities for 60 Years. 201
Table 48. Agency Cost Input Values. 202
Table 49. Summary of Deterministic Results. 204
Table 50. Summary of Probabilistic Results. 205

PART I: FLEXIBLE PAVEMENTS

CHAPTER 1. INTRODUCTION

BACKGROUND

In recent years, rapid energy development in Texas has caused significant damage to many farm-to-market (FM) roads, which traditionally have a thin asphalt surface layer plus a stabilized base directly over the subgrade. These roadways were often rehabilitated with full depth reclamation (FDR) and often 2 to 3 percent cement was added to the pulverized existing materials. These roadways performed well under normal traffic loads but failed dramatically under the energy sector truck loads. Figure 1 shows the damaged FM roads. The impact of overloading traffic on pavement damage is not only limited to FM roads, it also has significant influence on pavement life of state highways (SH) and even interstate highways (IH). There is an urgent need to repair many of these badly damaged roadways in all energy development areas.

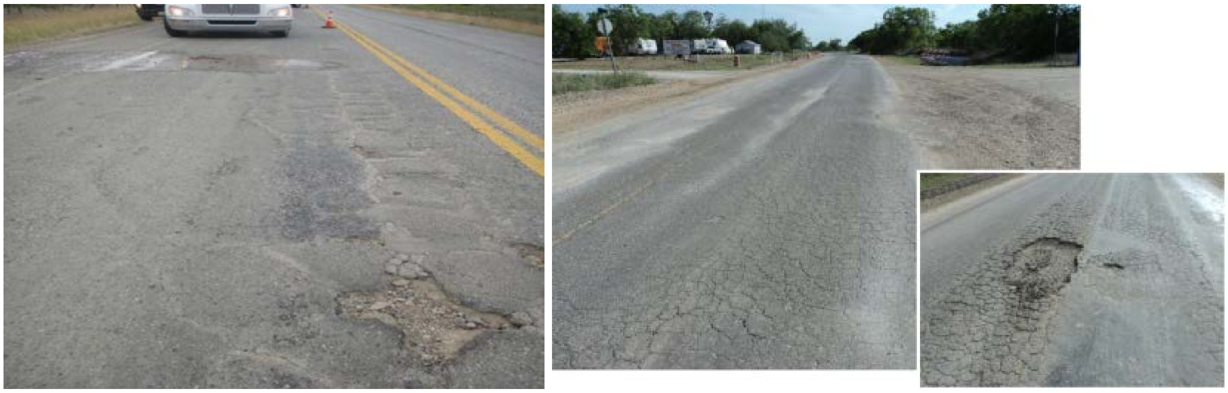

Figure 1. Pavement Damage Caused by Overload Trucks in Energy Development Areas.

CHALLENGES OF REPAIRING PAVEMENTS FOR ENERGY DEVELOPMENT AREAS

There are at least five challenges to address the urgent needs of repairing roadways in the energy development areas:

1. *Multiple types of roads*: The majority of the roads in energy development areas are thin FM roadways with often 6 in. of granular base with a thin surfacing layer. However, both SH and even IH are also impacted by the overloading traffic.
2. *Weak and non-uniform pavement structure of FM roads*: Existing FM roads typically have less than 2 in. of surface layer, and often a combination of multiple surface treatments, which are often very variable, especially if substantial maintenance has been performed.
3. *Early opening traffic requirement*: One requirement the Texas Department of Transportation (TxDOT) has placed on all rehabilitation work is that as there are no detours available for those FM roads, the existing roadway must be reopened to traffic at the end of each work day. This severely impacts the use of many of the

commonly used stabilizers such as cement or asphalt emulsions. Note that the opening traffic requirement for highways with multiple lanes (such as IH) may not be as bad as FM roads. For those highways with multiple lanes, cement, asphalt emulsions, other conventional stabilizers may be still applicable.

4. *Excessive traffic loads*: Not only have the truck traffic levels increased in many cases 20 to 50 times over the preexisting levels, but in some instances severely overloaded trucks are being found. In a study of weigh-in-motion (WIM) data collected, it was not uncommon to find trucks running at 50 to 60 percent overloaded. Real concerns have been expressed by pavement designers as to the inadequacy of both the 20-year design load estimates and the average of the 10 heaviest wheel loads daily (ATHWLD) both of which are required inputs within TxDOT flexible pavement design program.
5. *Available funds*: Many hundreds of miles have been severely damaged but only limited rehabilitation funds are available.

REHABILITATION OPTIONS FOR REPAIRING DAMAGED PAVEMENTS

In general many options are available for repairing damaged pavements, and sometimes it is not easy to determine which one is the best. However, the following two questions can assist in making better choice:

- What is wrong with existing pavement or the distress is limited to the surfacing (upper pavement layers) or it is a structural problem?
- What does TxDOT really want and what can they afford?

The answers to these two questions will narrow down the rehabilitation options to only those that will be cost-effective, considering the nature of the problem and the time frame. Another important consideration is the practicality of various rehabilitation methods. In additionally, traffic accommodation, weather conditions, and availability of resources can all have a significant influence on how a project is constructed may preclude certain options. Based on the nature of the problem, rehabilitation options are divided into two big categories:

- Surface rehabilitation.

  Surface rehabilitation measures often address problems usually within the top 2-in. to 4-in. surface layers. These problems are normally related to asphalt aging and top-down cracking that initiates at the surface. The most often used methods for this type of surface problem include 1) asphalt overlay, 2) milling and inlay, and 3) recycling.

  - Asphalt overlay.

    Paving a thin (1.5–2 in.) asphalt overlay on the existing surface is the simplest solution to a surface problem. The good parts of asphalt overlay are short working time and minimal impact on traffic and users. However, many active cracks in existing surface will reflect quickly through a new (thin) overlay. Thus, it is important to identify the active cracks and treat them before asphalt overlay. Additionally, repeated overlays increase road surface elevations that may cause drainage and access problems.

  - Milling and inlay.

    This method often mills the cracked layer and then replaces it with new asphalt mixes. This process is relatively fast, and other benefits include removing surface problem and maintaining pavement elevation.

  - Cold in place recycling.

    Generally, it recycles a relatively thin (4–6 in.) layer of asphalt material from the existing pavement. Figure 1 shows a cold in place recycling.

- Structural rehabilitation.

  Different from surface rehabilitation, the focus of structural rehabilitation is to fix the structural problems (such as fatigue cracking, deep rutting, etc.). In most cases pavement layer materials are still reusable. Sometime, it is often considered as a structural rehabilitation that a lower level of existing pavement is upgraded by strengthening the existing structure.

  There are three popular options for structural rehabilitation:

  - Total reconstruction.

    This option is often preferred when combined with an upgrading, which requires significant changes to the alignment of the road. In this case, some temporary road may be constructed to accommodate existing traffic.

  - Adding new layers.

    Thick asphalt overlays are often the easiest solution to a structural problem where the traffic volumes are high.

- FDR (or deep recycling).

  FDR often recycles to the depth in the pavement at which the problem occurs, thereby creating a new thick homogeneous layer that can be strengthened by the addition of stabilizing agents. Additional layers may be added on top of the recycled layer where the pavement is to be significantly upgraded. Stabilizing agents are usually added to the recycled material, especially where the material in the existing pavement is marginal and requires strengthening. Recycling aims for maximum recovery from the existing pavement. In addition to salvaging the material in the upper layers, the pavement structure below the level of recycling remains undisturbed.

RESEARCH OBJECTIVE

The main objectives of this project are as follows:

1. Determine traffic conditions (in terms of actual axle load level) for pavement designs in the energy development areas.
2. Assist local TxDOT districts in surveying pavements conditions of impacted areas using the state of the art nondestructive test equipment.
3. Develop materials options for handling the early trafficking requirement, which is critical in most recent projects.
4. Recommend improved pavement designs that are structurally adequate for overloaded vehicles.
5. Work with TxDOT districts that are currently being severely impacted, which include Laredo, San Antonio, Corpus, Odessa, San Angelo, Bryan, and Yoakum, to design, construct, and monitor test sections with new materials and design approaches.

Part I Organization

Part I is organized into six chapters. Chapter 1 provides background information relative to the project. Chapter 2 introduces WIM data analysis and traffic input for pavement design, and evaluates the difference of equivalent single axle load (ESAL) calculations from the traditional method and full load spectrum. Chapter 3 develops guidance for selecting optimal rehabilitation options for flexible pavements and presents laboratory test results including IDT and dynamic modulus for asphalt stabilized materials. Chapter 4 introduces several field projects with implementation of FDR including the test results obtained from nondestructive equipment. Pavement design catalogue for flexible pavements in energy development areas are developed based on Flexible Pavement Design System (FPS21) and Texas Mechanistic-Empirical Pavement Design and Analysis System (TxME) simulation results and presented in Chapter 5. Finally, Chapter 6 summarizes conclusions and recommendations for this project.

CHAPTER 2. WEIGH-IN-MOTION DATA ANALYSIS AND TRAFFIC INPUT FOR PAVEMENT DESIGN

TXDOT WEIGH-IN-MOTION SENSORS

TxDOT has deployed 41 permanent WIM sensors in 20 TxDOT districts, as shown in Table 1. Some districts have more than one WIM sensor, for example Laredo, Pharr, and Wichita Falls Districts have four WIM permanent stations each. Table 1 provides a listing of the WIM permanent stations by district along with the type (either bending plate or piezo) and the site name used in TxDOT GIS file of permanent stations. Figure 2 shows the location of the WIM permanent stations around the state.

Table 1. Permanent Stations of Type WIM and WIM/Piezo in Permanent Stations GIS File.

No.	Type	Site Name	District
1	WIM	BSIF	Laredo
2	WIM	BSIF	Laredo
3	WIM	BSIF	Pharr
4	WIM	BSIF	Pharr
5	WIM	BSIF	Laredo
6	WIM/Piezo	PZ-4142	Beaumont
7	WIM/Piezo	PZ-502	San Antonio
8	WIM	W-506	Wichita Falls
9	WIM	W-513	Waco
10	WIM	W-514	Dallas
11	WIM/Piezo	PZ-518	San Antonio
12	WIM	W-522	Pharr
13	WIM	W-523	Pharr
14	WIM	W-524	El Paso
15	WIM	W-525	Atlanta
16	WIM	W-526	Atlanta
17	WIM	W-527	Fort Worth
18	WIM	W-528	Wichita Falls
19	WIM	W-529	Wichita Falls
20	WIM	W-530	Wichita Falls
21	WIM	W-531	Laredo
22	WIM	W-532	Austin
23	WIM	W-533	Odessa
24	WIM	W-534	Corpus Christi
25	WIM	W-535	Corpus Christi
26	WIM	W-536	Austin
27	WIM	W-537	Lubbock
28	WIM	W-538	Corpus Christi
29	WIM/Piezo	PZ-539	Dallas
30	WIM	W-540	Odessa

No.	Type	Site Name	District
31	WIM	W-541	Atlanta
32	WIM	W-542	Beaumont
33	WIM	W-543	Lubbock
34	WIM	W-544	Brownwood
35	WIM	W-545	Lubbock
36	WIM	W-546	Paris
37	WIM	W-547	Amarillo
38	WIM	W-548	Waco
39	WIM	W-549	Fort Worth
40	WIM	W-550	Fort Worth
41	WIM/Piezo	PZ-800	Bryan

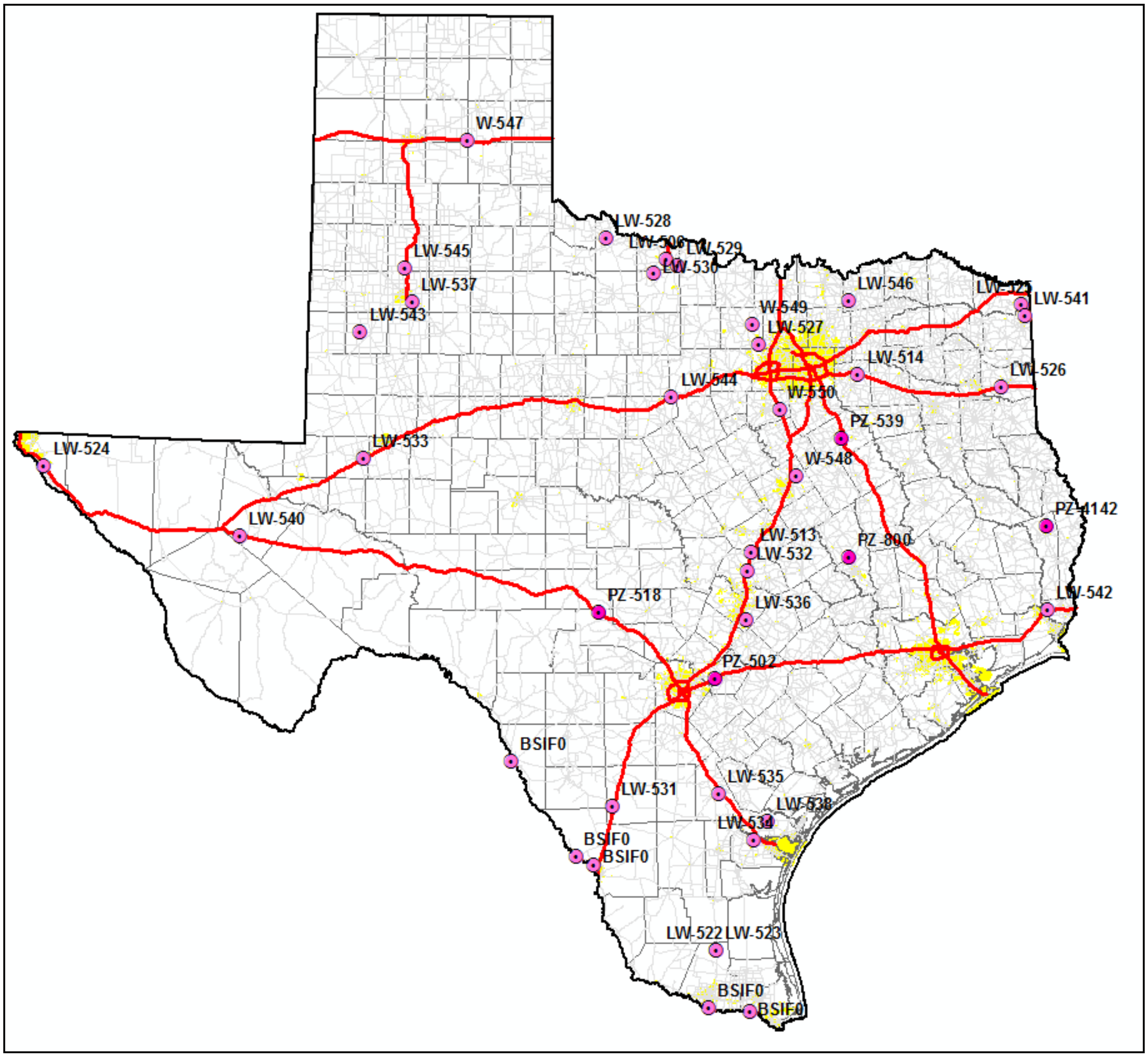
W-547
LW-528
LW-506
LW-529
LW-530
LW-545
LW-537
LW-543
LW-546
LW-525
LW-541
W-549
LW-527
LW-514
LW-526
LW-544
W-550
PZ-539
W-548
LW-524
LW-533
LW-540
PZ-4142
LW-513
LW-532
PZ-800
PZ-518
LW-536
LW-542
PZ-502
BSIF0
LW-535
LW-531
LW-538
LW-534
BSIF0
BSIF0
LW-522
LW-523
BSIF0
BSIF0

Figure 2. Location of TxDOT Permanent Stations for WIM Data Collection.

Not all WIM stations shown in the GIS file are active at all times. For example, Table 2 shows a query of the 2012 WIM data set that shows the total number of records (or vehicles weighed) for each month by station. Table 2 shows that there were no records collected for station 502, 540, and several others in January 2012. Table 2 provides a number of records for station 808, which did not appear in the GIS file. This station was removed in May 2012 and is no longer included in the GIS file.

Table 2. 2012 WIM Data Set: Number of Records by Station ID.

Station ID	Jan	Feb	Mar	Apr	May	Jun
142	26,326	26,414	27,253	221	29,605	12,533
502	-	-	-	1,738	151,909	63,918
506	105,219	89,111	111,037	84	58,621	48,290
513	287,551	279,010	321,890	3,864	319,916	139,926
518	74,692	72,519	80,472	1,118	79,924	37,698
522	47,409	44,922	50,690	36,725	48,759	49,754
523	100,298	95,635	108,547	1,650	99,519	47,252
524	192,634	161,309	118,980	2,582	147,073	75,901
525	69,160	69,014	73,191	759	67,040	32,354
526	227,622	216,976	239,969	2,329	209,353	99,815
527	71,507	69,404	76,550	642	79,778	30,380
528	72,428	69,762	80,082	1,099	88,390	39,038
529	103,622	124,638	96,027	1,705	137,654	62,421
530	23,845	24,629	25,262	293	27,756	11,524
531	207,241	193,680	224,575	2,563	109,658	90,920
532	34,827	35,603	38,431	391	40,290	19,954
533	300,811	301,761	314,126	3,083	298,895	148,373
535	36,345	46,762	53,880	433	58,292	26,859
536	50,782	49,674	59,452	473	62,344	29,002
537	64,788	61,329	69,481	731	72,289	31,787
538	24,051	24,837	29,439	29,052	30,315	28,905
539	185,643	185,392	201,740	2,626	212,793	89,823
540	46,512	4,719	30,283	691	-	-
541	6,718	3,003	5,388	80	9,462	3,585
542	244,796	-	276,589	2,901	22	66,857
543	8,882	8,868	10,563	100	10,929	4,515
544	160,445	170,333	180,487	2,487	161,128	72,641
800	2,277	2,053	2,653	12	2,268	814
808	1,414	1,731	634	-	-	-
Total	**2,777,845**	**2,433,088**	**2,907,671**	**100,432**	**2,613,982**	**1,364,839**

Table 2. 2012 WIM Data Set: Number of Records by Station ID. (Continued).

Station ID	Jul	Aug	Sep	Oct	Nov	Dec	Annual Total
142	27,590	14,815	27,224	28,298	28,442	19,107	267,828
502	212,866	84,814	221,375	244,589	275,027	223,059	1,479,295
506	144,292	57,170	104,987	105,234	166,289	408,035	1,398,369
513	302,321	177,259	284,449	280,146	411,096	238,600	3,046,028
518	76,268	42,177	80,334	85,590	97,269	70,417	798,478
522	46,662	48,855	45,171	51,199	50,518	49,270	569,934
523	93,800	52,776	96,029	107,460	125,452	89,426	1,017,844
524	169,125	87,168	166,561	173,112	211,111	160,770	1,666,326
525	57,956	38,364	67,085	70,391	82,763	60,000	688,077
526	204,018	115,943	208,168	216,479	257,004	175,322	2,172,998
527	67,324	38,506	69,168	76,609	87,833	65,243	732,944
528	85,021	47,810	72,458	78,893	111,648	80,959	827,588
529	139,051	75,039	136,126	132,609	164,760	113,730	1,287,382
530	23,650	12,944	24,931	25,804	29,170	24,044	253,852
531	202,051	110,275	192,977	208,764	208,305	161,631	1,912,640
532	41,803	24,360	40,530	44,822	58,950	39,392	419,353
533	302,278	158,610	281,365	73,262	-		2,182,564
535	56,558	31,316	58,769	59,605	72,301	56,386	557,506
536	60,332	22,283	58,262	71,527	89,918	65,289	619,338
537	52,644	161	61,832	67,716	82,062	39,246	604,066
538	29,266	30,400	28,352	28,246	24,881	24,279	332,023
539	18	3	21	131,577	231,300	184,339	1,425,275
540	-	-	-	-	-		82,205
541	8,258	4,961	8,398	8,370	9,121	5,127	72,471
542	293,440	172,621	314,708	336,519	363,403	277,993	2,349,849
543	9,302	4,851	8,491	11,755	13,840	8,935	101,031
544	155,172	89,246	154,864	178,693	195,176	154,772	1,675,444
800	1,023	852	2,153	2,278	2,100	1,509	19,992
808	-	-	-	-	-		3,779
Total	**2,862,089**	**1,543,579**	**2,814,788**	**2,899,547**	**3,449,739**	**2,796,880**	**28,564,479**

The data in the WIM file were provided by TxDOT’s Transportation Planning and Programming Division (TPP) in form of text files. Each text file contained records for all WIM stations for one month. For example, the January 2012 data set contained 2,777,845 records (Table 2). To make analysis of the data easier, researchers imported the data into an Oracle database.

The data in the WIM data set were formatted according to federal standards, as outlined in the Federal Highway Administration's (FHWA's) Traffic Monitoring Guide (*1*). Researchers created a data model to illustrate the structure of the weight data. Figure 3 shows the logical data model of the WIM data set using the example of the January 2012 table and the physical implementation using Microsoft® Access. Since tables for all months follow the same data structure, it is sufficient to show just one table. The following provides a brief description of each logical data model attribute:

- RECORD TYPE differentiates different types of data sets such as vehicle classification, speed, and WIM data. All records in the WIM data sets have a RECORD TYPE "W."
- FIPS STATE CODE provides the Federal Information Processing Standard (FIPS) code for the state where the data were collected. All records in the WIM data set have FIPS STATE CODE of "48" for Texas.
- STATION ID provides an identification for the WIM station, as shown in Table 2. Note that the STATION ID is different from the SITE NAME in the GIS file in that the STATION ID does not contain the station prefix, such as PZ or LW.
- DIRECTION OF TRAVEL provides a code for the direction of travel, which can be one of 10 possible values.
- LANE OF TRAVEL describes the lane in which the recorded vehicle was traveling, which is 1 for the rightmost lane, and 2 or higher for any other lane, counting from the rightmost lane. Zero indicates data with lanes combined.
- YEAR OF DATA is the year the data were recorded.
- MONTH OF DATA is the month the data were recorded.
- DAY OF DATA is the day the data were recorded.
- HOUR OF DATA is the hour the data were recorded.
- VEHICLE CLASS is a vehicle classification code following the Texas Vehicle Classification Scheme (Table 3) (*1*).
- OPEN is a field for special studies or state use, for example might contain vehicle speed or pavement temperature.
- TOTAL WEIGHT OF VEHICLE is the gross vehicle weight, in 1/10th of metric tons.
- NUMBER OF AXLES is the total number of axles in use by the vehicle, and determines how many of the following axle weight and axle spacing columns will be used for this record.
- A (B, C, D, etc.) AXLE WEIGHT is the total weight of the A (B, C, D, etc.) axle, in 1/10th of metric tons.
- A-B AXLE SPACING is the spacing between axle A and axle B, in 1/10th of a meter, B-C AXLE SPACING is the spacing between axle B and axle C, in 1/10th of a meter, etc.

Table 3. Texas Vehicle Classification Scheme (*1*).

Classification Code	Vehicle Type
1	Motorcycles, passenger vehicles, and small or short-wheel-based pickups
2	2 axles, 4-tire single-unit trucks (full-sized pickup trucks)
3	Buses (2 and 3 axles)
4	2-D, 6-tire single-unit vehicles (includes handicapped-equipped and mini school buses)
5	3 axles, single-unit vehicles
6	4 or more axles, single-unit vehicles
7	3 axles, single trailer (2S1)
8	4 axles, single trailer (2S2 or 3S1)
9	5 axles, single trailer (3S2, 3S2 split, or 2S3)
10	6 or more axles, single trailer (3S3, 3S4, etc.)
11	5 or less axles, multitrailers (2S1-2)
12	6 axles, multitrailers (2S2-2 or 3S1-2)
13	7 or more axles, trailers (3S2-2)
14	Unclassified (AVC and WIM) None

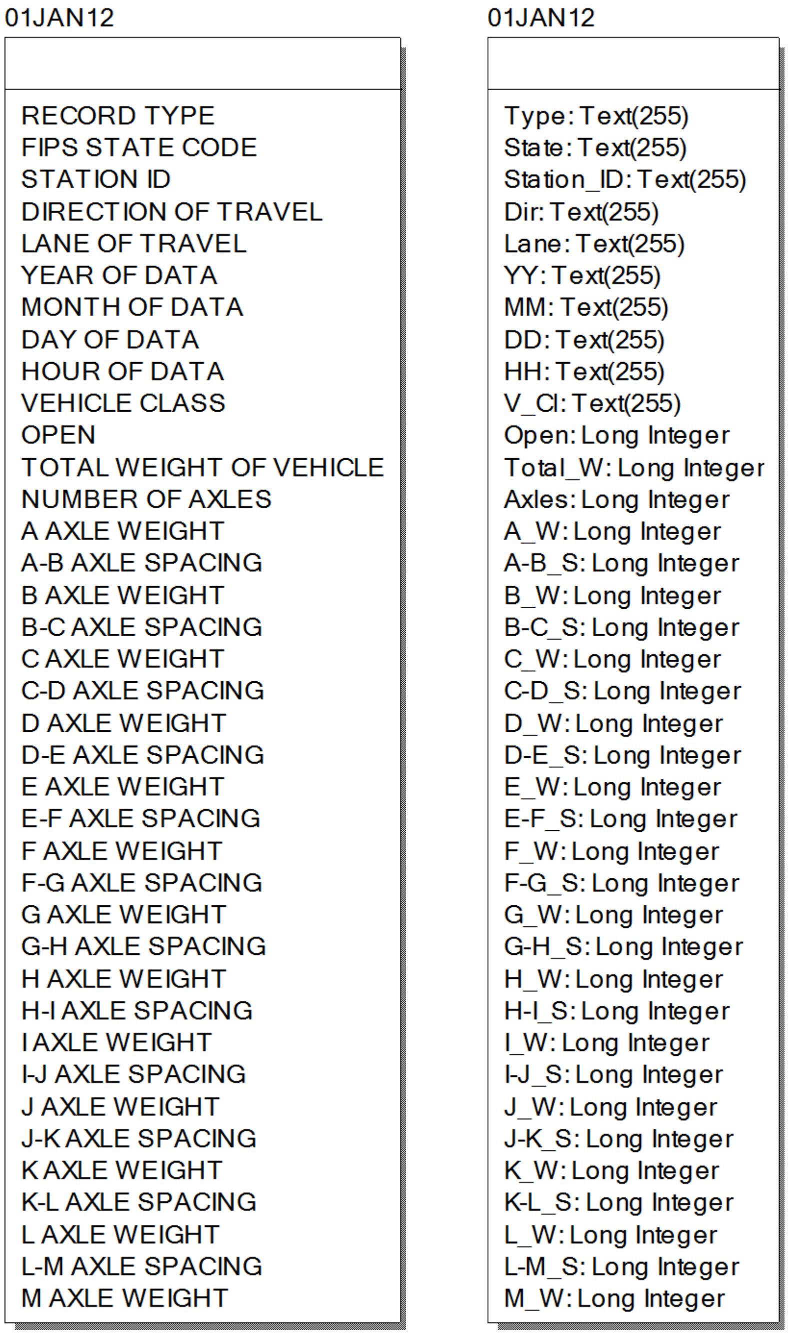

01JAN12	01JAN12
RECORD TYPE	Type: Text(255)
FIPS STATE CODE	State: Text(255)
STATION ID	Station_ID: Text(255)
DIRECTION OF TRAVEL	Dir: Text(255)
LANE OF TRAVEL	Lane: Text(255)
YEAR OF DATA	YY: Text(255)
MONTH OF DATA	MM: Text(255)
DAY OF DATA	DD: Text(255)
HOUR OF DATA	HH: Text(255)
VEHICLE CLASS	V_Cl: Text(255)
OPEN	Open: Long Integer
TOTAL WEIGHT OF VEHICLE	Total_W: Long Integer
NUMBER OF AXLES	Axles: Long Integer
A AXLE WEIGHT	A_W: Long Integer
A-B AXLE SPACING	A-B_S: Long Integer
B AXLE WEIGHT	B_W: Long Integer
B-C AXLE SPACING	B-C_S: Long Integer
C AXLE WEIGHT	C_W: Long Integer
C-D AXLE SPACING	C-D_S: Long Integer
D AXLE WEIGHT	D_W: Long Integer
D-E AXLE SPACING	D-E_S: Long Integer
E AXLE WEIGHT	E_W: Long Integer
E-F AXLE SPACING	E-F_S: Long Integer
F AXLE WEIGHT	F_W: Long Integer
F-G AXLE SPACING	F-G_S: Long Integer
G AXLE WEIGHT	G_W: Long Integer
G-H AXLE SPACING	G-H_S: Long Integer
H AXLE WEIGHT	H_W: Long Integer
H-I AXLE SPACING	H-I_S: Long Integer
I AXLE WEIGHT	I_W: Long Integer
I-J AXLE SPACING	I-J_S: Long Integer
J AXLE WEIGHT	J_W: Long Integer
J-K AXLE SPACING	J-K_S: Long Integer
K AXLE WEIGHT	K_W: Long Integer
K-L AXLE SPACING	K-L_S: Long Integer
L AXLE WEIGHT	L_W: Long Integer
L-M AXLE SPACING	L-M_S: Long Integer
M AXLE WEIGHT	M_W: Long Integer

Figure 3. Logical and Physical (Microsoft Access) Data Model of TPP WIM Data.

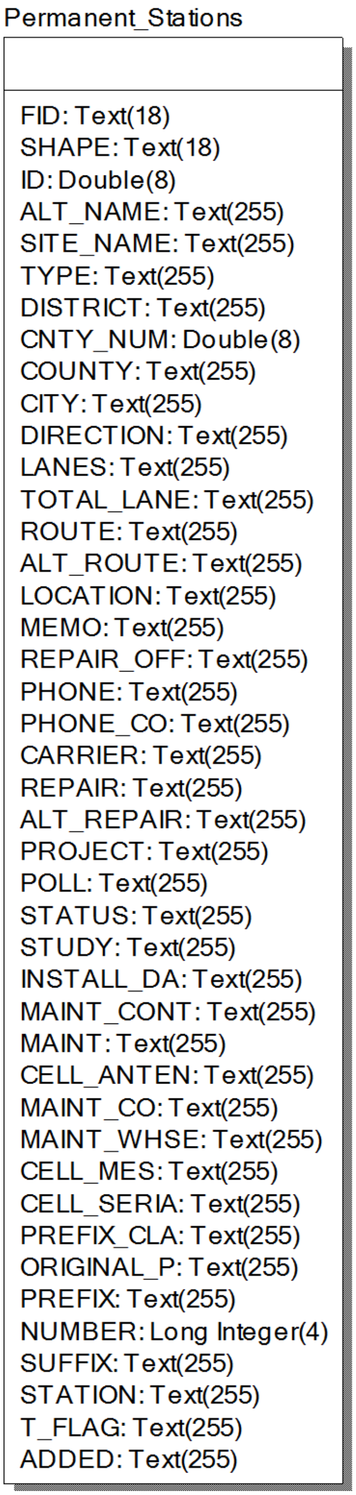

Permanent_Stations

FID: Text(18)
SHAPE: Text(18)
ID: Double(8)
ALT_NAME: Text(255)
SITE_NAME: Text(255)
TYPE: Text(255)
DISTRICT: Text(255)
CNTY_NUM: Double(8)
COUNTY: Text(255)
CITY: Text(255)
DIRECTION: Text(255)
LANES: Text(255)
TOTAL_LANE: Text(255)
ROUTE: Text(255)
ALT_ROUTE: Text(255)
LOCATION: Text(255)
MEMO: Text(255)
REPAIR_OFF: Text(255)
PHONE: Text(255)
PHONE_CO: Text(255)
CARRIER: Text(255)
REPAIR: Text(255)
ALT_REPAIR: Text(255)
PROJECT: Text(255)
POLL: Text(255)
STATUS: Text(255)
STUDY: Text(255)
INSTALL_DA: Text(255)
MAINT_CONT: Text(255)
MAINT: Text(255)
CELL_ANTEN: Text(255)
MAINT_CO: Text(255)
MAINT_WHSE: Text(255)
CELL_MES: Text(255)
CELL_SERIA: Text(255)
PREFIX_CLA: Text(255)
ORIGINAL_P: Text(255)
PREFIX: Text(255)
NUMBER: Long Integer(4)
SUFFIX: Text(255)
STATION: Text(255)
T_FLAG: Text(255)
ADDED: Text(255)

Figure 4. Physical Data Model of Permanent Stations GIS Data.

WIM DATA ANALYSIS

Researchers analyzed the data from WIM stations to create the files that can be imported in Traffic Input for Level 1-load spectra in TxME (as shown in Figure 5). In Figure 5, the main inputs for TxME include two-way annual average daily truck traffic (AADTT), vehicle class distribution and growth, monthly adjustment, and axle load distribution. As aforementioned, not all the WIM stations are active all the time. A total of 17 WIM stations have records for at least two years, which were selected for the analysis, and all these data can be used for Load Spectra inputs. In addition, portable WIM is used for monitoring traffic on SH 6 and FM 468. It is known that FM 468 is in the energy development area. Table 4 shows all the WIM stations for data analysis including road classification, highway or road name, WIM station ID, and their AADTT.

From Table 4, IH have a very large traffic volume compared with US or SH. For example, Station 513 on I-35, Station 502 on I-10, Station 526 on I-20 have the AADTT of 10,867, 8,005, and 7,704, respectively. Some US or SH have a much lower AADTT (less than 1000). Generally, FM roads has a very low AADTT. However, FM 468 has a much larger AADTT (i.e., 1062) due to a large amount of energy sector trucks.

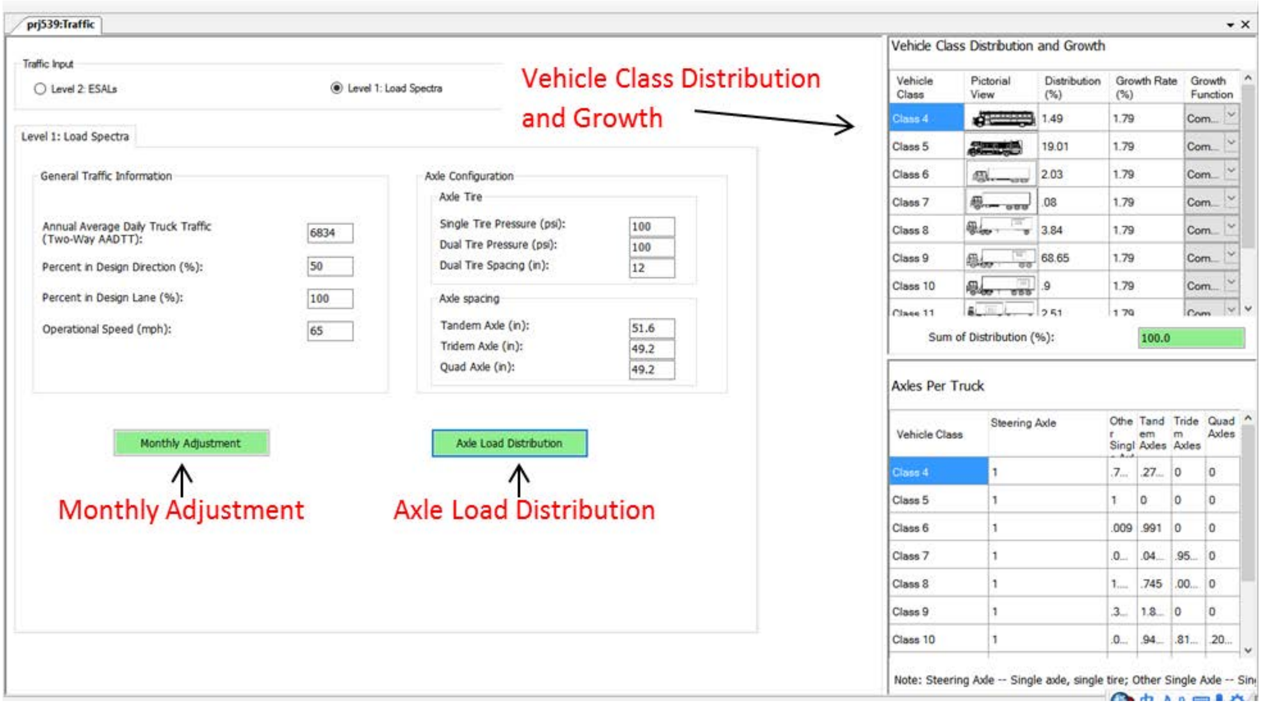

Traffic Input

○ Level 2: ESALs ● Level 1: Load Spectra

Level 1: Load Spectra

General Traffic Information

Annual Average Daily Truck Traffic (Two-Way AADTT): 6834
Percent in Design Direction (%): 50
Percent in Design Lane (%): 100
Operational Speed (mph): 65

Axle Configuration

Axle Tire
Single Tire Pressure (psi): 100
Dual Tire Pressure (psi): 100
Dual Tire Spacing (in): 12

Axle spacing
Tandem Axle (in): 51.6
Tridem Axle (in): 49.2
Quad Axle (in): 49.2

Vehicle Class Distribution and Growth

Vehicle Class	Pictorial View	Distribution (%)	Growth Rate (%)	Growth Function
Class 4		1.49	1.79	Com...
Class 5		19.01	1.79	Com...
Class 6		2.03	1.79	Com...
Class 7		.08	1.79	Com...
Class 8		3.84	1.79	Com...
Class 9		68.65	1.79	Com...
Class 10		.9	1.79	Com...
Class 11		2.51	1.79	Com

Sum of Distribution (%): 100.0

Axles Per Truck

Vehicle Class	Steering Axle	Other Singl	Tandem Axles	Tridem Axles	Quad Axles
Class 4	1	.7...	.27...	0	0
Class 5	1	1	0	0	0
Class 6	1	.009	.991	0	0
Class 7	1	.0...	.04...	.95...	0
Class 8	1	1....	.745	.00...	0
Class 9	1	.3...	1.8...	0	0
Class 10	1	.0...	.94...	.81...	.20...

Note: Steering Axle -- Single axle, single tire; Other Single Axle -- Sin

Figure 5. Load Spectrum Traffic Data Inputted in TxME.

Table 4. **WIM Stations Selected for Data Analysis**.

Highway Classification	Highway ID	Station ID	AADTT
Interstate Highways	I35	513	10,867
	I10	502	8,005
	I20	526	7,704
	I45	539	6,834
	I35	531	6,299
	I20	544	5,767
U.S. or State Highways	US287	506	4,182
	US287	528	3,247
	SH114	527	2,656
	SH130	532	2,269
	US59	535	2,000
	US82	530	919
	US96	142	846
	SH121	546	550
	SH6	Portable WIM	474
	US82	543	372
Farm to Market (FM) Roads	FM468	Portable WIM	1,062
	FM3129	541	251
	FM2223	800	142

COMPARISON OF ESAL CALCULATIONS FROM TRADITIONAL METHOD AND LOAD SPECTRA

ESAL is an important traffic input in the mechanistic-empirical (M-E) pavement design, which is defined as (*2*):

$$ESAL = \sum_{i=1}^{m} F_i n_i \tag{1}$$

Where,
m = the number of axle load groups.
F_i = the equivalent axle load factor (EALF) for the i*th*-axle load group.
n_i = the number of passes of the i*th*-axle load group during the design period.

ESAL is calculated using the following equation (*2*):

$$ESAL = \left(\sum_{i=1}^{m} p_i F_i \right) (ADT)_0 (T)(A)(G)(D)(L)(365)(Y) \qquad 2$$

Where,

p_i = the percentage of total repetitions for the i*th* load group.

F_i = the EALF for the i*th*-axle load group.

$(ADT)_0$ = the average daily traffic at the beginning of the design period.

T = the percentage of trucks in the ADT.

A = the average number of axles per truck.

G = the growth factor.

D = the directional distribution factor.

L = the lane distribution factor.

Y = the design period in years.

To conveniently compute ESAL, a term called truck factor is defined as follows:

$$T_f = \left(\sum_{i=1}^{m} p_i F_i \right) (A) \qquad 3$$

Where,

T_f = the number of 18-kip single-axle load applications per truck.

Substitute Equation 3 into Equation 2 to obtain (*2*):

$$ESAL = (ADT)_0 (T)(T_f)(G)(D)(L)(365)(Y) \qquad 4$$

Traditionally, ESAL is calculated using Equation 4, and truck factors for different classes of highways can be found in Table 6.10 in Huang's Book (*2*).

Another methodology for calculating ESAL is based on traffic load spectra, which is more complex but more accurate. One feature of TxME is to calculate ESAL based on the load spectra input. As aforementioned, a total of 19 WIM stations were selected for traffic data analysis. All these data can be used for load spectra input in TxME. Table 5 and Table 6 present the inputs for ESAL calculation and comparisons of ESAL calculations from traditional method (i.e., Equation 4 using truck factor) and load spectra in TxME, respectively. Four truck factors are selected from in Huang's Book (Table 6.10) for comparison. Annual growth rate for traffic is assumed 1.79 percent, and for a period of 20 years the total growth factor is 24.3. Figure 6 presents the graphical comparisons. ESALs calculated from all four truck factors are much lower than from

TxME load spectra. ESAL is significantly underestimated when using the traditional methodology (i.e., Equation 2). Generally, higher AADTT values generate higher cumulative ESALs, but they are not proportional all the time in the results from TxME load spectra. For example, although the AADTT of Station 513 was even higher than that of Station 526, the cumulative ESAL of Station 513 was less than that of Station 526, which is attributed to different axle load distributions since TxME load spectra includes the information of axle load distribution; whereas the ESALs calculated from truck factors show a different trend because its calculation considers AADTT instead of axle load distribution. Overall, the traffic load spectra can provide the best knowledge on traffic load condition, and TxME can directly analyze the impact of overloaded traffic (or load spectra) on pavement life, which is critical for designing pavements to support overloaded traffic areas.

Table 5. Inputs for ESAL Calculations.

Highway ID	Station ID	AADTT	Direction Distribution Factor	Lane Distribution Factor	Annual Growth Rate	Design Period (years)
I35	513	10,867	50%	100%	1.79%	20
I10	502	8,005	50%	100%	1.79%	20
I20	526	7,704	50%	100%	1.79%	20
I45	539	6,834	50%	100%	1.79%	20
I35	531	6,299	50%	100%	1.79%	20
I20	544	5,767	50%	100%	1.79%	20
US287	506	4,182	50%	100%	1.79%	20
US287	528	3,247	50%	100%	1.79%	20
SH114	527	2,656	50%	100%	1.79%	20
SH130	532	2,269	50%	100%	1.79%	20
US59	535	2,000	50%	100%	1.79%	20
US82	530	919	50%	100%	1.79%	20
US96	142	846	50%	100%	1.79%	20
SH121	546	550	50%	100%	1.79%	20
SH6	Portable WIM	474	50%	100%	1.79%	20
US82	543	372	50%	100%	1.79%	20
FM468	Portable WIM	1,062	50%	100%	1.79%	20
FM3129	541	251	50%	100%	1.79%	20
FM2223	800	142	50%	100%	1.79%	20

Table 6. Comparison of ESALs Calculated from Truck Factor and TxME Load Spectra.

Highway ID	Station ID	AADTT	ESAL @ Truck Factor (Urban-Interstate)=0.39	ESAL @ Truck Factor (Urban-principal)=0.21	ESAL @ Truck Factor (Rural-Interstate)=0.52	ESAL @ Truck Factor (Rural-Principal)=0.38)	ESAL from TxME-Load Spectra
I35	513	10,867	18,795,047	10,120,410	25,060,063	18,313,123	49,650,718
I10	502	8,005	13,845,068	7,455,036	18,460,090	13,490,066	32,748,557
I20	526	7,704	13,324,472	7,174,716	17,765,963	12,982,819	50,529,653
I45	539	6,834	11,819,762	6,364,487	15,759,682	11,516,691	37,354,536
I35	531	6,299	10,894,451	5,866,243	14,525,935	10,615,106	26,717,107
I20	544	5,767	9,974,329	5,370,793	13,299,106	9,718,577	28,243,048
US287	506	4,182	7,232,989	3,894,686	9,643,985	7,047,527	36,010,559
US287	528	3,247	5,615,857	3,023,923	7,487,809	5,471,861	17,228,683
SH114	527	2,656	4,593,691	2,473,526	6,124,922	4,475,904	13,479,223
SH130	532	2,269	3,924,355	2,113,114	5,232,473	3,823,730	7,682,393
US59	535	2,000	3,459,105	1,862,595	4,612,140	3,370,410	5,656,394
US82	530	919	1,589,459	855,862	2,119,278	1,548,703	3,120,864
US96	142	846	1,463,201	787,878	1,950,935	1,425,683	4,337,616
SH121	546	550	951,254	512,214	1,268,339	926,863	1,976,022
SH6	Portable WIM	474	819,808	441,435	1,093,077	798,787	1,830,420
US82	543	372	643,394	346,443	857,858	626,896	1,310,763
FM468	Portable WIM	1,062	1,836,785	989,038	2,449,046	1,789,688	11,437,641
FM3129	541	251	434,118	233,756	578,824	422,986	1,652,034
FM2223	800	142	245,596	132,244	327,462	239,299	516,928

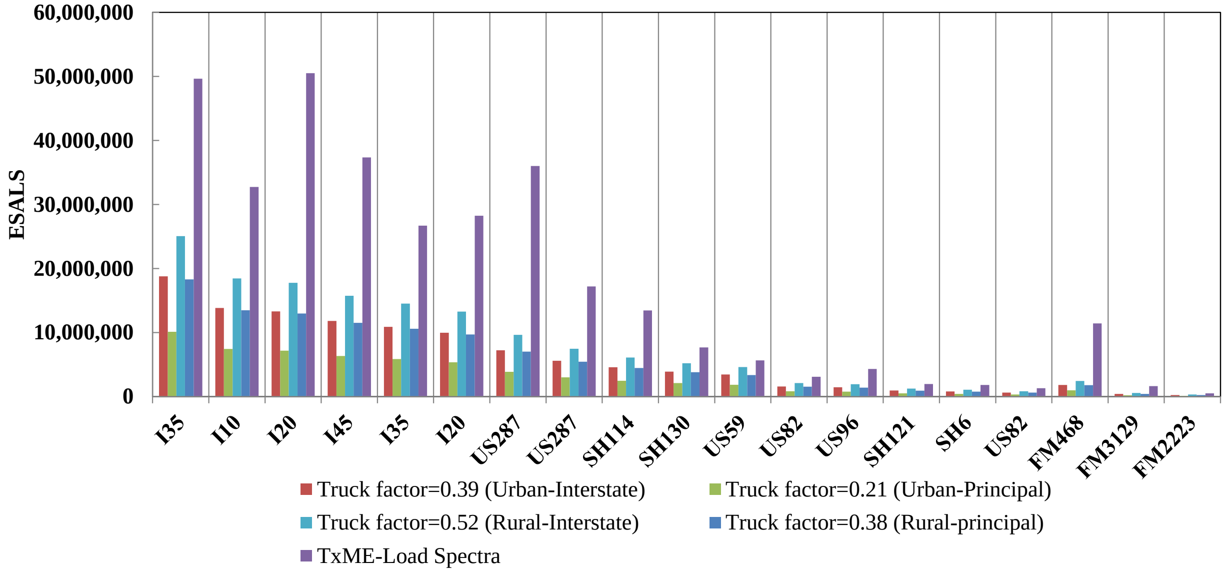

Figure 6. ESALs Calculated from Truck Factors and TxME Load Spectra.

COMPARISON OF TRAFFIC VOLUME AND LOADING FOR ENERGY AND NON-ENERGY AREAS

A better understanding of traffic volume and loading for different classes of highways is important for design of pavement structure for a specific area. In recent years, rapid energy development in Texas has caused significant damage to many FM roads. These roadways performed well under normal traffic loads but failed dramatically under energy sector trucks. The impact of overloading traffic on pavement damage is not only limited to FM roads, but also has significant influence on pavement life of US highways, SH, and IH.

Table 7 summarizes all the 19 WIM data sets including highway name, station ID, AADTT, and ESAL calculated from TxME load spectra. In addition, all the roads are classified in terms of traffic volume. Figure 7 to Figure 9 show the graphical comparisons of AADTT for IH, US or SH, and FM roads, respectively. All these IH have a much larger traffic AADTT (greater than 5000). I-20 and I-10 have the similar AADTT, but I-20 has a much larger ESAL (from TxME load spectra) than I-10 due to the difference of axle load distribution. US or SH have high, medium, and low AADTT, as shown in Figure 8. FM 468 is different from other FM roads because it is in the energy development area. When comparing FM 468 with US or SH, FM 468 has a little lower ESAL than SH 114, but it has a much lower AADTT (i.e., 1062) than SH 114 (i.e., 2656), which means the energy sector trucks on FM 468 has a much larger axle load than SH 114.

Table 7. Summary of All the 19 WIM Data Sets.

Highway Classification	Traffic Volume	Highway ID	Station ID	AADTT	ESAL from TxME Load Spectra (20 years)
Interstate Highways	High (AADTT ≥7000)	I35	513	10,867	49,650,718
		I10	502	8,005	32,748,557
		I20	526	7,704	50,529,653
	Medium (7000> AADTT ≥4000)	I45	539	6,834	37,354,536
		I35	531	6,299	26,717,107
		I20	544	5,767	28,243,048
U.S. or State Highways	High (AADTT ≥3000)	US287	506	4,182	36,010,559
		US287	528	3,247	17,228,683
	Medium (3000> AADTT ≥2000)	SH114	527	2,656	13,479,223
		SH130	532	2,269	7,682,393
		US59	535	2,000	5,656,394
	Low (AADTT<2000)	US82	530	919	3,120,864
		US96	142	846	4,337,616
		SH121	546	550	1,976,022
		SH6	Portable WIM	474	1,830,420
		US82	543	372	1,310,763
Farm to Market (FM) Roads	High (AADTT ≥1000)	FM468	Portable WIM	1,062	11,437,641
	Low (AADTT<1000)	FM3129	541	251	1,652,034
		FM2223	800	142	516,928

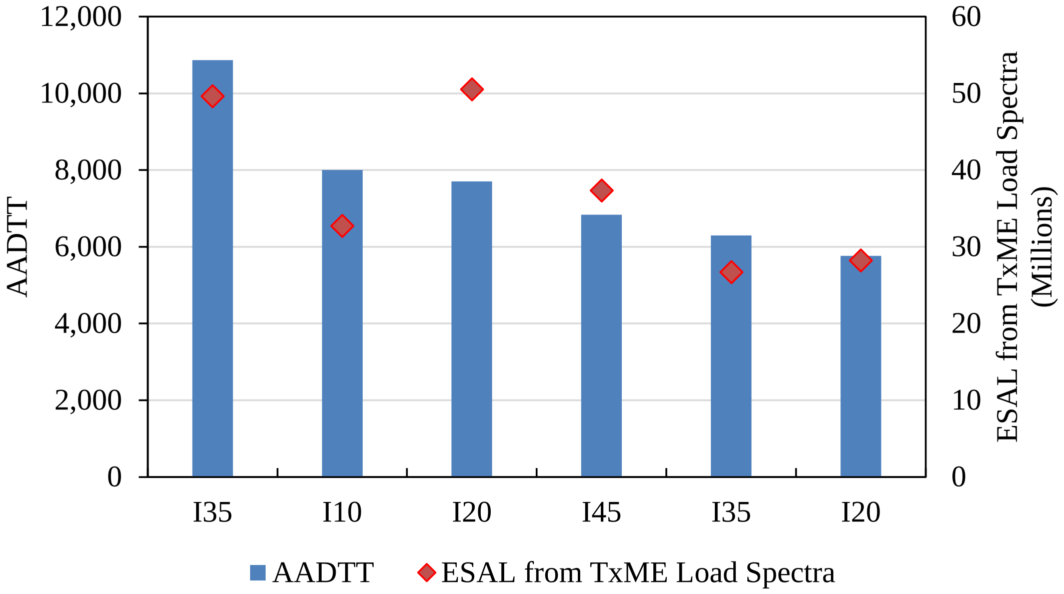

Figure 7. Comparison of AADTT for IH.

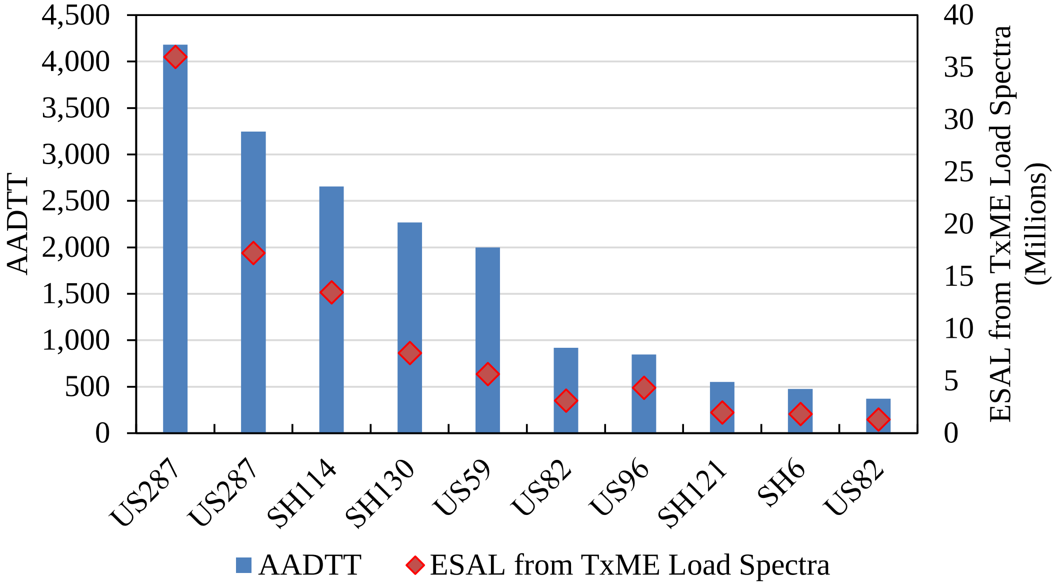

Figure 8. Comparison of AADTT for US or SH.

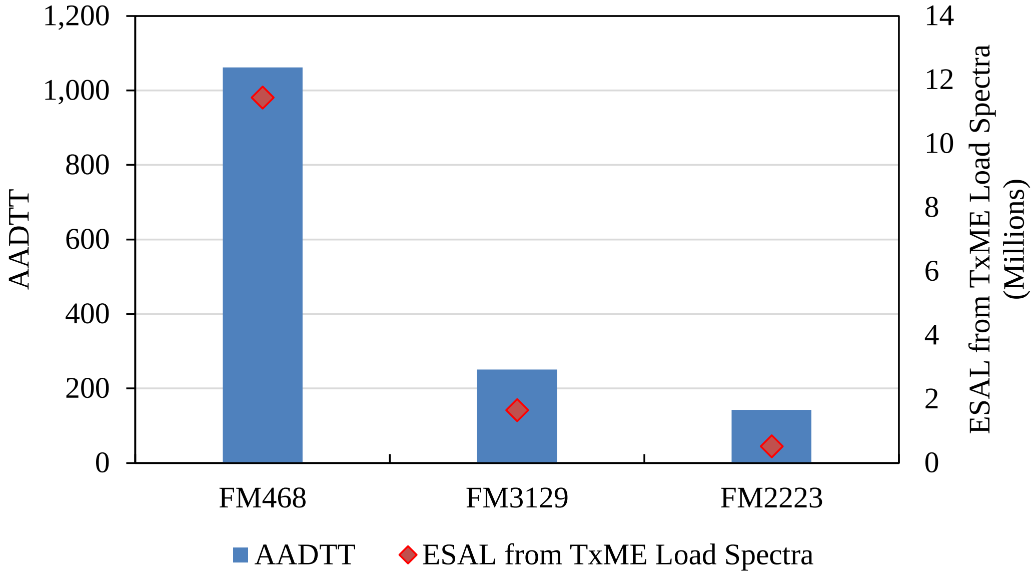

Figure 9. Comparison of AADTT for FM Roads.

COMPARISON OF PREDICTED PERFORMANCES FROM TXME WITH USE OF WIM TRAFFIC DATA INPUTS

In this section, a typical pavement structure is use for TxME simulations (as shown in Figure 10). The pavement structure is the same for all the simulations. The variable is the traffic input. The hot mix asphalt (HMA) layer is dense graded asphalt mixture, and the default values are used for the material properties. A total of 7 WIM data sets representing different traffic volume levels for each road type are selected for TxME load spectra inputs. IH have two cases of high and medium traffic volume. US or SH have three cases of high, medium, and low traffic volume. FM roads has two cases of high and low traffic volume. Table 8 summarizes the predicted pavement performances including total rut depths and asphalt concrete (AC) fatigue cracking area.

Figure 11 and Figure 12 present the graphical comparisons. For the rutting performance, IH has a much larger rut depths exceeding the failure criteria after 20 years, which is expected because IH have a very large AADTT. US 287 with a high AADTT in the group of US or SH has a rut depth close to the failure criteria. SH 130 and SH 6 have the rut depths far below the failure limit. FM 468 has a comparable rut depth with SH 130, which has a medium traffic volume in the group of US or SH. When looking at the fatigue performances, I-35, I-20, US 287, and FM 468 have the cracking areas exceeding the failure limit. Thus, the trucks in the energy development areas can cause significant damage to the FM roads due to very large axle loads.

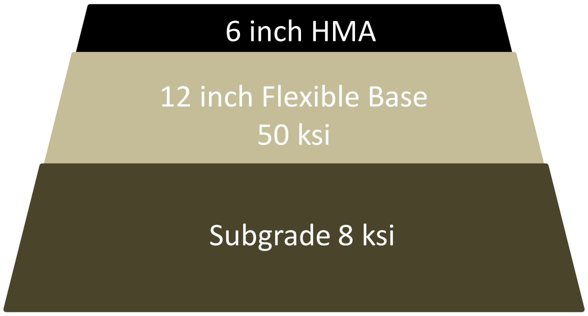

Figure 10. A Typical Pavement Structure.

Table 8. Summary of Predicted Pavement Performances Using Load Spectra Inputs.

Highway Classification	Traffic Volume	Highway ID	Station ID	AADTT	ESAL from TxME Load Spectra (20 years)	Results from TxME Load Spectra	
						Total Rut Depth (in.) (Limit:0.5)	AC Fatigue Cracking Area (%) (Limit:50)
Interstate Highways	High	I35	513	10,867	49,650,718	0.63	99.3
	Medium	I20	544	5,767	28,243,048	0.52	95.4
U.S. or State Highways	High	US287	506	4,182	36,010,559	0.48	94.2
	Medium	SH130	532	2,269	7,682,393	0.37	21.7
	Low	SH6	Portable WIM	474	1,830,420	0.21	0.08
Farm to Market (FM) Roads	High	FM468	Portable WIM	1,062	11,437,641	0.38	55
	Low	FM3129	541	251	1,652,034	0.22	0.22

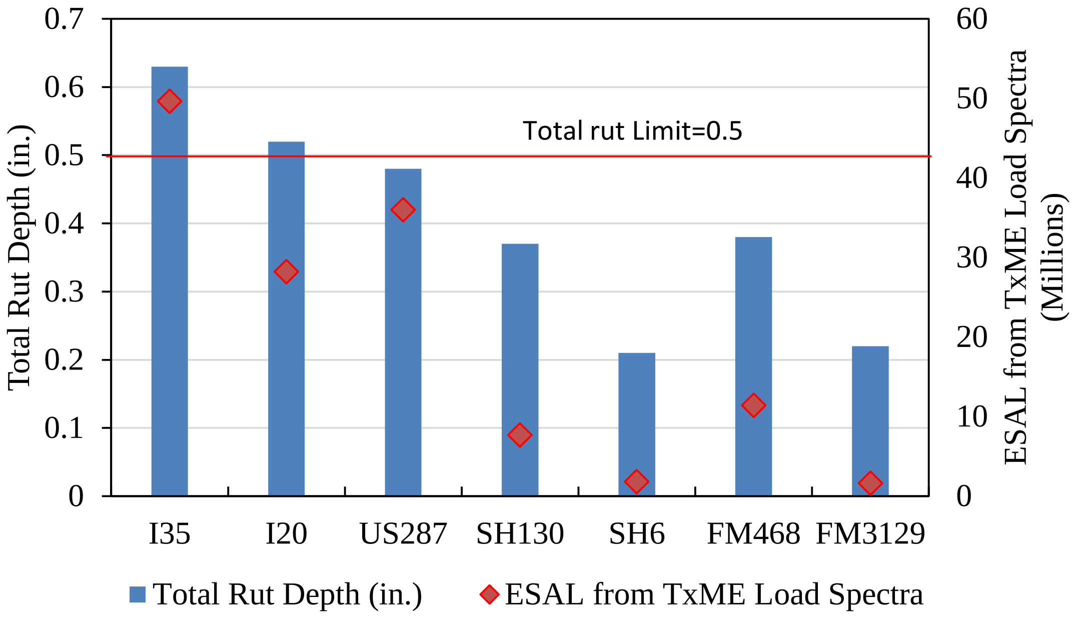

Figure 11. Total Rut Depths from TxME with Load Spectra Inputs.

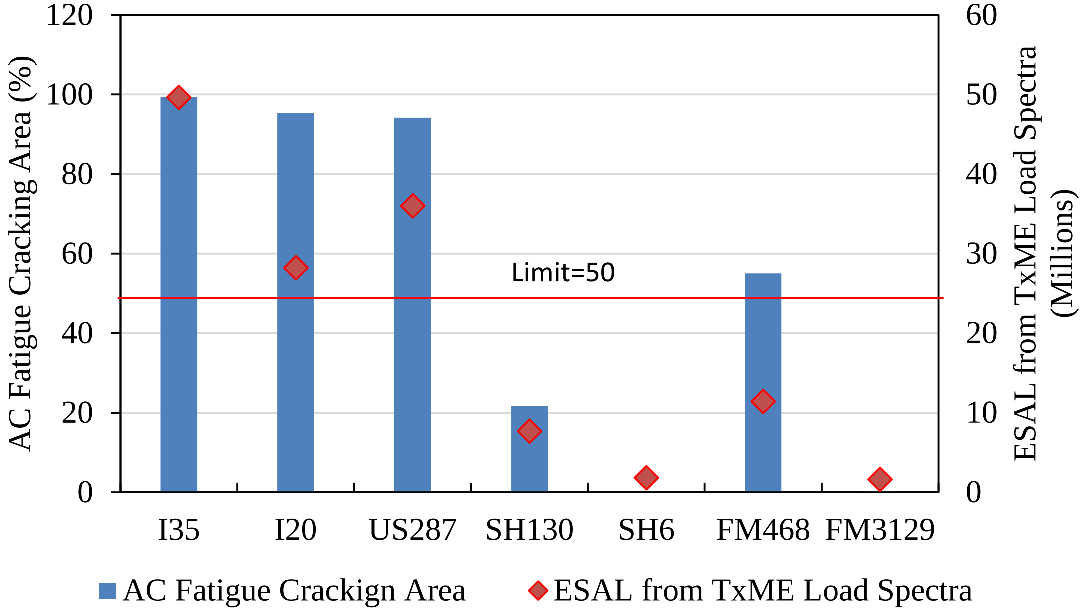

Figure 12. AC Fatigue Cracking Area from TxME with Load Spectra Inputs.

CHAPTER 3. FLEXIBLE PAVEMENT REHABILITATION OPTIONS

INTRODUCTION

Pavement repair and rehabilitation are important activities for all highway agencies. Many highway facilities, particularly those used by the energy sector, are experiencing early deterioration due to high traffic volumes and climate conditions, as well as service periods that extend, in some cases, well beyond the facilities’ design life. Coupled with this type of deterioration, reduced revenues and purchasing power make the decision process that much more critical. As the energy sector begins to recover, more and more miles of pavements are expected to require significant maintenance, rehabilitation, or repair (MRR). Factors such as these are cause for close examination of strategies for MRR of pavements to optimize the expenditure of limited repair funds. Therefore, better decision making, guidelines, and tools to evaluate and select appropriate MRR strategies are needed so that long-lasting, cost-effective rehabilitation solutions can be identified and implemented.

GUIDANCE FOR SELECTING OPTIMAL REHABILITATION OPTIONS

The purpose of selecting an appropriate rehabilitation alternative for energy sector roads is to provide sufficient pavement structural capacity and performance to support the heavy loads over its design life. This guidance will help engineers determine appropriate rehabilitation alternatives for flexible pavements with the consideration of existing pavement conditions, traffic loads, and material characteristics. Since most roads used by the energy sector are FM roads with surface treatments or a very thin asphalt layer, the most often-used rehabilitation strategy is FDR and then two-course surface treatment or an added asphalt layer. Thus, this guidance focuses on the use of FDR for roads in the energy sector.

As shown in Figure 13, the process of selecting an MRR alternative primarily includes six steps to reach a final decision for a sufficient pavement structural design and FDR mix design. Detailed information and procedure on each step are described in the following sections.

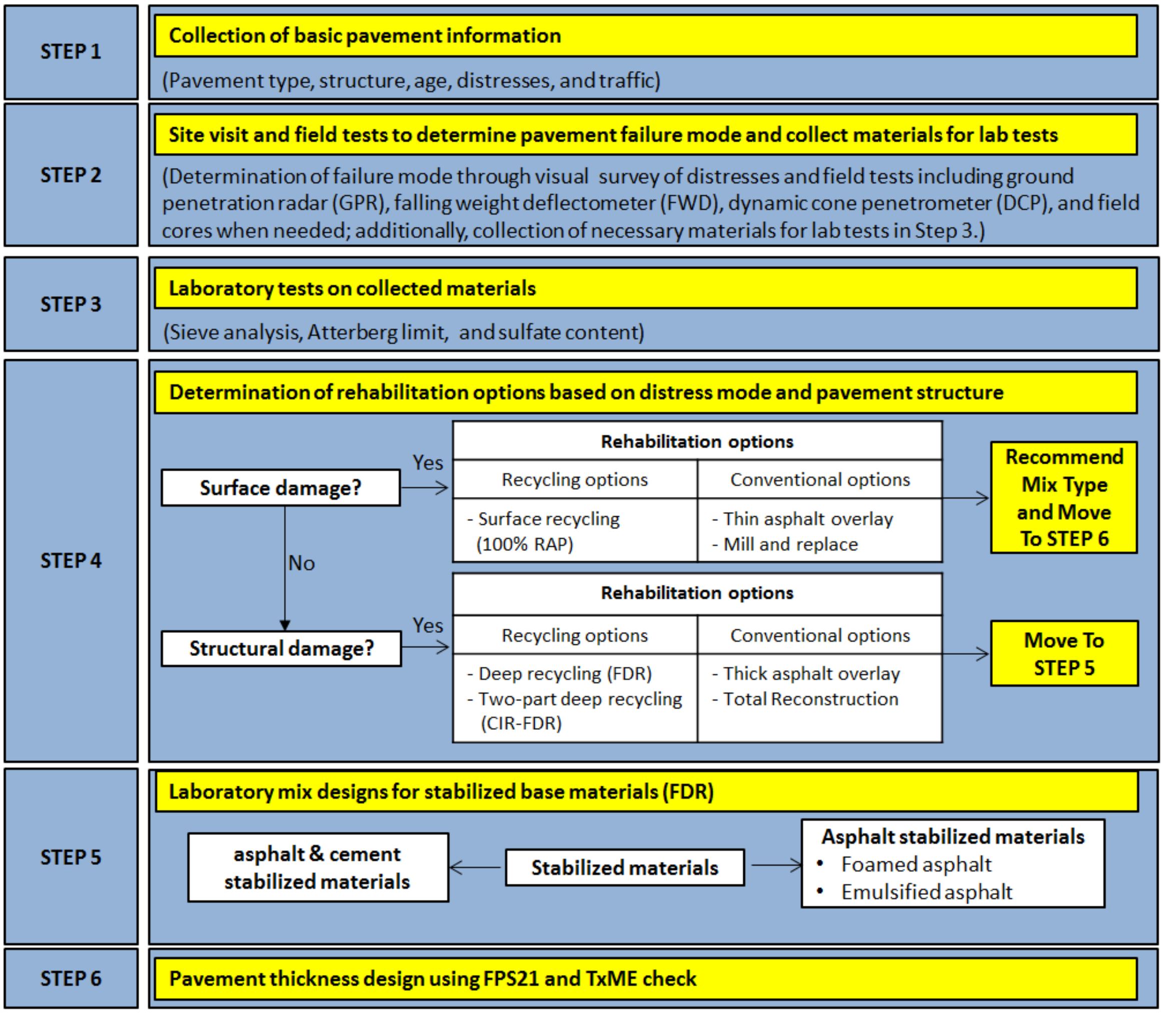
STEP 1
Collection of basic pavement information
(Pavement type, structure, age, distresses, and traffic)
STEP 2
Site visit and field tests to determine pavement failure mode and collect materials for lab tests
(Determination of failure mode through visual survey of distresses and field tests including ground penetration radar (GPR), falling weight deflectometer (FWD), dynamic cone penetrometer (DCP), and field cores when needed; additionally, collection of necessary materials for lab tests in Step 3.)
STEP 3
Laboratory tests on collected materials
(Sieve analysis, Atterberg limit, and sulfate content)
STEP 4
Determination of rehabilitation options based on distress mode and pavement structure
Surface damage?
Yes
Rehabilitation options
Recycling options
Conventional options
- Surface recycling (100% RAP)
- Thin asphalt overlay
- Mill and replace
Recommend Mix Type and Move To STEP 6
No
Structural damage?
Yes
Rehabilitation options
Recycling options
Conventional options
- Deep recycling (FDR)
- Two-part deep recycling (CIR-FDR)
- Thick asphalt overlay
- Total Reconstruction
Move To STEP 5
STEP 5
Laboratory mix designs for stabilized base materials (FDR)
asphalt & cement stabilized materials
Stabilized materials
Asphalt stabilized materials
• Foamed asphalt
• Emulsified asphalt
STEP 6
Pavement thickness design using FPS21 and TxME check

Figure 13. Pavement Rehabilitation Alternative Selection and Design Process for Energy Sector Roads.

Step 1: Collection of Basic Pavement Information

The existing pavement conditions, structure, and layer materials should be evaluated first. More specifically, to evaluate the existing pavements, the following information is typically needed (at a minimum): soil survey data, traffic data, climate data, pavement condition reports, maintenance records, and existing typical section (control-section-job number). Then, the information gathered should be reviewed; the brief output of the review will include (at a minimum) climate, current traffic, current pavement structure, material types, road condition, and potential problem areas.

Step 2: Site Visit and Field Tests to Determine Pavement Failure Mode and Collect Materials for Laboratory Tests

The main purpose of this step is to define the failure mode and collect materials for further laboratory tests. Generally, a site visit is needed to supplement data from Step 1. To this end, a visual inspection and several field tests are typically required in this step. Visual inspection provides observations such as drainage, geological changes, and valuable clues to recognize the cause of distress of the pavements. The failure mode and type of distress can be classified into the categories shown in Table 9.

Table 9. Failure Mode and Type of Distress.

Failure Mode	Distress Type	Description
Surface damage	Environmental damage Traffic damage	Raveling (stone loss) Thermal cracking Block cracking Rutting Stripping, bleeding, or polishing
Structural damage	Permanent deformation Cracking	Rutting in wheel paths Lateral shoving Longitudinal in wheel paths Alligator Other (transverse, etc.) Potholes, patches, etc.
Functional damage	Drainage Riding quality	Erosion, washouts, etc. Edge break Undulations, corrugations, etc.

Source: (*3*)

In most cases, a long roadway is not uniform over long distance in terms of subgrade, pavement structure, and associated maintenance/rehabilitation. Uniform sections can be identified visually by changes in distress pattern. However, some field tests should be considered to determine uniform sections by extracting core samples or using some forensic study tools, such as ground penetration radar (GPR), falling weight deflectometer (FWD), and dynamic cone penetrometer (DCP). The use of GPR is strongly recommended to determine layer thicknesses and identify changes in pavement structure and potential moisture issues in the pavement. Figure 14 shows an example screenshot of a GPR analysis and identifies the pavement structure. Both FWD and DCP can be used to identify the boundaries between the different uniform sections by assessing the in-situ properties such as the backcalculated modulus and bearing strength of the material in the different layers of the pavement, as shown in Figure 15. Core samples can be used to verify the thickness of the asphalt layers and to perform several laboratory tests for determining volumetric and material properties. Additionally, materials from each pavement layer and subgrade may be needed for further laboratory characterization, FDR mix design, and structural design. Lastly, new base materials may also be necessary for FDR mix design.

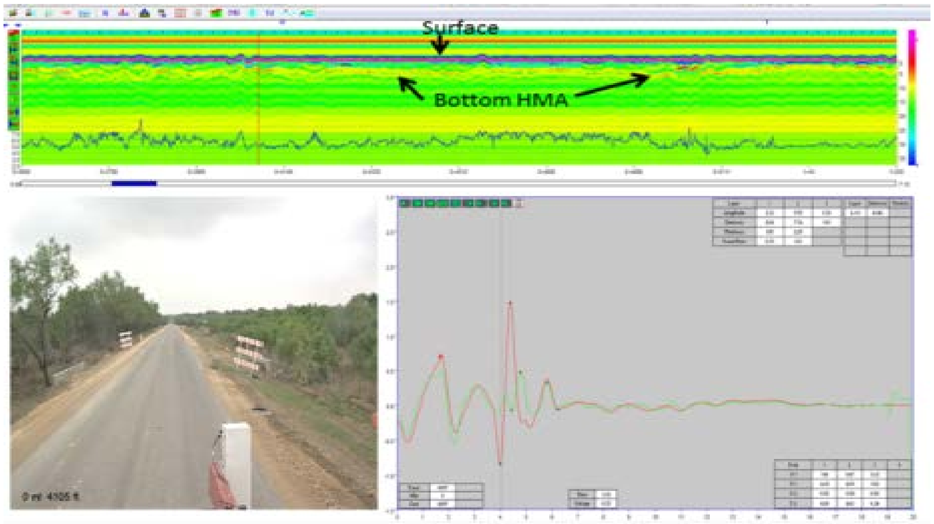

Figure 14. GPR Image Obtained on FM 99.

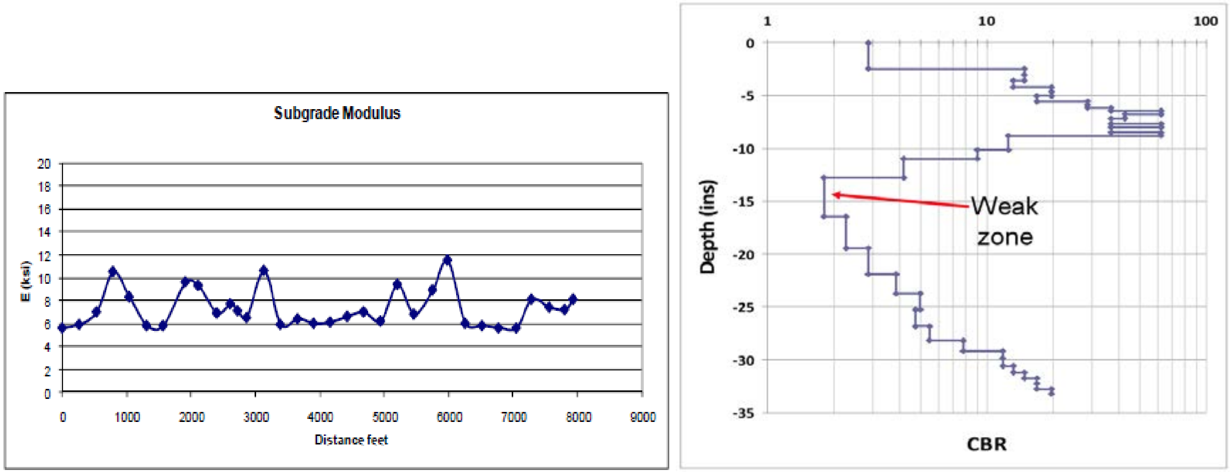

(a) FWD result (b) DCP result

Figure 15. Example of FWD and DCP Survey Results.

Step 3: Laboratory Tests on Collected Materials

Representative materials from existing layers and subgrade and from new materials (if necessary) should be properly collected and brought back for laboratory tests. As an example, Figure 16 shows new base, old base, and recycled asphalt pavement (RAP) (existing asphalt layer) collected from FM 99 for the laboratory evaluation. The most often-performed laboratory tests include sieve analysis, Atterberg limits, and sulfate content tests. The test results are used for the stabilizer selection process, as shown in Figure 15 (*4*). The detailed information from Step 2 and Step 3 should be summarized to make the final rehabilitation strategy in Step 4.

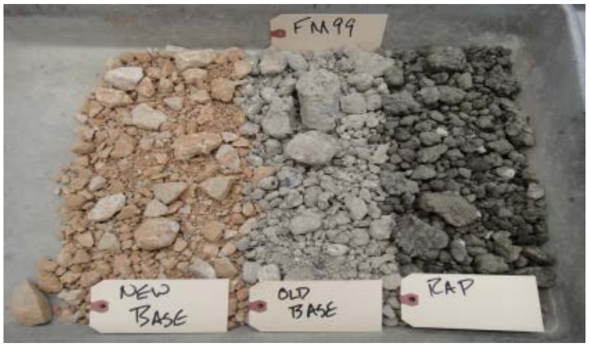
FM99
NEW BASE
OLD BASE
RAP

Figure 16. Materials Collected from FM 99.

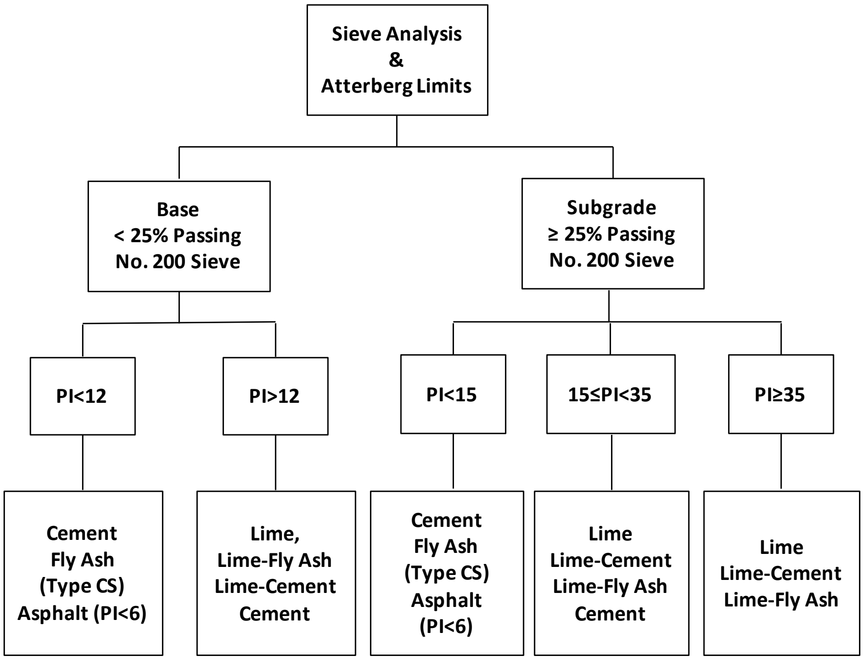
Sieve Analysis & Atterberg Limits
Base < 25% Passing No. 200 Sieve
Subgrade ≥ 25% Passing No. 200 Sieve
PI<12
PI>12
PI<15
15≤PI<35
PI≥35
Cement Fly Ash (Type CS) Asphalt (PI<6)
Lime, Lime-Fly Ash Lime-Cement Cement
Cement Fly Ash (Type CS) Asphalt (PI<6)
Lime Lime-Cement Lime-Fly Ash Cement
Lime Lime-Cement Lime-Fly Ash

Figure 17. Stabilizer Selection Guidelines.

Step 4: Determination of Rehabilitation of Options Based on Distress Mode and Pavement Structure

There are numerous options for maintaining and rehabilitating pavements. However, each option should be project specific. An appropriate rehabilitation alternative is often determined by the following three major factors:

- Existing pavement conditions and the pavement distress(es) that need(s) to be addressed.
- The quality of material in the recycling horizon.
- The outcome required (i.e., service life expectations).

Rehabilitation options are divided into two major categories based on the nature of the problem:

- Surface rehabilitation.
- Structural rehabilitation.

As illustrated in Figure 18, if the section is simply a candidate in the surface rehabilitation category (Figure 18a), three options are available:

- Surface recycling.
- Asphalt overlay.
- Mill and replace.

When the type of asphalt mix is recommended or determined, the pavement design is performed using the FPS21 and TxME for asphalt overlays.

For the second category, the structural rehabilitation category (Figure 18b and Figure 18c), three options are available:

- Deep recycling (e.g., FDR or two-part recycling).
- Thick asphalt overlay.
- Total reconstruction.

If the deep recycling option is determined, it is necessary to perform laboratory mix designs for stabilized materials as described in the next step. For thick asphalt overlay and total reconstruction options, again FPS21, TxACOL (for overlays), and TxME (for reconstruction) can used to develop pavement designs.

Step 5: Laboratory Mix Designs for Stabilized Materials for FDR Option

Figure 19 shows simplified steps for the mix design process. With the selected recycling option such as FDR, a series of laboratory tests for the combinations of materials should be performed to select the optimal stabilizer and its content. Typically, three primary stabilizers are used for FDR:

- Asphalt (foamed and emulsion).
- Cement.
- A combination of stabilizers.

But for energy sector roads with the requirement of same-day traffic opening, the stabilizers are narrowed down to two choices:

- Asphalt (foamed and emulsion).
- An asphalt-cement/lime combination.

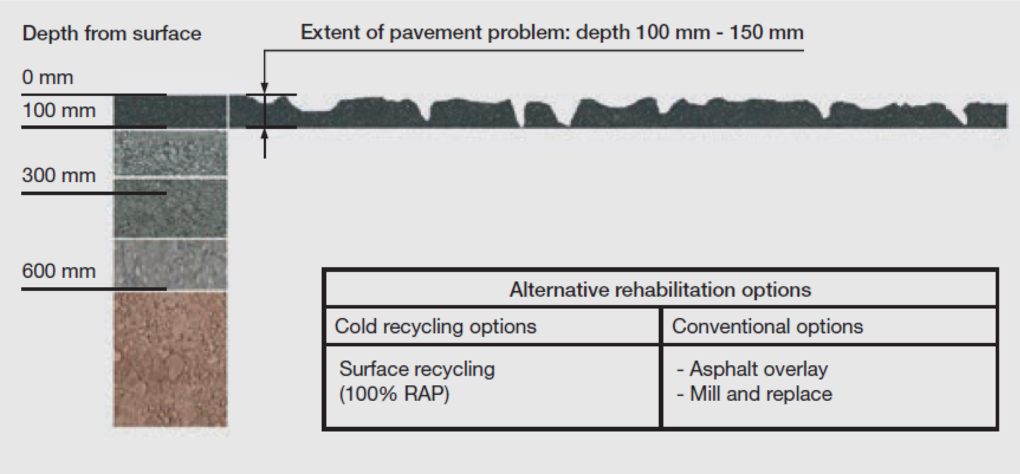
Depth from surface
Extent of pavement problem: depth 100 mm - 150 mm
0 mm
100 mm
300 mm
600 mm

Alternative rehabilitation options	
Cold recycling options	Conventional options
Surface recycling (100% RAP)	- Asphalt overlay - Mill and replace

(a) Rehabilitation options for upper pavement/surfacing distress

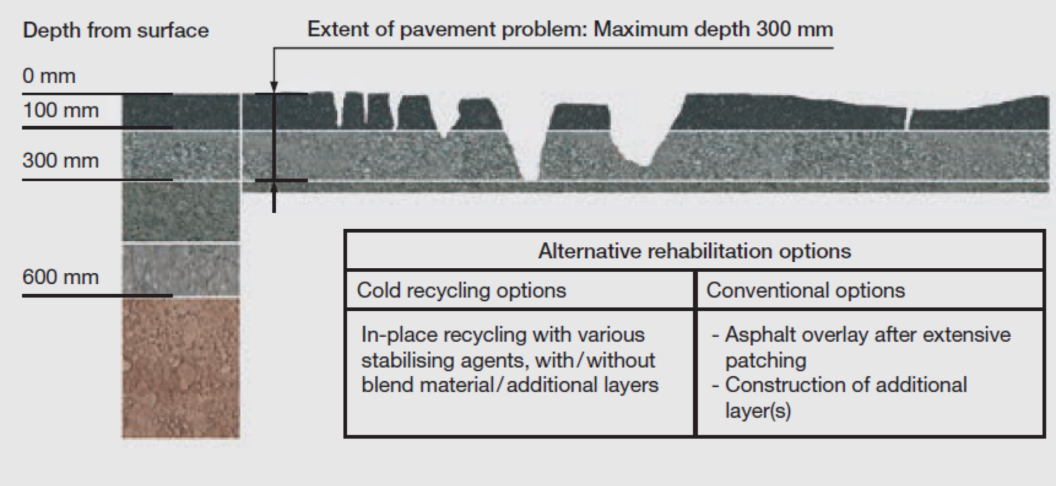
Depth from surface
Extent of pavement problem: Maximum depth 300 mm
0 mm
100 mm
300 mm
600 mm

Alternative rehabilitation options	
Cold recycling options	Conventional options
In-place recycling with various stabilising agents, with/without blend material/additional layers	- Asphalt overlay after extensive patching - Construction of additional layer(s)

(b) Rehabilitation options for structural distress in the upper pavement layers

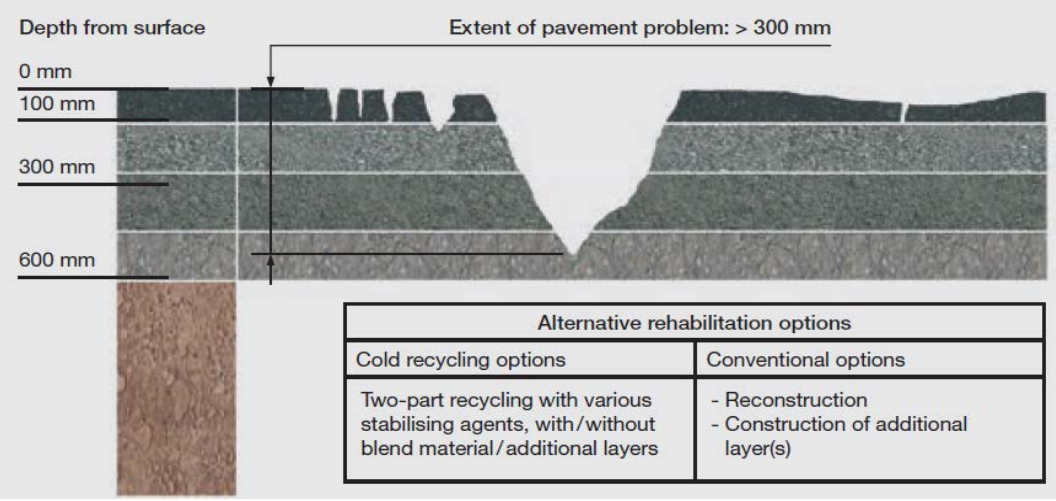
Depth from surface
Extent of pavement problem: > 300 mm
0 mm
100 mm
300 mm
600 mm

Alternative rehabilitation options	
Cold recycling options	Conventional options
Two-part recycling with various stabilising agents, with/without blend material/additional layers	- Reconstruction - Construction of additional layer(s)

(c) Rehabilitation options for deep-seated structural distress

Source: (*3*)

Figure 18. Three Different Cold Recycling Application Options.

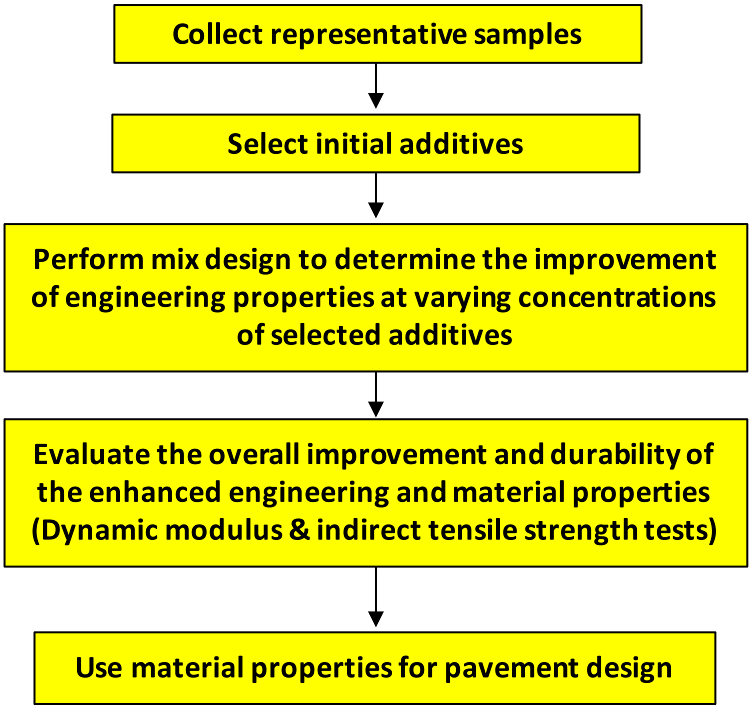
Collect representative samples
Select initial additives
Perform mix design to determine the improvement of engineering properties at varying concentrations of selected additives
Evaluate the overall improvement and durability of the enhanced engineering and material properties (Dynamic modulus & indirect tensile strength tests)
Use material properties for pavement design

Figure 19. Mix Design Process for Stabilized Materials.

It is very important to select the appropriate stabilizer type and its optimal amount for an effective resulting mix. Preliminary treatment options prior to the mix design can be selected based on the availability and costs of materials, agency experience, and material properties of existing pavement materials. Recently, the Texas A&M Transportation Institute (TTI), working with TxDOT, developed an FDR laboratory mix design procedure using small sizes of sample. The mix design produces a moisture-density curve and target stabilizer content based on the indirect tensile (IDT) strength test and the unconfined compressive strength. The IDT samples can be compacted using either a Superpave gyratory compactor or Texas gyratory compactor into 4 in. in diameter and 2 in. in height. The design procedure (TxDOT Specification 3279) has IDT strength requirements on both wet-conditioned and dry samples: a minimum dry strength of 45 psi and a minimum wet strength of 30 psi. Furthermore, supplemental tests can be performed to determine the modulus of stabilized materials for a further analysis using M-E pavement design methods. The dynamic modulus test can be used to determine the modulus of stabilized materials, as shown in Figure 20.

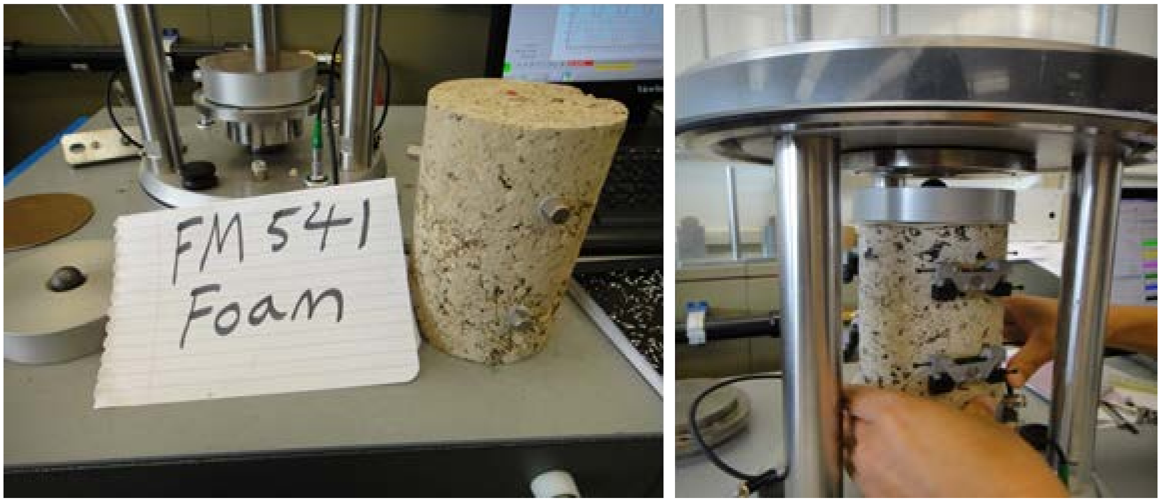

Figure 20. Dynamic Modulus Testing of Asphalt Stabilized Material.

Step 6: Pavement Thickness Design Using FPS21 and TxME Check

FDR projects must also be designed using FPS21. This could be to calculate the thickness of the flexible base to be placed over the stabilized subbase layer for heavily trafficked sections, or the thickness of the asphalt layer required to carry the design traffic loads over the stabilized base layer. For the reconstruction option, TxME can be used to check the pavement performance in terms of rutting and cracking; for the asphalt overlay option, TxACOL is available to predict both rutting and reflective cracking development in the design period of pavement life.

LABORATORY TESTS AND RESULTS FOR STABILIZED MATERIALS FOR FDR OPTION

Indirect Tension Test

To guide designers in their future FDR projects, several actual field test sections evaluated are used here as case studies for demonstration purposes. These case studies will help engineers perform a laboratory mixture design when an FDR option is selected. The three cases studies are FM 99 in Corpus Christi District, FM 906 in Paris District, and FM 541 in San Antonio. The laboratory tests include plasticity index (PI) test, moisture-density curve test, and IDT tests with different dosages of stabilizers.

FM 99 in Corpus Christi District, Texas

FM 99 is an extremely heavily trafficked energy development roadway in the Corpus Christi District of Texas; the limits of this project are from US 281A to the McMullen County line. The original plans stated that the roadway is 24 ft wide and has 1 in. of asphaltic materials as a surface layer and 6 in. of flexible base material. A test pit was dug in a representative area, and samples of the materials were obtained for stabilization design in the TTI lab.

The obtained materials were tested in the laboratory, and the measured PI was 9. For low PI material, cement, fly ash, and asphalt are recommended, as illustrated in Figure 17. Two designs were evaluated using an aggregate blend of 55 percent new base, 27 percent RAP, and 18 percent old base. Foamed asphalt and cement were selected as stabilizers. Two types of mix design with use of both foamed asphalt and cement (i.e., 2.4 percent foamed asphalt +1.5 percent cement, and 2.75 percent foamed asphalt + 1.5 percent cement) were evaluated.

The mix design was performed following TxDOT Special Specification 3279, which has the requirements about IDT strengths for both wet-conditioned and dry samples: a minimum dry IDT strength of 45 psi and a minimum wet IDT strength of 30 psi. A total of six samples with 4 in. in diameter and 2 in. in height are compacted for each mix design. These samples are then cured in the oven at 40°C for three days. After curing, three of the samples are submerged in water for 24 hours. After conditioning, the IDT test was performed on both the dry and wet samples. Figure 21 presents the compacted samples and the IDT test setup. Table 10 summarizes the test results including IDT test and unconfined compression strength (UCS). Two mix designs have the comparable IDT strengths. The higher dosage of asphalt foamed did not have a significant effect on the IDT strength.

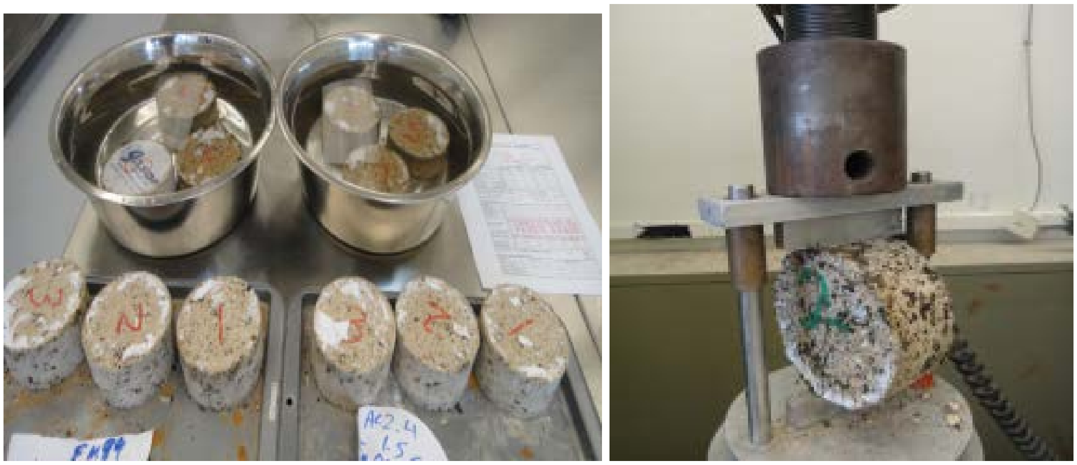

Figure 21. Samples Taken during the Moisture Conditioning and the IDT Test.

Table 10. IDT Results from Foamed Asphalt Samples from FM 99.

	TxDOT Test Method	**Spec. 3279 Requirement**	**1.5% Cement 2.4% Foam**	**1.5 Cement 2.75 Foam**
Dry IDT	Tex 226-F	45 psi	75 psi	77 psi
Wet IDT	Tex 226-F	30 psi	41 psi	39 psi
Min. UCS*	Tex 117-E	Report	171 psi	-
Dry density	-	-	121.5 lb/ft^3	122.4 lb/ft^3
Opt. % Mois.	-	-	7.3%	7.3%

FM 906 in Paris District, Texas

FM 906 is located in the Paris District of Texas; the limits of this project are from FM 196 to US 271. The net length of the roadway is 4.5 miles long. Materials were sampled from the test pit for further laboratory tests and stabilization design (as shown in Figure 22).

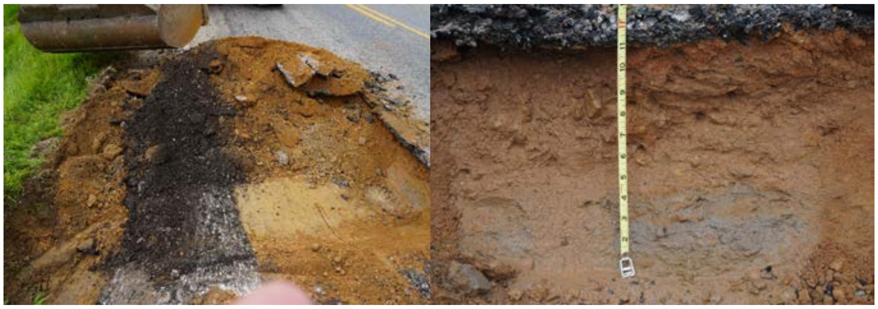

Figure 22. Test Pit on FM 906.

Figure 23 shows the materials used for the mix design including existing base, new base, and RAP. Table 11 presents the aggregate gradation for existing base and new base. The measured PIs are 7 and 4 for existing base and new base, respectively. Two combined gradations were evaluated:

- Combination 1: 75 percent existing base and 25 percent RAP.
- Combination 2: 42 percent existing base, 33 percent new base, and 25 percent RAP.

Table 12 presents the optimum moisture content (OMC) and dry density for the two combinations.

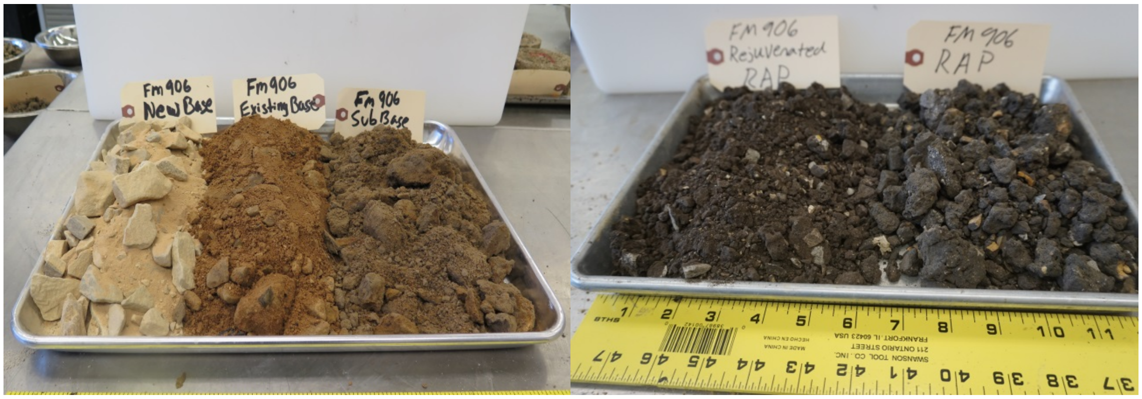

Figure 23. Pictures of Collected Soil Materials from FM 906.

Table 11. Aggregate Gradations for Existing Base and New Base.

Sieve Size	% Passing	% Passing
	Existing Base (EB)	New Base (NB)
1 ¾"	100	100
1 ¼"	99	95.4
¾"	90.5	78.5
3/8"	66	57.7
#4	55.3	44.1
#40	29	28.2

Table 12. OMC and Dry Density for Two Aggregate Combinations.

Combined Materials	OMC (%)	Dry Density (pcf)
Combination 1	5.4	133
Combination 2	6	131.1

After FDR was chosen for the test sections on FM 906, eight different designs, as shown in Table 13, were performed using both foamed asphalt and emulsion asphalt with and without cement. All designs consist of 25 percent RAP materials. The IDT tests were performed on these eight designs. Table 14 summarizes the test results. Based on the required IDT strengths in dry and wet conditions, Designs 2 and 5 are the best choices. Adding cement decreased the IDT strength for the case with addition of emulsion asphalt.

Table 13. Evaluated Stabilization Designs.

Design No.	Material %	% RAP	Foamed % (PG64-22)	Emulsion % (CSS-1H)	Additive
1	75% EB	25%	2.4	-	0%
2	75% EB	25%	2.4	-	1% Cement
3	42% EB 33% NB	25%	2.4	-	0%
4	42% EB 33% NB	25%	2.4	-	1% Cement
5	75% EB	25%	-	4	0%
6	75% EB	25%	-	4	1% Cement
7	42% EB 33% NB	25%	-	4	0%
8	42% EB 33% NB	25%	-	4	1% Cement

Table 14. IDT Test Results on Stabilization Designs.

Design No.	Material %	% RAP	Foamed % (PG64-22)	Emulsion % (CSS-1H)	Additive	Dry IDT (psi)	Wet IDT (psi)
1	75% EB	25%	2.4	-	0%	78.9	1.7
2	**75% EB**	**25%**	**2.4**	**-**	**1% Cement**	**73.3**	**33.5**
3	42% EB 33% NB	25%	2.4	-	0%	71.3	2.9
4	42% EB 33% NB	25%	2.4	-	1% Cement	49.3	37.9
5	**75% EB**	**25%**	**-**	**4**	**0%**	**76.4**	**50.2**
6	75% EB	25%	-	4	1% Cement	53.2	41.1
7	42% EB 33% NB	25%	-	4	0%	67.5	42.7
8	42% EB 33% NB	25%	-	4	1% Cement	56.0	49.5

FM 541 in San Antonio District, Texas

The FM 541 project is located in the San Antonio District and runs from I-37 to the Atascosa-Wilson County line, as shown in Figure 24. The existing pavement structure is 27 ft wide, and has 1.5 in. of seal coat as a surface layer and 9 in. of flexible base material. Figure 25 shows the existing pavement had rutting and patching on the surface prior to construction. Representative samples from several locations were obtained and returned to TTI for material evaluation and mix design.

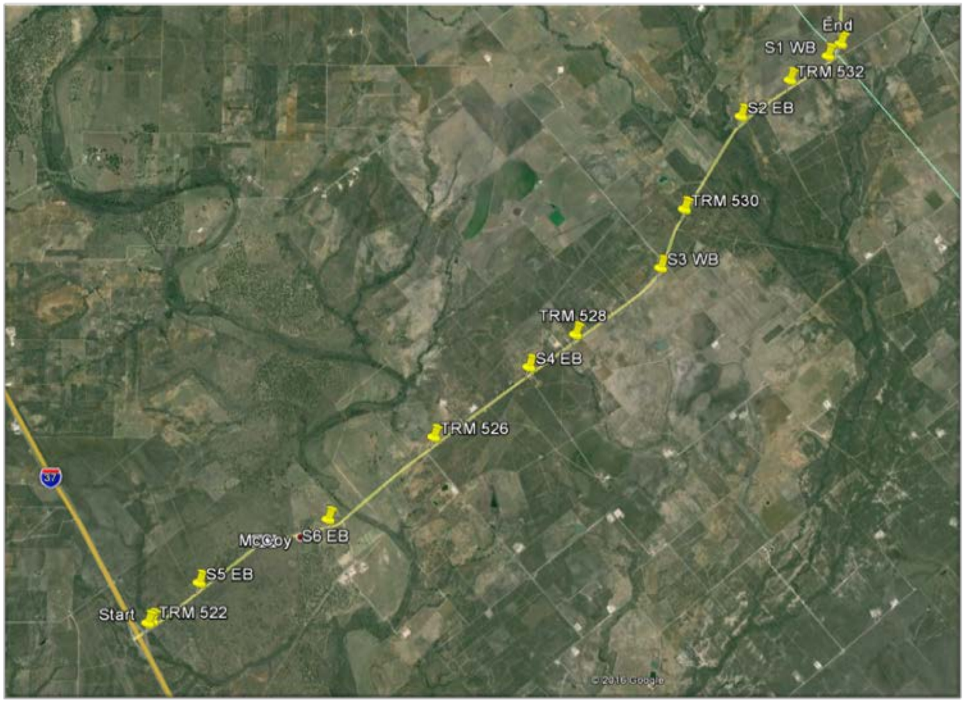

Figure 24. Location of the FM 541 Project.

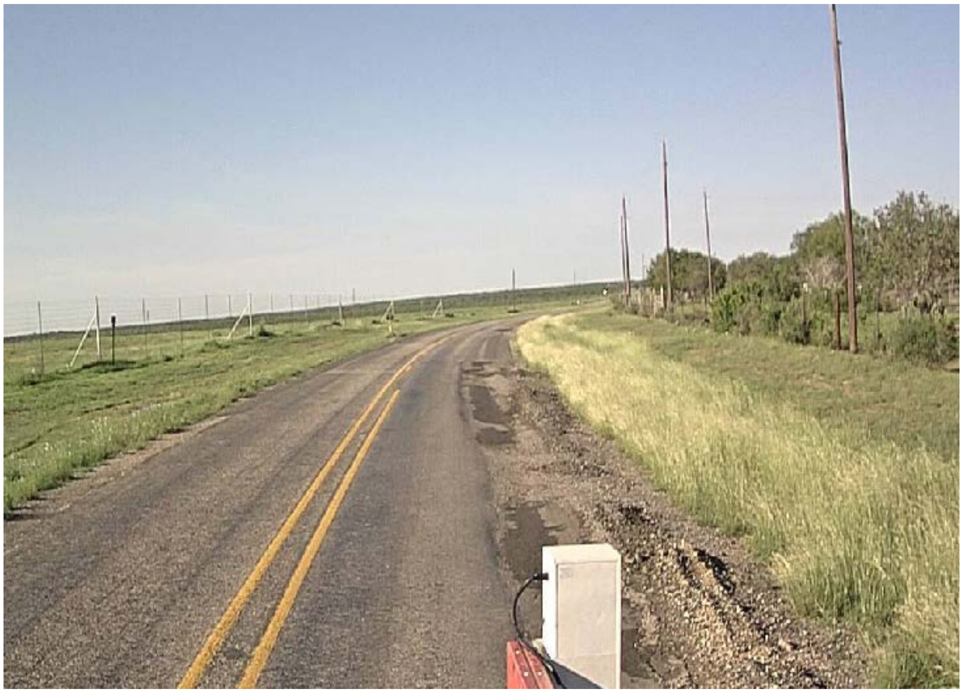

Figure 25. Pavement Condition prior to Construction.

Two mix designs were evaluated for an aggregate blend of 60 percent salvage material (RAP and old base) and 40 percent new base. Both cement and foamed asphalt were used for stabilizers. Table 15 presents the two mix designs with cement and foamed asphalt and IDT test results. The mix design with 1.0 percent cement and 2.4 percent foam asphalt meets the IDT requirements.

Table 15. IDT Results from Foamed Asphalt Samples from FM 541.

	TxDOT Test Method	**Spec. 3279 Requirement**	**1.0% Cement 2.4% Foam**	**1.0 Cement 2.75 Foam**
Dry IDT	Tex 226-F	45 psi	58 psi	68 psi
Wet IDT	Tex 226-F	30 psi	34 psi	28 psi
Min. UCS	Tex 117-E	Report	127 psi	97 psi
Dry Density	-	-	115.1 lb/ft^3	114.7 lb/ft^3
Opt. % Mois.	-	-	9.5%	9.1%

Comparisons of IDT Test Results

Three additives including foamed asphalt, emulsion asphalt, and cement are used for soil stabilizers. To have a better understanding of effects of these stabilizers on the mechanical property (i.e., IDT strength herein) of base materials, all the IDT test results obtained in the laboratory for the three FM roads are compared in Figure 26. All the dry IDT results pass the criteria. The major concern is about wet IDT strength. When the foamed asphalt was used for stabilizer, at least 1 percent cement also needs to be added in the mixture to improve the wet strength. For the cases of foamed asphalt without addition of cement (i.e., 2.4F+0C_B1 and

2.4F+0C_B2), the IDT strengths are very low. When the emulsion asphalt is used for stabilizer, there is no need to add cement to improve the wet strength.

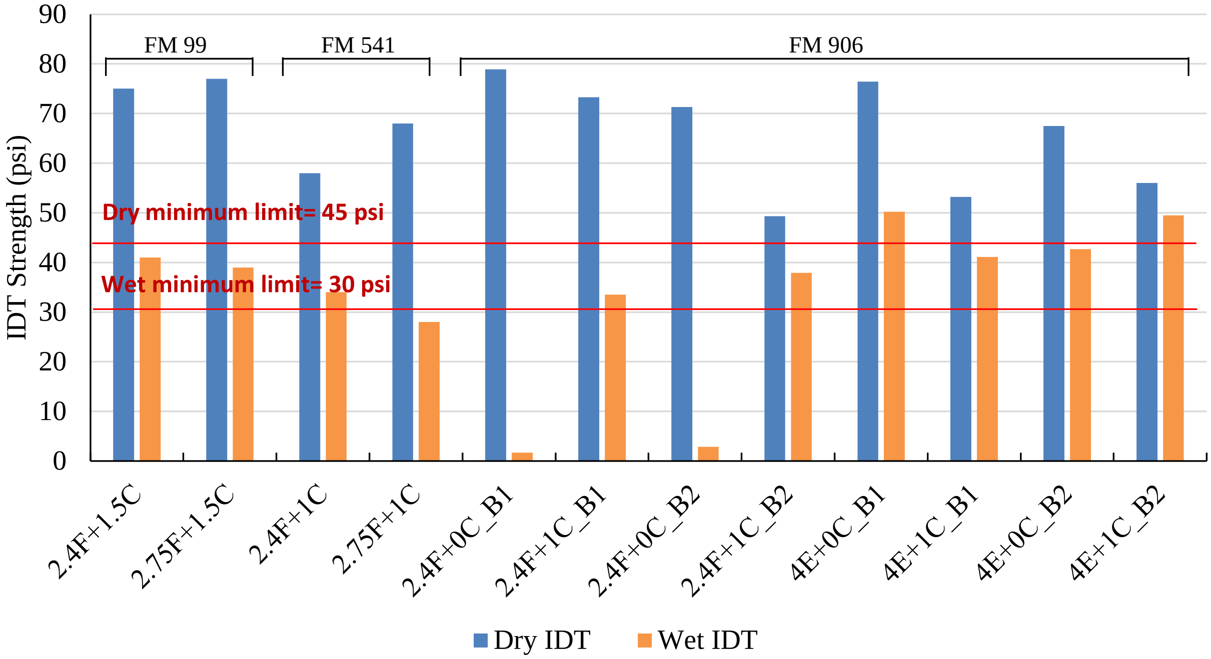

Figure 26. Comparison of All the IDT Test Results.

Legend: 2.4F+1.5C= 2.4% foamed asphalt+1.5% cement, 2.4F+0C_B1=2.4% foamed asphalt+0% cement for aggregate blend #1 in the case of FM 906, 4F+0C_B1=4% emulsion asphalt+0% cement for aggregate blend #1 in the case of FM 906

Characterization of Modulus of Stabilized Materials (FDR) Inputted in TxME

Modulus of a material is an important input in M-E pavement design software. One of the critical TxME inputs is the modulus of stabilized materials FDR mix. To use more accurate modulus values for stabilized base layers, researchers collected base materials from various field test sections and compacted them in the lab for dynamic modulus testing, as shown in Figure 27. At least two different stabilizers were used to treat each base material. Specimens were conditioned at 40°C for two different curing times of three days and seven days prior to testing, and then the dynamic modulus test was performed at 4°C, 20°C, and 40°C. Figure 28 to Figure 30 present the dynamic modulus obtained in the laboratory for three sections including FM 99, FM 541, and I-10. The modulus of stabilized materials does not keep the constant at different temperatures. The modulus decreases with an increase of the testing temperature. The modulus ranges from about 60 ksi to 700 ksi for different stabilized materials.

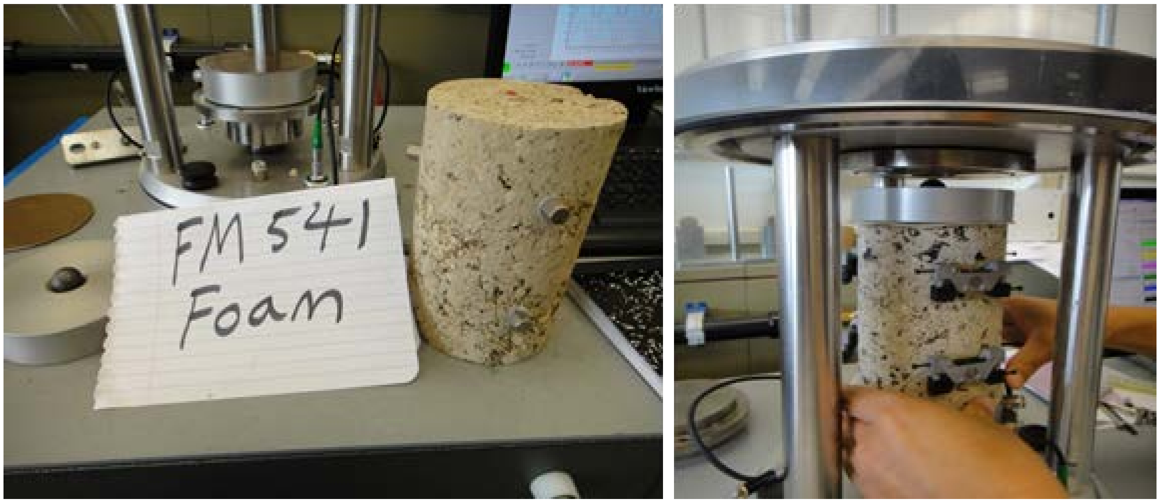

Figure 27. Dynamic Modulus Testing of Stabilized Materials (FDR).

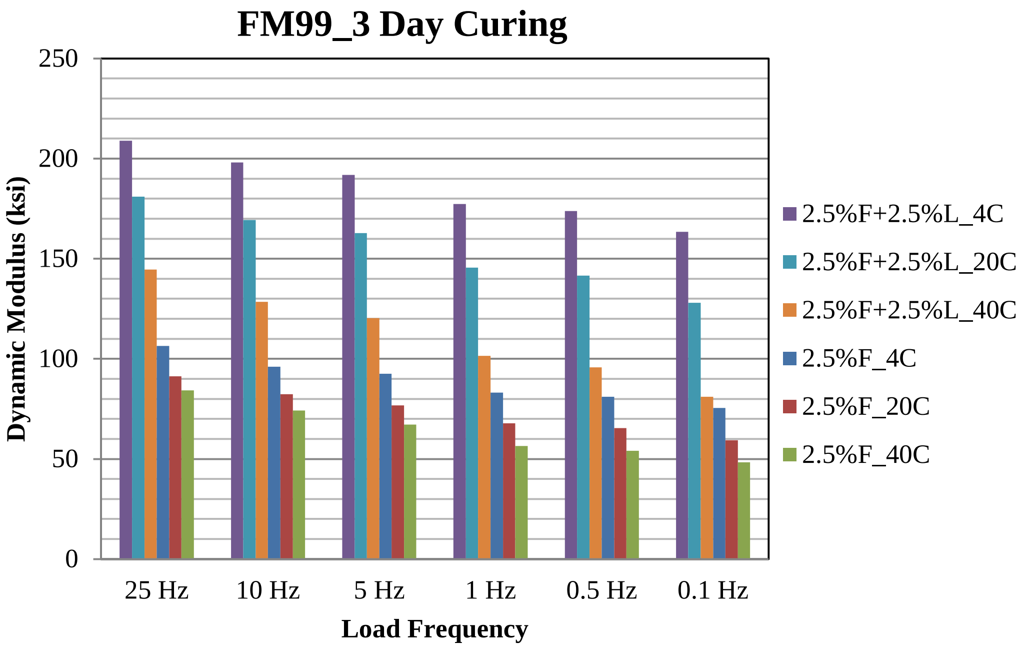

(a)

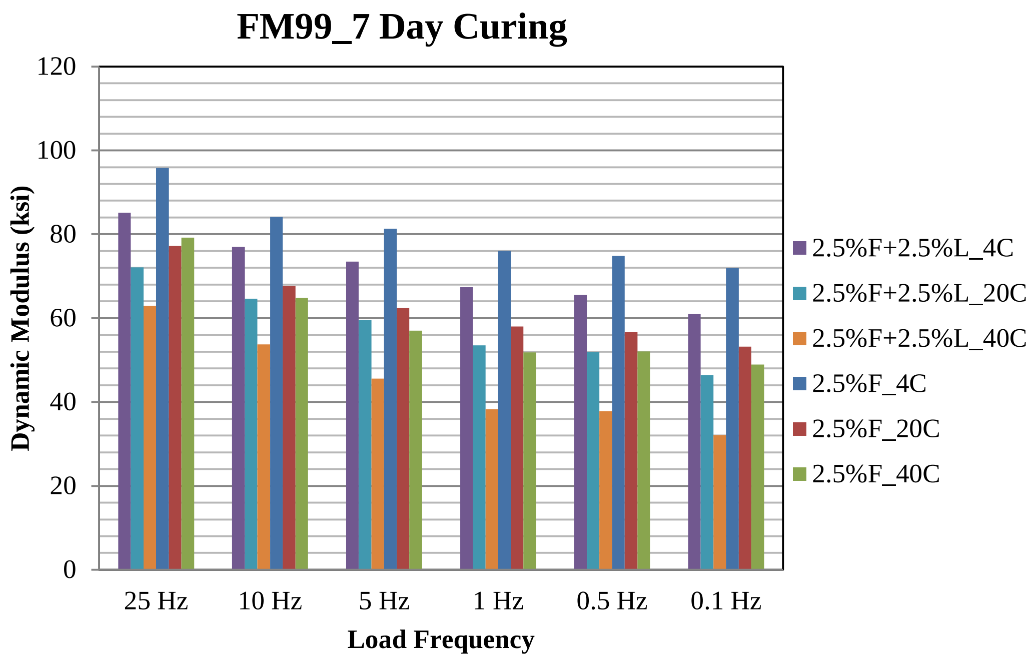

(b)

Figure 28. Dynamic Modulus for FM 99: (a) 3-Day Curing and (b) 7-Day Curing.

Legend: 2.5%F+2.5%L= 2.5% foamed asphalt+2.5% lime; 2.5%F= 2.5% foamed asphalt

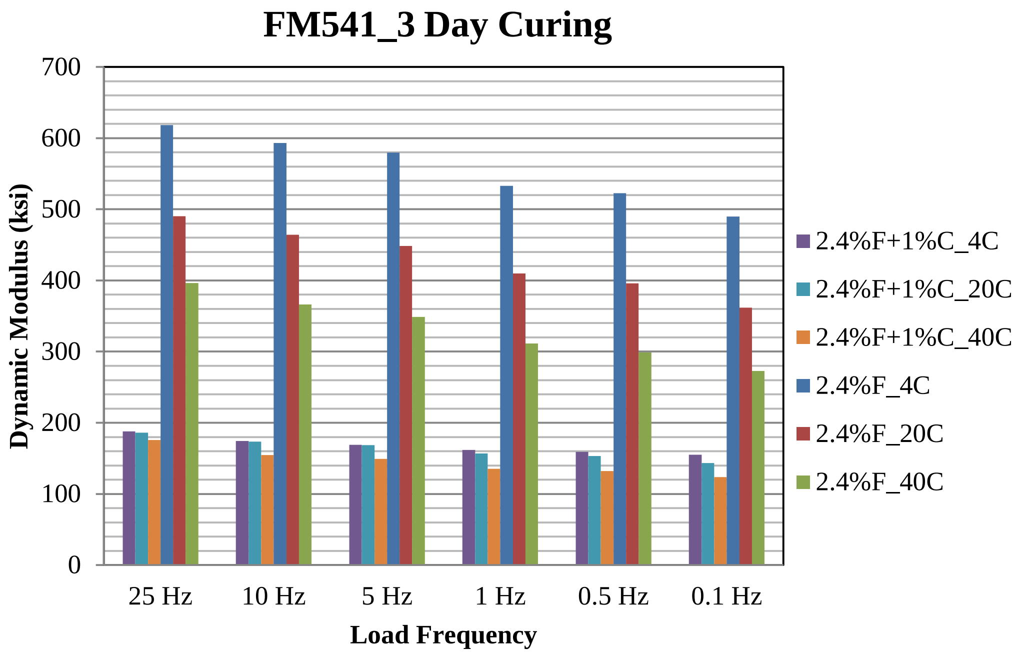

Figure 29. Dynamic Modulus for FM 541 (3-Day Curing).

Legend: 2.4%F+1%C= 2.4% foamed asphalt+1% cement; 2.4%F= 2.4% foamed asphalt

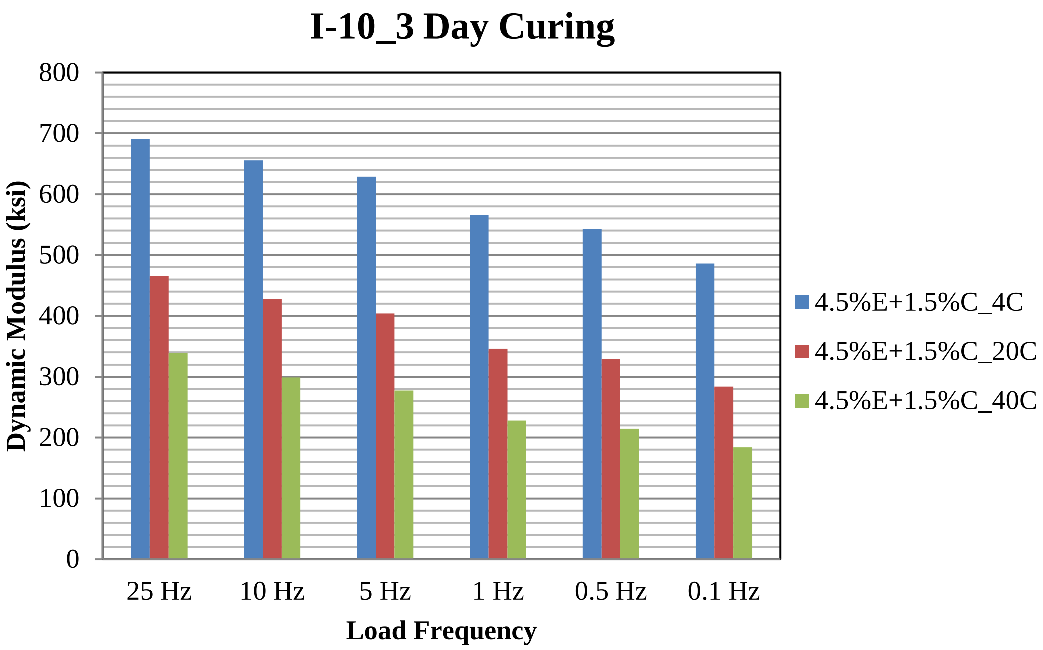

(a)

Legend: 4.5%E+1.5%C= 4.5% emulsion asphalt+1.5% cement

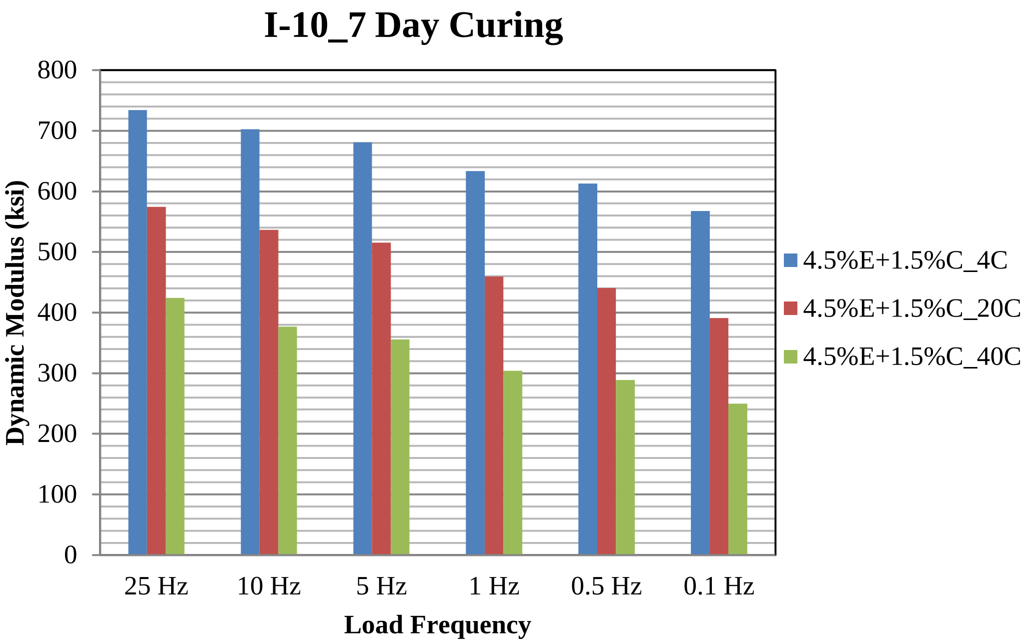

(b)

Figure 30. Dynamic Modulus for FM 541: (a) 3-Day Curing and (b) 7-Day Curing.

CHAPTER 4. FIELD PROJECTS WITH IMPLEMENTATION OF FDR

A total of five projects constructed with FDR option for FM roads, SH, and IH. The chapter presents the details of these five field projects including location of project, PI for subgrade, GPR and FWD prior to construction, pavement design, FWD after construction, and field performance monitoring.

FM 541 PROJECT

The FM 541 project is located in the San Antonio District (as shown in Figure 31), which is a rehabilitation project. The project includes excavating the subgrade and preparing the subgrade, placing salvaged base treated with lime and adding 12 in. of new flexible base, and performing a two-course surface treatment.

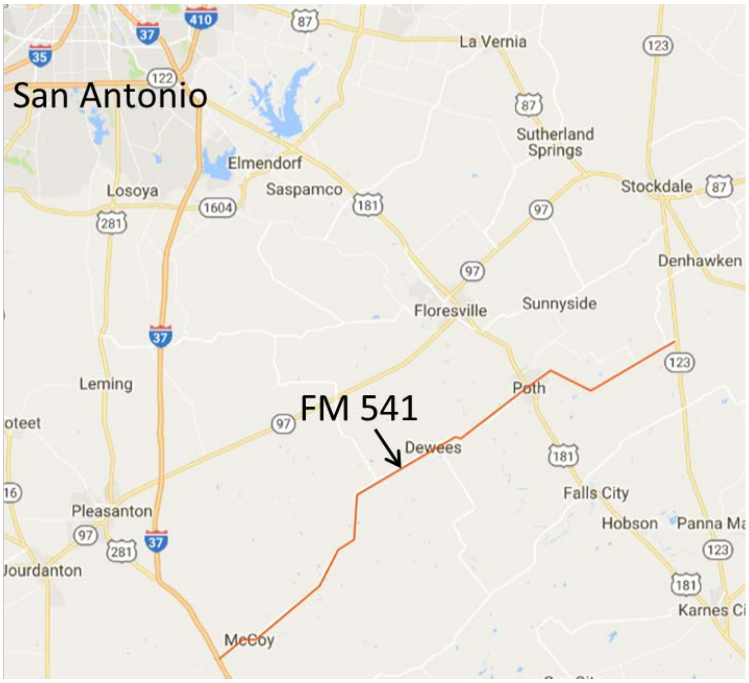
San Antonio
FM 541
La Vernia
Sutherland Springs
Elmendorf
Saspamco
Losoya
Stockdale
Denhawken
Floresville
Sunnyside
Poth
Dewees
Leming
Poteet
Pleasanton
Jourdanton
Falls City
Hobson
Panna Maria
Karnes City
McCoy

Figure 31. Location of FM 541.

PI for Subgrade

Figure 32 presents the soil map for PI. It can be seen that low PI is in the western portion while high PI is in the eastern portion. The western portion generally has the PI smaller than 12.6 while the eastern portion has the PI greater than 17.3.

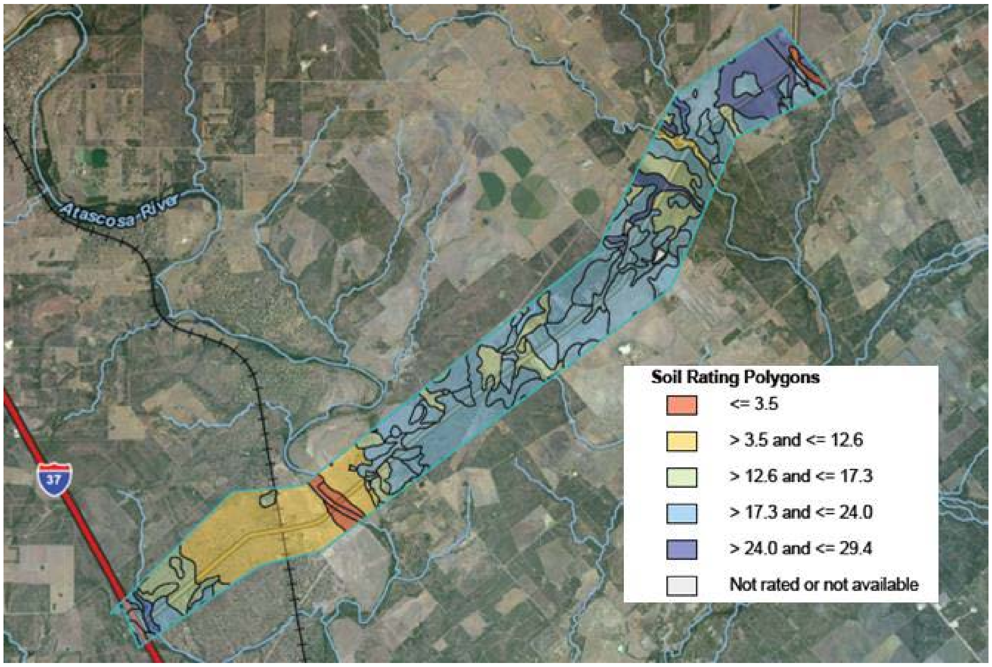
Atascosa River
37
Soil Rating Polygons
<= 3.5
> 3.5 and <= 12.6
> 12.6 and <= 17.3
> 17.3 and <= 24.0
> 24.0 and <= 29.4
Not rated or not available

Figure 32. Soil Map for PI.

GPR and FWD Results prior to Construction

The existing pavement structure is 27 ft wide, and has 1.5 in. of seal coat as a surface layer and 9 in. of flexible base material. The structural damage and layer thicknesses over the sections were found and verified by the GPR evaluation, as shown in Figure 33. Figure 34 presents FWD results. Based on the FWD, the western portion of the project had significantly improved subgrade conditions, which is consistent with prior observations from the soil map.

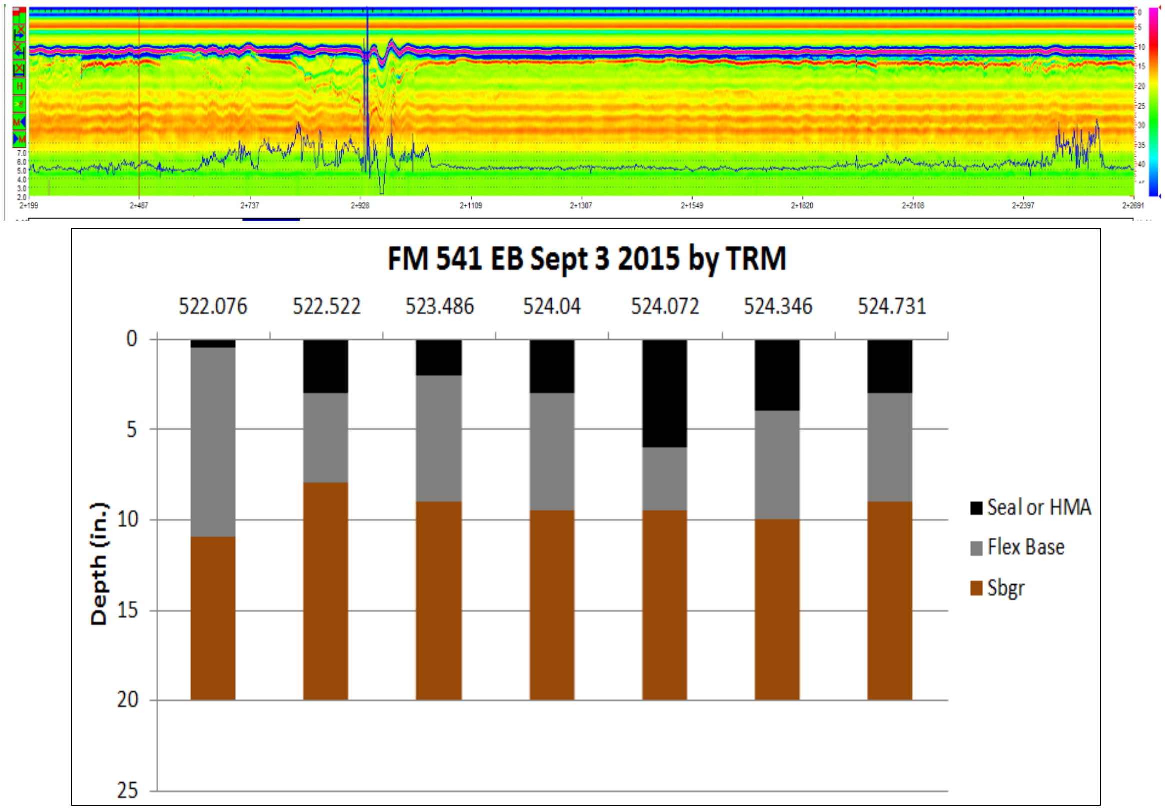

Figure 33. Structural Damage Found and Layer Thicknesses Verified by GPR Test.

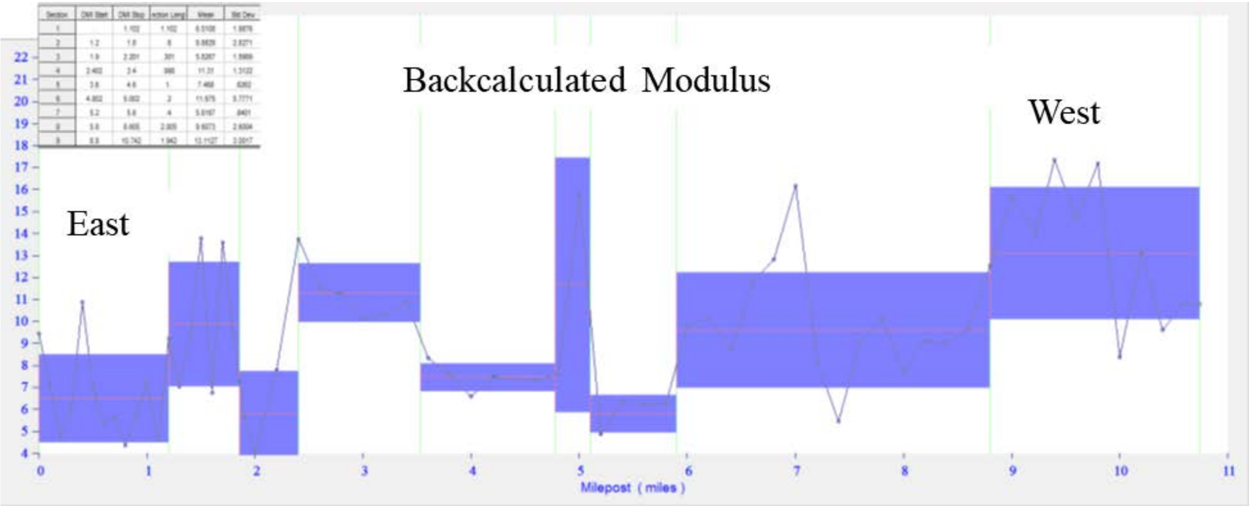

Figure 34. FWD Output from FM 541 Existing Pavement.

Pavement Design

A portion of the project implemented the FDR with foamed asphalt. Table 16 presents the traffic inputs for FPS design. Figure 35 presents the FPS pavement design for FM 541.

Table 16. Traffic Inputs for FM 541 in FPS Design.

Design Period (years)	20
ADT_beginning	1033
ADT_ending	1440
Total ESAL (million) after 20 years	2.4
Percent of trucks	30.9
Surface Treatment Modulus (ksi)	200
Modulus of stabilized base with foamed asphalt	300
Modulus of subgrade	7

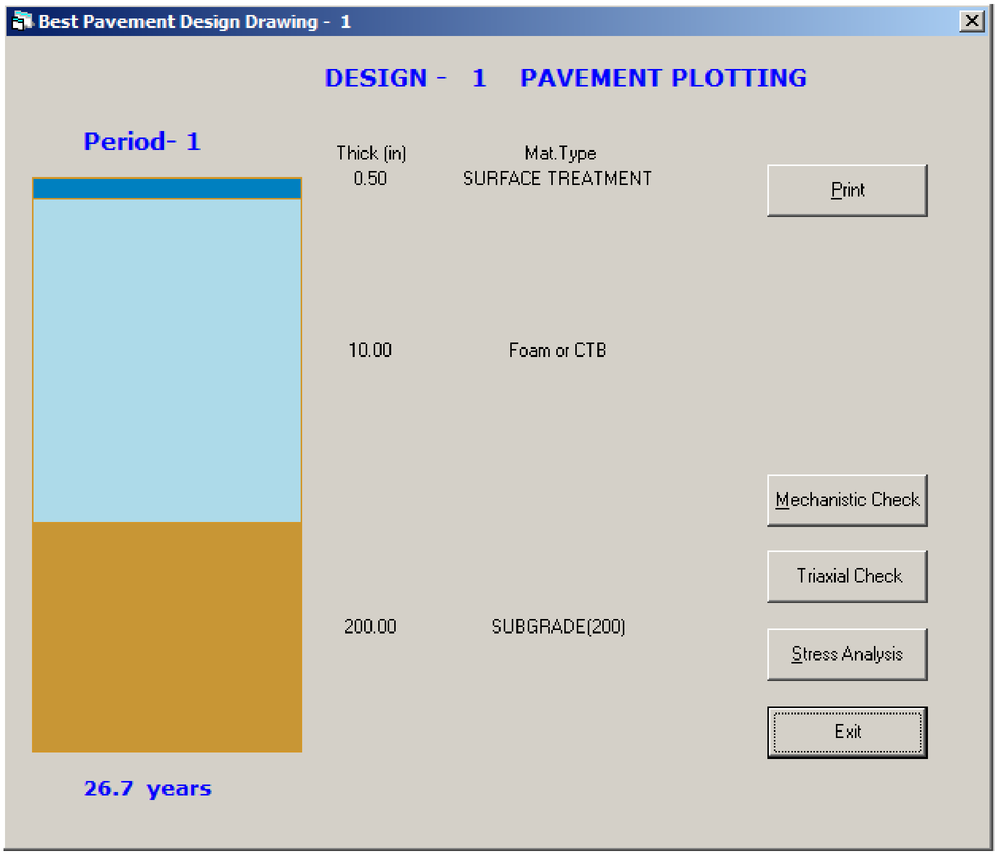
Best Pavement Design Drawing - 1
Print
Mechanistic Check
Triaxial Check
Stress Analysis
Exit

DESIGN - 1 PAVEMENT PLOTTING

Period- 1

Thick (in)	Mat.Type
0.50	SURFACE TREATMENT
10.00	Foam or CTB
200.00	SUBGRADE(200)

26.7 years

Figure 35. Pavement Design for FM 541.

Construction

The western portion of the project was suitable for FDR and constructed using 2.4 percent of foamed asphalt and 1 percent of cement for a 10-in. treatment depth. Figure 36 presents the construction sequence. The section was completed in October 2015.

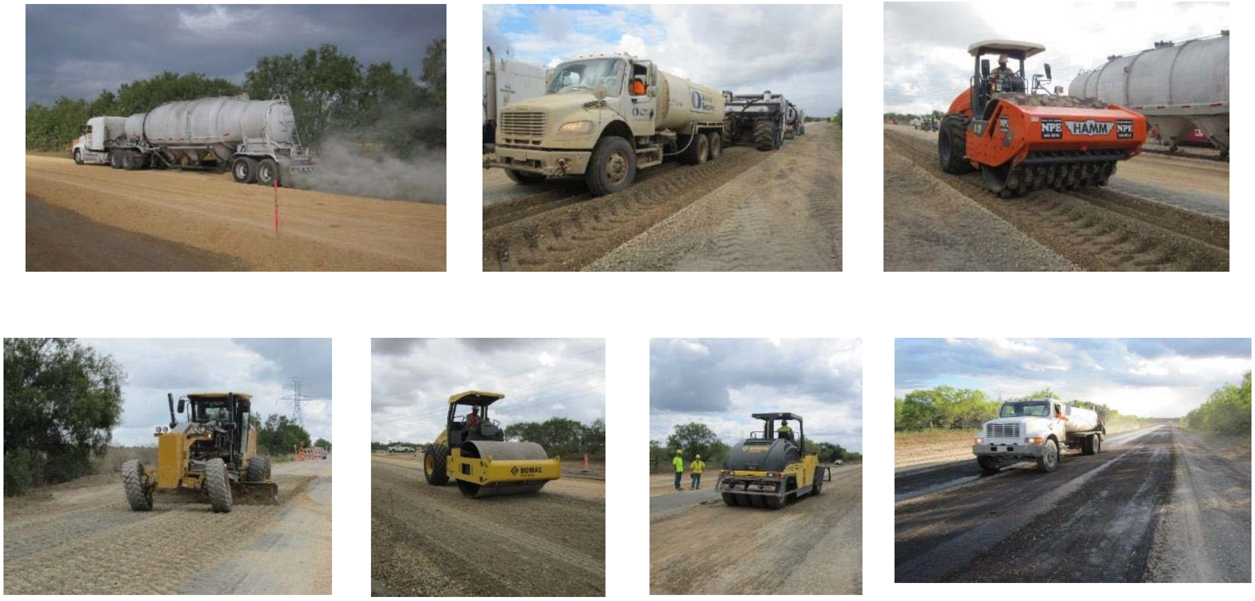

Figure 36. Typical Construction Sequence.

FWD Results after Construction

It is important for the pavement layers to achieve the designed modulus value so that the designed pavement may perform as expected. The FWD test can be used to monitor layer moduli of pavements after construction. FM 541 employed a foamed asphalt (2.4 percent) with 1 percent cement to treat the base layer. During construction, the cement was evenly distributed. The FWD test was conducted to monitor the modulus after construction. Figure 37 shows the FWD testing and backcalculated moduli of the section two weeks after construction. As shown in Figure 37, the measured deflections were uniform and the average base moduli value was around 280 ksi, which was a reasonable match with the modulus measured in the laboratory.

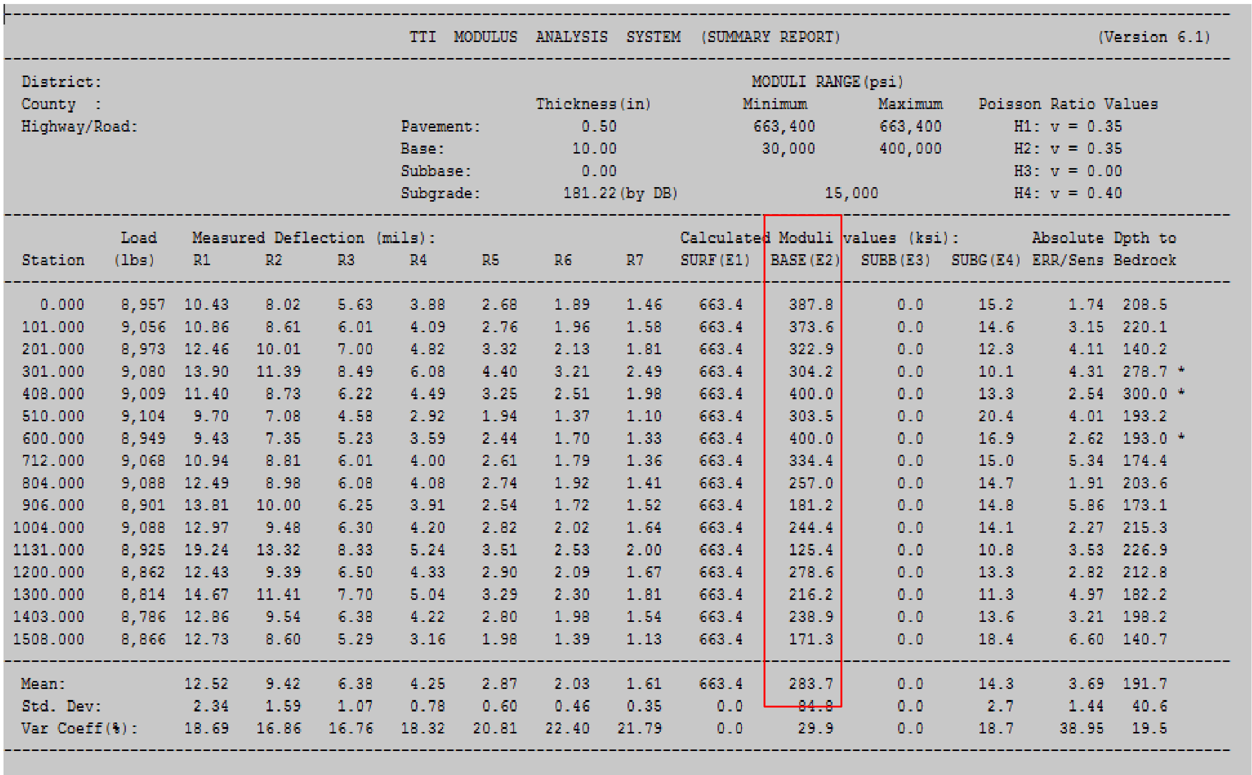

```
|------------------------------------------------------------------------------------------------------------------------------
                                            TTI  MODULUS  ANALYSIS  SYSTEM  (SUMMARY REPORT)                        (Version 6.1)
-------------------------------------------------------------------------------------------------------------------------------
 District:                                                                      MODULI RANGE(psi)
 County  :                                           Thickness(in)          Minimum        Maximum    Poisson Ratio Values
 Highway/Road:                            Pavement:       0.50              663,400        663,400        H1: v = 0.35
                                          Base:          10.00               30,000        400,000        H2: v = 0.35
                                          Subbase:        0.00                                            H3: v = 0.00
                                          Subgrade:     181.22(by DB)                15,000               H4: v = 0.40
-------------------------------------------------------------------------------------------------------------------------------
            Load    Measured Deflection (mils):                                   Calculated Moduli values (ksi):       Absolute Dpth to
 Station    (lbs)   R1        R2       R3       R4       R5       R6       R7     SURF(E1)  BASE(E2)  SUBB(E3)  SUBG(E4)  ERR/Sens Bedrock
-------------------------------------------------------------------------------------------------------------------------------
   0.000    8,957  10.43     8.02     5.63     3.88     2.68     1.89     1.46     663.4     387.8       0.0      15.2       1.74  208.5
 101.000    9,056  10.86     8.61     6.01     4.09     2.76     1.96     1.58     663.4     373.6       0.0      14.6       3.15  220.1
 201.000    8,973  12.46    10.01     7.00     4.82     3.32     2.13     1.81     663.4     322.9       0.0      12.3       4.11  140.2
 301.000    9,080  13.90    11.39     8.49     6.08     4.40     3.21     2.49     663.4     304.2       0.0      10.1       4.31  278.7 *
 408.000    9,009  11.40     8.73     6.22     4.49     3.25     2.51     1.98     663.4     400.0       0.0      13.3       2.54  300.0 *
 510.000    9,104   9.70     7.08     4.58     2.92     1.94     1.37     1.10     663.4     303.5       0.0      20.4       4.01  193.2
 600.000    8,949   9.43     7.35     5.23     3.59     2.44     1.70     1.33     663.4     400.0       0.0      16.9       2.62  193.0 *
 712.000    9,068  10.94     8.81     6.01     4.00     2.61     1.79     1.36     663.4     334.4       0.0      15.0       5.34  174.4
 804.000    9,088  12.49     8.98     6.08     4.08     2.74     1.92     1.41     663.4     257.0       0.0      14.7       1.91  203.6
 906.000    8,901  13.81    10.00     6.25     3.91     2.54     1.72     1.52     663.4     181.2       0.0      14.8       5.86  173.1
1004.000    9,088  12.97     9.48     6.30     4.20     2.82     2.02     1.64     663.4     244.4       0.0      14.1       2.27  215.3
1131.000    8,925  19.24    13.32     8.33     5.24     3.51     2.53     2.00     663.4     125.4       0.0      10.8       3.53  226.9
1200.000    8,862  12.43     9.39     6.50     4.33     2.90     2.09     1.67     663.4     278.6       0.0      13.3       2.82  212.8
1300.000    8,814  14.67    11.41     7.70     5.04     3.29     2.30     1.81     663.4     216.2       0.0      11.3       4.97  182.2
1403.000    8,786  12.86     9.54     6.38     4.22     2.80     1.98     1.54     663.4     238.9       0.0      13.6       3.21  198.2
1508.000    8,866  12.73     8.60     5.29     3.16     1.98     1.39     1.13     663.4     171.3       0.0      18.4       6.60  140.7
-------------------------------------------------------------------------------------------------------------------------------
 Mean:             12.52     9.42     6.38     4.25     2.87     2.03     1.61     663.4     283.7       0.0      14.3       3.69  191.7
 Std. Dev:          2.34     1.59     1.07     0.78     0.60     0.46     0.35       0.0      84.8       0.0       2.7       1.44   40.6
 Var Coeff(%):     18.69    16.86    16.76    18.32    20.81    22.40    21.79       0.0      29.9       0.0      18.7      38.95   19.5
-------------------------------------------------------------------------------------------------------------------------------
```

Figure 37. FWD Test on FM 541 Section after Two Weeks after Construction.

Field Performance Monitoring

The field survey was conducted two years after construction. Figure 38 shows the pictures of pavement surface and rutting measurement. No cracks were observed in the pavement. The average rutting depth measured is 2.9 mm.

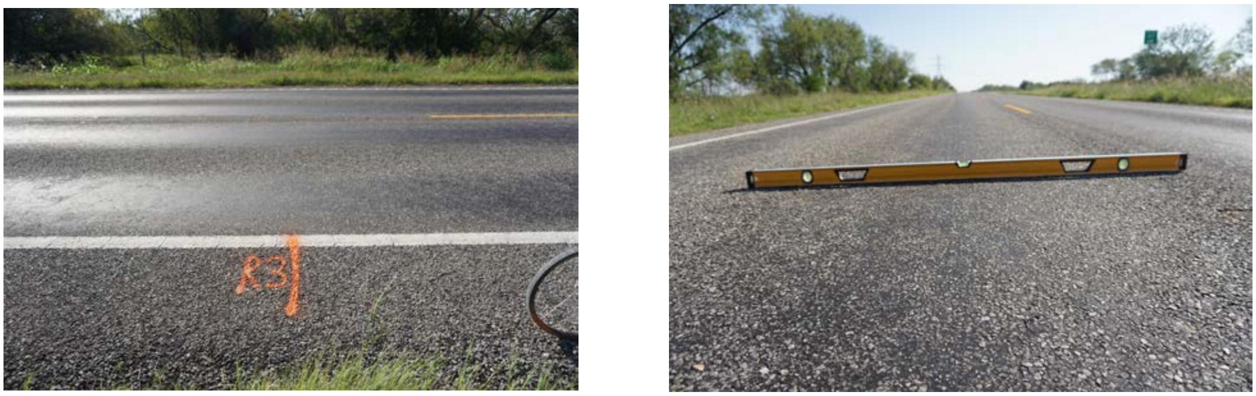

Figure 38. Pictures of Pavement Surface and Rutting: (a) No Cracking and (b) Rutting.

SH 202 PROJECT

The SH 202 project is located in Corpus Christi District and runs from US 181 to US 183. Figure 39 shows its location.

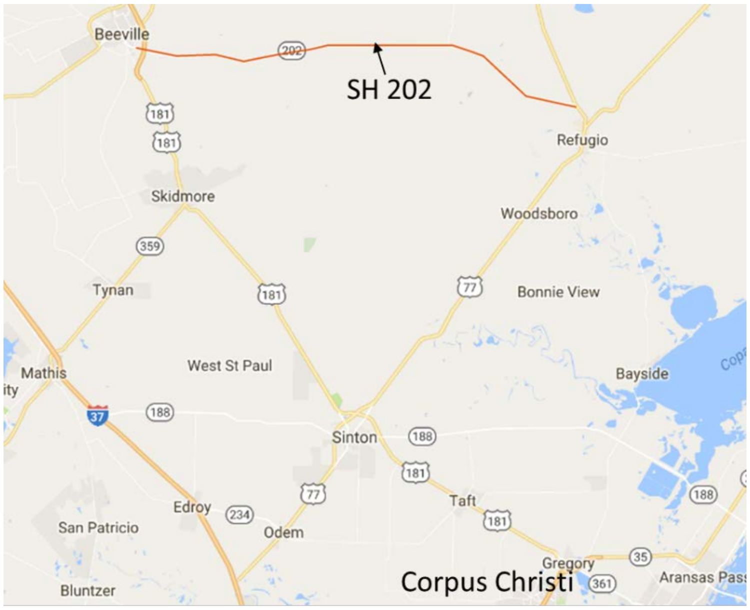

Beeville
202
SH 202
181
181
Refugio
Skidmore
Woodsboro
359
Tynan
181
77
Bonnie View
Mathis
West St Paul
Bayside
37
188
Sinton
188
181
Edroy
234
77
Taft
181
188
San Patricio
Odem
Gregory
35
Corpus Christi
361
Aransas Pass
Bluntzer

Figure 39. Location of SH 202.

PI for Subgrade

Figure 40 presents the soil map for PI. Most of the area has a PI less than 20.

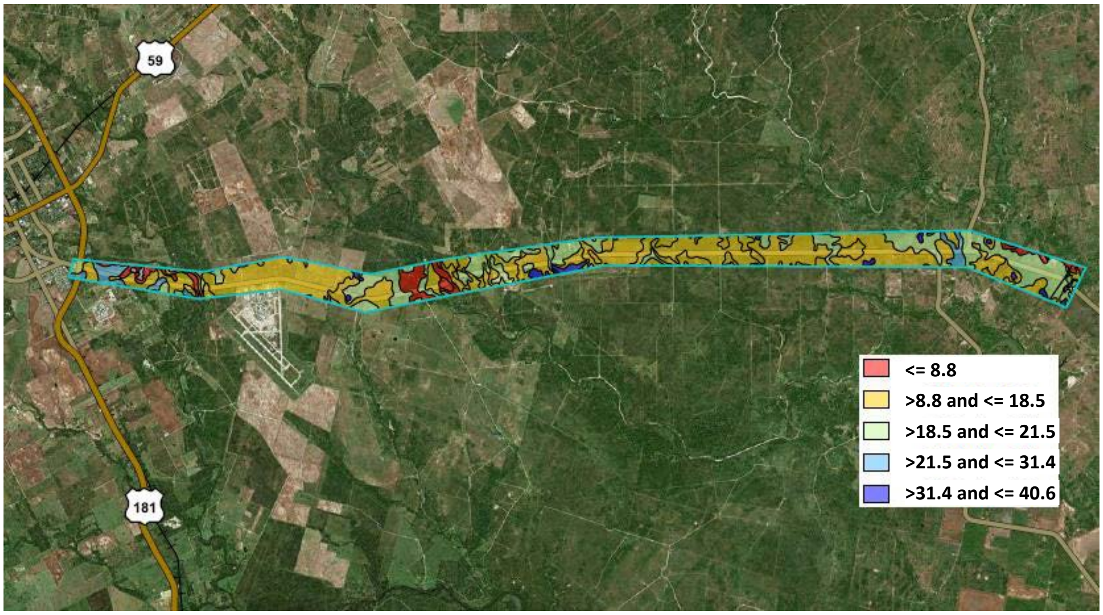

59
181
🟥 <= 8.8
🟨 >8.8 and <= 18.5
🟩 >18.5 and <= 21.5
🟦 >21.5 and <= 31.4
🟦 >31.4 and <= 40.6

Figure 40. Soil Map for PI.

GPR and FWD Results Prior to Construction

Figure 41 and Figure 42 presents GPR and FWD results. From GPR results, there are variations in surface thickness that could be attributed to maintenance activities. FWD results indicate that the modulus of base has a large variation indicating the deterioration of the stabilized base. The subgrade modulus is 11.5 ksi.

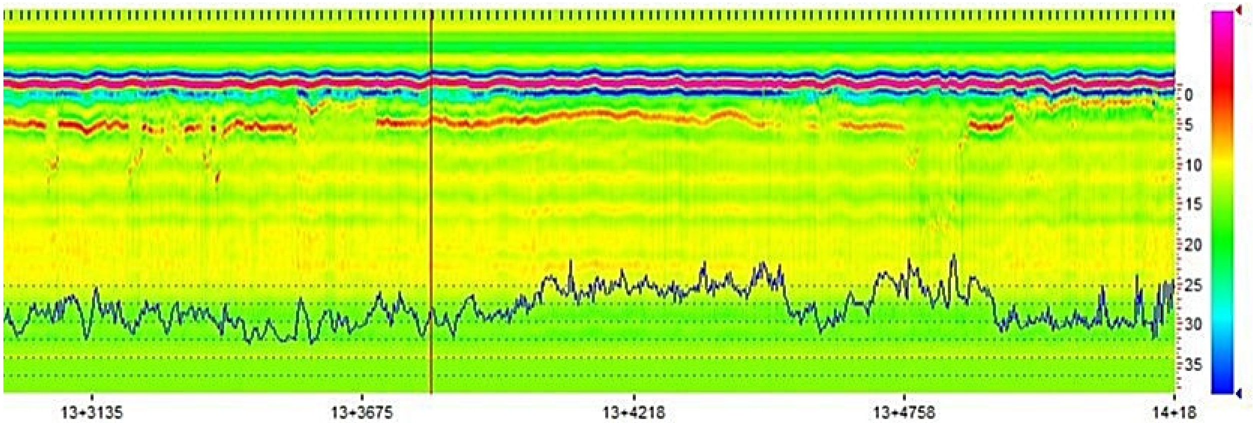

Figure 41. Example of GPR Test Results.

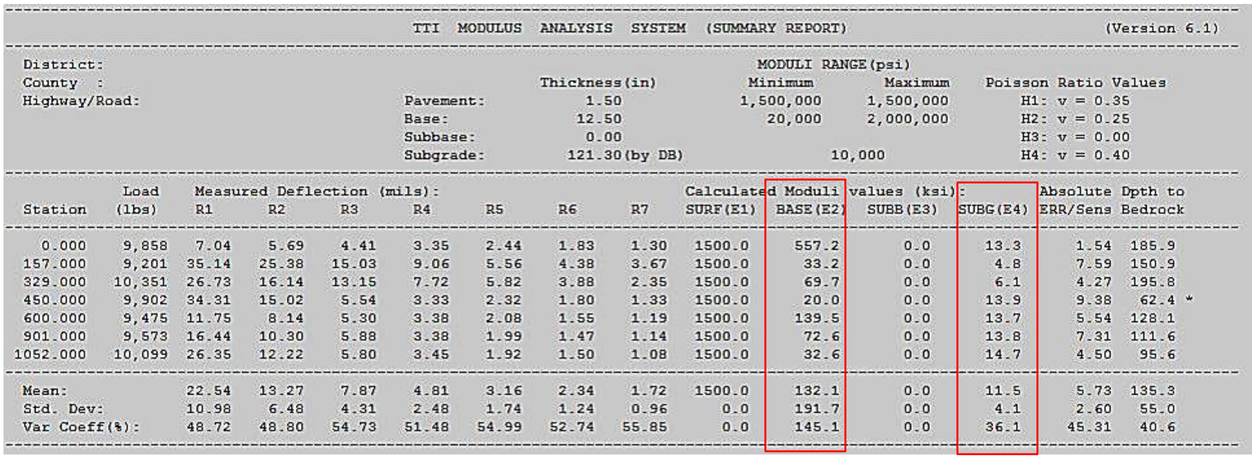

```
-------------------------------------------------------------------------------------------------------------
                                        TTI  MODULUS  ANALYSIS  SYSTEM  (SUMMARY REPORT)              (Version 6.1)
-------------------------------------------------------------------------------------------------------------
 District:                                                                 MODULI RANGE(psi)
 County   :                                          Thickness(in)       Minimum        Maximum    Poisson Ratio Values
 Highway/Road:                         Pavement:          1.50           1,500,000      1,500,000      H1: v = 0.35
                                       Base:             12.50              20,000      2,000,000      H2: v = 0.25
                                       Subbase:           0.00                                         H3: v = 0.00
                                       Subgrade:        121.30(by DB)              10,000              H4: v = 0.40
-------------------------------------------------------------------------------------------------------------
            Load    Measured Deflection (mils):                                    Calculated Moduli values (ksi):   Absolute Dpth to
 Station   (lbs)    R1      R2      R3      R4      R5      R6      R7     SURF(E1)  BASE(E2)  SUBB(E3)  SUBG(E4)  ERR/Sens Bedrock
-------------------------------------------------------------------------------------------------------------
   0.000   9,858   7.04    5.69    4.41    3.35    2.44    1.83    1.30    1500.0     557.2      0.0      13.3      1.54  185.9
 157.000   9,201  35.14   25.38   15.03    9.06    5.56    4.38    3.67    1500.0      33.2      0.0       4.8      7.59  150.9
 329.000  10,351  26.73   16.14   13.15    7.72    5.82    3.88    2.35    1500.0      69.7      0.0       6.1      4.27  195.8
 450.000   9,902  34.31   15.02    5.54    3.33    2.32    1.80    1.33    1500.0      20.0      0.0      13.9      9.38   62.4 *
 600.000   9,475  11.75    8.14    5.30    3.38    2.08    1.55    1.19    1500.0     139.5      0.0      13.7      5.54  128.1
 901.000   9,573  16.44   10.30    5.88    3.38    1.99    1.47    1.14    1500.0      72.6      0.0      13.8      7.31  111.6
1052.000  10,099  26.35   12.22    5.80    3.45    1.92    1.50    1.08    1500.0      32.6      0.0      14.7      4.50   95.6
-------------------------------------------------------------------------------------------------------------
 Mean:            22.54   13.27    7.87    4.81    3.16    2.34    1.72    1500.0     132.1      0.0      11.5      5.73  135.3
 Std. Dev:        10.98    6.48    4.31    2.48    1.74    1.24    0.96       0.0     191.7      0.0       4.1      2.60   55.0
 Var Coeff(%):    48.72   48.80   54.73   51.48   54.99   52.74   55.85       0.0     145.1      0.0      36.1     45.31   40.6
-------------------------------------------------------------------------------------------------------------
```

Figure 42. FWD Output from SH 202 Existing Pavement.

Pavement Design

A total of 5 million ESALs was assumed for traffic input for pavement design. The moduli of stabilized FDR layer, flexible base, and surface treatment were 150 ksi, 40 ksi, and 200 ksi, respectively. The final pavement design chosen by TxDOT is FDR treatment of 10 in. with 3 percent cement and then 6 in. of new flexible base with a three-course surface treatment.

Construction

The project was constructed from spring 2016 through fall 2016. Figure 43 shows the construction sequence on SH 202.

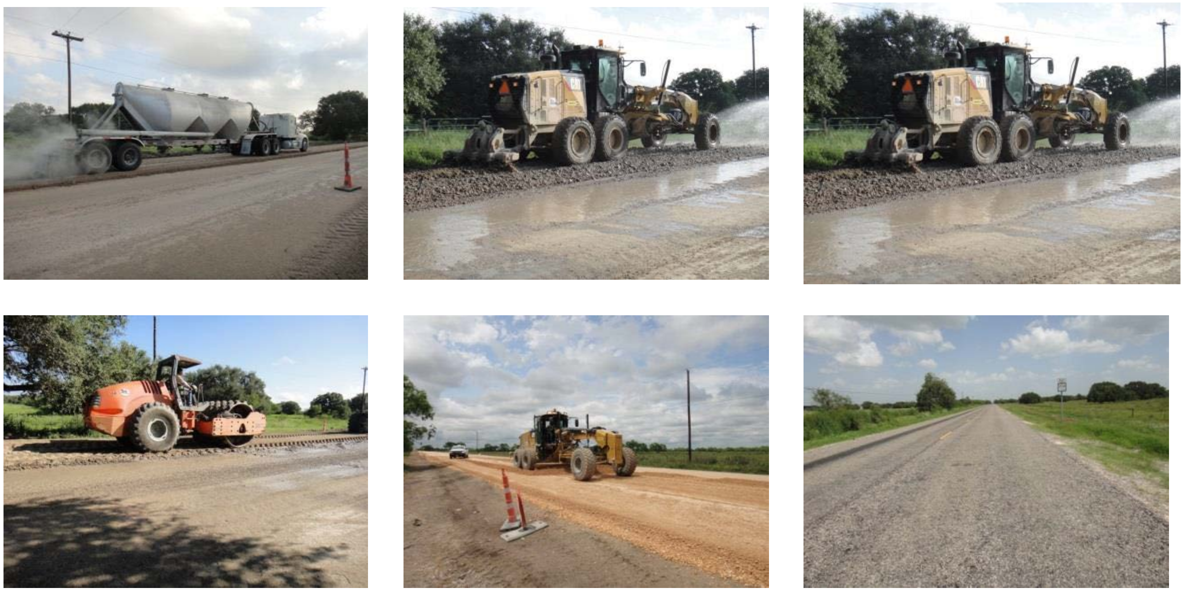

Figure 43. Construction Sequence on SH 202.

FWD Results after Construction

Figure 44 shows the comparison of FDR layer modulus at different ages. It is clear that FDR layer modulus is significantly improved after 8 months. The modulus is a reasonable value.

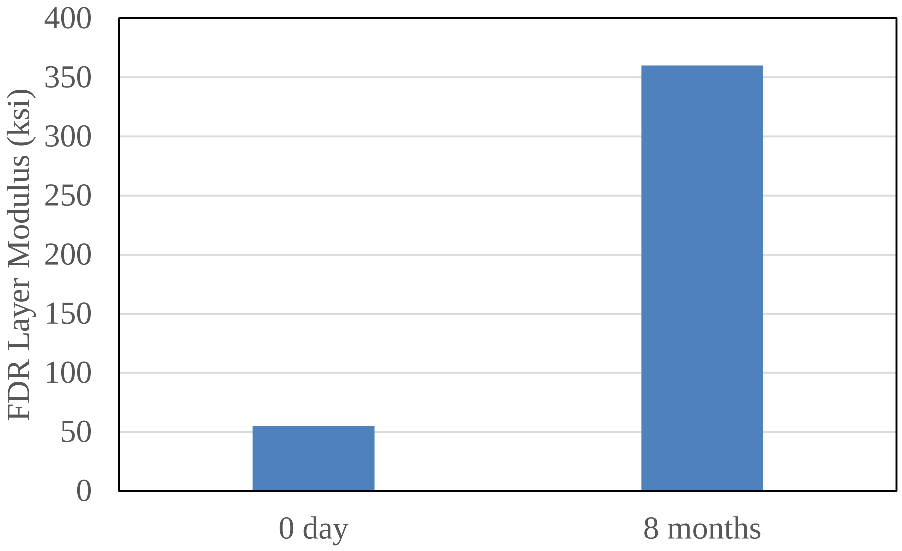

Figure 44. FWD Test Results on SH 202.

Field Performance Monitoring

The field survey was conducted one year after construction. Figure 45 shows the pictures of pavement surface and rutting measurement. No cracks were observed in the pavement. The average rutting depth measured is 5.2 mm.

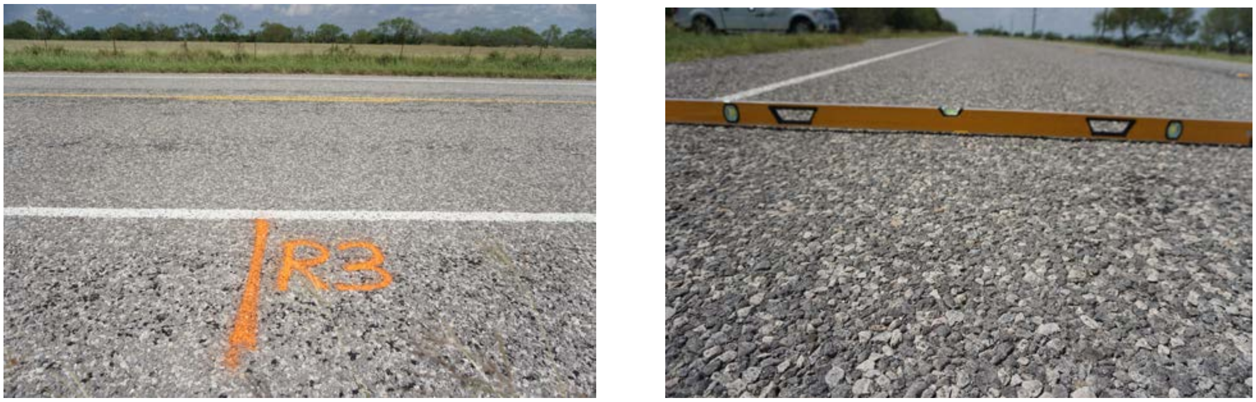

Figure 45. Pictures of Pavement Surface and Rutting: (a) No Cracking and (b) Rutting.

I-10 PROJECT

The I-10 project is located in Reeves County, as shown in Figure 46. The soil survey, GPR, and FWD prior to construction were not performed.

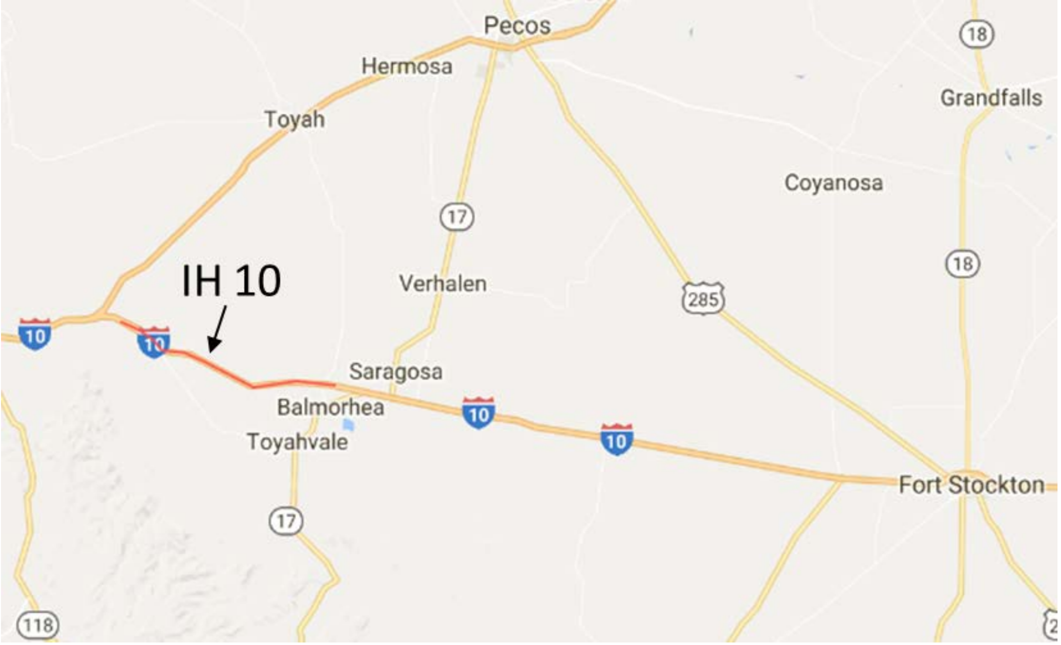
Pecos
Hermosa
Toyah
Grandfalls
Coyanosa
17
18
18
IH 10
Verhalen
285
10
10
10
10
Saragosa
Balmorhea
Toyahvale
Fort Stockton
17
118

Figure 46. Location of I-10.

Pavement Design and Construction

The pavement design consists of 7-in. flexible base to remain in place, 9 in. of emulsion-treated base, and 4 in. of HMA with modulus values of 35, 250, and 500 ksi, respectively. The modulus of subgrade is assumed as 22 ksi. For FDR layer, 4.5 percent asphalt emulsion and 1 percent cement was used. Construction was completed in winter 2016.

FWD Results after Construction

Figure 47 shows the FDR layer modulus after construction. The stabilized layer treated with emulsion shows a much higher modulus value exceeding the design input after 8 months.

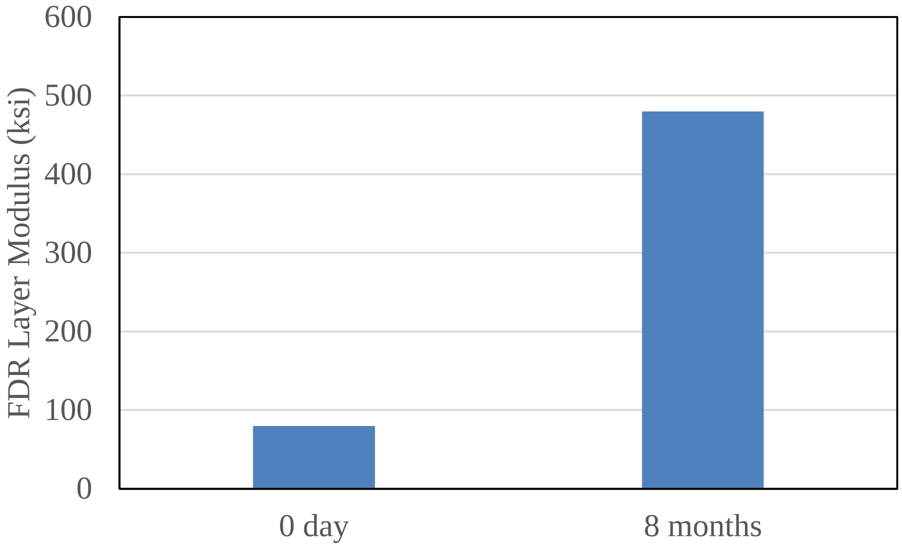

Figure 47. FWD Test Results on I-10.

Field Performance Monitoring

The field survey was conducted one year after construction. Figure 48 shows the pictures of pavement surface and rutting measurement. No cracks were observed in the pavement. The average rutting depth measured is 6.4 mm.

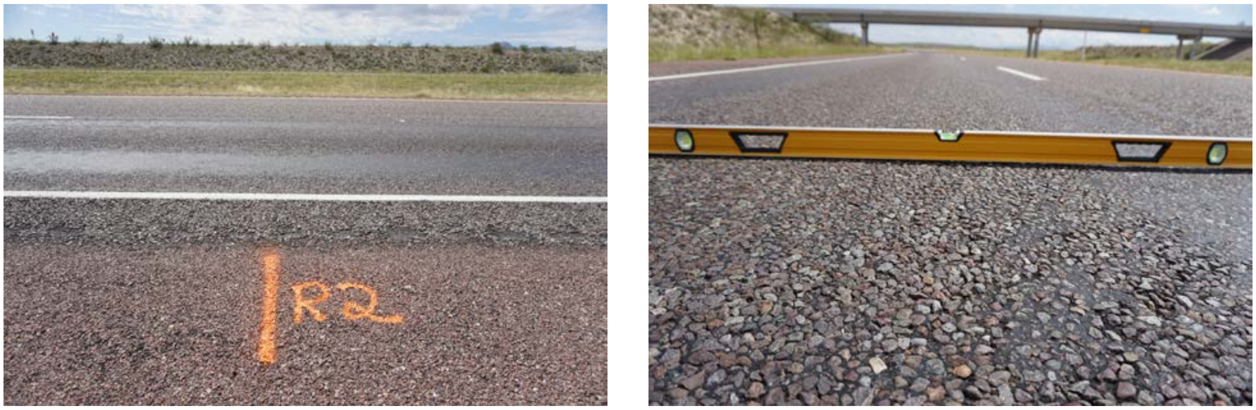

Figure 48. Pictures of Pavement Surface and Rutting: (a) No Cracking and (b) Rutting.

SH 7 PROJECT

The SH 7 project is located in Bryan District, as shown in Figure 49.

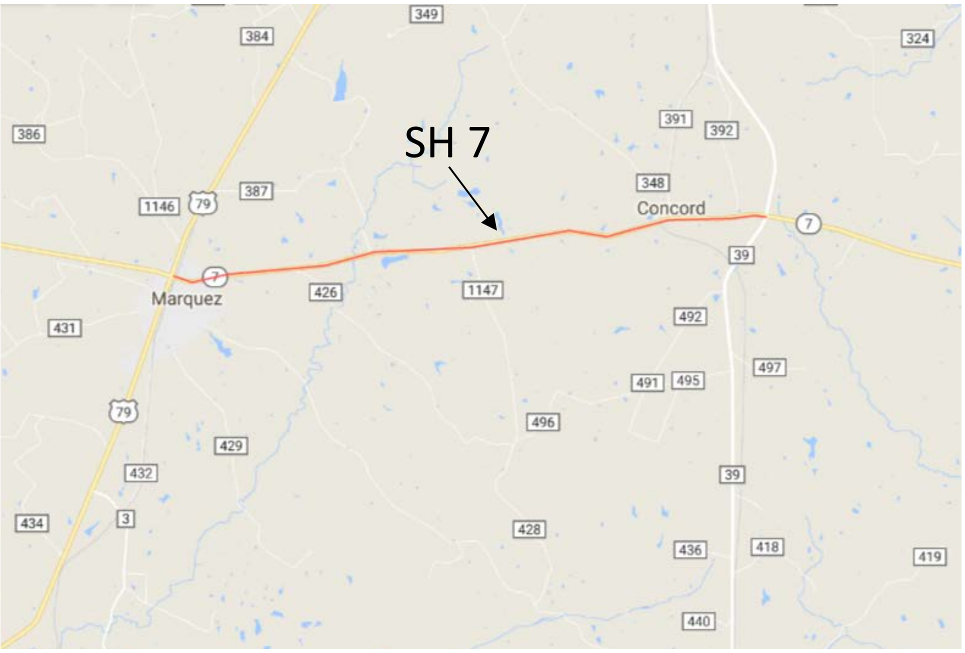
SH 7
Marquez
Concord
349
384
324
386
391
392
348
1146
79
387
7
39
426
1147
492
431
491
495
497
79
496
429
432
39
434
3
428
436
418
419
440

Figure 49. Location of SH 7.

PI for Subgrade

Most of the area has a PI less than 17.

FWD Results Prior to Construction

The subgrade modulus is about 20 ksi, which is a high value.

Pavement Design and Construction

A total of 5.8 million ESALs was assumed for traffic input for pavement design. The foamed stabilized base modulus was assumed as 300 ksi. The pavement design includes 0.5-in. surface treatment, 10-in. FDR treatment, and 4-in. subbase. Ten-inch FDR treatment include two sections: one use 2.4 percent foamed asphalt with 1 percent cement and the other use only 2.4 percent foamed asphalt. The project was constructed in August 2016.

FWD Results after Construction

Figure 50 shows the FDR layer modulus one month after construction. The only foamed stabilized layer did not achieve the design modulus while the layer treated with foamed and cement had a much higher modulus exceeding the design input.

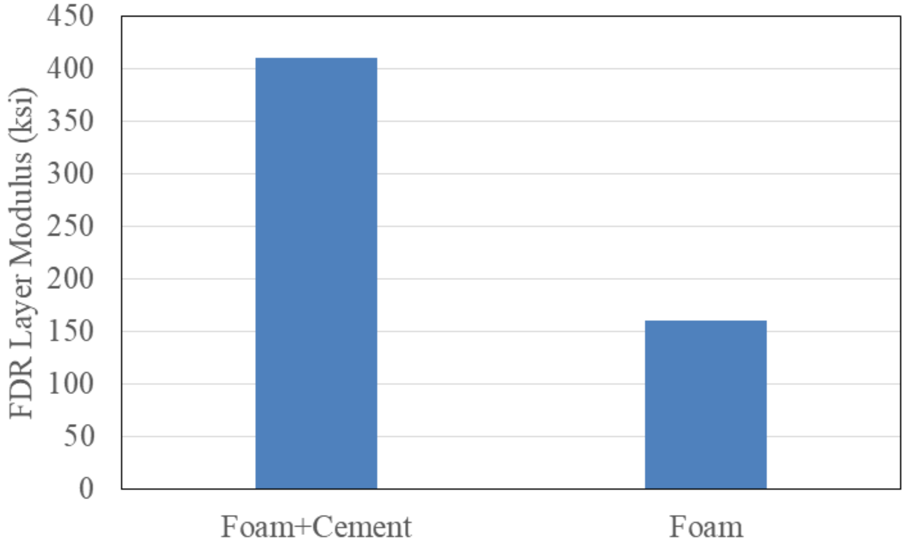

Figure 50. FWD Test Results on SH 7.

Field Performance Monitoring

The field survey was conducted one year after construction. There is no cracking or rutting observed.

FM 99 PROJECT

FM 99 is an extremely heavily trafficked energy development roadway in the Corpus Christi District of Texas; the limits of this project are from US 281A to the McMullen County line. The original plans stated that the roadway is 24 ft wide and has 1 in. of asphaltic materials as a surface layer and 6 in. of flexible base material. Figure 51 shows the condition of the existing pavement, indicating severe alligator cracks and potholes on the surface of the pavement. Figure 52 shows the location of the project.

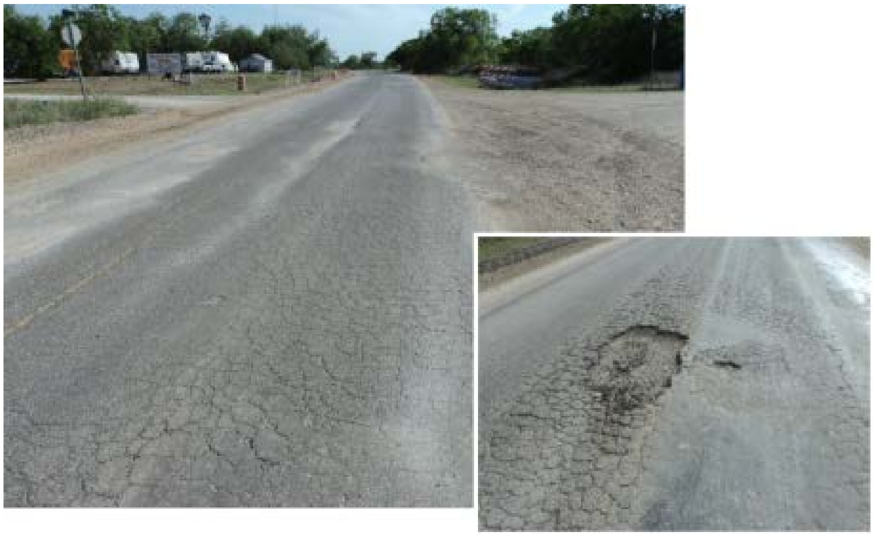

Figure 51. Condition of FM 99 prior to Rehabilitation.

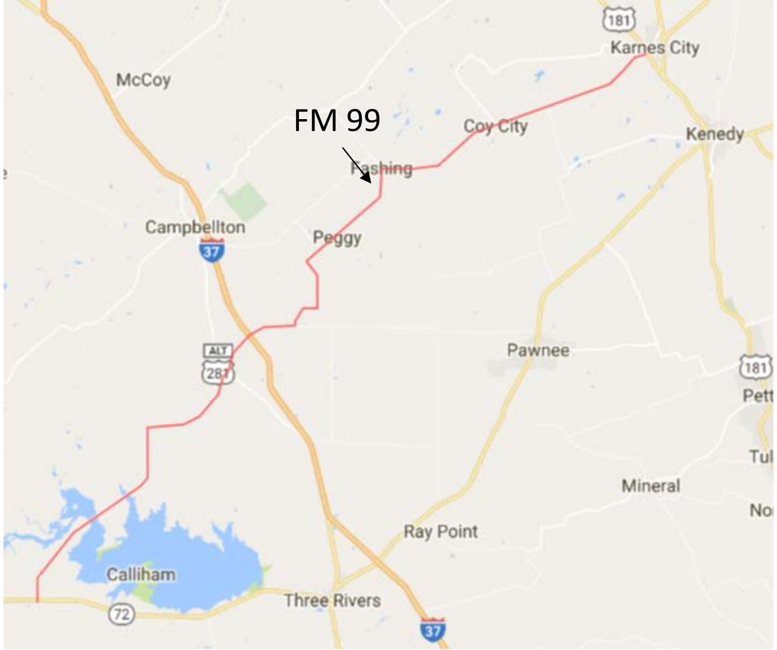
181
Karnes City
McCoy
FM 99
Coy City
Kenedy
Fashing
Campbellton
37
Peggy
ALT
281
Pawnee
181
Pett
Tul
Mineral
No
Ray Point
Calliham
72
Three Rivers
37

Figure 52. Location of FM 99.

GPR Results Prior to Construction

GPR was used to examine the test section variability along the way and to check layer thicknesses. The main finding from the GPR was that the asphalt layer was not 1-in. thick but instead varied between 3 and 5 in. However, the structure in the 1-mile test section was uniform.

Pavement Design and Construction

The information of pavement design is not available at this time, but the project consisted of three FDR treatments: foamed asphalt treatment (11 in.), cement treatment (11 in.), and cement treatment (8 in.) with 6 in. flexible base overlay. The FDR layer treated with 2.4 percent foamed asphalt and 1.5 percent cement. All the foamed work was completed in around June 2014.

FWD Results after Construction

The FWD was performed on 11-in. foamed section two weeks after construction, and the stabilized modulus was 506 ksi, which is an excellent value. The modulus of cement treated base (11 in.) was 410 ksi measured two months after construction. For the section with 8 in.-base and 6 in.-flexible base overlay, the modulus of flexible base was 147 ksi while the modulus of foamed treated subbase was 323 ksi.

Field Performance Monitoring

The field survey was conducted three years after construction. Figure 53 shows the pictures of pavement surface and rutting measurement. A total of 15 spots were surveyed and the distance between two spots was about 76 m. Cracks were observed at two spots, as shown in Figure 53. The average rutting depth measured is 4.0 mm.

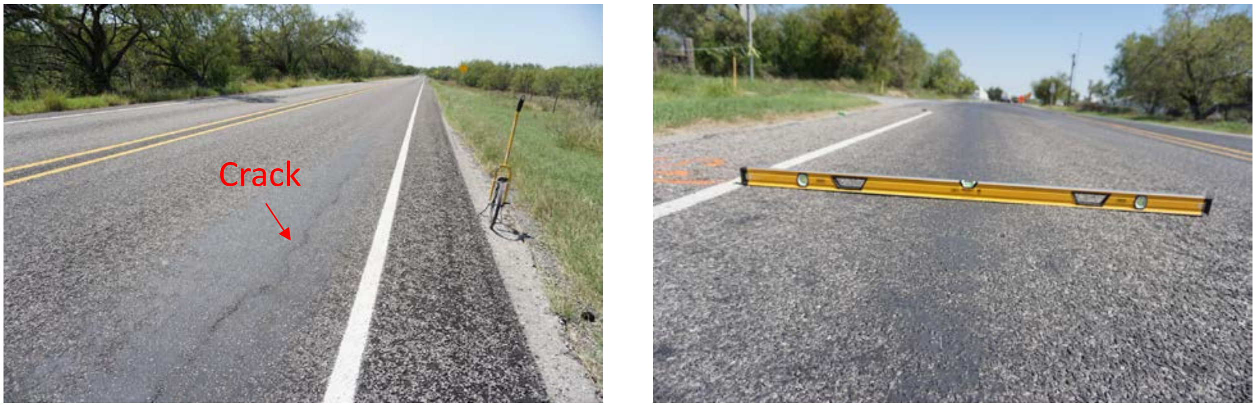

Figure 53. Pictures of Pavement Surface and Rutting: (a) Cracking and (b) Rutting.

CHAPTER 5. PAVEMENT DESIGN CATALOGUE FOR PAVEMENTS IN ENERGY DEVELOPMENT AREAS

INTRODUCTION

Texas has undergone a boom in the production of natural gas and crude oil since 2008 due to improvements in the practice of hydraulic fracturing (fracking) of oil and gas bearing rock formations. This development of energy sources in Texas and throughout the United States has tremendously impacted the global economy by increasing the world’s supply of gas and petroleum, which has driven the cost of energy down significantly. While the recent energy development has had a positive economic benefit to Texas, it has had severe impacts on the condition of the state’s highway system estimated to be approximately $2 billion per year.

The process of fracking requires the movement of equipment, materials, and water to establish and complete wells, produce oil, and re-frack on a periodic basis. This can translate into 1000 to 2000 loaded trucks per well and with a rate of well completion on the order of 10,000 to 15,000 per year, a total of 10,000,000 to 30,000,000 additional truck trips are being generated annually on SH. The locations of these wells within Texas are generally in rural areas where the traditional traffic has been largely passenger vehicles with occasional agriculture-related truck traffic. The pavements on these rural roads were vastly under-designed for the amount of traffic they are currently serving. Many of these pavements have suffered severe distress in the form of fatigue cracking, edge cracking and deterioration, and rutting.

OBJECTIVE

The objective of the work presented here was to develop a simplified approach to estimating the required pavement section for roads planned for widening and reconstruction in the form of pavement design catalogs. It is intended for use by TxDOT District Maintenance and Design Engineers to obtain a quick assessment of the pavement structural section for a 10-year design life.

METHODOLOGY FOR DEVELOPING PAVEMENT DESIGN CATALOG

Currently TxDOT designs flexible pavements with the computer program FPS21, and then the Texas Triaxial method is employed to check whether or not the pavement designs have enough structural thickness above the subgrade to avoid shear failure. The Texas Triaxial method is appropriate for those pavements with aggregate base materials (i.e., flex base). Thus, researchers generated pavement design curves with FPS and, when appropriate, used the Texas Triaxial check for various scenarios that maintenance supervisors and engineers often find on roadways. Analysis of available traffic data in energy affected areas was used to establish traffic loading as a function of the number of gas or oil wells being served. These traffic loadings were then added to the typical non-energy related traffic loadings. The result is a simplified pavement design catalog based on the design curves for various traffic levels in energy affected areas.

Pavement rehabilitation practices associated with the repair of oil and gas development and production activities typically involve some type of pavement strengthening operations either performed by maintenance forces or a maintenance or construction contract. These operations include deep patches, widening of the roadway or rehabilitation of the entire roadway section. The determination of the structural thickness of the pavement is an important part of selecting a maintenance or rehabilitation alternative for a particular roadway.

Typical rehabilitation sections used by TxDOT in the oil and gas fields employ FDR to pulverize and widen the existing roadway, the placement of a flexible base over the FDR, followed by an asphalt bound surface, which is either a surface treatment or HMA. FDR operations are sometimes performed without the addition of a stabilizer. The use of portland cement at a level of 2 to 3 percent (cement modified [CM]) with the FDR operation is common. Districts increasingly are using asphalt emulsions and foamed asphalt as binders in full depth recycling operations. Flexible base is often placed on top of the FDR layer. Some districts have used portland cement as a stabilizer with the new flexible base material. The use of portland cement stabilization as a base course is discouraged if a surface treatment or thin HMA layers are to be used as a wearing or surface layer, as reflection cracking will occur.

There are two types of structures typically used in the rehabilitation of energy sector roads. One of these is a 4-layer pavement structure, a FDR of the existing pavement, followed by a granular base layer plus either a surface treatment or an HMA layer. The other is a 3-layer pavement where FDR is performed and placed on the subgrade and overlaid with either an asphalt surface mix or a two-course surface treatment or HMA. Figure 54a shows a typical 4-layer pavement structure. Generally, the FDR thickness is a minimum of 6 in., and typically stabilized with portland cement, asphalt emulsion, or foamed asphalt. For surface layers, there are four options: 1) two-course surface treatment, 2) 2-in. asphalt layer, 3) 4-in. asphalt layer, and 4) 6-in. asphalt layer. Figure 54b shows a 3-layer pavement structure. The pavement design process is used to determine the thickness of the flexible pavement layer for the 4-layer option and to determine the thickness of FDR for the 3-layer structure.

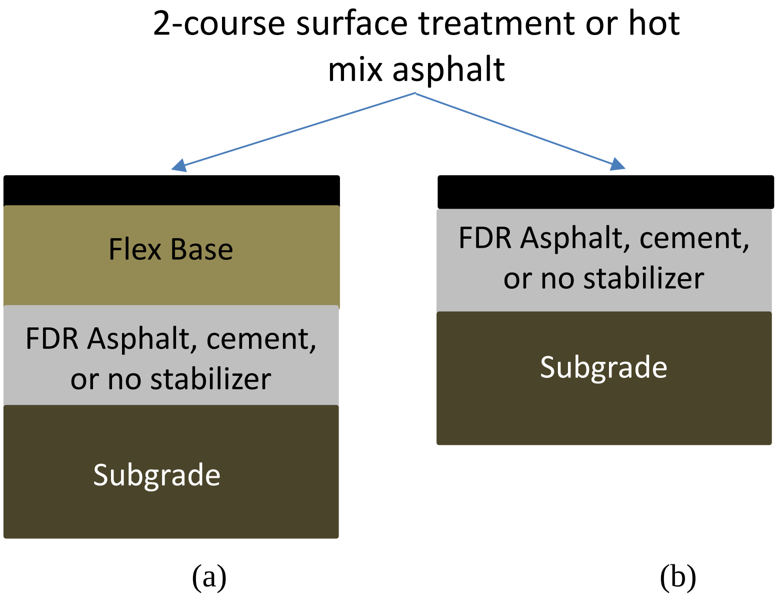
2-course surface treatment or hot mix asphalt
Flex Base
FDR Asphalt, cement, or no stabilizer
Subgrade
FDR Asphalt, cement, or no stabilizer
Subgrade
(a)
(b)

Figure 54. (a) 4-Layer Pavement Structure for Rehabilitation and (b) 3-Layer Pavement Structure for Rehabilitation.

Two types of wearing or surface courses are typically used on oil and gas development and production impacted roadways: surface treatments or HMA. Typically, a double surface treatment is placed on top of the new flexible base material. It is recommended that a minimum of 4 in. of HMA be used in the south Texas districts. It is possible to use 2 in. of asphalt as a surface course when a stabilized FDR is placed directly below as a base course.

FPS21 Key Inputs

As mentioned earlier, FPS21 was used to determine the structural sections for the design catalog, after which a check on the Texas Triaxial criteria was performed. After discussing with the technical experts of this project panel, the following key parameters for FPS21 pavement design were selected:

- Length of analysis period: 10 years.
- Minimum time to first overlay: 8 years.
- Minimum time between overlays: 8 years.
- Design confidence level: C-95 percent.
- Initial serviceability index:
  - HMA: 4.5.
  - Surface treatment: 4.0.
- Final serviceability index: 2.5.
- ADT beginning: 4500.
- ADT, end 20 year: 7000.

- 18 kip ESALs (20 years): 0.1, 0.5, 1, 2, 3, 5, 10, 15, and 20 million.
- Pavement material properties: see Table 17.

Table 17. Pavement Material Properties for FPS21 Pavement Design.

Layer	Materials	Properties		Thickness (inch)	Comments
		Resilient Modulus (ksi)	Triaxial Class		
Surface	Surface treatment			Less than 1	Single and double surface treatments utilized
	Hot mix asphalt	500		4 and 6	New flexible base used with FDR subbase
Base	Flexible base	50		6 to 12	
	High stabilization	300		6 to 11	No flexible base used with these
	Medium stabilizatio	200		6 to 13	
	Low stabilization	100		6 to 15	
Subbase	FDR-salvaged	75		6 and 8	No stabilizer
	FDR-PC	150			
	FDR-asphalt	100			
Subgrade		7	5.8		
		10	5		
		20	3		

FDR-PC-full depth recycling with Portland cement as modifier (2 to 3 percent)
FDR-Asphalt-full depth recycling with asphalt emulsion or foamed asphalt as a stabilizer

**High, medium, and low levels of base stabilization should be based on the amount of material passing the No. 200 sieve, the PI of the material, and the amount of asphalt binder (emulsion or foam) used to obtain high, low, or medium modulus (stiffness).*

Texas Triaxial Key Inputs

The Texas Triaxial criteria were applied to the designs with flex base layers to ensure an adequate thickness to avoid shear failures in the subgrade. Discussions with the technical experts of this IAC panel led to the following inputs for the Texas Triaxial check of the FPS21 designs:

- Load level factor: Waive use of 1.3 factor for any case.
- Texas Triaxial Class (TTC):
  - 7 ksi ---------- TTC=5.8.
  - 10 ksi --------- TTC=5.0.
  - 20 ksi ----------TTC=3.5.
- Cohesiometer value (Cm):
  - FDR-PC: Cm=800.
  - FDR-Asphalt: Cm=300.
  - FDR-salvaged: Cm=100.

- HMA: Cm=550, regardless of HMA thickness.
- Always use the highest Cm value of the materials being incorporated. For example, if the pavement structure has two layers: FDR-PC and HMA, use Cm value corresponding to FDR-PC.

Fatigue Cracking and Rutting Evaluation

The M-E design approach used in FPS21 evaluates the potential for fatigue cracking and structural rutting. These two distresses are the product of a pavement that is too weak for the traffic, and must be accounted for in the structural design as they are among the most expensive problems to fix. In FPS21, the Asphalt Institute fatigue and rutting criteria were used as per the equations shown below. The fatigue equation is:

$$N_f = 7.92\times10^{-2}(\varepsilon_t)^{-3.291}(E_{AC})^{-0.854} \tag{5}$$

Where:

N_f = Number of loading cycles to failure.

ε_t = Tensile strain at the bottom of the HMA pavement layer.

E_{AC} = Modulus of the asphalt layer.

The rutting equation is:

$$N_f = 1.365\times10^{-9}(\varepsilon_v)^{-4.477} \tag{6}$$

Where:

N_f = Number of loading cycles to failure.

ε_v = Vertical compressive strain at the top of the subgrade.

If fatigue cracking or rutting failure was likely for a particular structure at a given design traffic loading, structure was not recommended for consideration.

PAVEMENT DESIGN CURVES FOR 4-LAYER PAVEMENTS

The 4-layer pavement structures were analyzed at the traffic levels presented above through FPS21 and Texas Triaxial check. Additionally, fatigue cracking for all asphalt concrete surfaced pavements and rutting potential for all pavements were analyzed. The subgrade modulus values were selected with typical values for the Eagle Ford Shale (EF) representing a soft condition (< 7 ksi), the typical values for the Permian Basin (PB) representing a stiff condition (>15 ksi), and the medium subgrade as being bracketed by the stiff and soft subgrades. A total of 24 pavement design curves were developed for the 4-layer cases, and these are described below.

These curves show the required thickness of flexible base for a 10-year pavement design for the subgrade modulus, surface type, and the 20-year forecasted traffic:

- Pavement surface layer: Surface treatments.
  - FDR with no stabilizer.
  - FDR with PC.
  - FDR with asphalt.
- Pavement surface layer: 4-in. HMA.
  - FDR with no stabilizer.
  - FDR with PC.
  - FDR with asphalt.
- Pavement surface layer: 6-in. HMA.
  - FDR with no stabilizer.
  - FDR with PC.
  - FDR with asphalt.

Figure 55 shows the type of design curves developed for the 4-layer pavements. In this case, the curves are for a double surface treatment over flex base over an asphalt stabilized FDR over subgrade. Figure 55(a) illustrates the flex base thickness required for different levels of traffic, FDR subbase thickness, and subgrade stiffness. Figure 55(b) shows the Triaxial Classification check for the same materials and conditions.

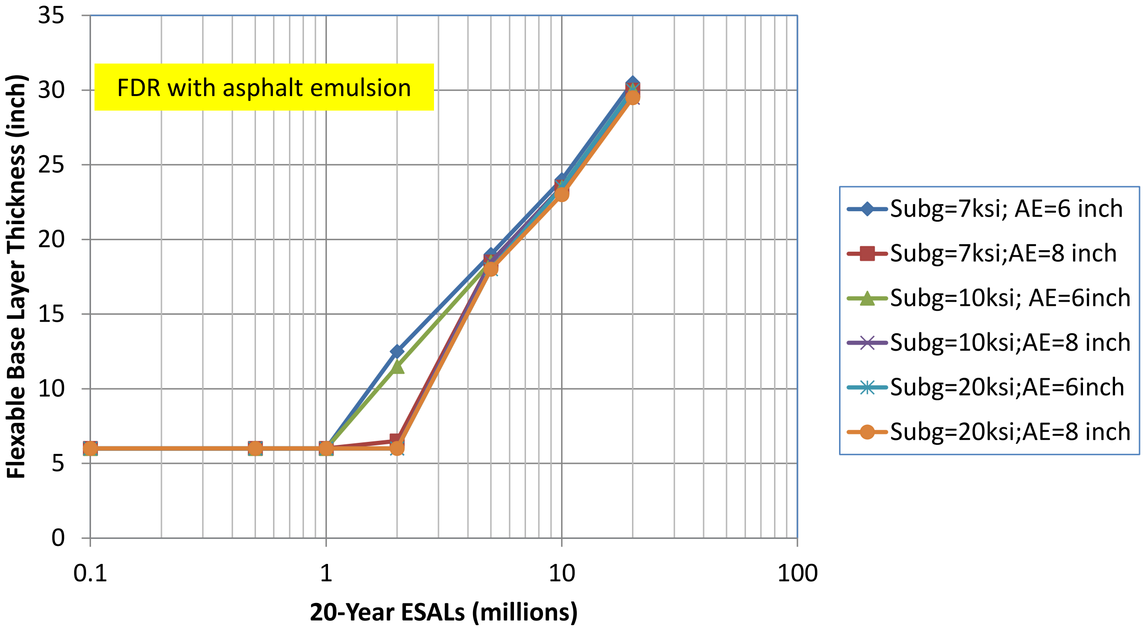

(a)

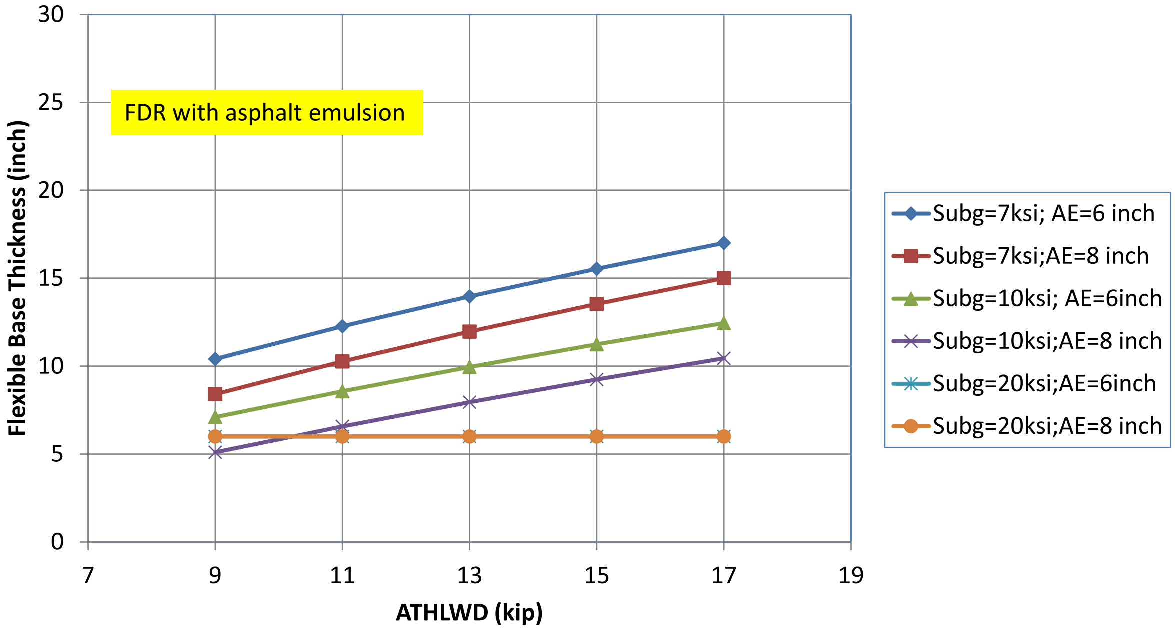

(b)

Figure 55. Pavement Design Curves for FDR with Asphalt Stabilization and Surface Treatments: (a) FPS Curves and (b) Triaxial Check.

PAVEMENT DESIGN CURVES FOR 3-LAYER PAVEMENTS

The 3-layer pavement structures were analyzed at the traffic levels presented above through FPS21. Additionally, fatigue cracking for all asphalt concrete surfaced pavements and rutting potential for all pavements were analyzed. A total of 36 pavement design curves were developed for the 3-layer cases, and these are described below.

These curves show the required thickness of stabilized base over subgrade for a 10-year pavement design for the subgrade modulus, stabilized base modulus, surface type, and the 20-year forecasted traffic. The subgrade modulus values were selected with typical values for the EF representing a soft condition (< 7 ksi), the typical values for the PB representing a stiff condition (> 15 ksi), and the medium subgrade as being bracketed by the stiff and soft subgrades. The stabilized base modulus values are ranked as stiff (300 ksi), medium (200 ksi), and soft (100 ksi). These values are somewhat subjective but the choice should reflect the amount of material passing the No. 200 sieve, the amount of high PI material present, and the degree of stabilization for the FDR base. The amount of minus No. 200 material will be dictated by the quality of the existing base course and the potential for clay soils to be picked up and incorporated into the base during the mixing process.

The thickness design curves for each combination of subgrade and base stiffness are as follows:

- Surface treatment surface.
- 2-in. AC surface.
- 4-in. AC surface.
- 6-in. AC surface.

Figure 56 shows the design curves for a 4-in. asphalt surface over the FDR base and three subgrade modulus values. For these pavements, the Triaxial check was not needed since flex base was not used. These graphs were used to obtain the required depth of FDR base at different levels of traffic.

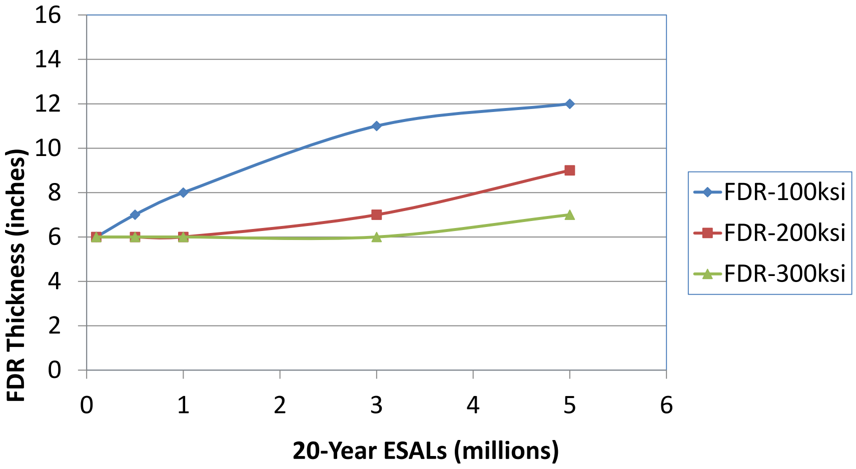

(a) Subgrade modulus= 7 ksi

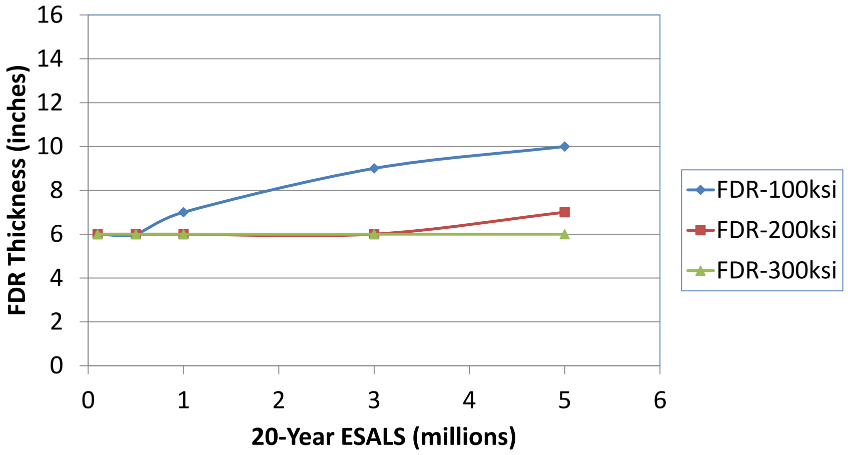

(b) Subgrade modulus=10 ksi

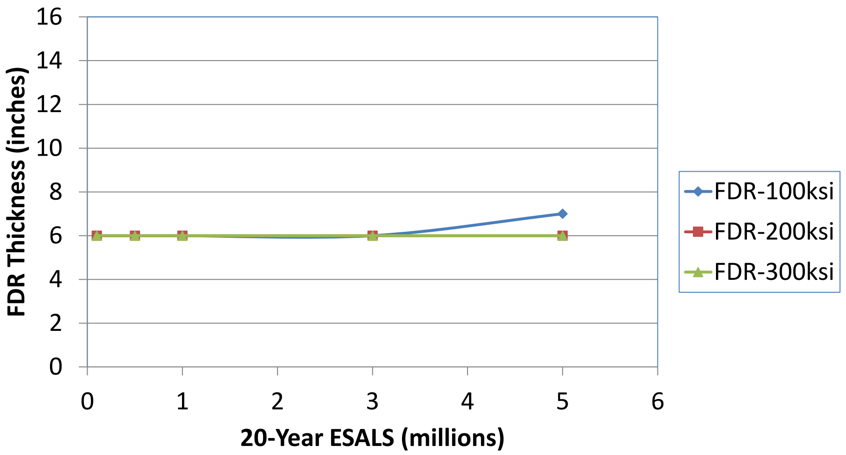

(c) Subgrade modulus= 20 ksi

Figure 56. 3-Layer Design Curves for 4-in. AC Surface.

TRAFFIC ANALYSIS

A systematic approach was taken to determine the ESALs in connection with the development and operation of typical horizontal, hydraulically fracked oil and gas wells in the EF, PB, and Barnett Shale (BS) regions of the state. The general process to determine ESALs for individual wells involved the following:

- Determining the number of trucks per well activity phase over a 20-year period. Truck volumes were estimated by relying on information in the literature from around the country as well as information gathered by TxDOT and data available from the FracFocus database (for the amount of water and sand used for fracking operations).
- The axle weight distribution was estimated for the truck types used for each phase of well development. This was accomplished by analyzing WIM data, which was tied to video logs of the weighed vehicles.
- The axle weight distribution for each truck type used was applied to the number of trucks per well development or operation phase and, with this information, the American Association of State Highway and Transportation Officials (AASHTO) road test equations were used to estimate the number of ESALs for each phase.
- The total number of ESALs from the development and operation phases was determined for arriving and departing trucks from an average well in the EF, PB, and BS formations. The variation in traffic generated per well in different regions is due to factors such as the amount of horizontal drilling versus vertical drilling, whether the products are primarily gas or oil, and the likely presence of pipelines. From the arriving and departing ESALs, the larger value was used for pavement design. Table 18 shows this information.

- The data in Table 18 were used with the number of wells served on a given route to calculate ranges of 20-year ESALs in each region. Thus, a maintenance supervisor or engineer can use a well count in an area to estimate the traffic level for design purposes.

Table 18. ESALs per Well during Development and Operation for Different Texas Formations (*5*).

	BS Region	EF Region	PB Region
Number of trucks	5,413	15,170	10,324
ESALs per well after 20 years (trip to well)	5,804	10,641	6,151
ESALs per well after 20 years (trip from well)	3,823	13,694	10,792

Next, it was necessary to determine the ATHWLD for the Triaxial check of the pavement section for the 4-layer cases where flex base is used. This estimate was provided by Figure 57, which shows the relationship between ATHWLD and ESAL.

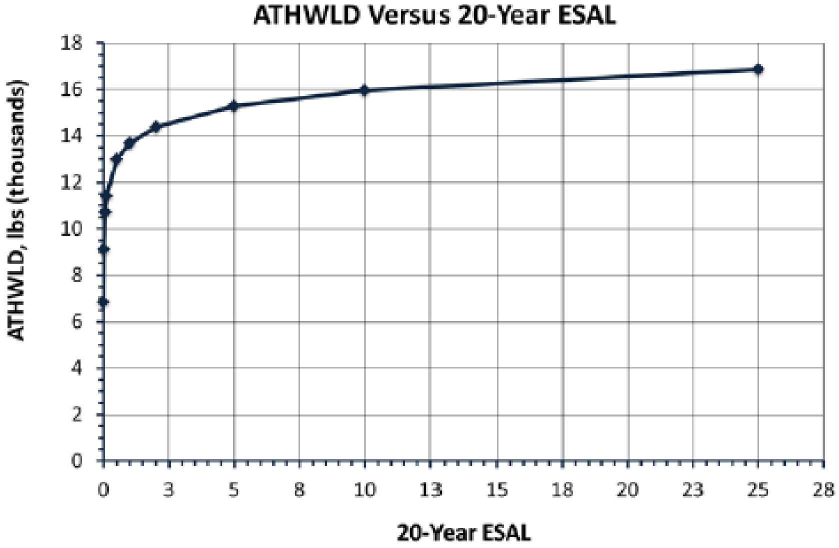

Figure 57. ATHWLD for 20-Year ESAL Level.

PAVEMENT DESIGN CATALOG TABLES

Once the 20-year ESAL level and the ATHWLD were determined for the number of wells served, the values were entered into graphs like those presented in Figure 55 to determine the flexible base thickness for each pavement structure and traffic level for the 4-layer pavement structures. The project panel of engineers decided upon a minimum flexible base thickness of 6 in. and a maximum of 12 in. for the 4-layer structures. The governing base thickness from FPS21 and the Texas Triaxial Classification check was determined, and the fatigue check was used to preclude premature failure. Also, sections requiring base thicknesses in excess of 12 in. were precluded as they exceeded the recommended maximum.

A similar procedure was used for the 3-layer pavements, except that a Triaxial check was not performed because there was no flexible base material used. In this case, the depth of thickness for the FDR base was determined by using graphs like those in Figure 56.

4-Layer Pavement Catalog (Surface, Flex Base, FDR, and Subgrade)

Table 19 shows the final form of the pavement design catalog for 4-layer pavements. To use it, the number of wells serviced by a particular route should be determined. There are three areas identified for the well count: BS, PB, and EF. If the expected traffic exceeds the maximum number of wells for a given region or 5 million ESALs, then a more formal approach to pavement design is recommended. Next, the subgrade stiffness should be determined. Soft subgrades are expected in the EF area, and stiff subgrades are expected in the PB. The engineer should use the general history of soil behavior in an area to select the subgrade stiffness. The type and thickness of FDR is located on the left column, and these are designated as CM, asphalt emulsion, or non-stabilized at either 6 in. or 8 in. Next locate the column with the desired surface type, either double-course surface treatment (2CST) or four, or 6-in. concrete (AC) or HMA. The resulting base thickness will be at the intersection of these. The blank boxes indicate sections that are not recommended for design due to possible premature failure.

As previously stated, the designs in Table 19 for flex base thickness had an additional check against the TxDOT Triaxial Classification to preclude shear failure in the subgrade, which explains the sometimes sudden jumps in required thickness of flexible base from one cell to another. In general, it is advisable to avoid the use of seal coat and 4-in. thick asphalt surfaces in high traffic (> 3 million ESAL) pavements as structural rutting and fatigue cracking may occur. However, 2CST may be used with 12 in. of flex base over a stiff subgrade for traffic up to 4 million ESAL. At higher traffic levels, HMA is the preferred surface material and a minimum thickness of 4 in. is recommended for this heavy traffic. The FPS-21 thickness design procedure should be used to determine the necessary pavement section.

As an example using Table 19 to determine the structural requirements for a pavement, assume a road is located in the EF (soft subgrade, modulus < 7 ksi) with approximately 125 wells expected. The existing roadway has an adequate amount of surface and base to allow for a FDR treatment to a depth of 8 in. With the CM option, the pavement section would be a 2CST over 10 in. of flex base over 8 in. of CM subbase. This may be compared with the asphalt emulsion or non-stabilized subbase option where 12 in. of flex base is required for the same surface and same thickness of subbase. These are illustrated in Figure 58. Surface treatments should not be used when predicted 20-year ESALs are at 5.0 million and above.

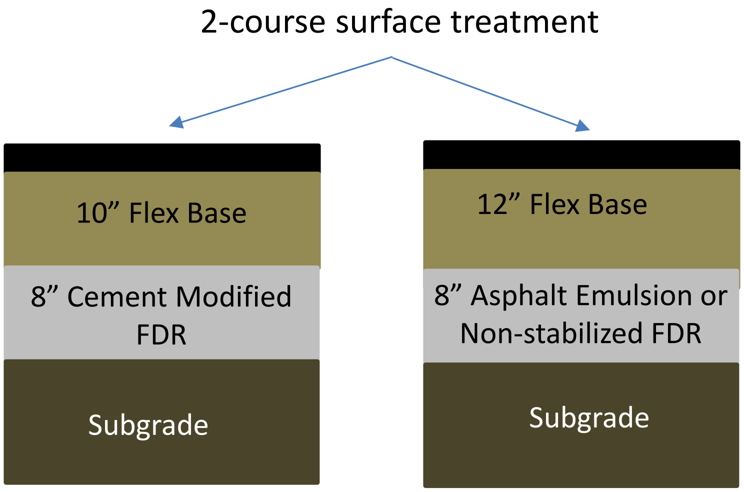
2-course surface treatment
10” Flex Base
8” Cement Modified FDR
Subgrade
12” Flex Base
8” Asphalt Emulsion or Non-stabilized FDR
Subgrade

Figure 58. Comparison of Pavement Sections Using Table 19 for 2 Million ESAL, Soft Subgrade, and 8 In. of FDR.

Table 19. Pavement Design Catalog for 4-Layer (Surface, Flex Base, FDR, Subgrade) Pavement. Numbers in Table Are Flex Base Thickness in Inches.

Traffic ESAL	**< 0.5 Million**			**0.5-1.5 Million**			**1.5-3.0 Million**			**3.0-4.0 Million**			**4.0-5.0 Million**			**> 5.0 Million**
EF #Wells	<10			10-90			90-200			200-270			270-340			Use Formalized Design
PB #Wells	<20			20-110			110-250			250-340			340-440			
BA #Wells	<40			40-210			210-470			470-640			640-810			
Eagle Ford (Subgrade Modulus < 7 ksi)																
Surface	2CST	4" HMA (PG 64-22)	6" HMA (PG 64-22)	2CST	4" HMA (PG 64-22)	6" HMA (PG 64-22)	2CST	4" HMA (PG 64-22)	6" HMA (PG 64-22)	2CST	4" HMA	6" HMA (PG 64-22)	2CST	4" HMA	6" HMA (PG 64-22)	
CM 6"	11	7	6	12	8	6	12	9	7	-	-	7	-	-	7	
CM 8"	9	6	6	10	6	6	10	7	6	-	-	6	-	-	6	
AE/NS 6"	12	8	6	12	9	7	12	10	7	-	-	8	-	-	8	
AE/NS 8"	12	6	6	12	7	6	12	10	7	-	-	8	-	-	8	
Medium Subgrade (7< Subgrade Modulus < 15 ksi)																
CM 6"	7	6	6	10	6	6	12	6	6	-	-	6	-	-	6	
CM 8"	6	6	6	7	6	6	10	6	6	-	-	6	-	-	6	
AE/NS 6"	12	6	6	12	6	6	12	6	6	-	-	6	-	-	6	
AE/NS 8"	12	6	6	12	6	6	12	6	6	-	-	6	-	-	6	
Permian Basin (Subgrade Modulus >15 ksi)																
CM 6"	6	6	6	6	6	6	10	6	6	12	-	6	-	-	6	
CM 8"	6	6	6	6	6	6	10	6	6	12	-	6	-	-	6	
AE/NS 6"	6	6	6	6	6	6	12	6	6	12	-	6	-	-	6	
AE/NS 8"	6	6	6	6	6	6	12	6	6	12	-	6	-	-	6	

Legend:
EF #Wells = number of wells serviced by road in the Eagle Ford Shale
PB #Wells = number of wells serviced by road in the Permian Basin
BS #Wells = number of wells serviced by road in the Barnett Shale
CM 6" = Cement Modified FDR, 6 in. thick
CM 8" = Cement Modified FDR, 8 in. thick
AE/NS 6" = Asphalt Emulsion FDR or Non-stabilized FDR, 6 in. thick
AE/NS 8" = Asphalt Emulsion FDR or Non-stabilized FDR, 8 in. thick
PG 64-22= dense-graded HMA with PG 64-22

■ *Not recommended due to premature failure expected*

3-Layer Pavement Catalog (Surface, FDR Base, and Subgrade)

The designs presented in are for surfaces placed directly on stabilized FDR bases. The stabilization in this case may be cement modification, asphalt emulsion, or foamed asphalt. The traffic level categories are at the top of the table, and there are three cases of subgrade stiffness as in Table 20. In Table 20, the degree of stabilization is considered to be related to the stiffness. This should be determined by the amount of material passing the No. 200 sieve, the likelihood of high PI material contaminating the FDR, and the amount of stabilization present. There are three levels of stabilized FDR base stiffness along the left side of the table: high (modulus = 300 ksi), medium (modulus = 200 ksi), and soft (modulus = 300 ksi). Because of the stiffness and thickness of the FDR bases, all the sections presented in Table 20 passed the mechanistic criteria for rutting and fatigue.

An example for using Table 20 is to compare medium stiffness stabilized FDR base thicknesses for a road serving 80 wells in the PB with a high stiffness subgrade for surface treatment, 2 in. of asphalt mix surface, and 4 in. of asphalt mix surface. Reading the chart shows that the surface treatment requires 8 in. of FDR, a 2-in. asphalt surface requires 7 in., and a 4-in. asphalt surface needs 6 in., as seen in Figure 59.

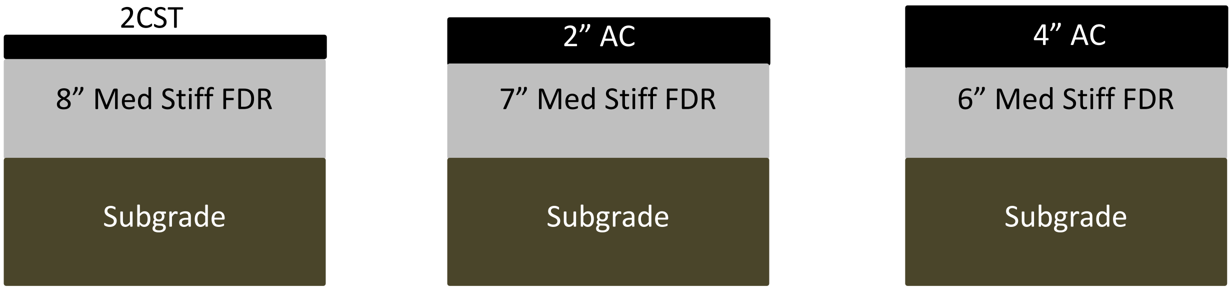

Figure 59. Comparison of Pavement Sections Using Table 20 for 80 Wells in PB with Stiff Subgrade and Medium Stiffness FDR.

Table 20. Pavement Design Catalog for 3-Layer (Surface, FDR, Subgrade) Pavement. Numbers in Table Are Flex Base Thickness in Inches.

Traffic ESAL	**< 0.5 Million**				**0.5-1.5 Million**				**1.5-3.0 Million**			
EF #Wells	<10				10-90				90-200			
PB #Wells	<20				20-110				110-250			
BA #Wells	<40				40-210				210-470			
Eagle Ford (Subgrade Modulus < 7 ksi)												
Surface	2CST	2" HMA (PG 64-22)	4" HMA (PG 64-22)	6" HMA (PG 64-22)	2CST	2" HMA (PG 64-22)	4" HMA (PG 64-22)	6" HMA (PG 64-22)	2CST	2" HMA (PG 64-22)	4" HMA (PG 64-22)	6" HMA (PG 64-22)
Stiff Base	8	6	6	6	9	7	6	6	10	8	6	6
Med Base	9	7	6	6	11	9	6	6	11	9	7	6
Soft Base	11	9	7	6	14	11	9	7	15	12	10	8
Medium Subgrade (7 ksi <Subgrade Modulus <15 ksi)												
Stiff Base	7	6	6	6	8	7	6	6	9	7	6	6
Med Base	8	6	6	6	10	8	6	6	10	8	6	6
Soft Base	10	8	6	6	13	10	8	6	13	11	9	6
Permian Basin (Subgrade Modulus >15 ksi)												
Stiff Base	6	6	6	6	7	6	6	6	7	6	6	6
Med Base	7	6	6	6	8	7	6	6	8	7	6	6
Soft Base	8	6	6	6	10	8	6	6	10	8	6	6

Legend:
EF #Wells = number of wells serviced by road in the Eagle Ford Shale
PB #Wells = number of wells serviced by road in the Permian Basin
BS #Wells = number of wells serviced by road in the Barnett Shale
Stiff base (FDR) modulus= 300 ksi
Medium base (FDR) modulus= 200 ksi
Soft base (FDR) modulus= 100 ksi
PG 64-22= dense-graded HMA with PG 64-22

■ *Not recommended due to premature failure expected*

Table 21. Pavement Design Catalog for 3-Layer (Surface, FDR, Subgrade) Pavement. Numbers in Table Are Flex Base Thickness in Inches (continued).

Traffic ESAL	**3.0-4.0 Million**				**4.0-5.0 Million**				**>5.0 Million**
EF #Wells	200-270				270-340				Use Formalized Design
PB #Wells	250-340				340-440				
BA #Wells	470-640				640-810				
Eagle Ford (Subgrade Modulus < 7 ksi)									
Surface	2CST	2" HMA (PG 64-22)	4" HMA (PG 64-22)	6" HMA (PG 64-22)	2CST	2" HMA (PG 64-22)	4" HMA (PG 64-22)	6" HMA (PG 64-22)	
Stiff Base	-	8	7	6	-	8	7	6	
Med Base	-	10	8	6	-	11	9	6	
Soft Base	-	14	12	9	-	15	12	9	
Medium Subgrade (7 ksi < Subgrade Modulus < 15 ksi)									
Stiff Base	-	8	6	6	-	8	6	6	
Med Base	-	9	7	6	-	10	7	6	
Soft Base	-	12	10	7	-	13	10	7	
Permian Basin (Subgrade Modulus > 15 ksi)									
Stiff Base	-	7	6	6	-	7	6	6	
Med Base	-	8	6	6	-	8	6	6	
Soft Base	-	9	7	6	-	10	7	6	

Legend:
EF #Wells = number of wells serviced by road in the Eagle Ford Shale
PB #Wells = number of wells serviced by road in the Permian Basin
BS #Wells = number of wells serviced by road in the Barnett Shale
Stiff base (FDR) modulus= 300 ksi
Medium base (FDR) modulus= 200 ksi
Soft base (FDR) modulus= 100 ksi
PG 64-22= dense-graded HMA with PG 64-22

■ *Not recommended due to premature failure expected*

TxME Verification for the Pavement Design Catalog

After obtaining the pavement design catalog using the FPS21, TxME was used for further verification of the pavement design catalog based on the simulated rutting and fatigue results. In the TxME simulation, several types of asphalt mixtures can be choices for HMA layer. In all the simulations herein, the HMA layer used dense-graded with PG 64-22 (Type D). The traffic input was the same as that used in FPS21. The analysis period was 10 years. Although the total number of ESALs for 20 years was used for the traffic input, the actual total number of ESALs for the 10-year analysis period was less than a half of the total number of ESALs for 20 years. San Antonio, TX, was selected as the climate station. All the designs in the catalog have been verified in TxME and pass the rutting and fatigue failure criteria.

Table 22 and Table 23 show the pavement designs selected from Table 19 and Table 20 for 4-layer design and 3-layer design, respectively. These selected pavement designs used for demonstration of TxME simulation results. The value of 10 ksi was used for the medium subgrade modulus in the simulation. The rutting limit was 0.5 in., and the fatigue cracking area limit was 50 percent.

For 4-layer designs, the 2CST showed a higher rutting depth than the HMA layer, but still was below the rutting limit. The designs with HMA layer (either 4-in. HMA or 6-in. HMA) and different FDR layers (i.e., CM, asphalt emulsion, and no stabilizer) showed the comparable rutting depth and fatigue cracking area. Thus, the cost of the pavement construction was the key factor for the final selection of the pavement design.

For 3-layer designs, the 2CST with stiff FDR base had the similar rut depth compared with medium FDR base. The designs with a HMA layer (i.e., 2-in. HMA or 4-in. HMA) and a FDR base layer (i.e., stiff FDR, medium FDR, or soft FDR) exhibited comparable rut depths. The fatigue cracking area was very low for all the cases presented herein.

Table 22. 4-Layer Designs Selected for Demonstration of TxME Results.

Traffic ESAL	**1.5-3.0 Million** (select 3.0 million for TxME verification)			**4.0-5.0 Million** (select 5.0 million for TxME verfication)		
EF #Wells	90-200			270-340		
PB #Wells	110-250			340-440		
BA #Wells	210-470			640-810		
Medium Subgrade (7 < subgrade modulus < 15 ksi)						
Surface	2CST	4" HMA (PG 64-22)	6" HMA (PG 64-22)	2CST	4" HMA (PG 64-22)	6" HMA (PG 64-22)
CM 6"	12	6	6	-	-	6
CM 8"	10	6	6	-	-	6
AE/NS 6"	12	6	6	-	-	6
AE/NS 8"	12	6	6	-	-	6

Table 23. 3-Layer Designs Selected for Demonstration of TxME Results.

Traffic ESAL	**1.5-3.0 Million** (select 3.0 million for TxME verification)			**4.0-5.0 Million** (select 5.0 million for TxME verfication)		
EF #Wells	90-200			270-340		
PB #Wells	110-250			340-440		
BA #Wells	210-470			640-810		
Medium Subgrade (7 ksi < subgrade modulus < 15 ksi)						
Surface	2CST	2" HMA (PG 64-22)	4" HMA (PG 64-22)	2CST	2" HMA (PG 64-22)	4" HMA (PG 64-22)
Stiff Base	7	6	6	-	8	6
Med Base	8	6	6	-	10	7
Soft Base	10	8	6	-	13	10

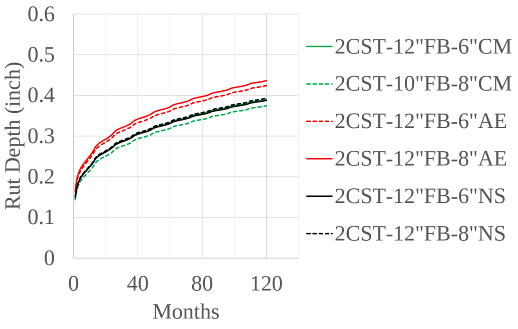

(a) 2CST

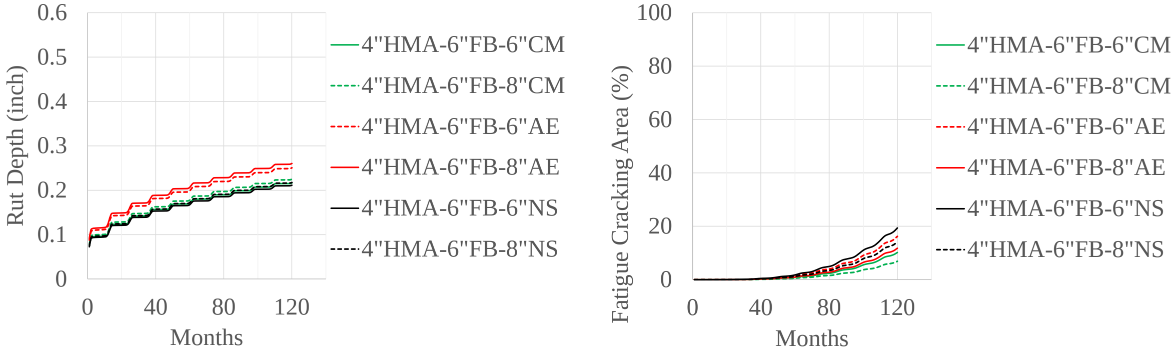

(b) 4-in. HMA

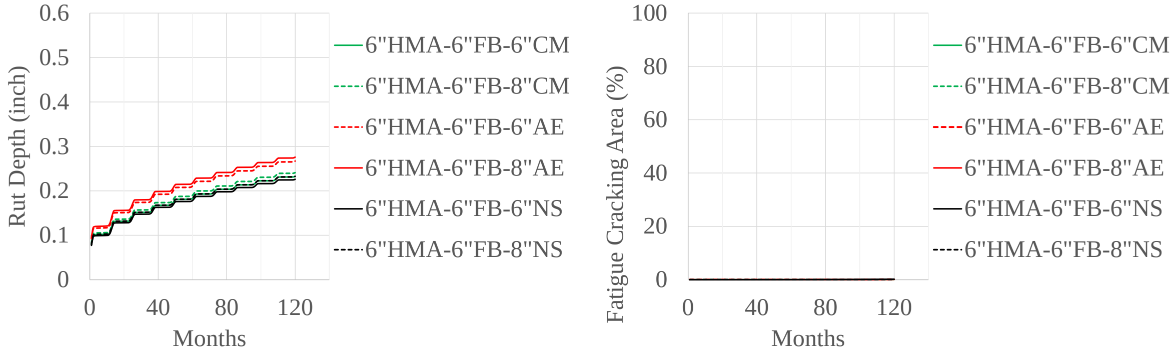

(c) 6-in. HMA

Figure 60. Four Layers: TxME Results for Subgrade Modulus 10 ksi and 3.0 Million ESAL.

(Legend example: 2CST-12”FB-6”CM= double-course surface treatment+12 in. flexible base+6 in. cement-modified layer)

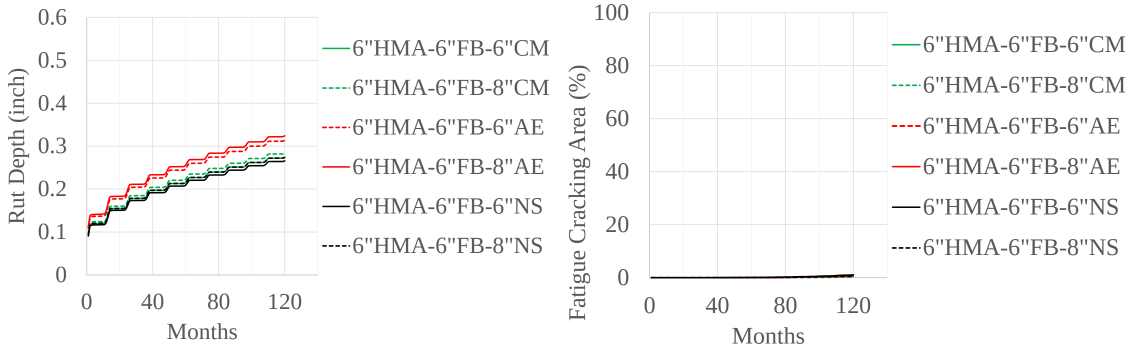

Figure 61. Four Layers: TxME Results for Subgrade Modulus 10 ksi and 5.0 Million ESAL.

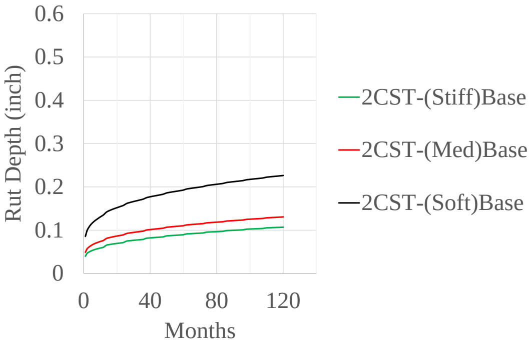

(a) 2CST

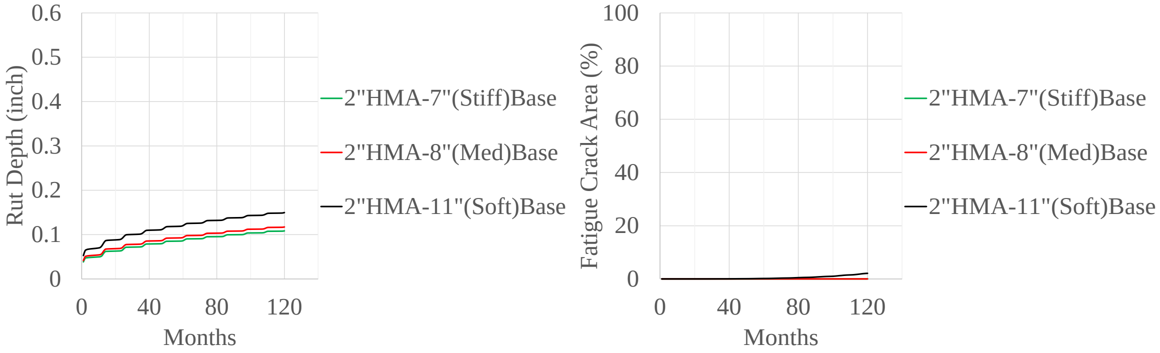

(b) 2-in. HMA

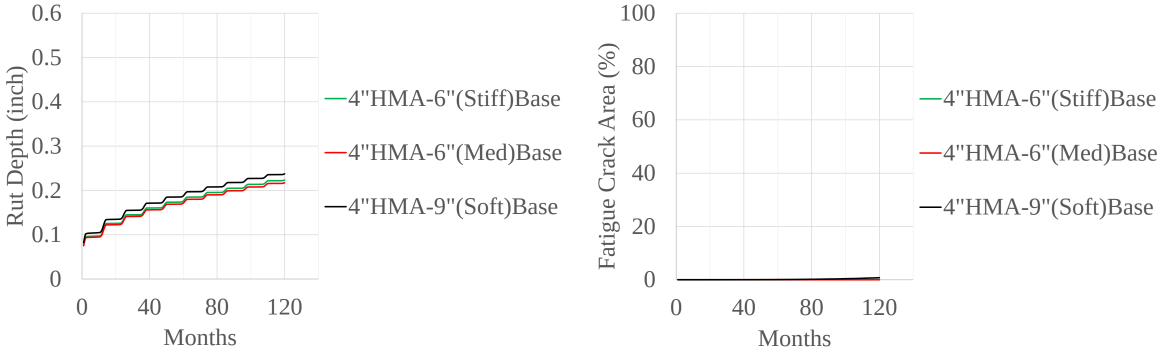

(c) 4-in. HMA

Figure 62. Three Layers: TxME Results for Subgrade Modulus 10 ksi and 3.0 Million ESAL.

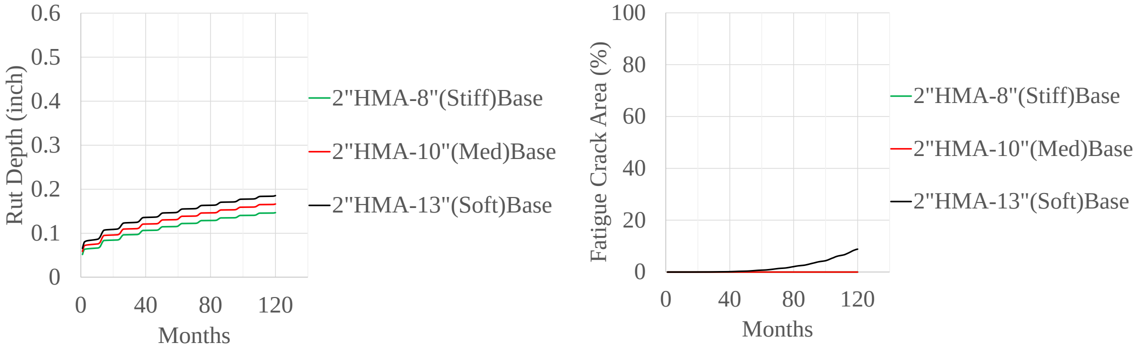

(a) 2-in. HMA

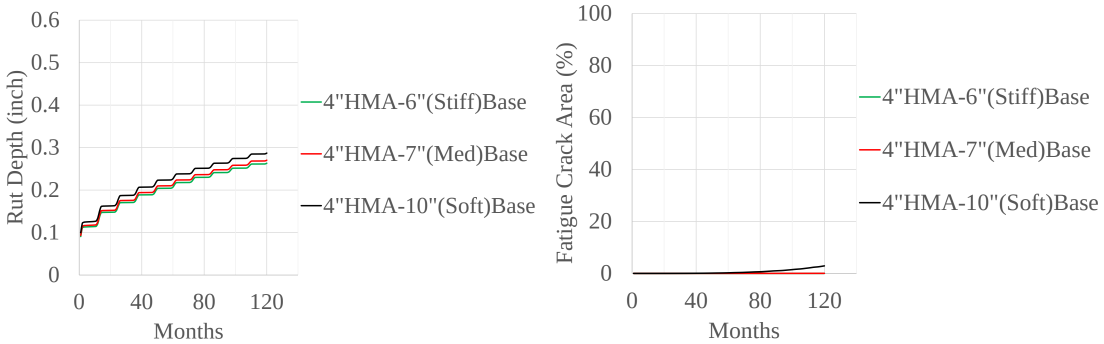

(b) 4-in. HMA

Figure 63. Three Layers: TxME Results for Subgrade Modulus 10 ksi and 5.0 Million ESAL.

CHAPTER 6. CONCLUSIONS AND RECOMMENDATION

CONCLUSIONS

Based on the research presented in this report, the following conclusions and recommendation are made:

- Total ESAL for a design period calculated from the tradition method (i.e., using the equation based on ADT) is much lower than from the TxME-load spectra, which means the total ESAL is significantly underestimated when using the tradition methodology.
- The ESAL calculation based on the AADTT may not be accurate while the calculation from TxME-load spectra is more accurate. For the FM road in energy development area, the AADTT could be much lower than the US or SH with medium traffic volume, but the ESAL calculated from TxME-load spectra indicated that it could have the similar ESAL with the US or SH. For example, FM 468 has a much lower AADTT but the comparable ESAL value with SH 114. Thus, it is recommended that the ESAL calculated from TxME-load spectra should be used for the design for the roads in the energy development areas.
- The guidance for selecting optimal flexible pavement rehabilitation options has been proposed and demonstrated in this report.
- The IDT test is used for laboratory mix design for FDR option. When the foamed asphalt is used for stabilizer, at least 1 percent cement also needs to be added in the mixture to improve the wet strength to meet the IDT requirement. Emulsion asphalt as a stabilizer generally can meet both the dry and wet IDT strength requirements, and there is no need to add cement to improve the wet strength.
- The test methodology using dynamic modulus for FDR stabilizer materials is explored, and it can be used for determining modulus input in M-E design software such as TxME. The dynamic modulus test results indicate that the temperature can affect the modulus of asphalt stabilized materials including foamed asphalt and emulsion asphalt as stabilizers.
- Nondestructive tests are used for the projects with implementation of FDR. The FWD test results after construction indicate that the modulus of FDR layer improved significantly with the increase of curing time and the modulus of FDR layer treated with cement or foamed asphalt plus cement or emulsion has an excellent value exceeding 300 ksi. However, the FDR layer treated with only foamed asphalt without cement could have a lower modulus (i.e., < 200 ksi).
- The pavement design catalog used for energy development areas has been developed based on FPS21. In addition, TxME has been used to verify all the designs in the catalog that pass the failure criteria for the rutting and fatigue.

RECOMMENDATION

The field projects with implementation of FDR should be further monitored for the pavement performance.

PART II: RIGID PAVEMENTS

CHAPTER 1. ANALYSIS OF TEXAS RCC FIELD PERFORMANCE DATA

INTRODUCTION

Part II examine roller compacted concrete (RCC) pavements currently in-place in Texas to assess the performance this pavement type. The sites are in areas of high energy sector traffic most of the sites have large traffic loads. The research visually surveys RCC pavements and uses the falling weight deflectometer (FWD) to evaluate their effectiveness. Some drainage tests were also looked at for the pavement joints. Common distresses are noted in the report along with the test data, the analysis, and some recommendations for RCC pavements. The sites visited re the Pioneer Natural Resources USA, SEC Energy Products & Services, Bella Vista Community, and Solms Rd. Additional data from previous tested sites in Brownsville, TX, are also included in the report. The report includes site photos and figures for reference.

The Pioneer Natural Resources facility is located outside of Victoria, TX. The site is an 8-in. RCC pavement used by heavy truck traffic for oil field equipment. The visual survey of the site noted that the majority of the area had no drainage and outer areas experienced some separation in slab jointing. The notable distresses were blowups throughout the center of the entire site. Heavy cracking was found on the higher traffic routes, and signs of the joints separating sufficient enough that drainage is occurring under the pavement layer. FWD testing yielded high deflections in much of the site and in compared to the other sites visited.

The SEC Energy site is located in north-central Houston and is used for transporting and constructing large energy equipment and products. The pavement is 15-in. thick pavement, and the joints are interlocked with staggered lifts poured. The pavement visually looked in good condition with the only major distress noted that the longitudinal joints are beginning to spall. The joints were all tightly compressed allowing no drainage through joints. This site was visited once in the summer and then again in the winter to compare the FWD results between the two.

The Bella Vista site is actually two sites in the community of Plum Grove, right outside of Splendora, TX, which is north of Houston. The site is paved with RCC throughout both areas but one area also has pavement with different base materials thatwere compared in the research. The pavement condition was great but the site is fairly new and some areas are not yet open to traffic. The only noted distress for this site was longitudinal joint separation around the long curves/bends in the road.

Solms Rd. is located in New Braunfels, TX, and is a city street that experiences heavy truck traffic. The road extended farther down but only the immediate section north of I-10 was tested. The pavement is much older than the other sites and visually does not look to be performing well at first. Visually the pavement has a higher amount of cracking but the cracks all appear to be tight with good load transfer. The longitudinal joint was experiencing some spalling of the pavement but mostly spalling of the repair material overlaid where the joint had maintenance done.

Overall the sites showed some common distresses, and each site visitedhas been overloaded with heavier and higher amounts of traffic. The sites are each compared and all FWD test data are tabulated in the field report. The performance of each is discussed in further detail with the proper reference figures and charts.

OBJECTIVE

Part II focused on RCC pavements across Texas to assess the quality and effectiveness of this pavement type. The pavement assessment reported herein consists of cracking ,performance surveys,running FWD, and permeability testing to determine actual deformation characteristics and to investigate common distresses to provide improvements for the design and use of RCC in selected Texas Department of Transportation (TxDOT) construction projects.

TESTING PLAN

The research will look at sites with different design thicknesses, ages, and traffic demands. Each site is discussed in detail with a summary provided at the end of each section. An overall summary of the all the sites is also included. Each site was examined during periods of warmer weather, and a few sites were examined during colder conditions for comparison.

SITES

- The performance data of RCC were collected from the following locations:The performance data of RCC were collected from the following locations:Pioneer Natural Resources USA, 15555 US Hwy 77 N, Victoria, TX 77904 (Figure 64–Figure 74).
- Standard Equipment Company (SEC) Energy Products & Services Complex, 9523 Fairbanks North Houston Rd, Houston, TX 77064 (Figure 75–Figure 87).
- Bella Vista Community, Bella Vista Dr./Plum Grove Rd, Cleveland, TX, 77327 (Figure 88–Figure 98).
- Solms Rd., North Solms Rd., New Braunfels, TX 78132 (Figure 99–Figure 106).
- Brownwood—Central Texas (Figure 107–Figure 110).

Pioneer, Victoria, TX

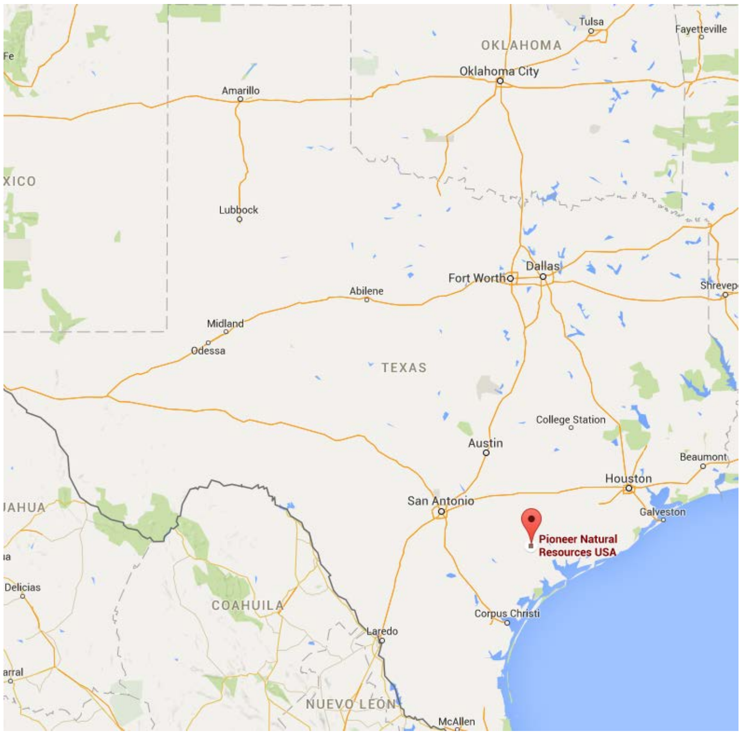
OKLAHOMA
Tulsa
Fayetteville
Oklahoma City
Amarillo
Lubbock
Dallas
Fort Worth
Shrevep
Abilene
Midland
Odessa
TEXAS
College Station
Austin
Beaumont
Houston
San Antonio
Galveston
Pioneer Natural Resources USA
COAHUILA
Delicias
Corpus Christi
Laredo
NUEVO LEON
McAllen

Figure 64. Map of Pioneer National Resources USA.

Site Description

The Pioneer site is a 60+ acre paved site (Figure 65 and Figure 66) used for storing and servicing heavy oil field equipment used by Pioneer Natural Resources. The site has three main buildings, one employee parking lot, a fueling station, and the rest is for storage space. The site was paved with RCC pavement with the employee parking area paved with a different RCC pavement section (same slab thickness but with a 12–18 in. stabilized subgrade). All buildings are on Portland cement concrete (PCC) foundations. Truck traffic is diverted in one direction around the facility; and currently with Pioneer's high production rate majority of truck traffic comes into the front service area and after a 24 hours maintenance routine is sent back out into the field, meaning that majority of the storage area for trucks is never used (Figure 67).

Drainage of the site consists of one concrete culvert paved at the front of the property and a low point graded to the north portion of the property. No inlets or underground drainage were present. Eighty percent plus of the property drains to the graded low point on the north side, which then drains from natural slope to the creek behind the property. Joint sealant was not used in the construction, and joint/crack separation is present and on-going. With the joints separating so much, a large amount of water is likely infiltration the pavement and is seemingly running between the base course and the pavement.

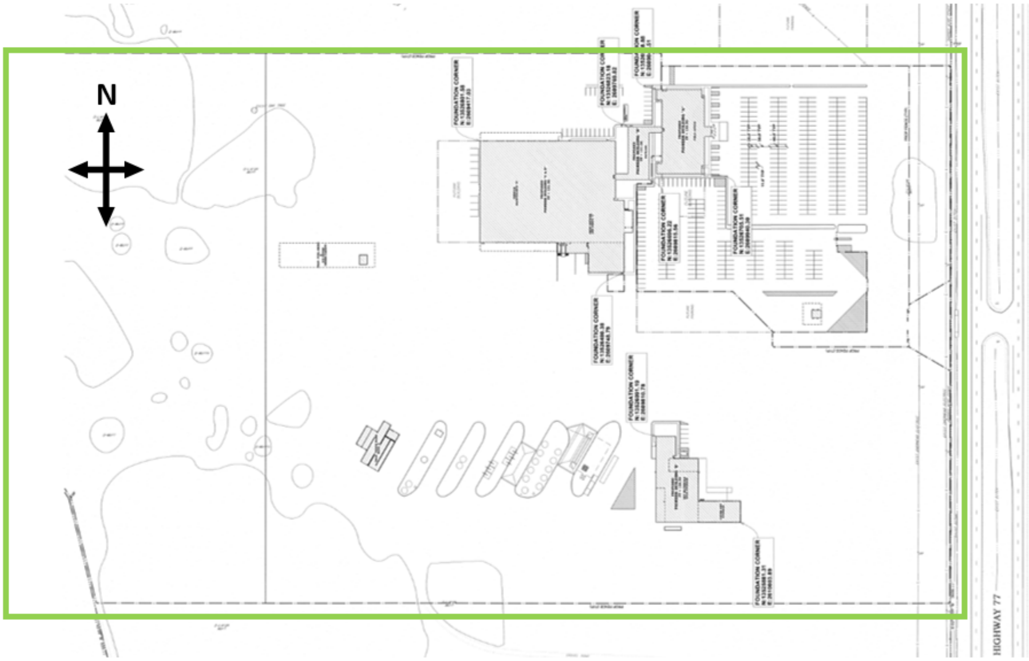
N
HIGHWAY 77
FOUNDATION CORNER

Figure 65. Pioneer Site Layout.

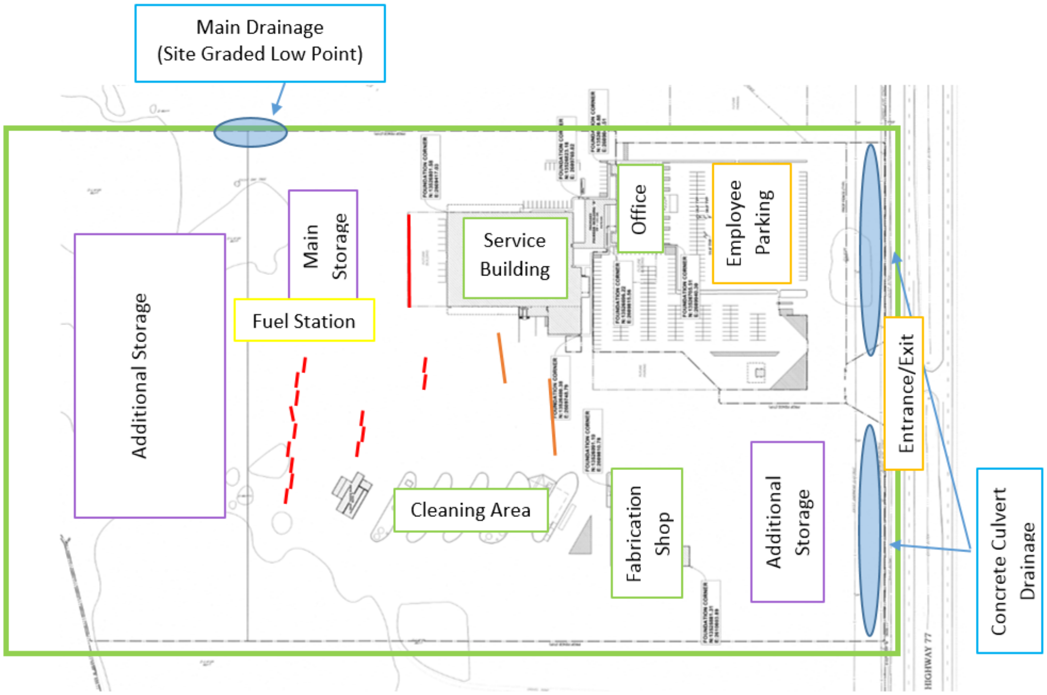
Main Drainage
(Site Graded Low Point)
Additional Storage
Main Storage
Fuel Station
Service Building
Office
Employee Parking
Entrance/Exit
Cleaning Area
Fabrication Shop
Additional Storage
Concrete Culvert Drainage
HIGHWAY 77

Figure 66. Pioneer Site Layout with Captions.

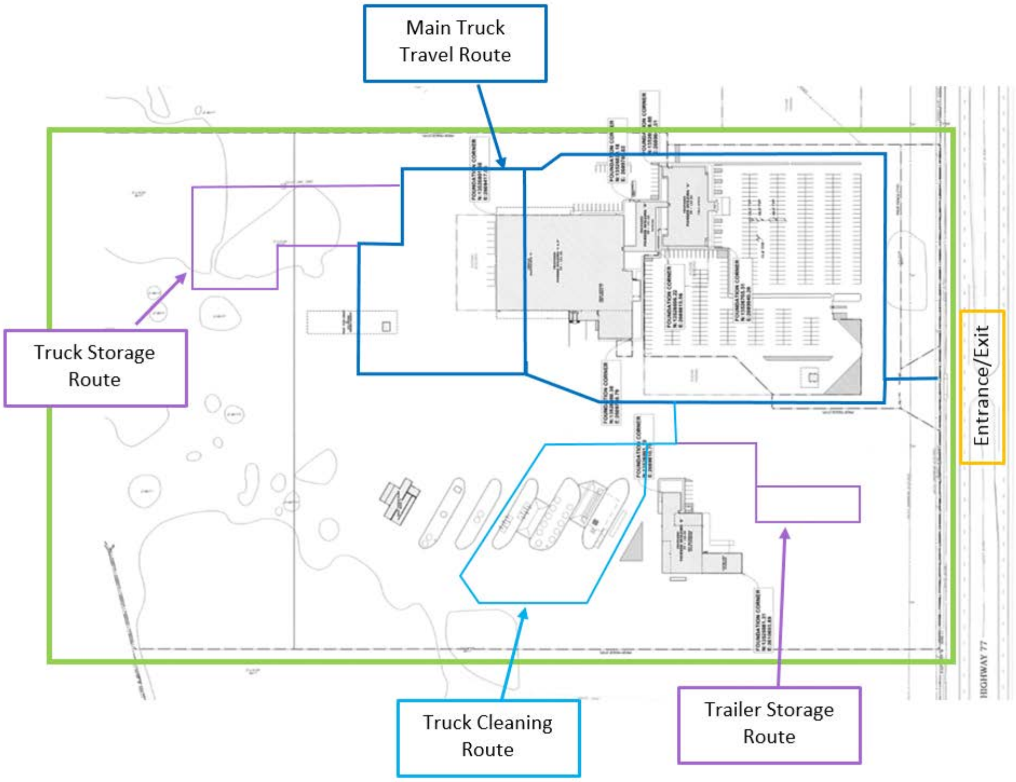
Main Truck Travel Route
Truck Storage Route
Entrance/Exit
Truck Cleaning Route
Trailer Storage Route
HIGHWAY 77

Figure 67. Pioneer Site Layout with Traffic Routes.

Pavement Section Details

For the Pioneer site, the following pavement section details were obtained:

- *Age*: 2 years (constructed summer 2013).
- *Structure:*
    - Layer 1: 8-in. RCC.
    - Subgrade: 6-in. stabilized subgrade.

Testing Description

The following testing list and condition were maintained to collect the required performance data:

- *Testing Performed:* July 9, 2015 (around 12:00 p.m.), Temp. = 90°F (dry conditions, minimal rainfall recently).
- *Tests:*
    - FWD.
    - Joint infiltration test.
    - Visual distress survey.

The FWD testing was performed following ASTM D4694. The FWD testing was performed on numerous joints around the facility (Figure 68), and the process used was to test within 6 in. of the approach side and then test within 6 in. from the leave side of the joint. Majority of testing was performed on transverse joints with some transverse cracks and longitudinal joints tested as well. FWD testing was also performed on key distress points and transition points of patching or PCC areas.

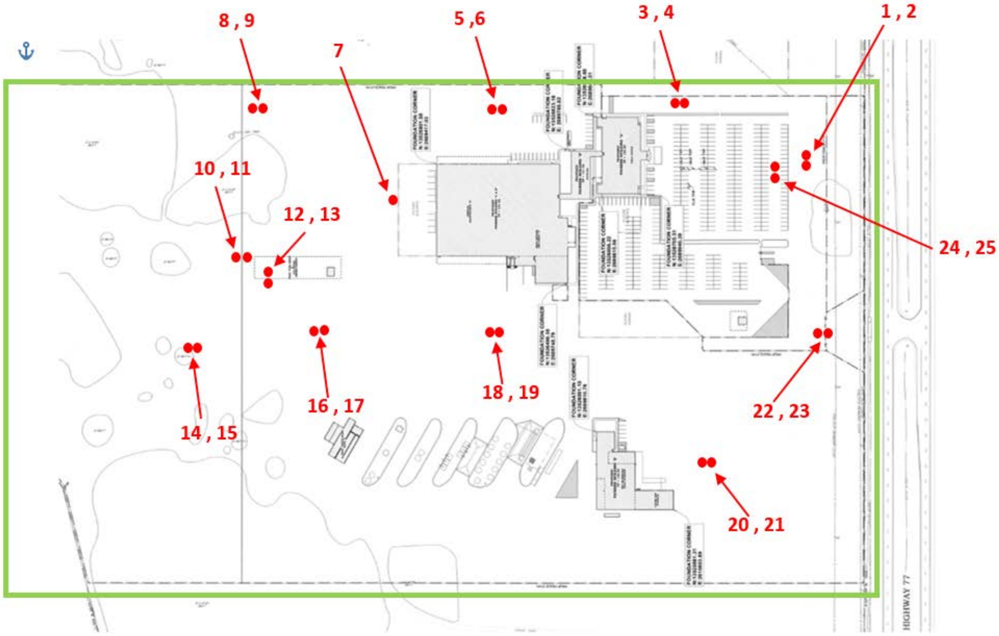

Figure 68. Pioneer FWD Testing Locations.

Infiltration tests were performed on each type of joint present and on distressed areas of faulting or separation (Figure 69). Note that the site has some major issues with slabs shifting and faulting. These distress have caused many of the joints to separate and open up substantially that many of the infiltration tests were difficult to seal against the free flow of the water along the joint rather than into the subgrade. To better summarize this, most of the joints were unsealed and have opened so wide the water freely flowed down the joint itself. Consequently, the test results from most of the locations did not indicate the permeability of the subgrade layer. This infiltration issue is also shown in the photo, located in the appendix, taken of the PCC cut-out in the fueling area that regularly fills with water immediately after being pumped out.

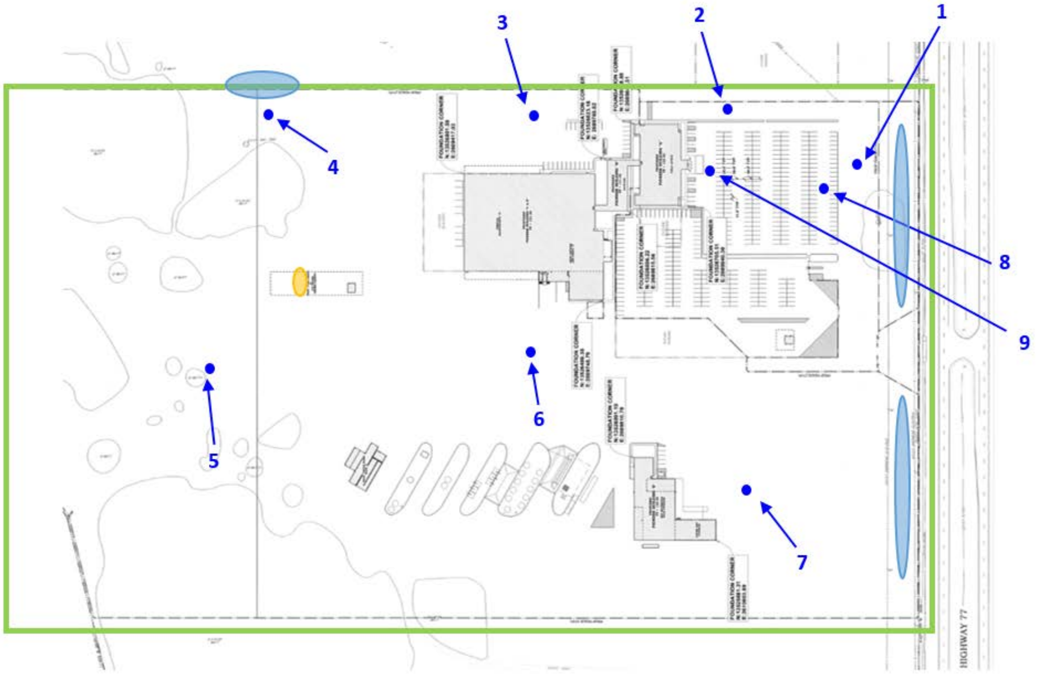

Figure 69. Pioneer Infiltration Testing Locations.

Distress Survey Results

The entire site was examined on foot and the following distresses were found:

- Faulting.
- Slab/joint separation (App. B, Figure 145).
- Blow-ups (App. B, Figure 147, Figure 148).
- Slab cracking (App. B, Figure 146).
- Corner breaks (App. B,Figure 144).
- Patching.

The majority of the truck traffic travels along a constant short route down the north end to the service bay, and then right back out through the center of the property. The areas of higher truck traffic exhibited higher distress quantities and severity. The faulting was found across the site with the high severity locations being in the heavier traffic lanes. Joint separation in the higher traffic lane exceeded ½ in. to the point that uninhibited water infiltration of joints was of high certainty. Many of the slabs experienced high enough deflections to visually observe the movement. This together with FWD data show signs of erosion of layers below the slabs. The blowups were found on the site where two of the five positions noted where the blow-ups occurred have been repaired using a FD PCC patch. Figure 70 shows the positions where the blow-up occurred.

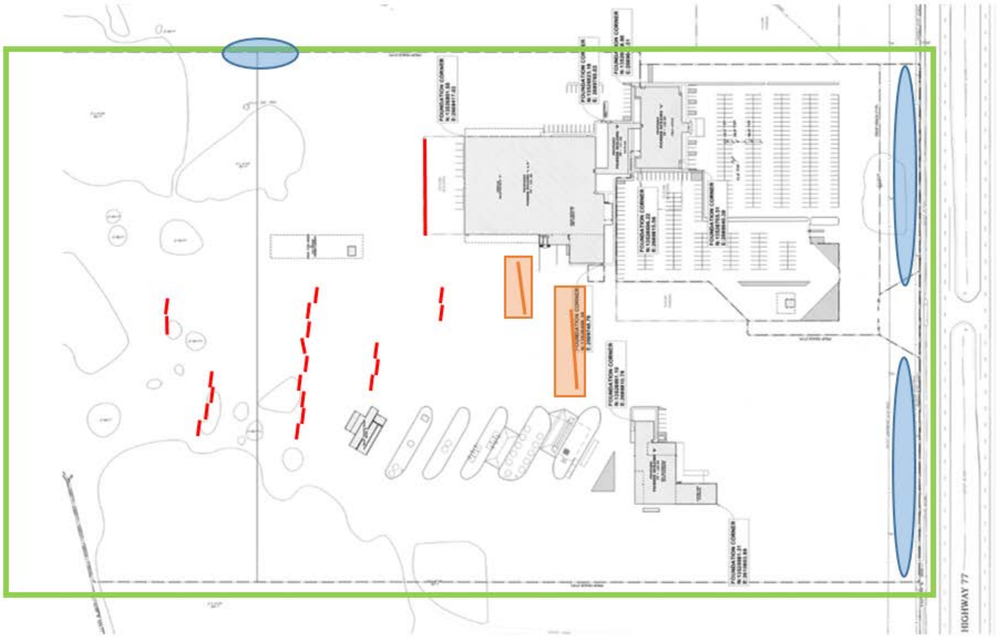

Figure 70. Pioneer Distress Locations.

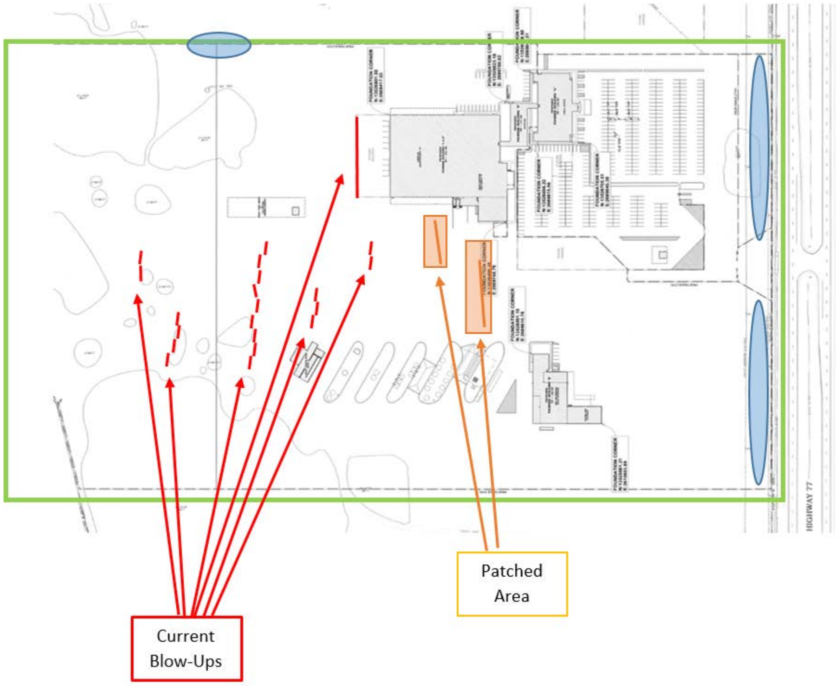
HIGHWAY 77
Patched Area
Current Blow-Ups

Figure 71. Pioneer Distress Locations with Captions.

Analysis of the data taken from the FWD was carried on according to the discussion provided in Appendix A. Key data from this analysis consisted of the effective pavement thickness (h_e), the composite k-Value of the subgrade, and the load transfer efficiency (LTE) of the joint or crack. Figure 72, Figure 73, and Figure 74 show these data. Based on the data shown in Figure 72, the pavement section is structurally deficient and highly variable. The pavement was nominally 8-in. thick that looked structurally to be much less than that varying from 2 to 7.5 in. These data are mainly representing the stiffness of cracks, joints, slab edges, and corners, but this is where the stiffness is needed, andthey suggest that a significant amount of erosion has taken place particularly in light of the quality of surface drainage that has existed at the site over the years.

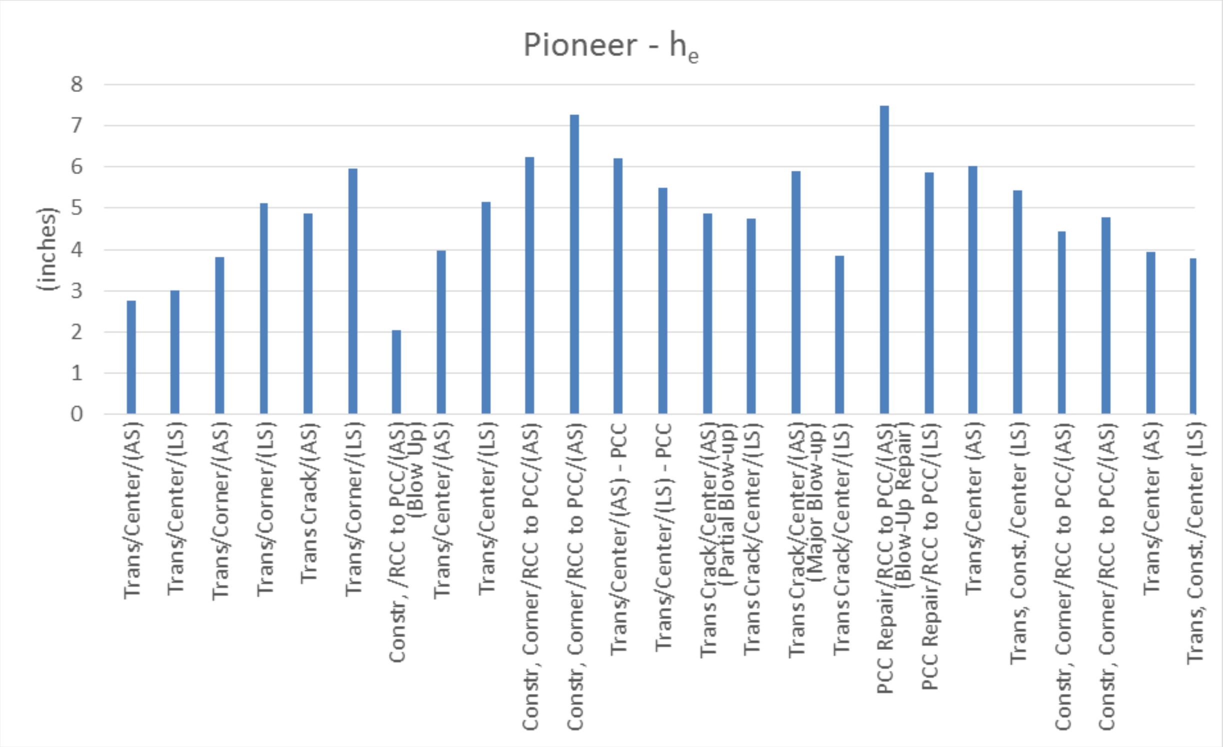

Figure 72. Pioneer Effective Thickness Chart.

Figure 73 shows the back calculated k-values. The variability is typically of subgrade support but the range in the values suggests some areas have high moisture contents and are possibility saturated again pointing to the quality of the drainage being very poor. Figure 74 shows the LTE results and again indicates the lack of stiffness along several cracks and corner slab areas. But there are areas of good stiffness, which is what is expected with RCC pavement—tight cracks with good LTE. LTE less than 80 percent is considered to be poor.

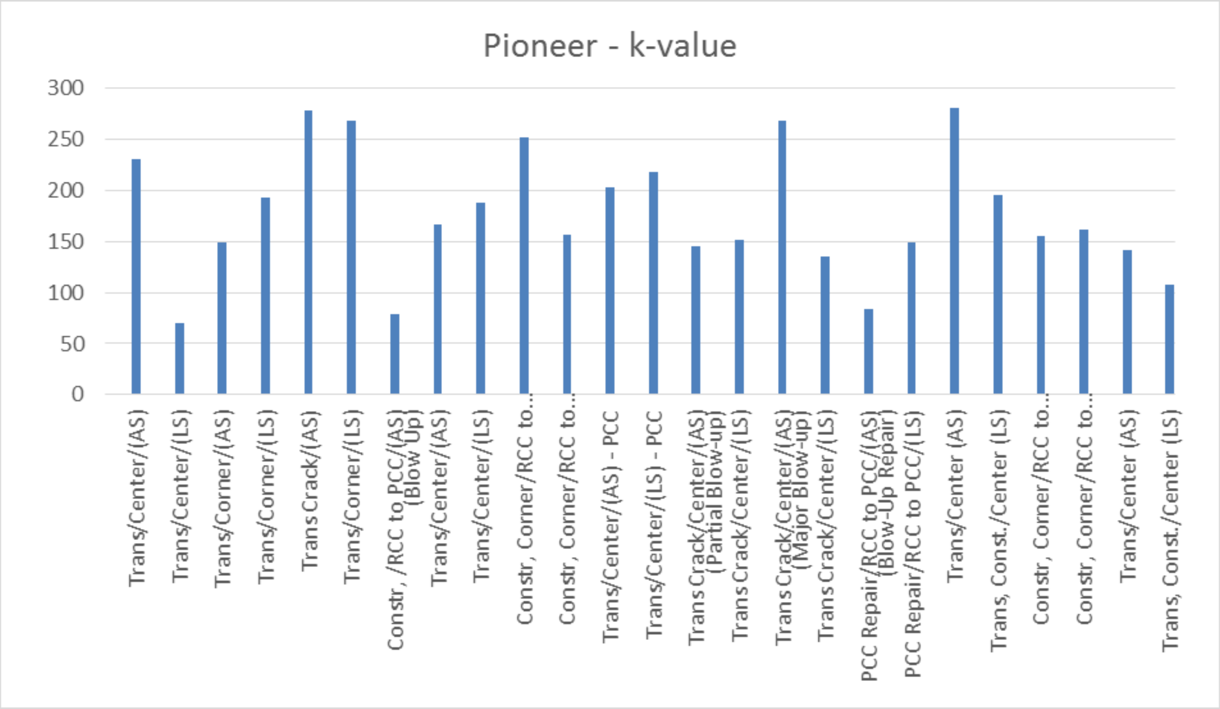

Figure 73. Pioneer k-Value Chart.

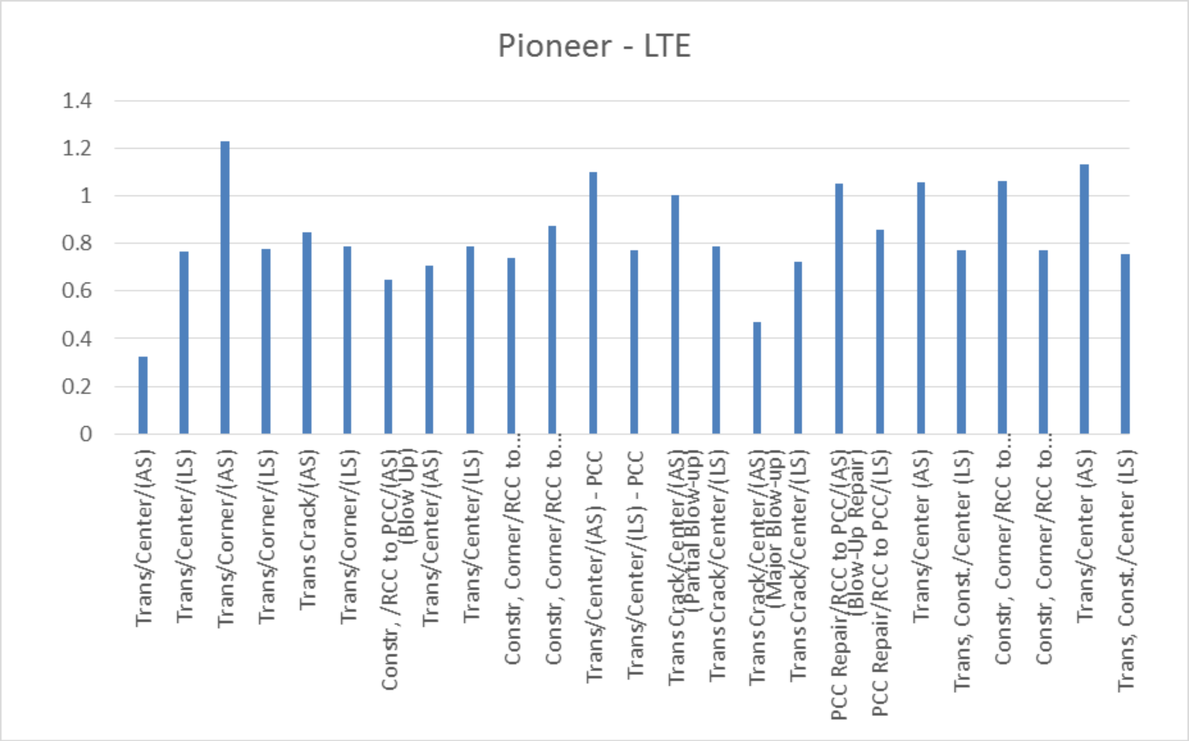

Figure 74. Pioneer Load-Transfer Efficiency Chart.

Standard Equipment Company (SEC)

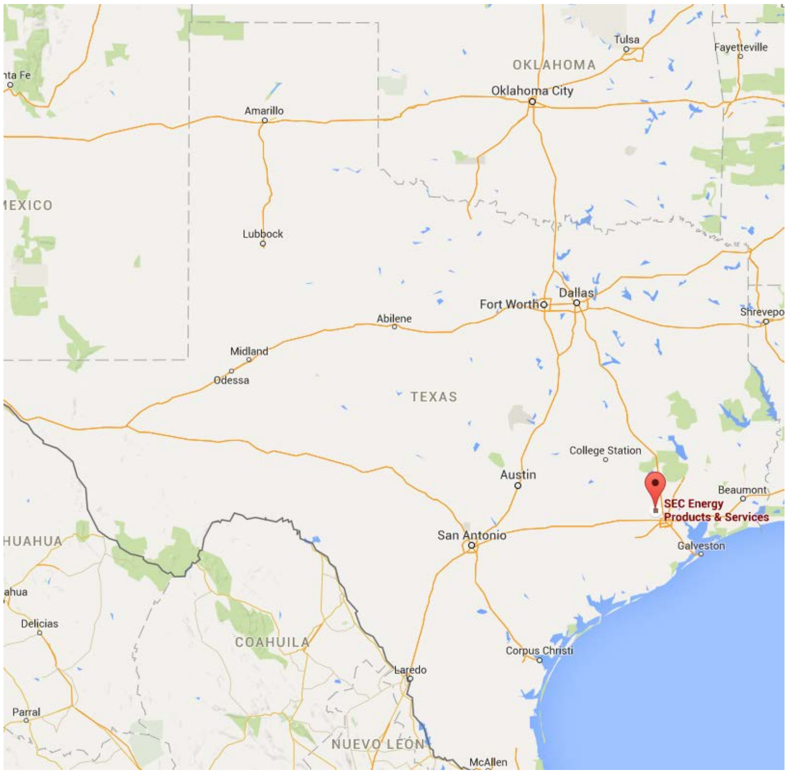

nta Fe
Tulsa
Fayetteville
OKLAHOMA
Oklahoma City
Amarillo
EXICO
Lubbock
Fort Worth
Dallas
Shrevepo
Abilene
Midland
Odessa
TEXAS
College Station
Austin
Beaumont
SEC Energy Products & Services
HUAHUA
San Antonio
Galveston
ahua
Delicias
COAHUILA
Corpus Christi
Laredo
Parral
NUEVO LEÓN
McAllen

Figure 75. Map of SEC Energy Products and Services.

Site Description

The site is located in north Houston in an industrial area. The front portion of the site is fully paved with RCC pavement that has 15 ft sawcut transverse joints, which is becoming more of a common feature of RCC paving. The mid-section is paved with jointed PCC, while the back portion not paved and looks to be made of a compacted limestone base material (Figure 76 and Figure 77). The travel paths are for trucks are in one direction, while the fork lifts and moving equipment travel in any area not occupied by building space. The building foundations are all made of PCC while the RCC is paved in the employee parking lot and the travel lanes of the front portion.

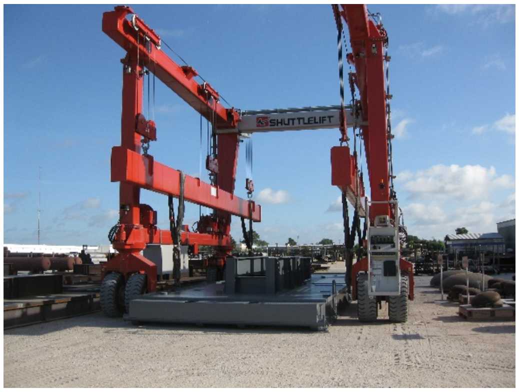
SHUTTLELIFT

Figure 76. Heavy Duty Industrial Fork Lift.

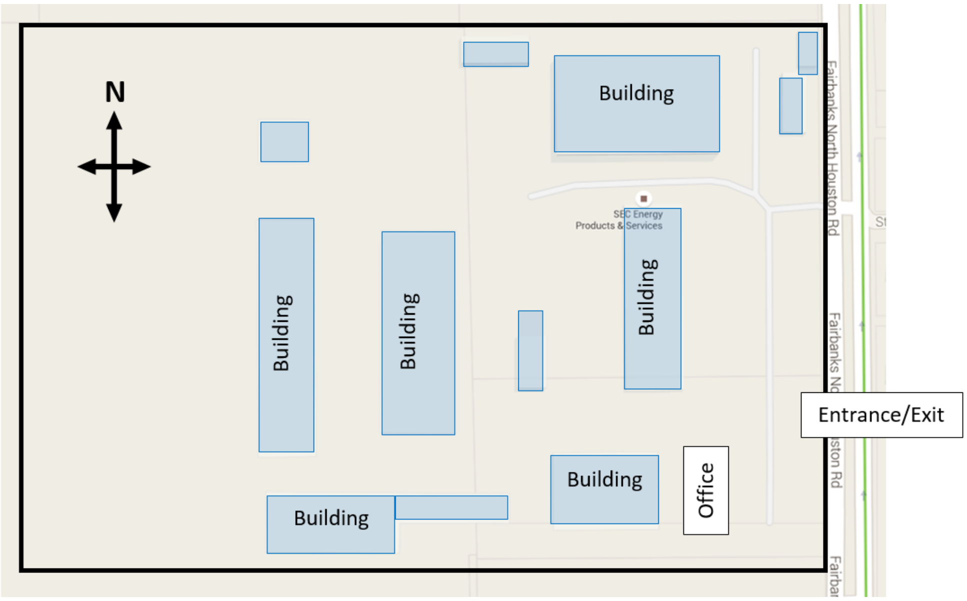
N
Building
SEC Energy Products & Services
Building
Building
Building
Building
Building
Office
Entrance/Exit
Fairbanks North Houston Rd
Fairbanks N
ston Rd
Fairban

Figure 77. SEC Building/Site Layout.

The traffic for the site includes heavy duty tractor trailer trucks, heavy duty industrial fork lifts, cranes/lifting equipment, and heavy duty building materials (Figure 78). The SEC produces large scale industrial components used in natural gas and petroleum production. The scale of equipment is of the highest magnitude and the loads are representative of the largest design loads applicable to almost any project. The site itself is densely compacted with fabrication buildings and material storage.

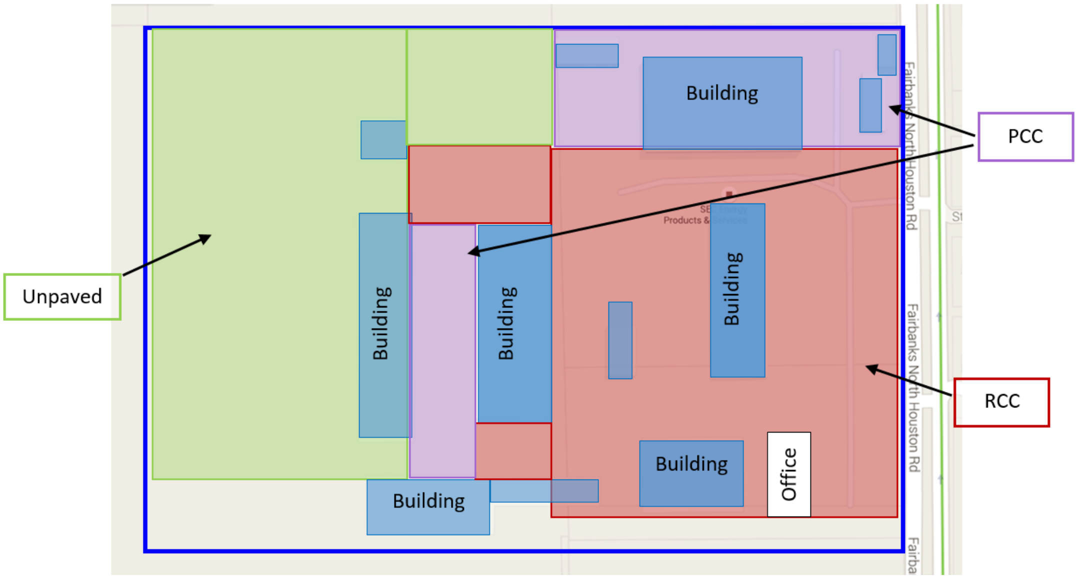
Building
PCC
Unpaved
Building
Building
Building
RCC
Building
Office
Building
Fairbanks North Houston Rd
Fairbanks North Houston Rd
SEC Energy Products & Services

Figure 78. SEC Pavement Types Layout.

Figure 79 shows the main traffic route. The yellow line travels the path of the standard tractor trailers, while the red line represents the travel of the cranes and the largest loads. The purple route represents the path that the heavy duty fork lifts and materials travel daily.

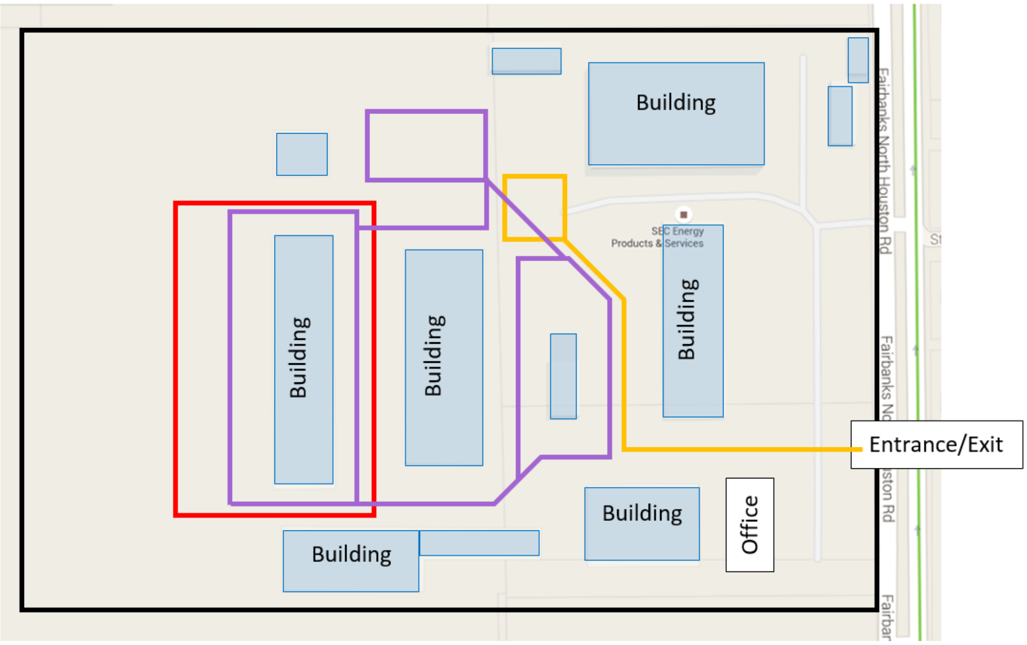
Building
SEC Energy Products & Services
Building
Building
Building
Entrance/Exit
Building
Office
Building
Fairbanks North Houston Rd
Fairbanks North Houston Rd

Figure 79. SEC Major Traffic Routes.

Pavement Specifications

For the SEC location, the following pavement section details were obtained:

- *Age*: 6 years.
- *Structure:*
    - Layer 1: Two-lift 14-in. RCC.
    - Layer 2: 6-in. cement treated base.
    - Subgrade: natural subgrade.

The RCC layer was paved in two 7-in. lifts for compaction purposes. The longitudinal construction joints are designed as a stair-step connection or staggered joint with the intent of creating better load transfer.

Testing Description

The following testing list was performed to collect the required performance data:

- *Testing Performed:*
    - July 20, 2015 (around 12:00 p.m.), Temp. = 90°F, (dry conditions, minimal rainfall recently).
    - December, 2015 (around 12:00 p.m.), Temp. = 65°F, (dry conditions, minimal rainfall recently).
- *Tests:*
    - FWD.
    - Joint infiltration test.
    - Visual distress survey.

The FWD testing was performed following ASTM 4694. The FWD testing was performed on numerous joints around the facility (Figure 82), and the process used was to test within 6 in. of the approach side and then test within 6 in. from the leave side of the joint. Drop locations included transverse joints, longitudinal joints, center of slabs, constructions joints, RCC to PCC transition joints, and PCC joints as well for comparison and analysis. FWD testing was also performed on key distress points found in the RCC portion.

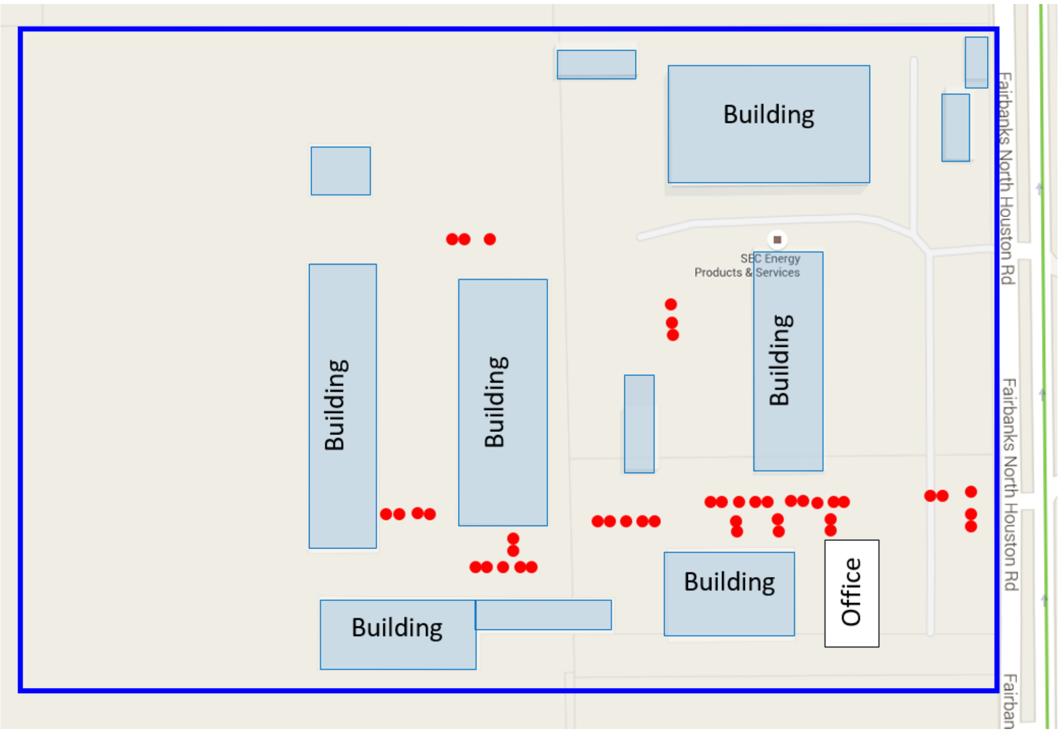
Building
Building
Building
Building
Building
Building
Office
SEC Energy Products & Services
Fairbanks North Houston Rd
Fairbanks North Houston Rd
Fairban

Figure 80. SEC July 2015 FWD Testing Positions Layout (App C and D Figures).

Initially infiltration tests were to be run on each of the sawcut joints tested with the FWD, but upon performing a handful of tests, it was determined that the data would not be applicable. Further explanation is provided under the Test Results section.

Test Results

The entire site was surveyed and the following distresses were found:

- Spalling (mostly on longitudinal joints).
- Minor transverse cracking.
- Minor faulting.
- Possible delamination.

A major distress found was spalling along several longitudinal construction joints. Selected joints that demonstrated this type of distress was tested with the FWD to assess the load transfer and possibly determine the source of the issue. In Figure 81, the red line represents the location of the joint tested.

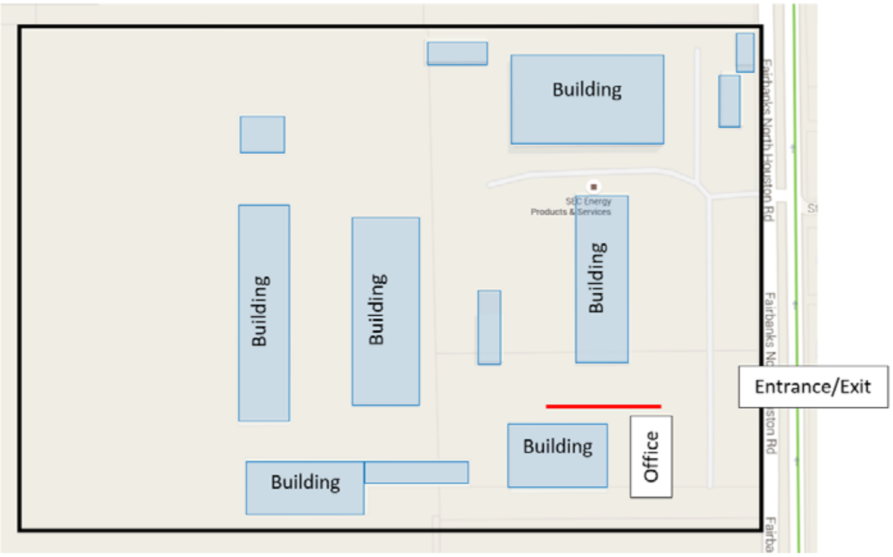

Figure 81. SEC Longitudinal Joint Further Examined.

For the infiltration testing, the first 5 sawcut joints were tested at 20 in., 6 in., and 3 in. of pressure head. Each test yielded no infiltration of any water through the joint. Upon closer examination, it was determined that the joints were compressed so tight from expansion that the joints resembled fully sealed joints. Joint sealant was present in the RCC paved section (PCC pavement did have silicone sealants).

From the FWD data, Figure 80 to Figure 85 were generated illustrating the slab effective thickness (h_e), backcalculated subgrade modulus (k-Value), and the joint LTE determined during hot and cooler weather temperature conditions. The hot weather h_e and k-values indicate the likelihood that there is delamination or separation between the two lifts that were placed to pavement the 14-in. RCC pavement section. The average effective thickness was less than 8 in. particularly along the slab edges and corners. However, during cooler weather, this values increased to approximately 10.5 to 11 in. meaning the separation was considerably reduced. This increased thickness was perhaps reflected in the higher LTE results under cooler weather conditions. The test data suggest the degree of slab separation (as reflected in the h_e values) is a function of climatic conditions.

Several areas of the pavement exhibited an open texture that over time may have contributed to the amount of drying shrinkage that may have taken place. A way to reduce the texture that typically is formed on the surface of RCC. In App E, Figure 155 and Figure 156show that paving RCC without rolling can also be closed at the surface with a troweling operation. This effect would also likely improve the curing quality of the RCC surface.

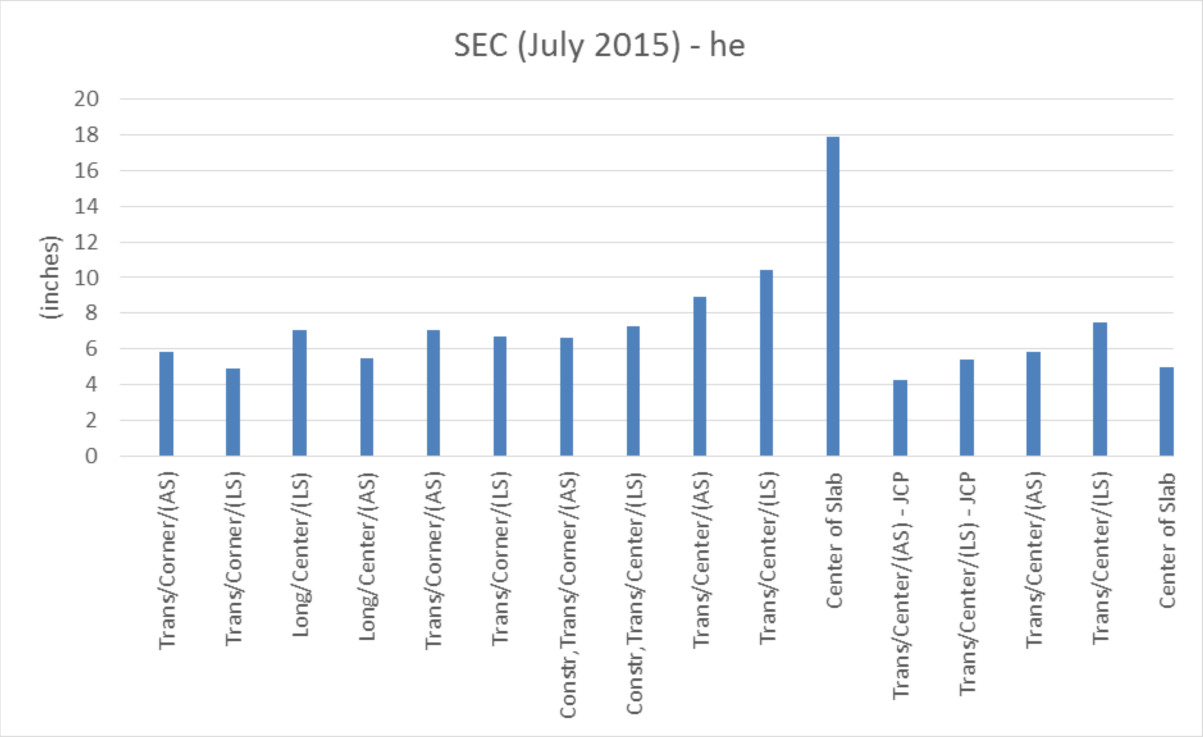

Figure 82. SEC Effective Thickness (July 2015).

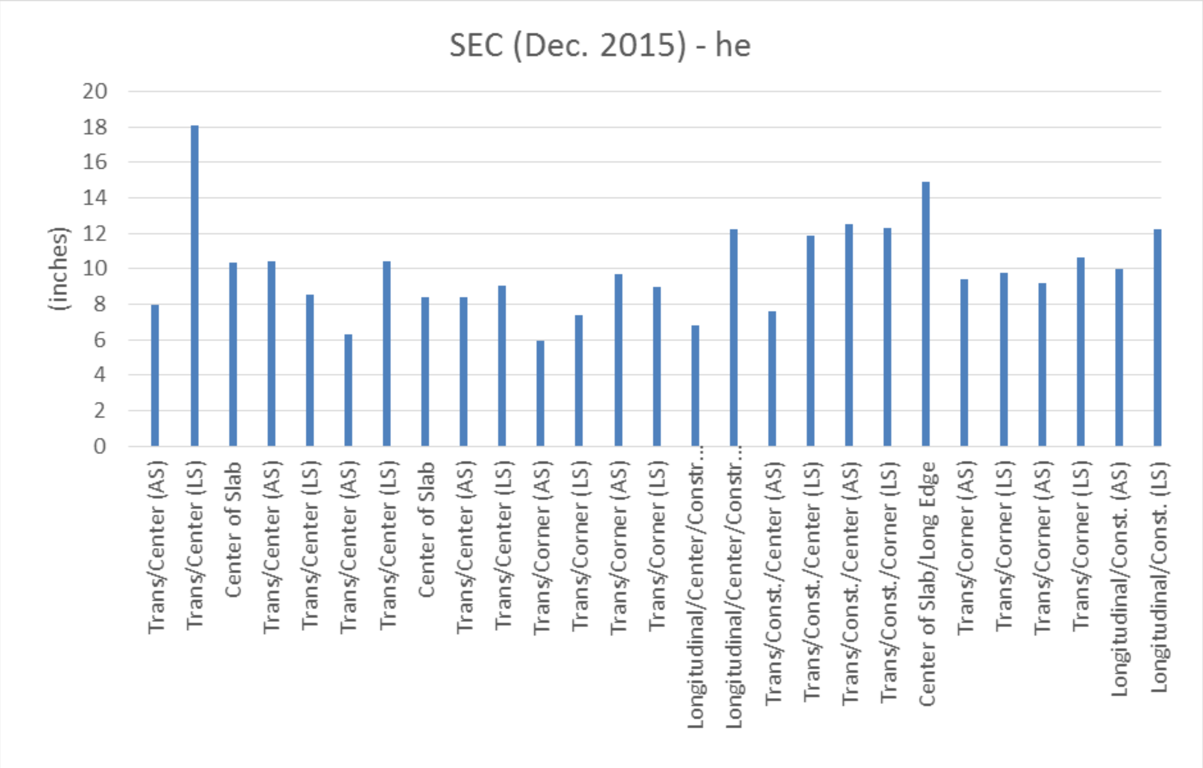

Figure 83. SEC Effective Thickness (December 2015).

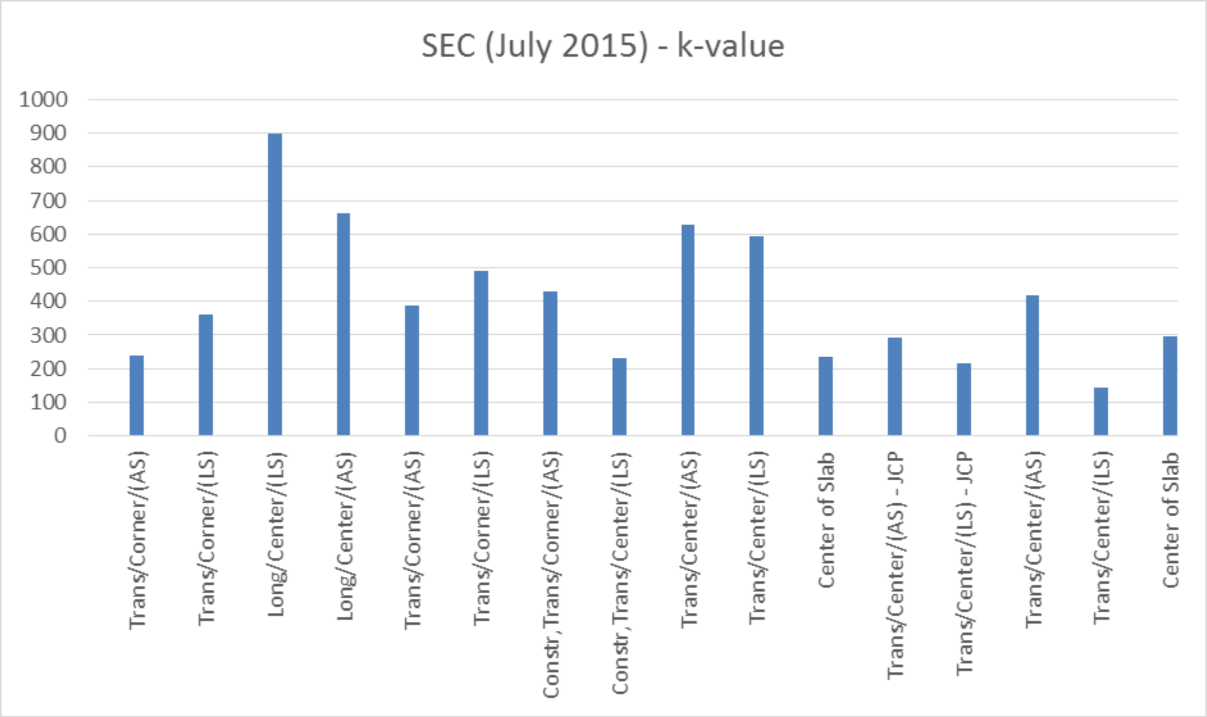

Figure 84. SEC k-Value (July 2015).

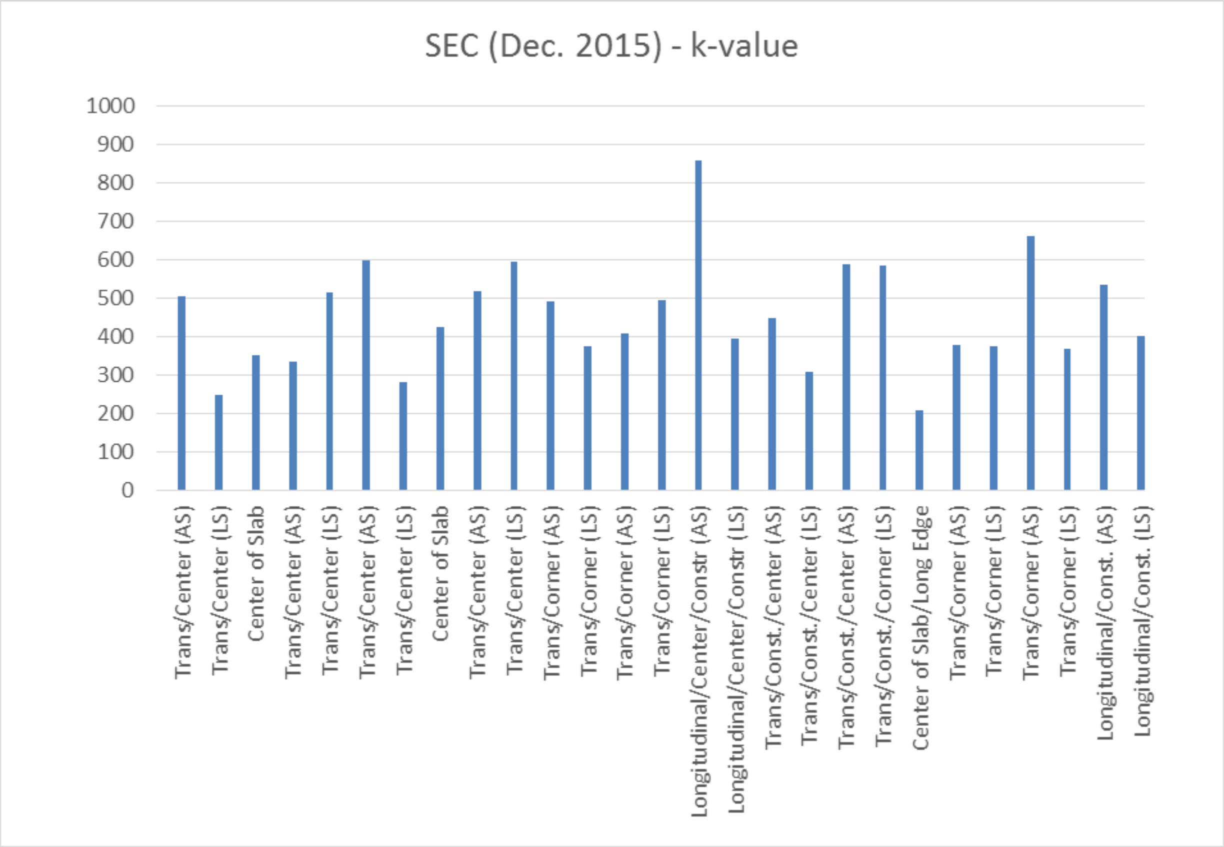

Figure 85. SEC k-Value (December 2015).

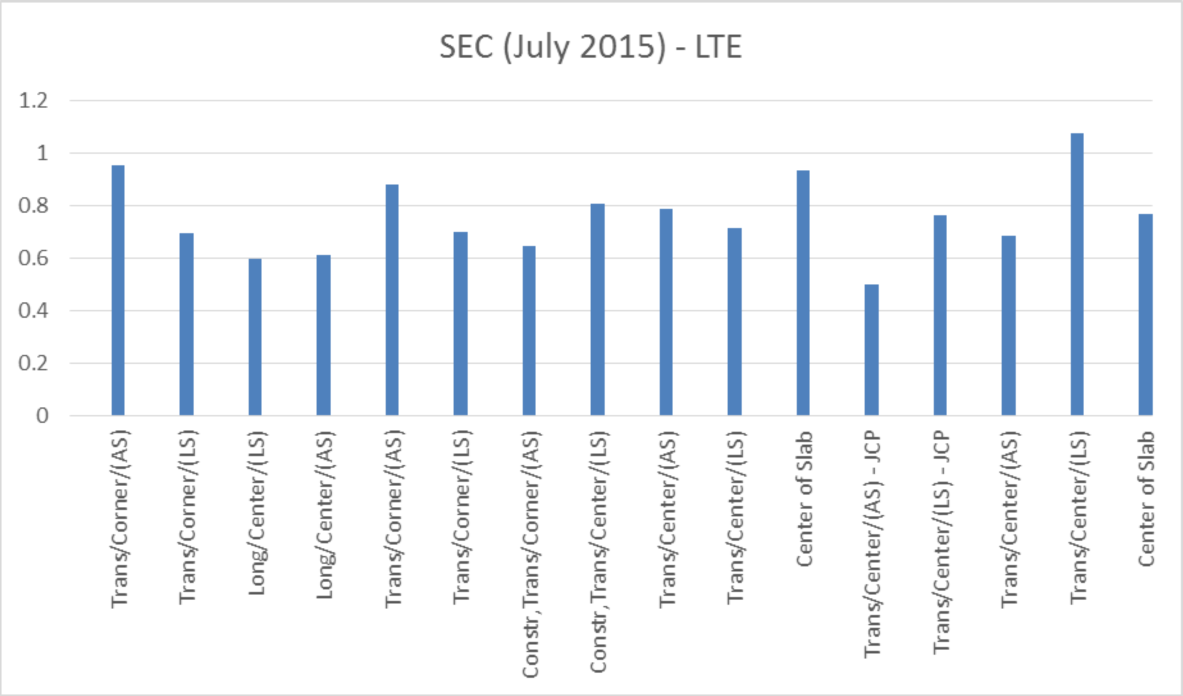

Figure 86. SEC LTE(July 2015).

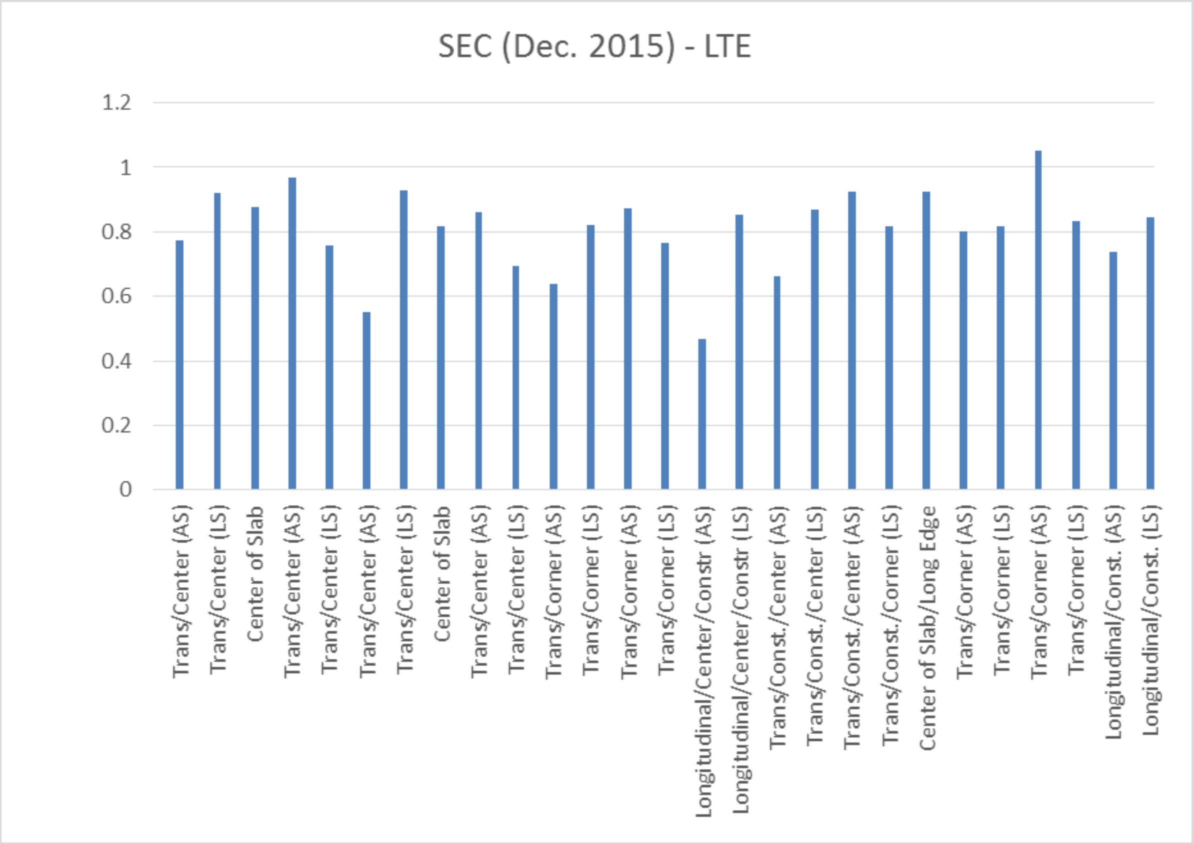

Figure 87. SEC LTE(December 2015).

Bella Vista (Cleveland, TX)

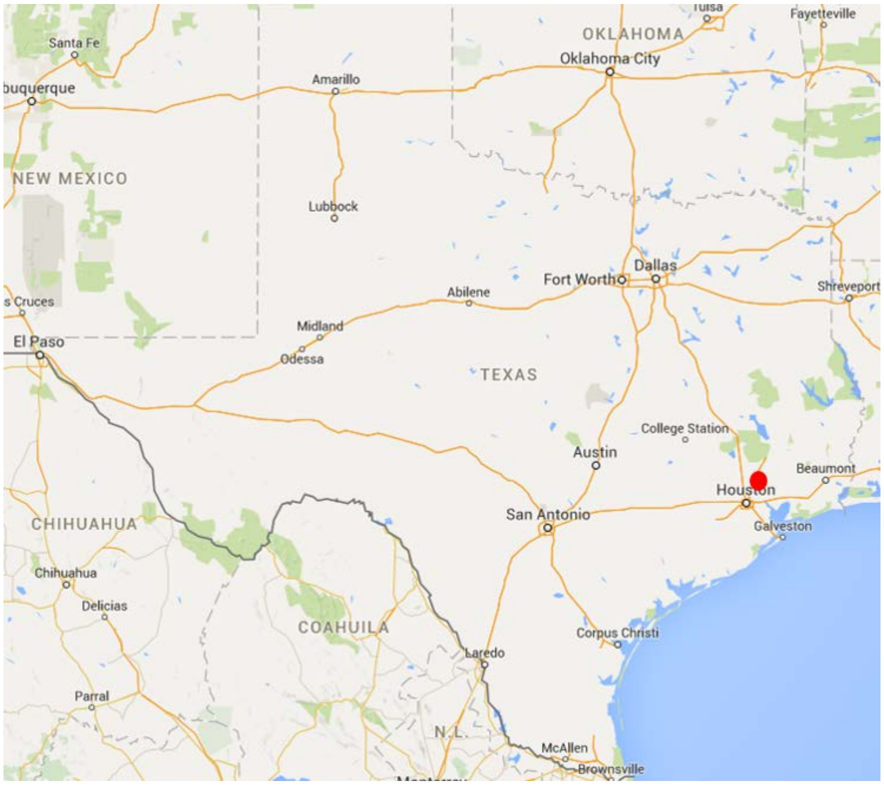
OKLAHOMA
Oklahoma City
Tulsa
Fayetteville
Santa Fe
Albuquerque
Amarillo
NEW MEXICO
Lubbock
Fort Worth
Dallas
Shreveport
Abilene
Las Cruces
El Paso
Midland
Odessa
TEXAS
College Station
Austin
Beaumont
Houston
San Antonio
Galveston
CHIHUAHUA
Chihuahua
Delicias
COAHUILA
Corpus Christi
Laredo
Parral
N.L.
McAllen
Brownsville

Figure 88. Map of Bella Vista Community.

Site Description

The Bella Vista Site is actually two separate communities, of the same design, that are located within a few miles of each other (Figure 86). The communities are a part of Plum Grove, which is outside of Cleveland, TX (North of Houston). The communities experience residential traffic and dump-truck traffic moving materials for building the houses. The area is currently only partially inhabited so traffic grow in the near future is expected. The majority of the pavements in the communities are recently paved and sit on one type of stabilized base, but there are older sections of RCC that consist of an asphalt base and sections with no base.

Pavement Specifications

For the Bella Vista location, the following pavement section details were obtained:

- *Age*: 1 to 4 years.
- *Structure*:
  - Layer 1: 5-in. RCC pavement.

- Subgrade: Site 1—6-in. cement stabilized (App. F, Figure 160 and Figure 161); Site 2—A: 6-in. cement stabilized, B: natural subgrade (no base layer; App. F, Figure 164).

Layout

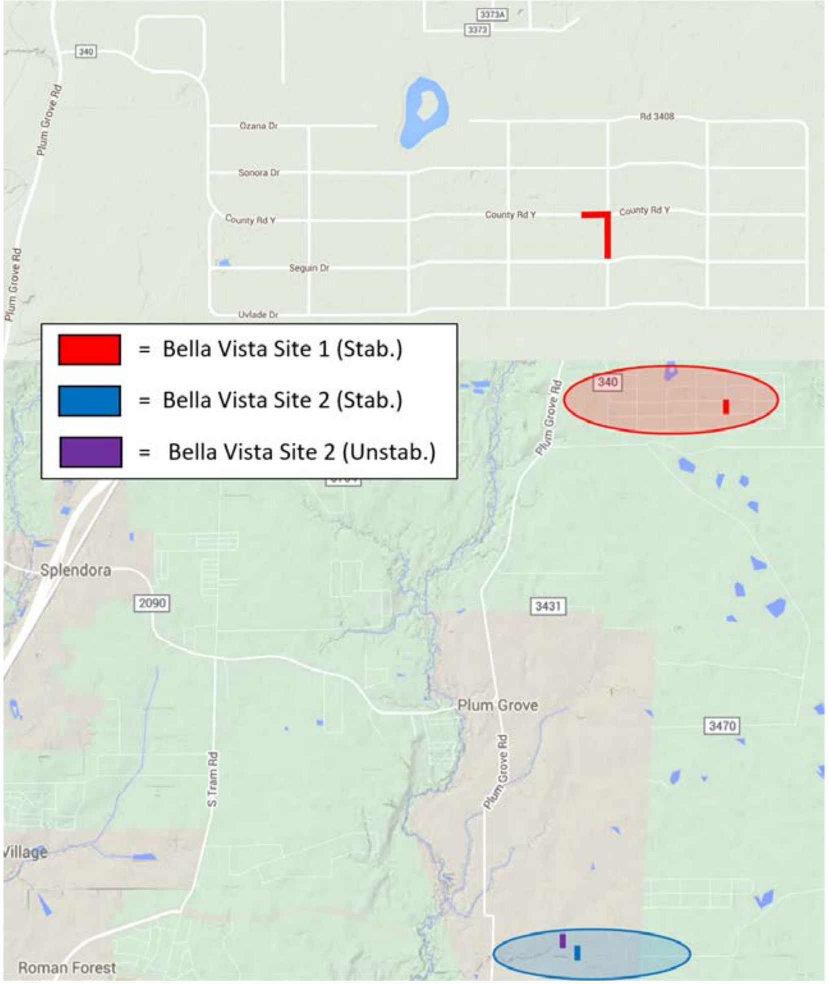
3373A
3373
340
Plum Grove Rd
Ozana Dr
Sonora Dr
County Rd Y
Seguin Dr
Uvlade Dr
Rd 3408
County Rd Y
County Rd Y
Plum Grove Rd
🟥 = Bella Vista Site 1 (Stab.)
🟦 = Bella Vista Site 2 (Stab.)
🟪 = Bella Vista Site 2 (Unstab.)
340
Plum Grove Rd
Splendora
2090
3431
Plum Grove
3470
S Tram Rd
Plum Grove Rd
Village
Roman Forest

Figure 89. Bella Vista Site Layout with Testing Layout.

Testing Description

The site was initially surveyed in July 2015 and then again during a site visit for FWD testing in December 2015 covering two section of RCC pavement. A distress survey was also conducted along with infiltration testing transverse cracks and longitudinal joints. Some of the longitudinal joints had separated along curved sections; these had yielded full flow/infiltration through the joint. However, all the transverse joints were tightly closed and in some case blow-ups had occurred after a heavy rainfall event.

Field Surveys/Tests

The following testing list was performed to collect the required performance data:

- Distress surveying.
- FWD.
- Paving operations.

Results

Some areas of the recently paved RCC sections had been subjected to extensive flooding and were submerged for a number of days, many blowups, and expansive movement. This has possibly led to blow ups and joint separation (App. E , Figure 153,Figure 155 and Figure 159 that under normal circumstance would not occur. It is likely the flooding affects the degree of friction between the slab and base layer allowing thermal movements to occur over broad areas of the pavement that appeared to be under considerable compressive stress (App. F, Figure 162 and Figure 163).

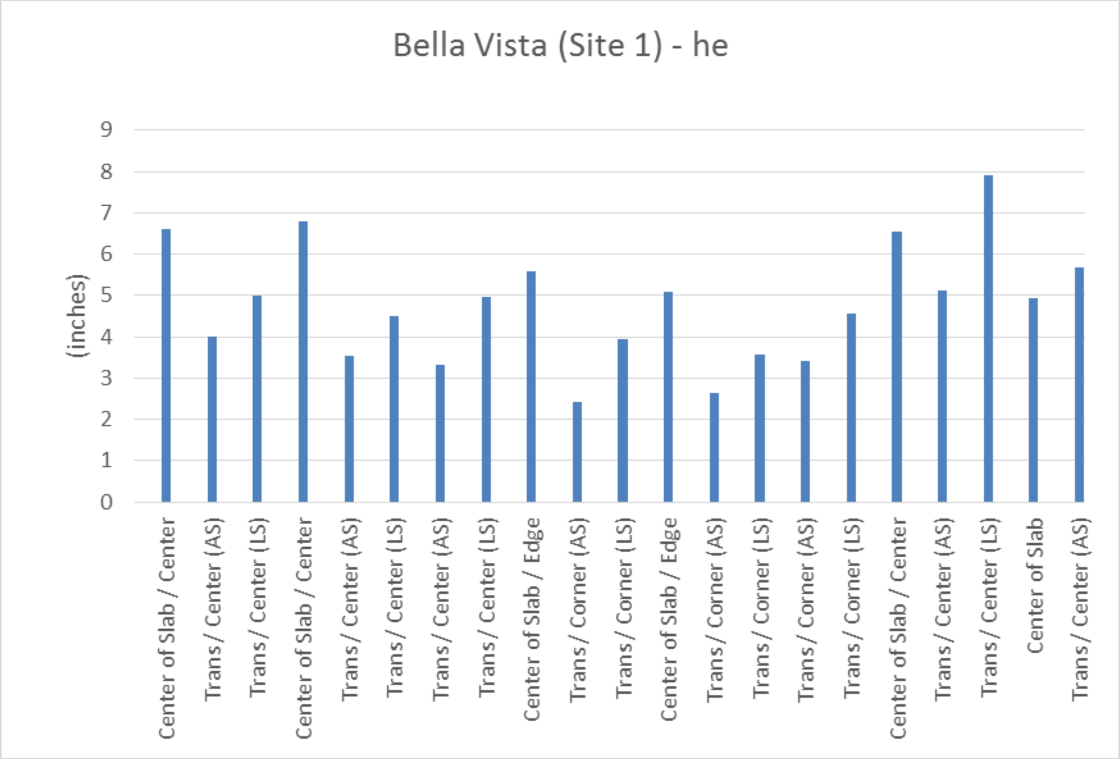

Figure 90. Bella Vista Effective Thickness for Site 1.

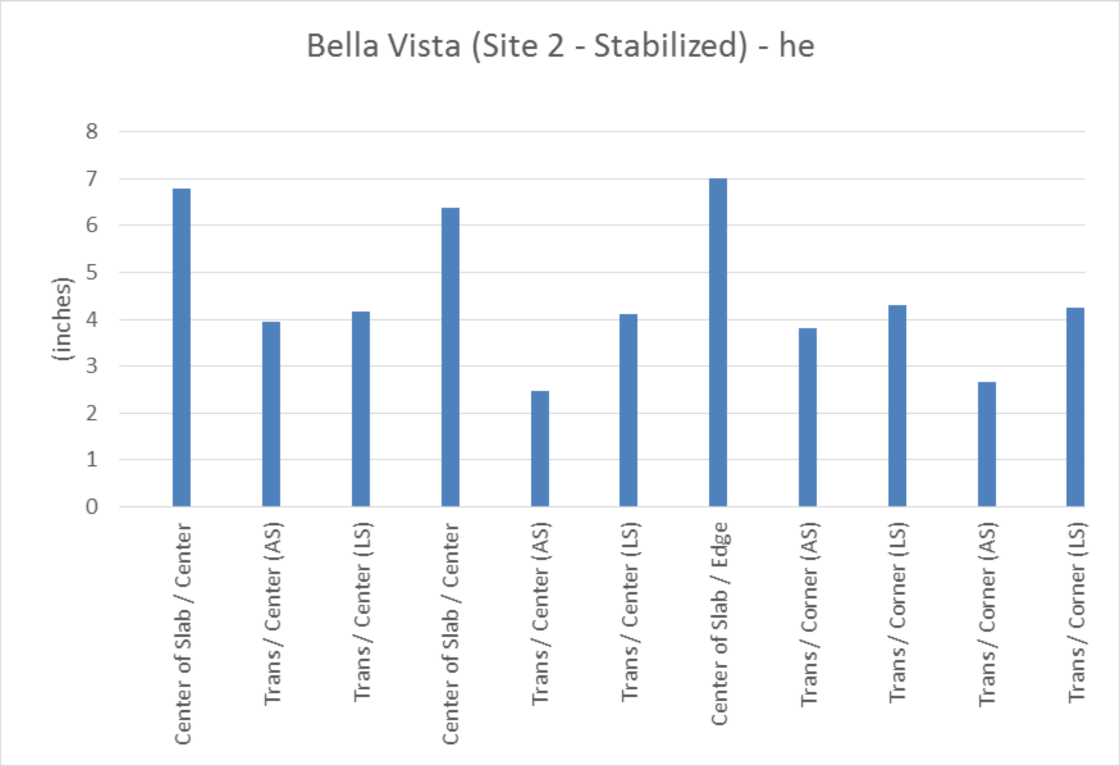

Figure 91. Bella Vista Effective Thickness for Site 2—Stabilized.

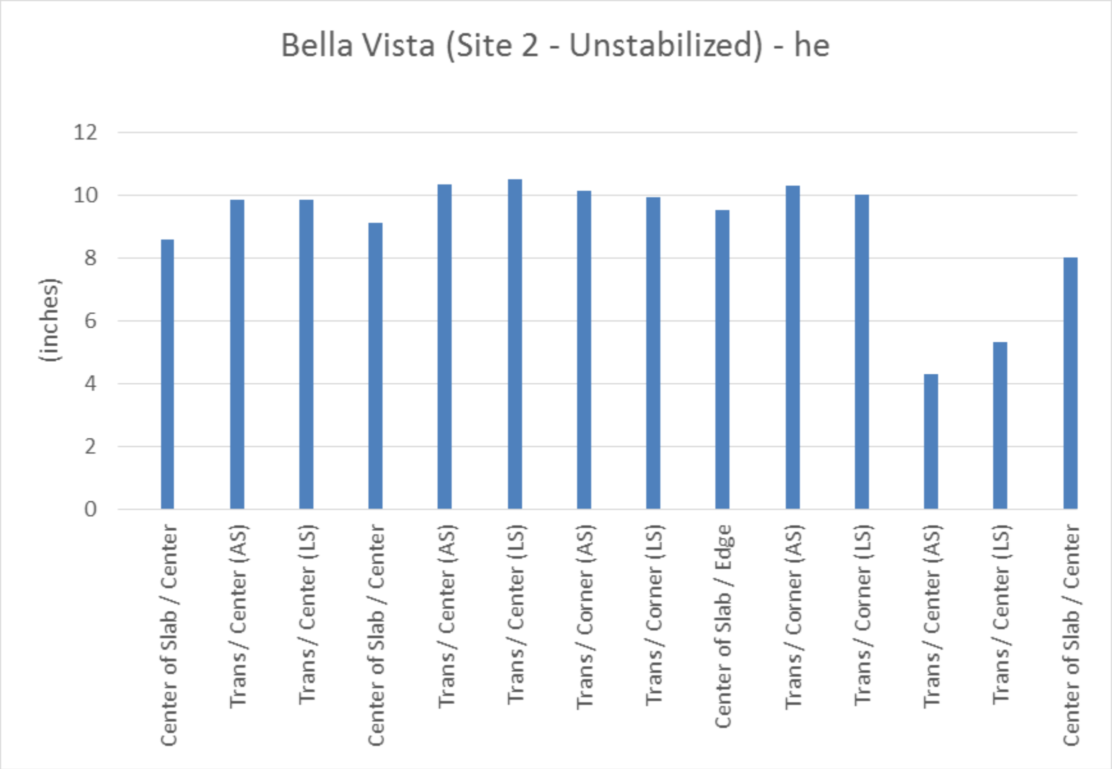

Figure 92. Bella Vista Effective Thickness for Site 2—Unstabilized.

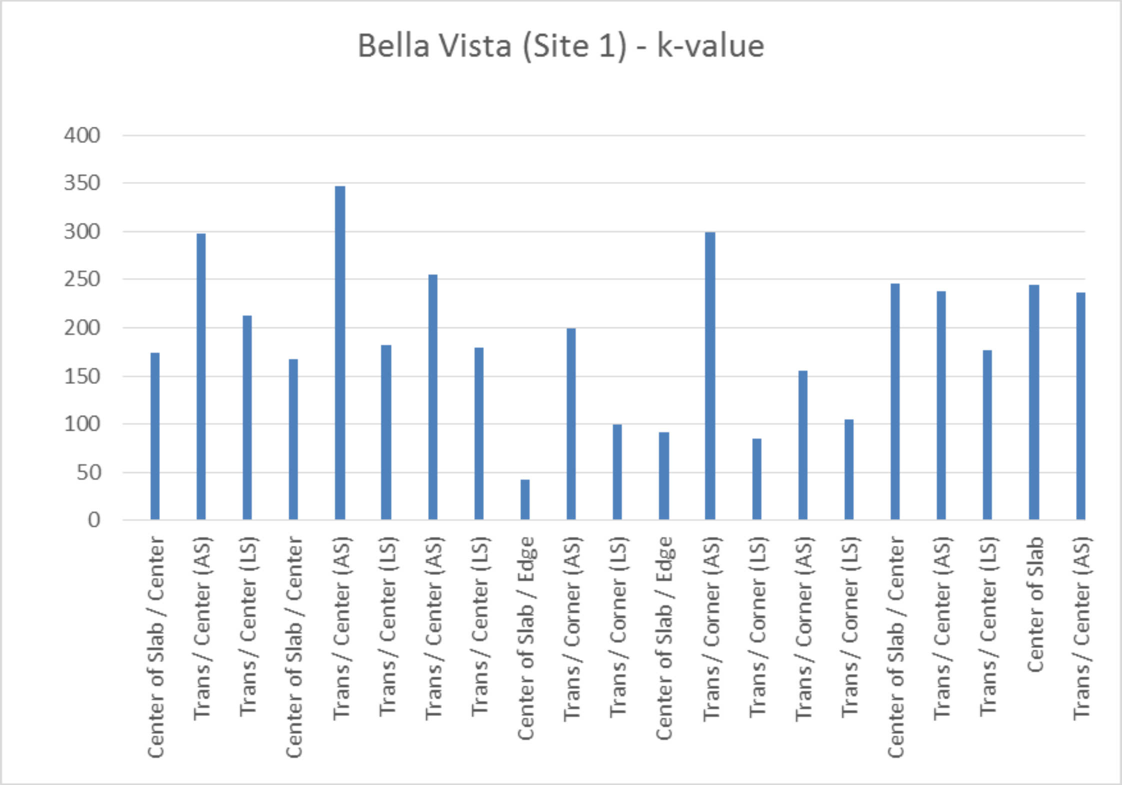

Figure 93. Bella Vista k-Value for Site 1.

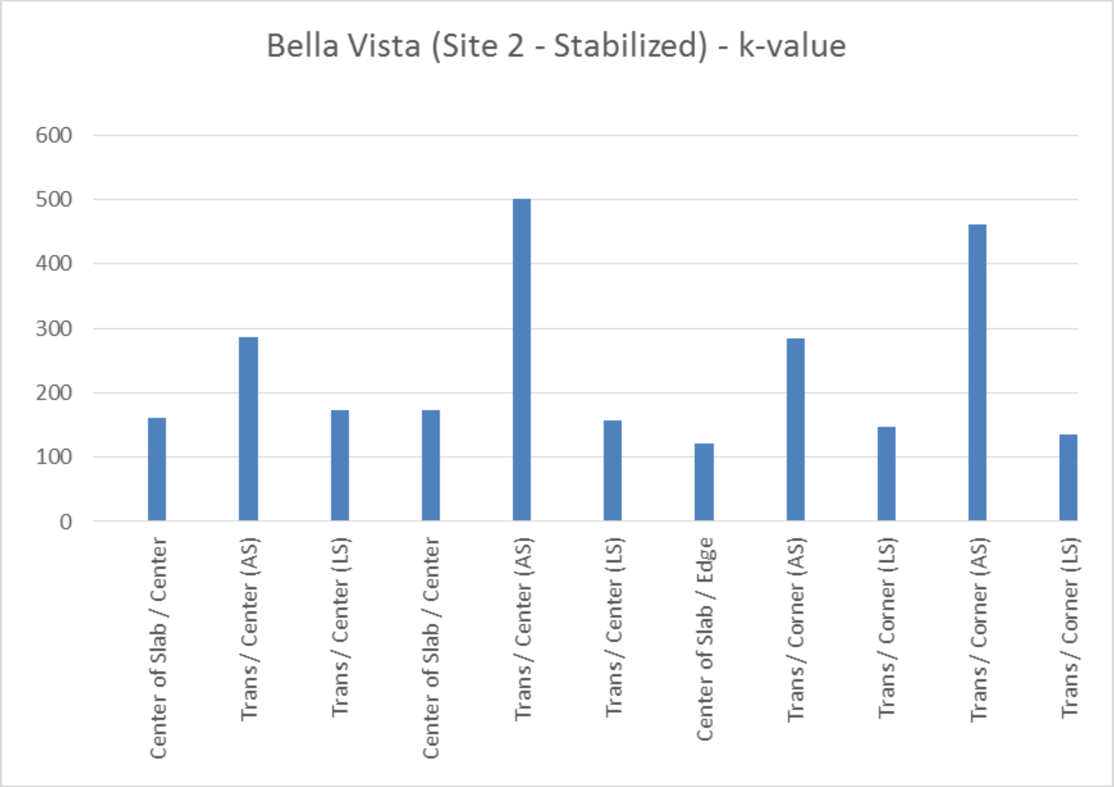

Figure 94. Bella Vista k-Value for Site 2—Stabilized.

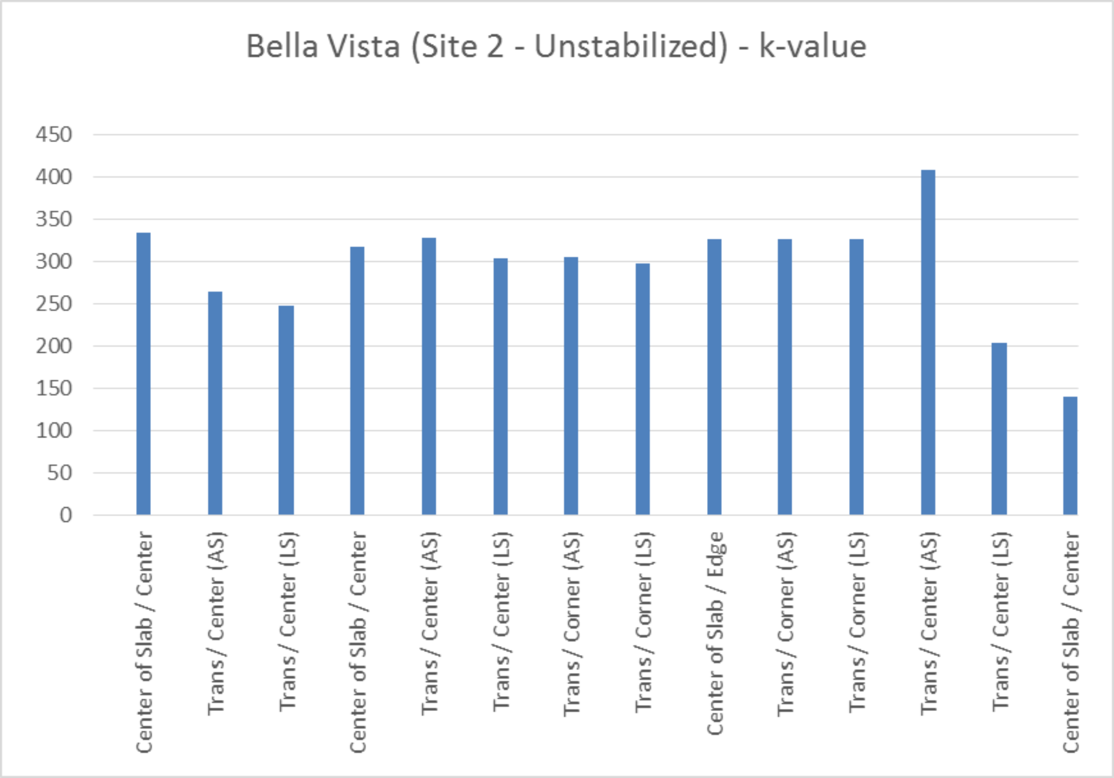

Figure 95. Bella Vista k-Value for Site 2—Unstabilized.

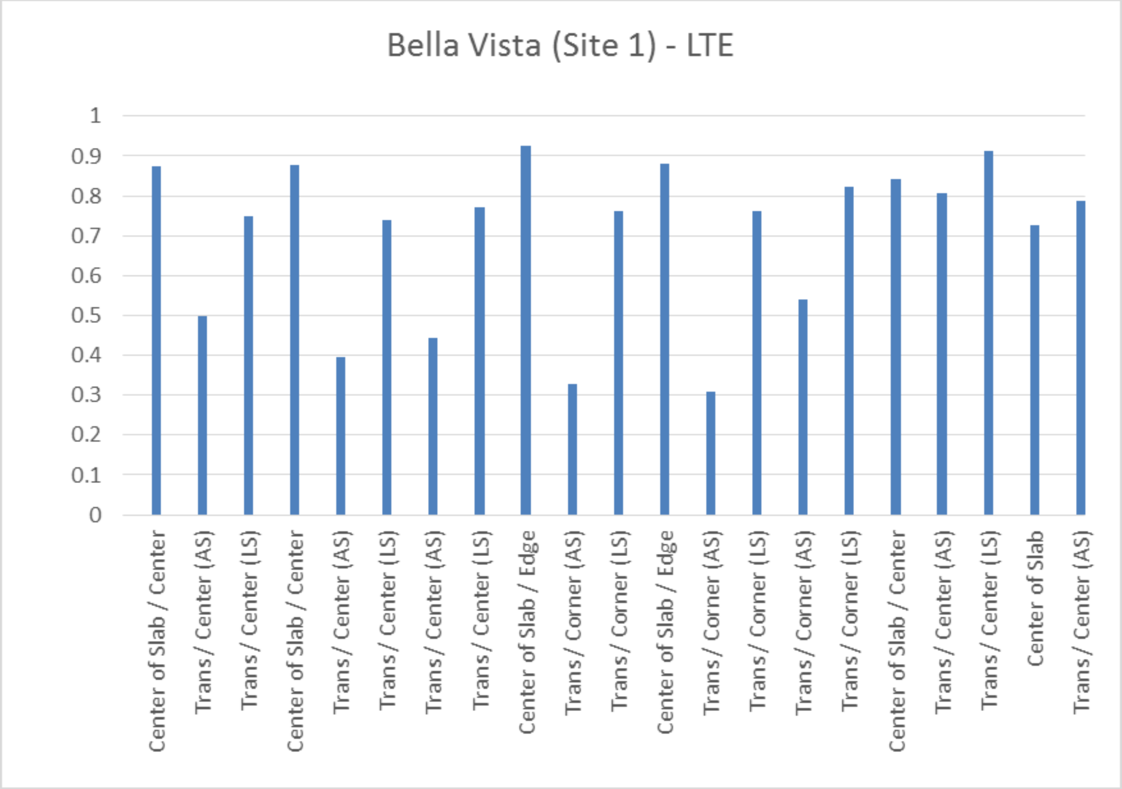

Figure 96. Bella Vista LTE for Site 1.

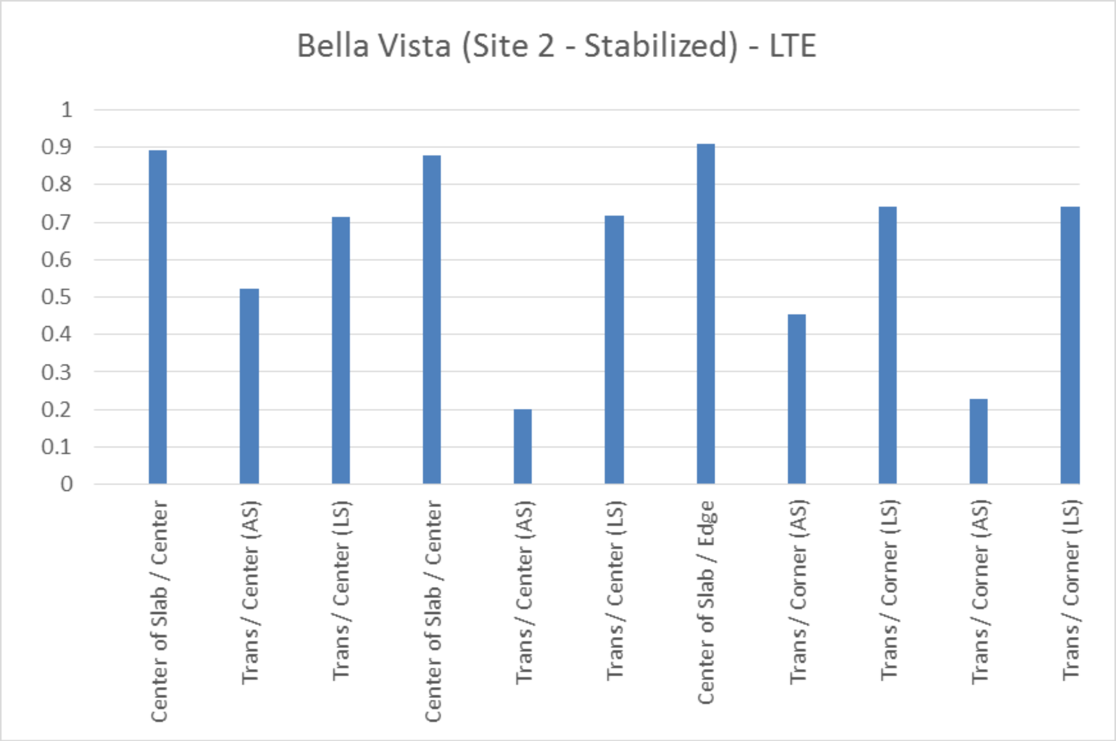

Figure 97. Bella Vista LTE for Site 2—Stabilized.

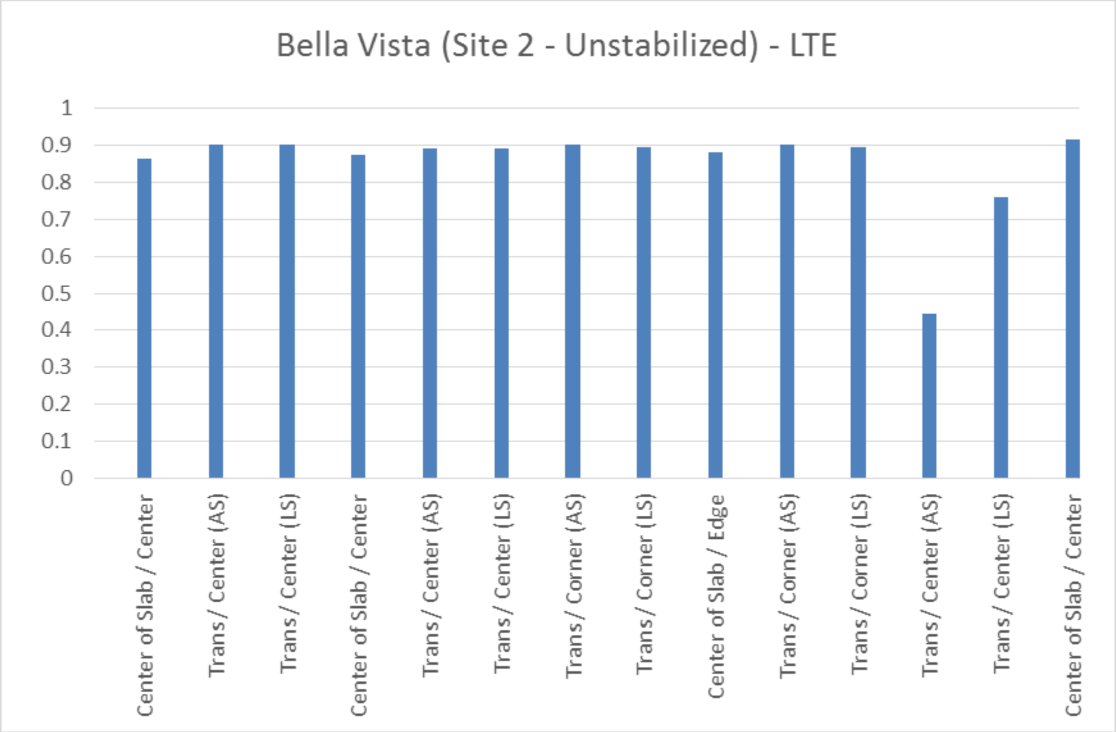

Figure 98. Bella Vista LTE for Site 2—Unstabilized.

Figure 87–Figure 96 (App. F, Figure 157 and Figure 158) were generated using the FWD data collected. The purpose of these data is to look at the effect of stabilization on RCC behavior, and it appears that base support does have a significant effect. The requirement for base support does however depend upon the load and traffic requirements as part of the design of the pavement. The inclusion of stabilization effected the effective thickness somewhere between a half to an inch and the effect of a stiffer subgrade (greater k-values) is approximately double that.

Solms Rd.

Location

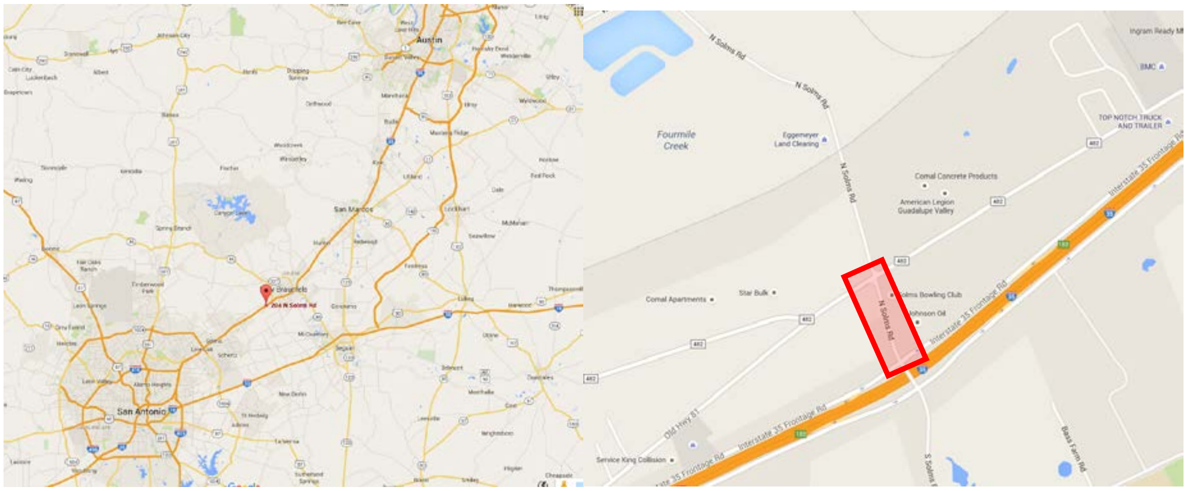
Austin
San Marcos
New Braunfels
204 N Solms Rd
San Antonio
N Solms Rd
Fourmile Creek
Eggemeyer Land Clearing
Comal Concrete Products
American Legion Guadalupe Valley
Solms Bowling Club
Johnson Oil
Comal Apartments
Star Bulk
Old Hwy 81
Interstate 35 Frontage Rd
Service King Collision
S Solms Rd
Bass Farm Rd
Ingram Ready Mix
BMC
TOP NOTCH TRUCK AND TRAILER
482

Figure 99. Map of Solms Rd.

Site Description

Solms Rd. is located in New Braunfels, TX, and is considered a residential street although the truck traffic on this route is significant—approximately 1500 trucks per day mainly servicing Cemex operations located to the west of the roadway. The road extends both north and south of I-10, but for this, researchers looked at the short section initially north of the interstate. As noted, the section is heavily used by truck traffic, many of which hauling rock and large materials.

Pavement Specifications

For the Solms Rd. location, the following pavement section details were obtained:

- *Age*: 3+ years.
- *Structure*:
  - Layer 1: 8-in. RCC pavement.
  - Base: 6-in. stabilized material.

Layout

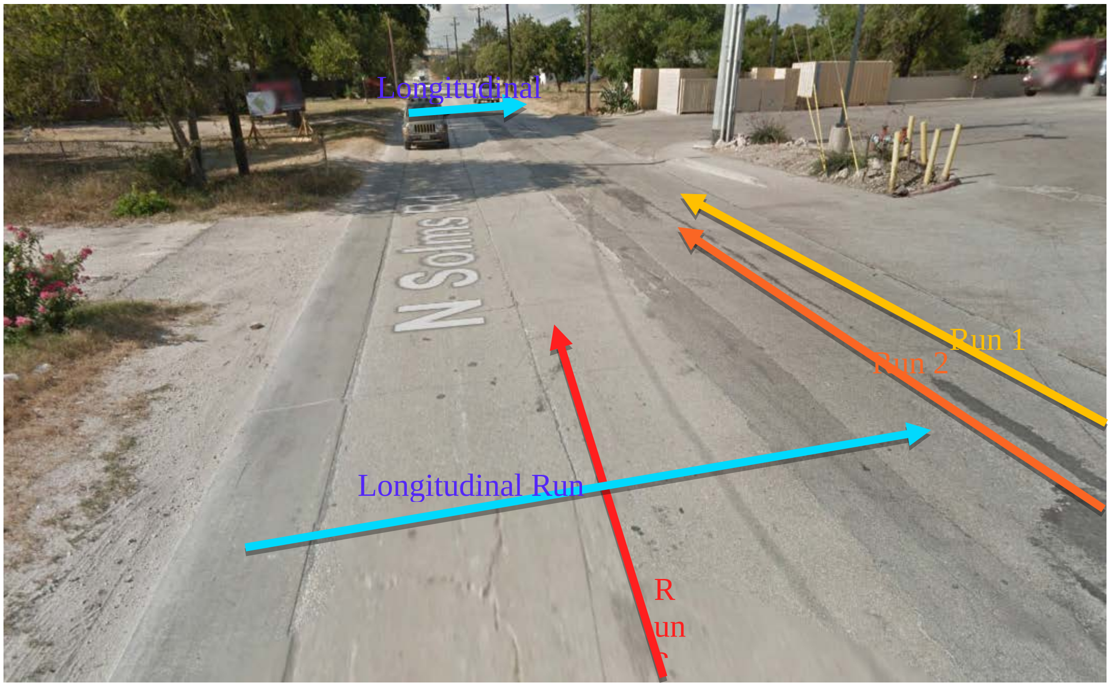

Figure 100. Solms Rd.—FWD Testing Patterns.

Testing Description

The following testing list was performed to collect the required performance data:

- *Testing Performed*:
  - Distress surveying.
  - FWD.

Results

Figure 97 to Figure 104 were generated from the FWD data collected from the site (App. G, Figure 167–Figure 169). Despite the amount of cracking this pavement has been subjected to (which much of it is curling and warping related; App. G, Figure 166), a portion of the pavement structure shows good stiffness as seen in Figure 97 but lower in Figure 98 suggesting that at least in part of the RCC pavement is bonded to the stabilized base layer. This is further illustrated by the back calculated k-values shown in Figure 101 and Figure 102, where they are more representative of the subgrade in Figure 101 due to the greater stiffness of that section and higher in Figure 102 due to the lower stiffness of that section of pavement. These stiffness differences are further delineated by the consistent LTE results shown in Figure 103 and Figure 104. Areas, such as those shown in App. G, Figure 169, tended to shown poor stiffness wherever they are located.

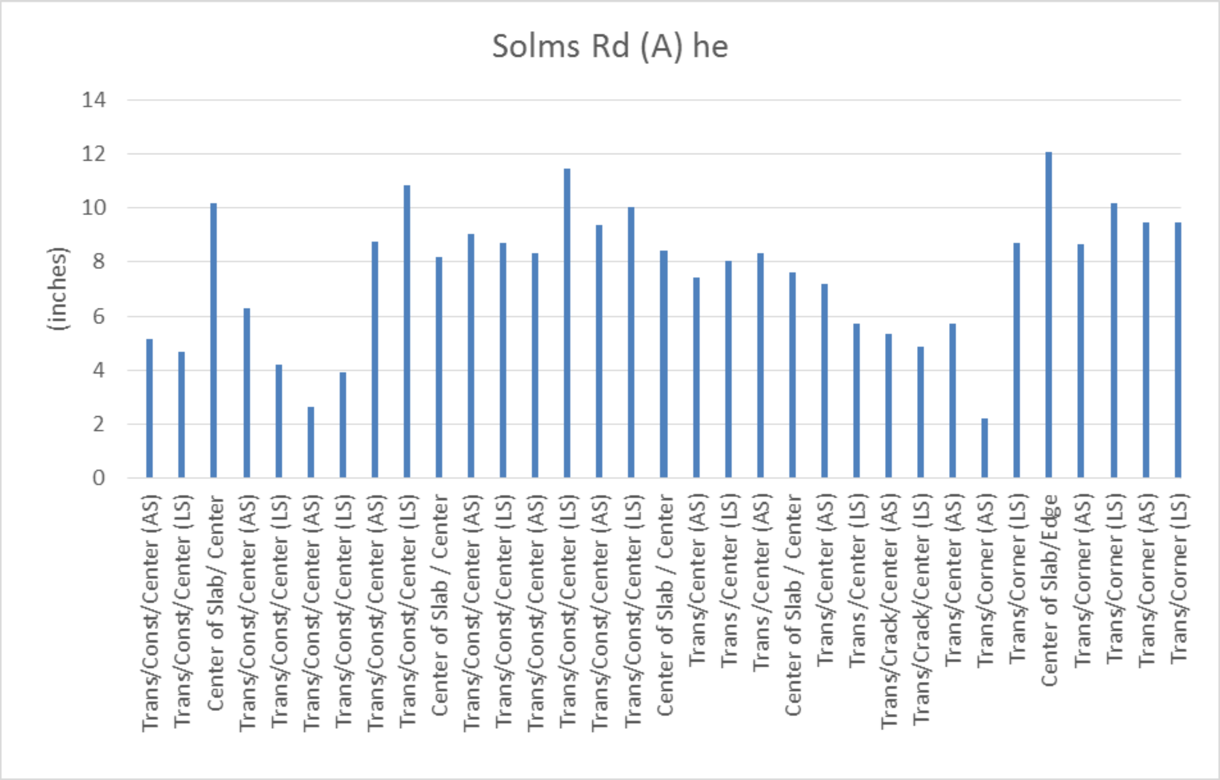

Figure 101. Solms Rd. (A) Effective Thickness.

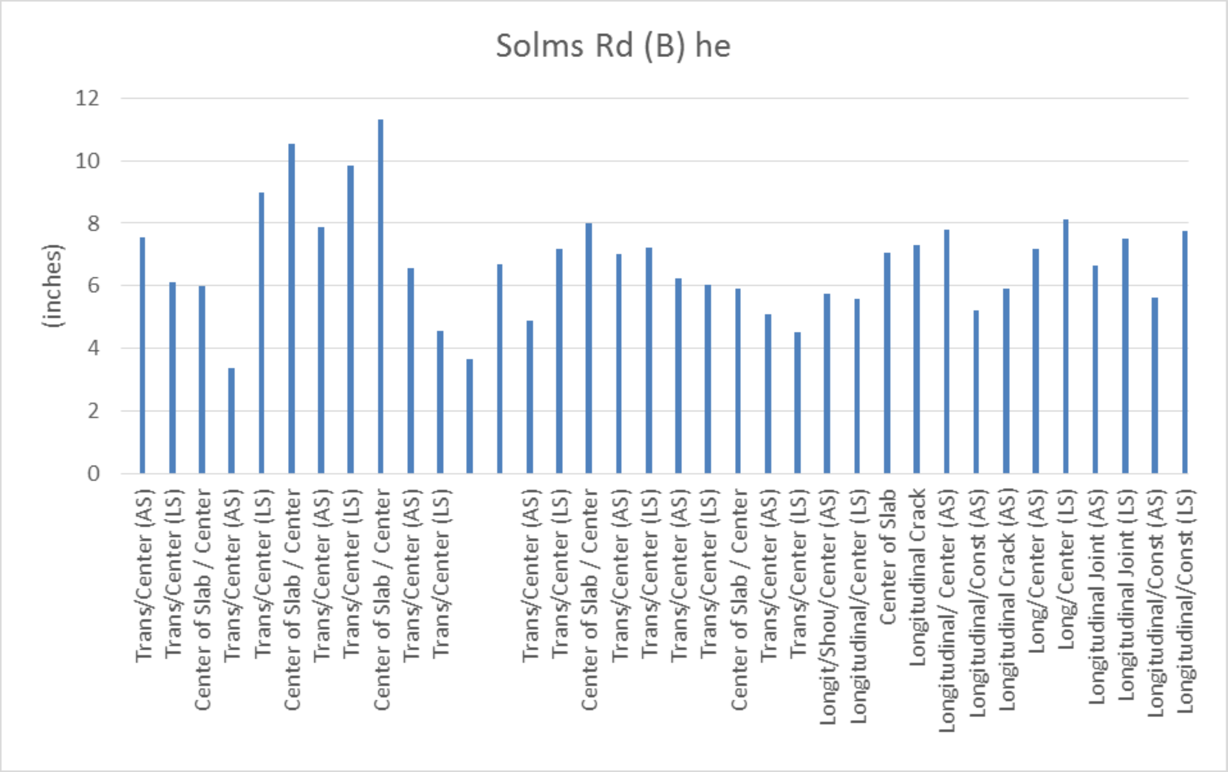

Figure 102. Solms Rd. (B) Effective Thickness.

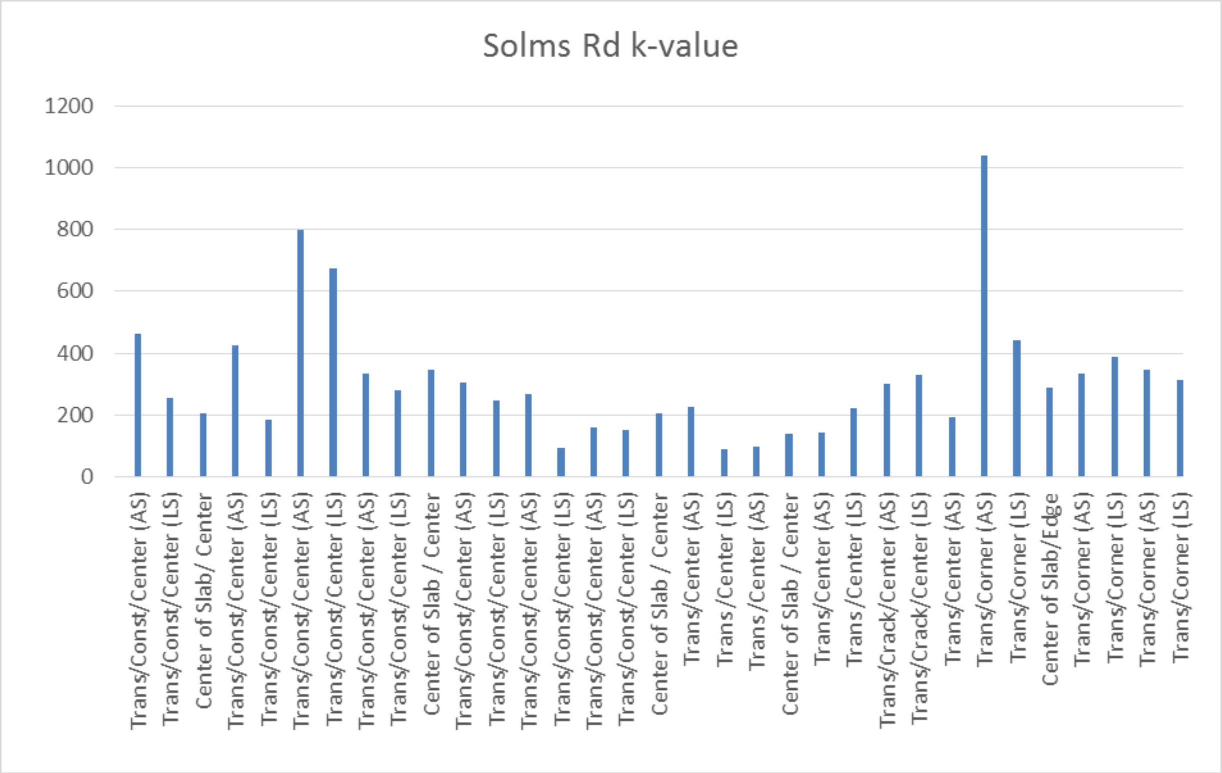

Figure 103. Solms Rd. (A) k-Value.

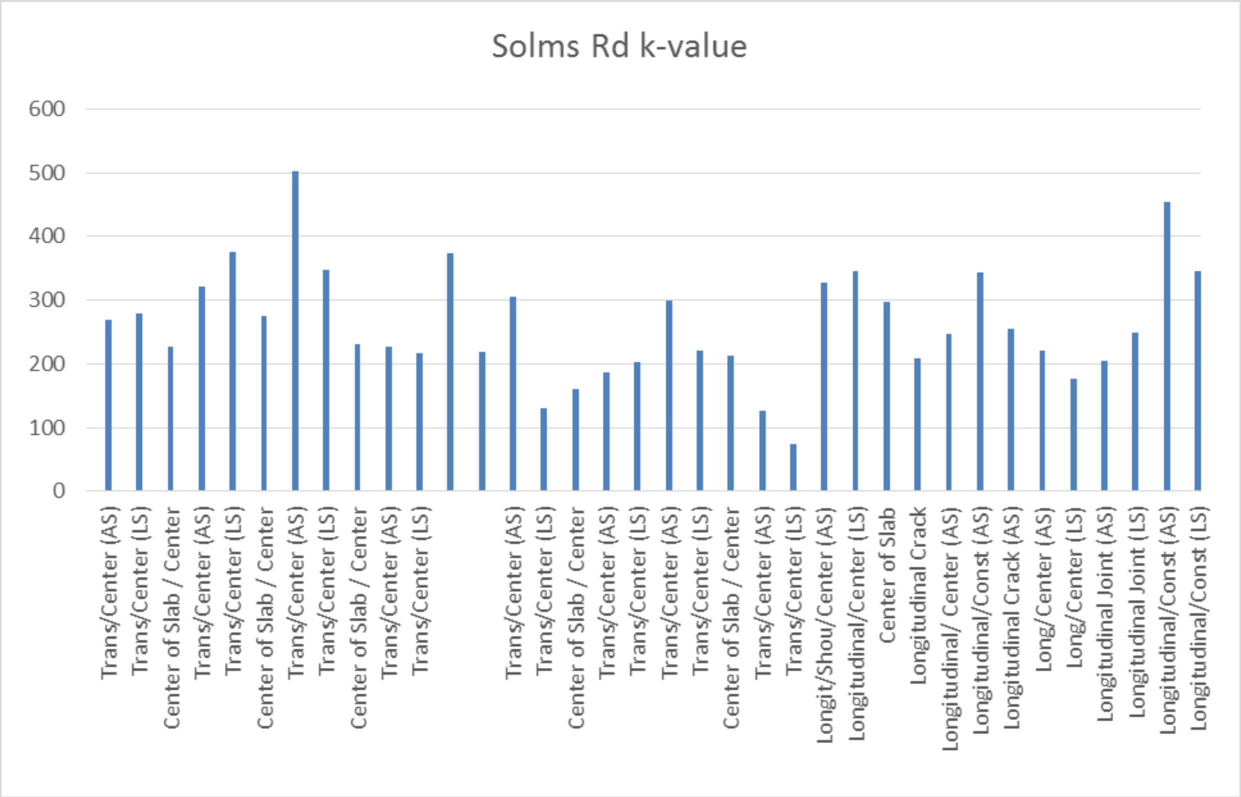

Figure 104. Solms Rd. (B) k-Value.

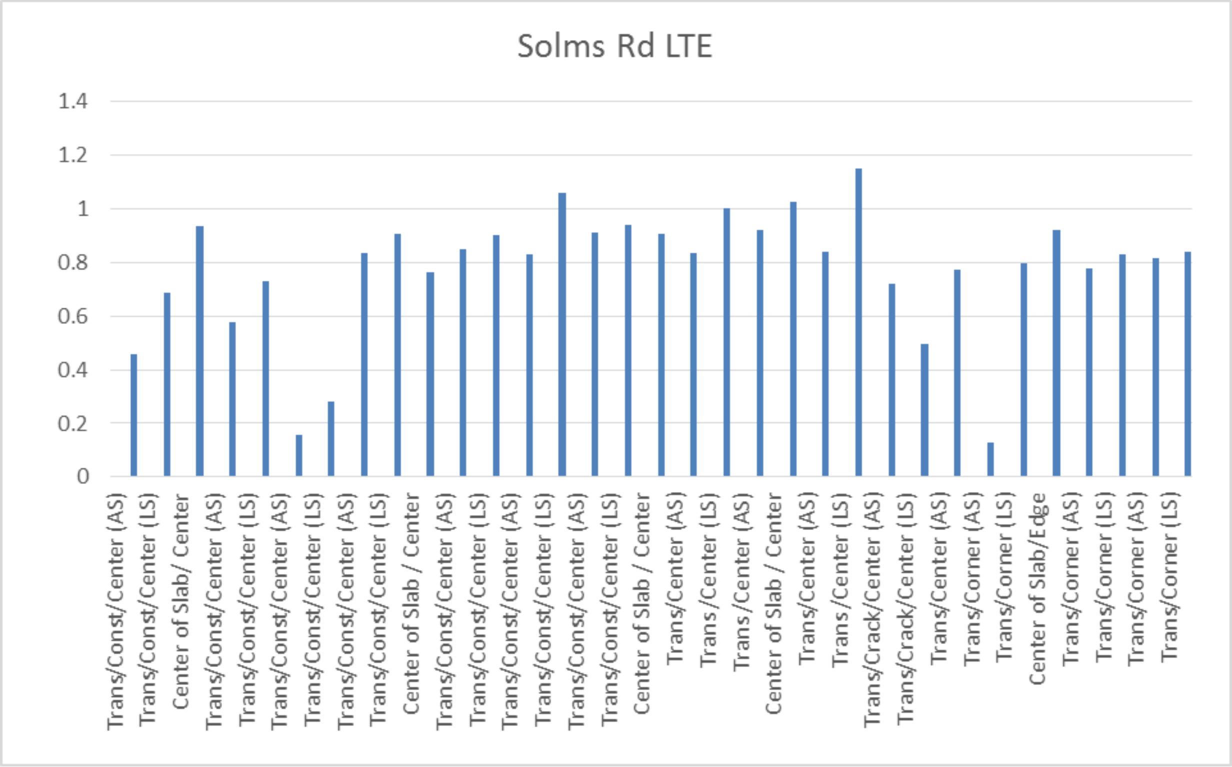

Figure 105. Solms Rd. (A) LTE.

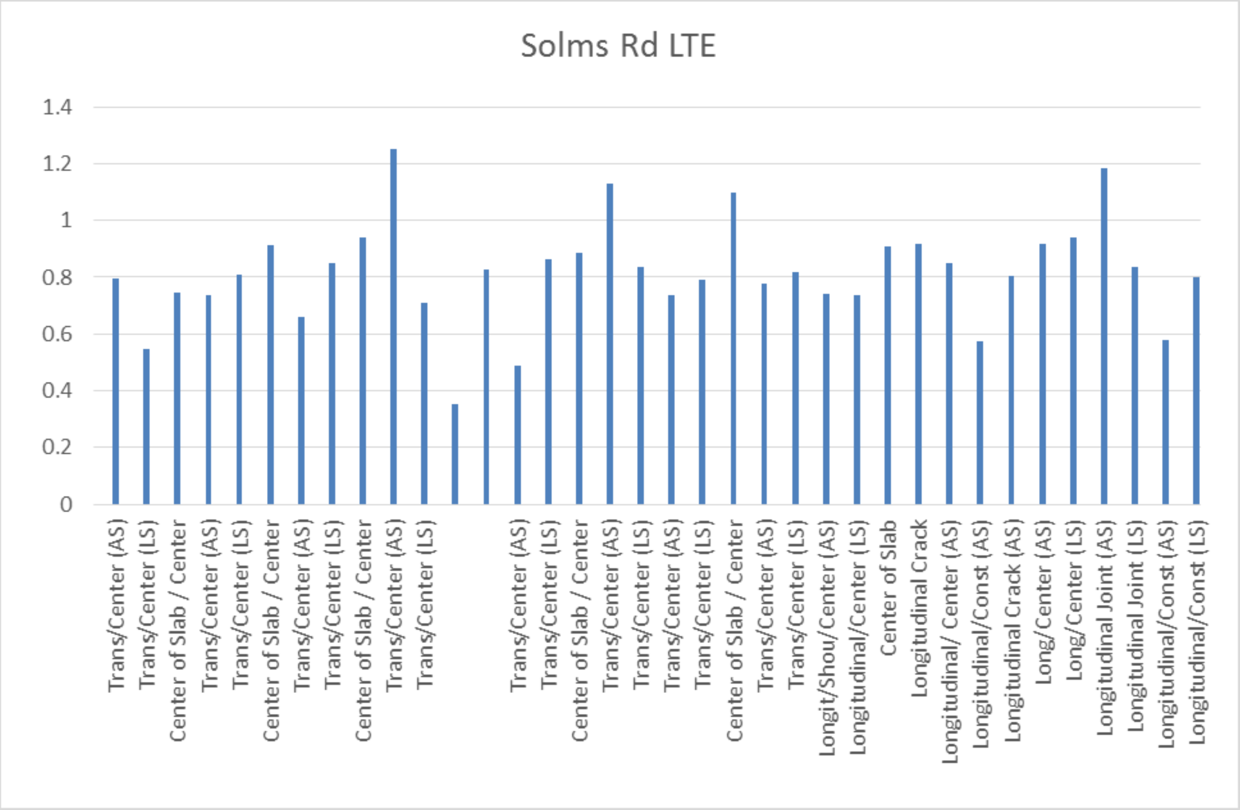

Figure 106. Solms Rd. (B) LTE.

Brownwood, Tx

Location

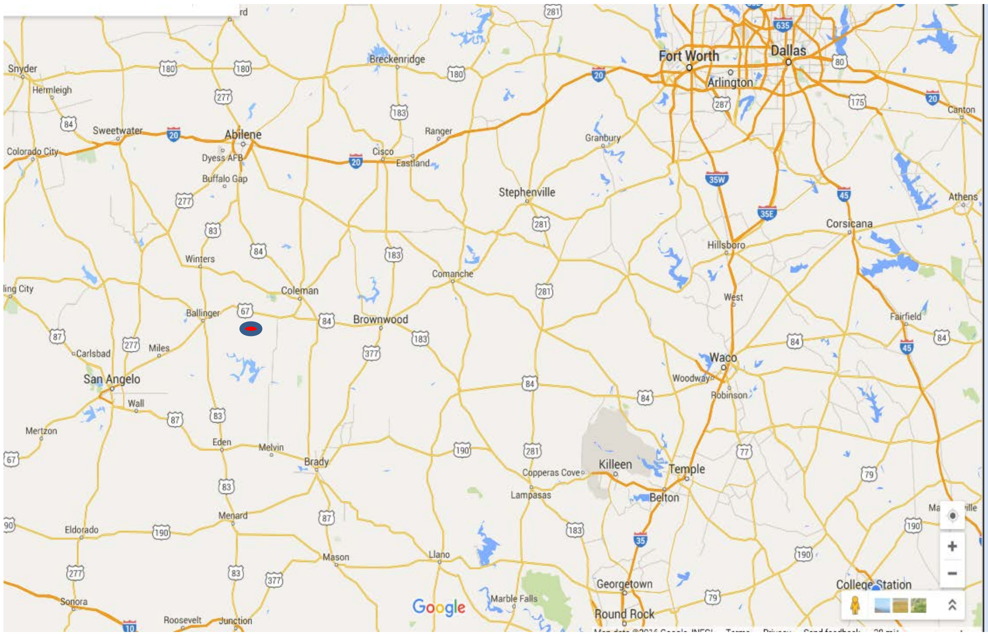
Snyder
Hermleigh
Sweetwater
Abilene
Dyess AFB
Buffalo Gap
Colorado City
Breckenridge
Cisco
Eastland
Ranger
Fort Worth
Dallas
Arlington
Canton
Granbury
Stephenville
Athens
Corsicana
Hillsboro
Winters
Comanche
Coleman
Ballinger
Brownwood
West
Fairfield
Waco
Woodway
Robinson
Carlsbad
Miles
San Angelo
Wall
Mertzon
Eden
Melvin
Brady
Copperas Cove
Killeen
Temple
Belton
Lampasas
Eldorado
Menard
Mason
Llano
Georgetown
Round Rock
Marble Falls
Sonora
Roosevelt
Junction
College Station
Google

Figure 107. Map of Location near Brownwood, Texas.

Site Description

This site is rest area constructed under TxDOT funding.

Pavement Specifications

For the Brownwood location, the following information were used for pavement section details as well as for testing description

- *Age*: constructed 1999.
- *Structure*:
  - Layer 12 in.; two lift construction.
  - Stabilized base 4 in.
- *Layout*: Not available.
- *Testing Description:* Testing was carried by TxDOT to determine the structural characteristics of the RCC pavement placed at the rest area.
- *Tests*: FWD.

Results

Figure 105 to Figure 108 show results of the analysis. Effective thickness shown in Figure 101 along the edges and corners of the RCC slabs suggests that some separation as confirmed by

TxDOT coring results has taken place between the lifts used to place the RCC pavement section. Nonetheless, the separation is not severe and tends to indicate that a certain amount of friction does exist between the lifts despite the separation. Some loss of LTE has occurred possibly due to the spacing of the cracks and their associated opening.

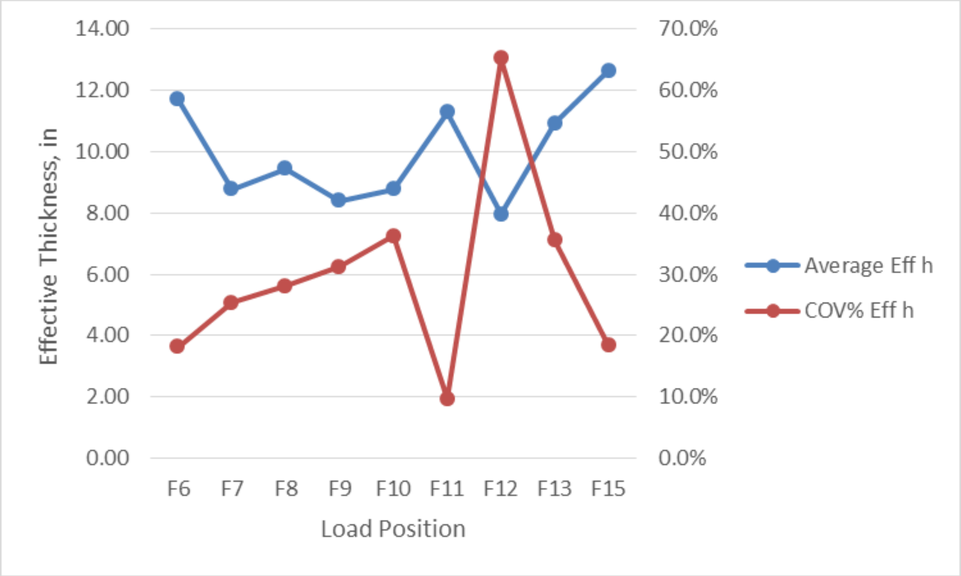

Figure 108. Effective Thickness—Brownwood Rest Area RCC.

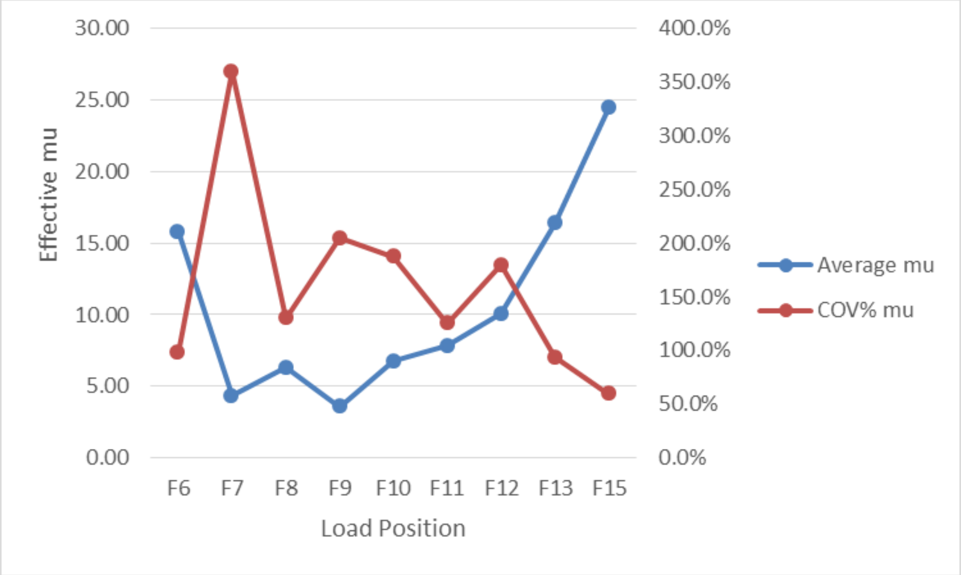

Figure 109. Effective µ Brownwood Rest Area RCC.

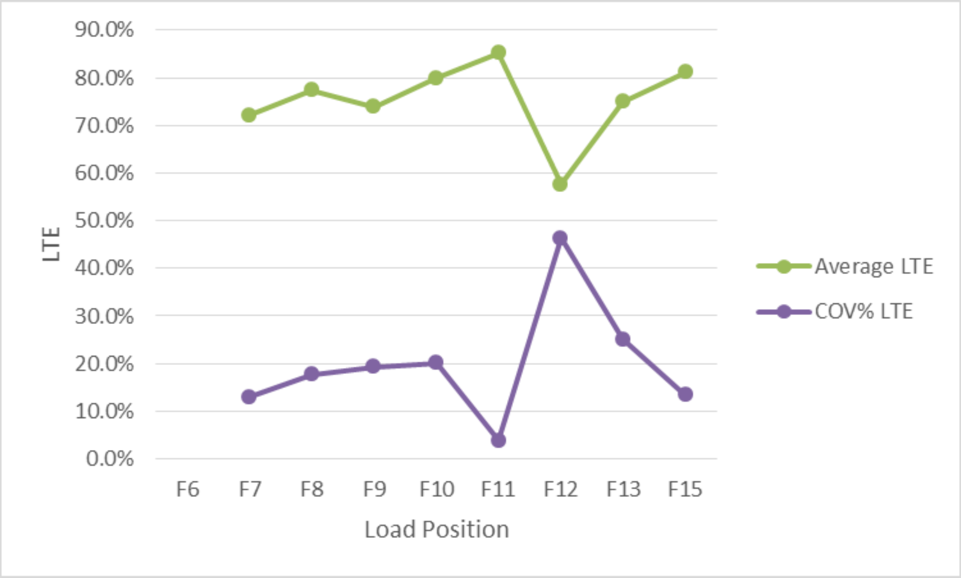

Figure 110. LTE Brownwood Rest Area.

FIELD RESEARCH SUMMARY

Evaluation of the field surveys and the FWD testing is still under way but the following points can be made to date on a preliminary basis:

- Both good and poor sections of RCC pavement were visited in Texas.
- RCC tends to have an open surface texture and may contribute to increased drying shrinkage requiring a higher degree of curing protection.
- RCC paving and layout must be done for the drainage scheme for the entire project that adequately addresses and minimizes the accumulation and ponding or standing of water on the pavement surface. Surface drainage may be the key to long-term performance.
- Longitudinal joints should not be subjected to high loading frequency.
- Transverse joints are typically under compression restraint and if tightly closed will carry heavy loads effectively.
- Two lift construction tends to be problematic and may result in the separation between consecutive lifts.
- Blow ups may occur in RCC but likely at weakened joints or break points in grade.
- Apparently it is possible to get strength in RCC without the use of rolling operations particularly if the pavement is placed on a stiff base layer.

CONCLUSION/RECOMMENDATIONS

No conclusions are drawn at this time other than the use of RCC in heavy traffic situations is certainly feasible and has been done in Texas in recent projects. However, certain precautions are important to take relative to drainage and layout of longitudinal joints relative to the location and travel paths of the heavily loaded vehicles.

CHAPTER 2. FIELD ANALYSIS OF THE INTERSECTION OF US 181/SH 123 IN KARNES CITY, TEXAS

INTRODUCTION

In the previous section, a field investigation of RCC pavements placed in Texas was conducted to assess the performance their performances. In this section of field investigation, assessment of current condition of a site located in Karnes City, Texas, is conducted through field and laboratory testing. These testing are essential to create different viable options to reconstruct the roadway that will test different design techniques to improve future use.

SITE DESCRIPTION

The intersection is laid out in a T shape format with SH 123 (also known as Business 181) ending into US 181. The intersection has a large leg for northbound US 181 traffic to exit on SH 123 at higher speeds but that section will not be included in this project. The small leg from southbound SH 123 to US 181 is included in the scope. US 181 has two northbound lanes, one southbound lane, and a split southbound used for merging traffic on and off US 181. A raised concrete median in the shape of a triangle is located at the center of the split southbound lane and another raised concrete median is located inside the SH 123 and the small leg described before. There are two traffic signal poles with one extending over the constant flow southbound lane and the other extending over the two southbound lanes immediately north of the intersection.

For the full length of US 181 the center median is an asphalt concrete paved culvert with inlets at low points. The intersection of US 181 for this project is the low point between the north and south boundary of the scope of work. Directly underneath the intersection is a concrete culvert that drains out and north along the west side of SH 123. A grassy drainage culvert runs the full length of the west side of US 181 and another runs along the east side of US 181 north of SH 123. The large triangle shaped area inside 181/123 and the large leg or exit ramp, currently drains to the southeastern portion where a concrete culvert drains underneath the ramp. The change in grade from the roadway of US 181 down to the large triangle area is very steep in upwards of 5 ft of rise for 5 or less feet of run. The area engineers have expressed major concerns for any change in drainage of this area specific.

CURRENT SITE CONDITION

The site is currently constructed of HMA throughout both section of the intersection. SH 123 has been reconstructed for the most part with 12 in.+ of AC and up to 24 in. of asphalt and cement treated base layers. The subgrade is these areas is still presenting problems even with the full depth repair areas. The southbound lane of SH 123 has some areas with the 8 in. AC layer and 12 in. cement treated base. The majority of US 181 is constructed of 8 in. AC layer and a 12 in. cement treated base with some small areas of patching. A distress survey was conducted to record keys areas of interest with the results in the testing section.

TESTING/DATA COLLECTION PERFORMED

The data collection and testing was divided into two parts field and laboratory testing. For testing the current pavement surface condition, the field testing was conducted at the intersection and it included the following testing:

- FWD.
    - Data collection system used: TTI FWD.
      Load weights = 6,000 lb, 9,000 lb, 12,000 lb, 16,000 lb (9,000 lb results used following ASTM standards).
    - Sensor locations = 0 in., 12 in., 24 in., 36 in., 48 in., 60 in., 72 in. from center of load plate to measure parameters such as deflections, bonding, modulus and subgrade interaction.
- Visual distress survey.
- Coring.
- DCP.

To assess the condition of subgrade and base materials, laboratory testing was conducted to investigate the need for stabilization of existing subgrade for the future concrete overlays. The subgrade materials were obtained from the intersection of US 181/SH 123 in Karnes City while base materials were collected from Martin Marietta quarry in San Antonio. The laboratory testing included the following:

- Moisture-density relations for subgrade, base, and stabilized base and subgrade materials.
- Seven-days compressive strength testing for stabilized subgrade and base material samples.
- pH testing for subgrade materials to determine lime percentage in subgrade stabilization.
- Capillarity testing.
- Site testing external parameters:
    - FWD testing—date: August 2015/temp: 90°F/time: 10:00 a.m.
    - Coring/DCP/subgrade and base sampling – date: October 2015/temp: 70°F/time: 10:00 a.m.
    - GPR data (data acquired 1–2 years prior to project).
    - Traffic data—recent and past traffic counts are being obtained by the interim district engineer.

FIELD RESULTS/FINDINGS

Distresses Observed

The following distress types were found:

- Fatigue cracking.
- Alligator cracking.
- Rutting.
- Bleeding.
- Stripping/layers debonding.

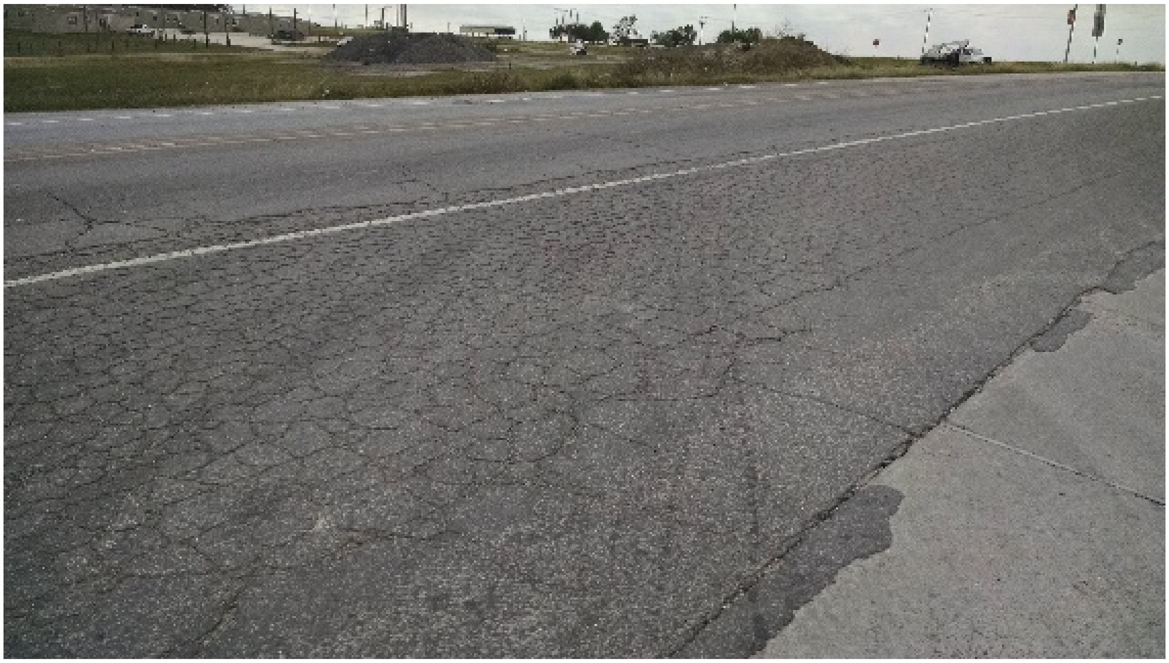

Figure 111. Alligator Cracking Distress Located on SH 123, Approach Lane toward US 181.

From visual inspection alligator cracking was found heavily along SH 123 and in the southbound split lane from the intersection on. The stripping was assumed after looking at FWD data and was proven when the cores in locations 1 and 2 easily came apart at 4 in. and 6 in. depth.

FWD Analysis

FWD data were collected in the outer wheel path of each lane. The intersection was divided into sections and five runs were made to collect the entire site data. Each run is described below and the colors correspond to those in Figure 112:

- Run 1 runs down the southbound lane of SH 123 (light blue).
- Run 2 beginning in the turning lane of the southbound US 181 split and goes through the intersection and down the northbound lane of SH 123 (pink).
- Run 3 is the length of the southbound constant flow lane on US 181 (blue).
- Run 4 is the length of the northbound lane of US 181 (red).
- Run 5 starts at the end of SH 123 and goes through the intersection and down the lower half of the southbound split (yellow).

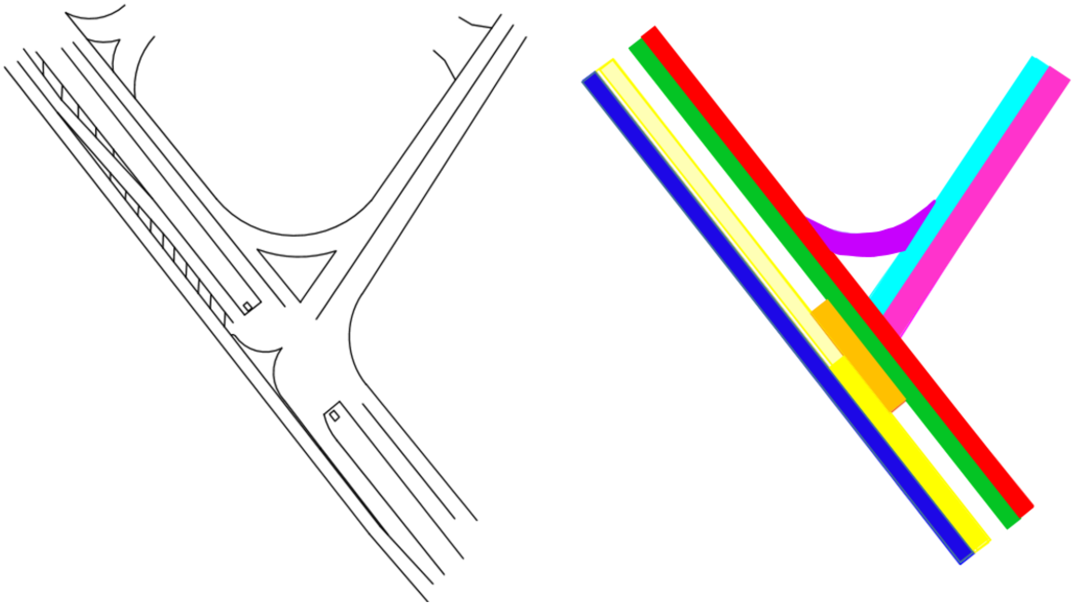

Figure 112. US 181 Intersection Breakdown Layout.

The complete FWD data are located in the appendices. From the FWD data, researchers used the ModulusSetupTexas2015 program to compile results and come up the following parameters.

Table 24. FWD R1 Sensor Deflection Data.

Run #	**Block Section Color**	**Section Description**	**R1 Sensor Deflections (mils)**				
			Average	***Minimum***		***Maximum***	
				Value	*Location*	*Value*	*Location*
1	Light Blue	SH 123 Southbound Lane		4.76	923	40.9	858
2	Pink	SH 123 Northbound Lane		3.65	57	46.18	263
3	Blue	US 181 Southeast-bound (Constant Traffic Flow Lane)		16.01	500	31.05	50
4	Red	US 181 Northwest-bound Outer Lane		10.04	209	27.7	509
5	Orange/Yellow	Through Intersection & Down Southeast-bound Split Lane	**46.03**	20.19	0	55.59	255

Table 25. FWD Calculated Subgrade Modulus.

Run #	Block Section Color	Section Description	Calculated Subgrade Modulus (ksi)				
			Average	Minimum		Maximum	
				Value	*Location*	*Value*	*Location*
1	Light Blue	SH 123 Southbound Lane					
2	Pink	SH 123 Northbound Lane					
3	Blue	US 181 Southeast-bound (Constant Traffic Flow Lane)					
4	Red	US 181 Northwest-bound Outer Lane					
5	Orange/Yellow	Through Intersection & Down Southeast-bound Split Lane	**1.8**	1.1	384	2.7	0

Table 26. FWD Calculated Base Layer Modulus.

Run #	Block Section Color	Section Description	Calculated Base Modulus (ksi)				
			Average	Minimum		Maximum	
				Value	*Location*	*Value*	*Location*
1	Light Blue	SH 123 Southbound Lane					
2	Pink	SH 123 Northbound Lane					
3	Blue	US 181 Southeast-bound (Constant Traffic Flow Lane)					
4	Red	US 181 Northwest-bound Outer Lane					
5	Orange/Yellow	Through Intersection & Down Southeast-bound Split Lane	**51.8**	50	63	64.3	0

Table 27. FWD Calculated Surface Layer Modulus.

Run #	Block Section Color	Section Description	Calculated Surface Modulus (ksi)				
			Average	Minimum		Maximum	
				Value	*Location*	*Value*	*Location*
1	Light Blue	SH 123 Southbound Lane					
2	Pink	SH 123 Northbound Lane					
3	Blue	US 181 Southeast-bound (Constant Traffic Flow Lane)					
4	Red	US 181 Northwest-bound Outer Lane					
5	Orange/Yellow	Through Intersection & Down Southeast-bound Split Lane	**340**	340	All	340	All

Figure 113 shows the max deflections (0 in.- sensor/center of load plate). Run 5 demonstrated the highest deflections. The large deflections are found over a 200 ft span, which leads one to believe there is insufficient subgrade support in that area, and it must addressed in the coming design schemes.

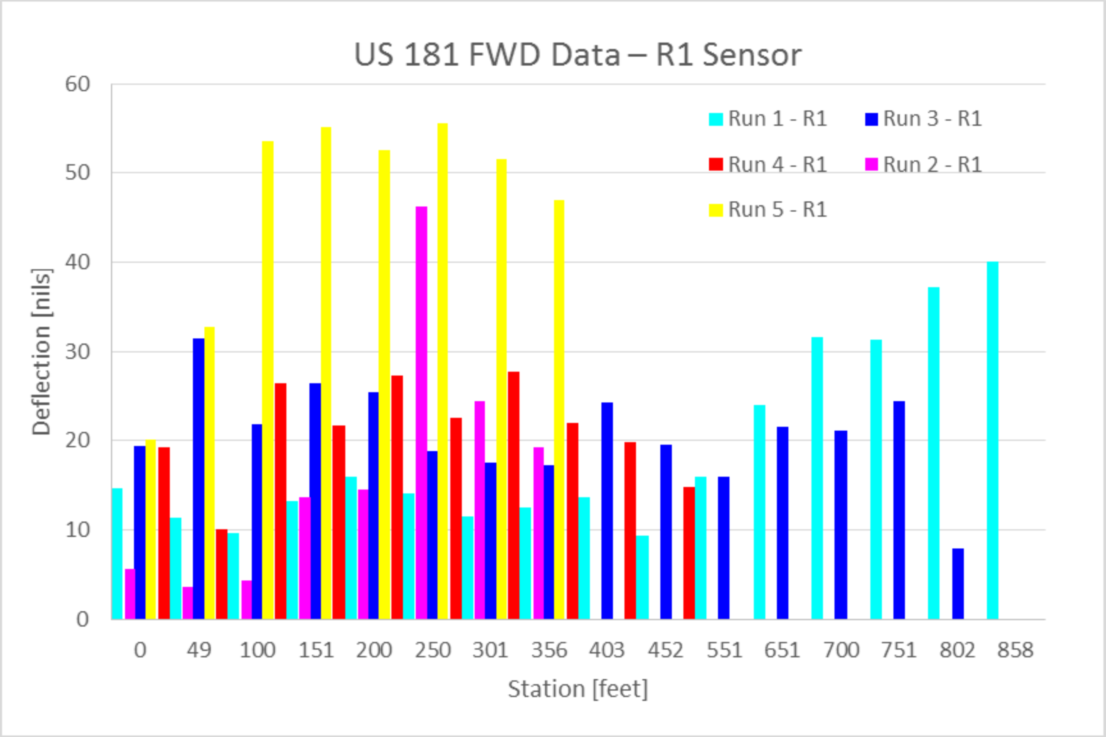

Figure 113. FWD Deflection Data of Sensor at Load Plate Center Plot.

From the plot. the section 5 exhibited the most deflection as compared to the rest of the site. Run 2 showed a spike in the area where heavy alligator cracking was present. Run 1 shows an increase at the end, which is the length through the small leg and onto US 181.

Coring

Figure 114 shows cores were taken at four locations labeled. The locations were selected by the project committee accounting for key distressed areas and heavy traffic areas. The cores were cut 8 in. into AC layer and then extracted as undisturbed as possible. DCP was used to first estimate base layer thickness and then the auger was used to remove the base material that was collected for testing as well. The DCP was also run of the undisturbed subgrade to determine subgrade modulus. At each location two or more cores were taken to get the most accurate representation of the location. Some DCP data were inaccurate due to base material still being present but those areas are addressed in the DCP data section.

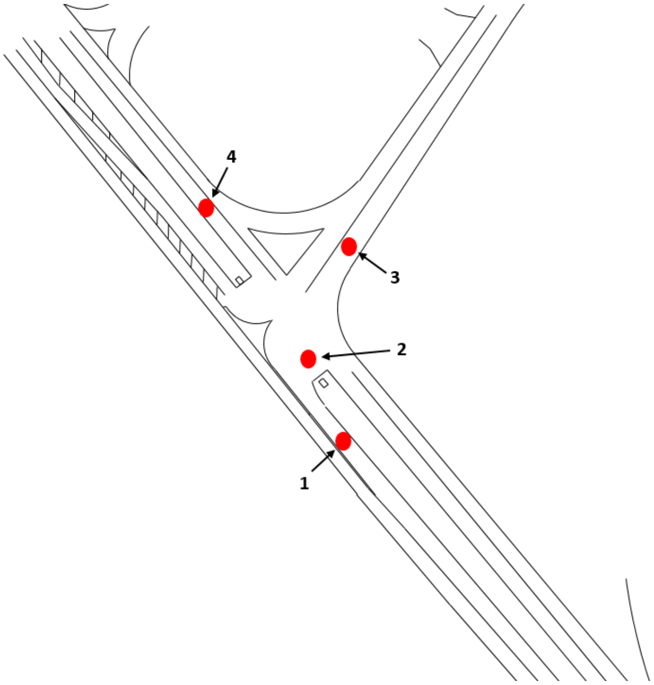

Figure 114. US 181/SH 123 Core and DCP Locations.

Coring Field Notes

At Location 1, researchers were able to drill the hot mix, remove the base layer with the auger, and run DCP on the subgrade. The three cores were drilled for this location to get a solid sample. First specimens exhibited stripping of the asphalt layers.

At Location 2, researchers drilled the hot mix and could not remove all the base layer with the auger. Researchers removed most of the base and ran DCP. No stripping was present with these cores. The base layer of cement stabilized. Base layer was hard enough that the second core was drilled to try and penetrate base layer. Researchers were unable to penetrate the base with auger more than 6 in. DCP ran through base layer and into subgrade.

Location 3 was a full depth repair section. Researchers drilled approximately 11 in. of hot mix and ran into a solid base layer (LRA base probably). The hot mix layer and then base layer were too thick to penetrate even an inch with DCP after 50+ blows. Section thickness was addressed in the analysis.

At Location 4, researchers were able to drill the hot mix layer, then ran DCP through the base, to establish base layer thickness and then into the subgrade. This location was taken first and DCP was ran through the base and subgrade layers. Material of each was collected for further testing of composition, erosion, and any other parameters.

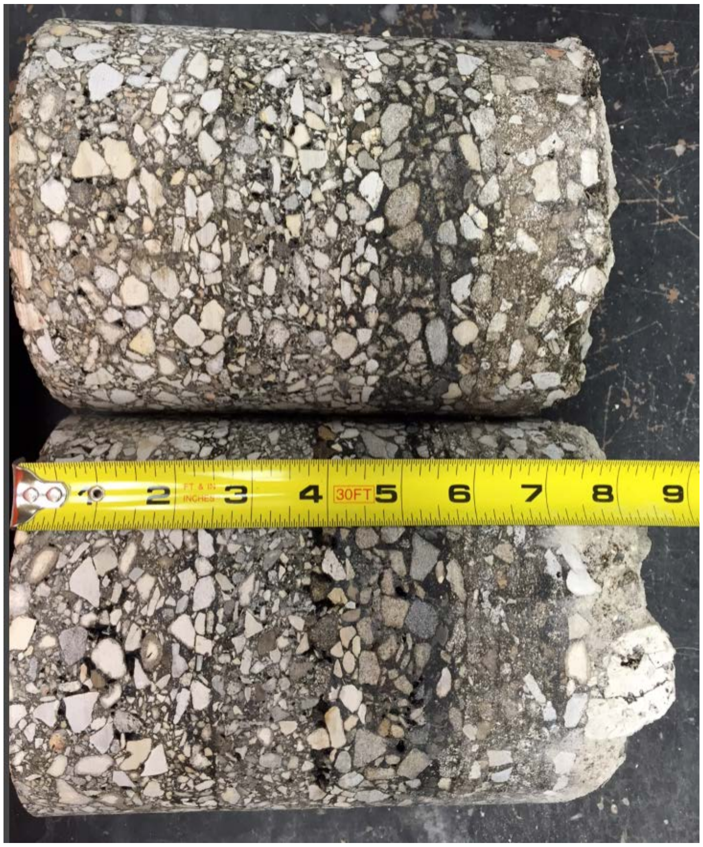

Figure 115. Core Location 4 Existing Material Samples.

DCP

Researchers were able to successfully run DCP tests on locations 1 and 2. Location 3 contained an asphalt concrete layer of more than 12 in. in the first core (Core bit only 14 in. deep) and 12 in. in the second core but then the base layer was stiff up to 24 in. So location 3 gave less than an inch of penetration for 50+ blows. Location 4 was cored and tested two days prior to the project team visiting the site for the coring of the rest of the site. The operator ran the DCP test starting at the top of the base layer and down 18 in., which did penetrate into the subgrade. This result verified the depth of the base layer for this location, but the modulus data yielded are invalid due to them including the base.

Table 28. DCP Calculated Parameters.

Core Location	Layers Tested	Penetrating Rate [mm/blow]	Modulus [ksi]
1	Subgrade	21.070	10.854
2	Base & Subgrade	17.211	12.547
3	Base	N/A	N/A
4	Base & Subgrade	7.866	21.995

LABORATORY RESULTS/FINDINGS

In the laboratory work, the moisture-density relationships for subgrade and base materials were established using the TxDOT testing manual procedures. To predict the amount of lime required for stabilization of subgrade materials, pH values were measured for different subgrade samples. Additionally, 7-days compressive strength of lime stabilized subgrade and cement stabilized base materials were tested to evaluate the effectiveness of chosen percent of stabilization. In moisture-density testing and compressive strength testing, stabilized samples were always compared to non-stabilized samples for evaluation. As mentioned before, subgrade materials were collected from site with help of Karnes municipality personnel and equipment while base materials were collected from the Martin Marietta quarry in San Antonio.

Relation of Moisture and Density

The moisture and density relationship was employed to determine the OMC for non-stabilized and stabilized base and subgrade material. For this testing, Tex 113-E and Tex 114-E were used. These procedures require molding at least 4 specimens with different moisture contents to determine the OMC and maximum dry density. Table 29 shows the tested materials and the associated optimum moisture and maximum density. Figure 116–Figure 121 show each case by the Tex 113-E and 114-E excel calculation sheet.

Table 29. Materials Tested and Their OMC and Maximum Dry Density.

Material Type	OMC (%)	Maximum Dry Density (pcf)
Base material only	8.6	137.1
Base material+6% cement	9.9	134.5
Subgrade only at 2 to 3 ft depth	16.1	108.3
Subgrade only at less than 2 ft	8	115.2
Subgrade only at more than 3.5 ft	13.5	80.6
Subgrade material+ 4% lime	11.8	112.1

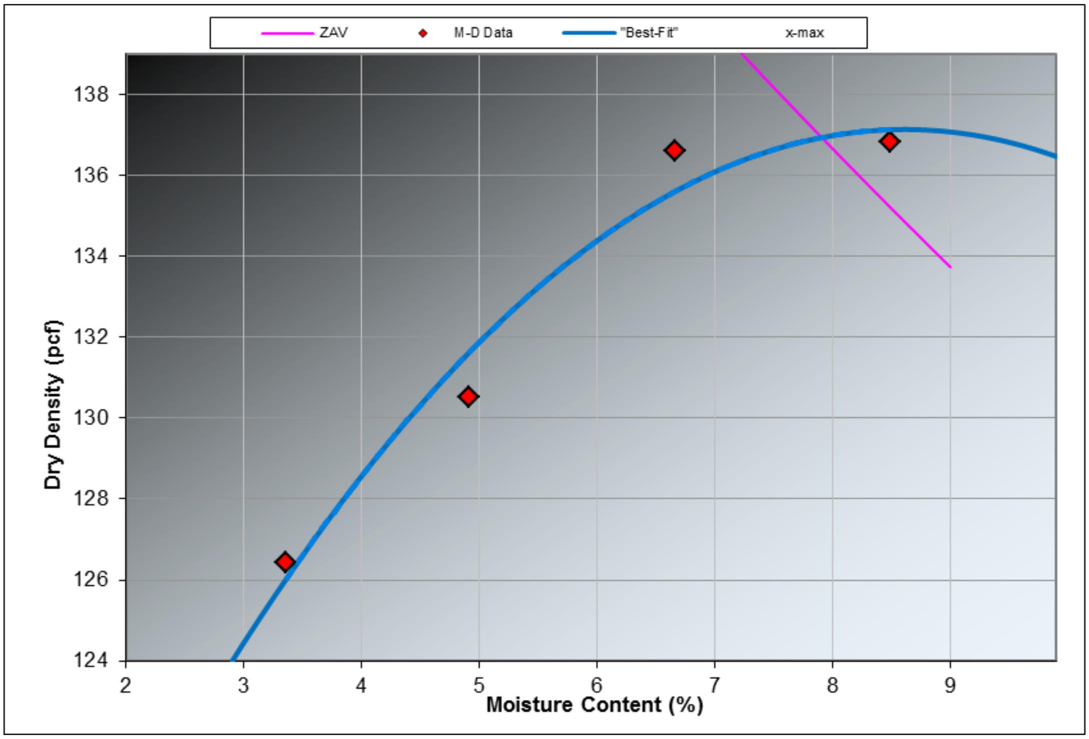

Figure 116. Moisture-Density Relation for Base Materials Only.

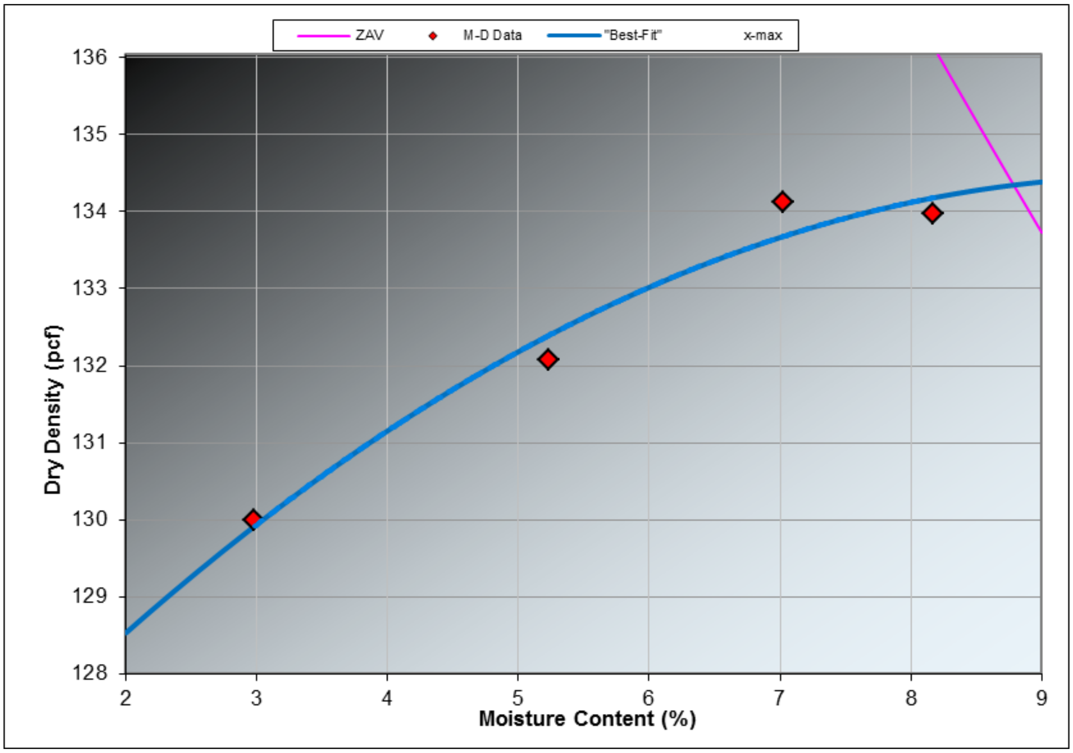

Figure 117. Moisture-Density Relation for Base Materials+6 Percent Cement.

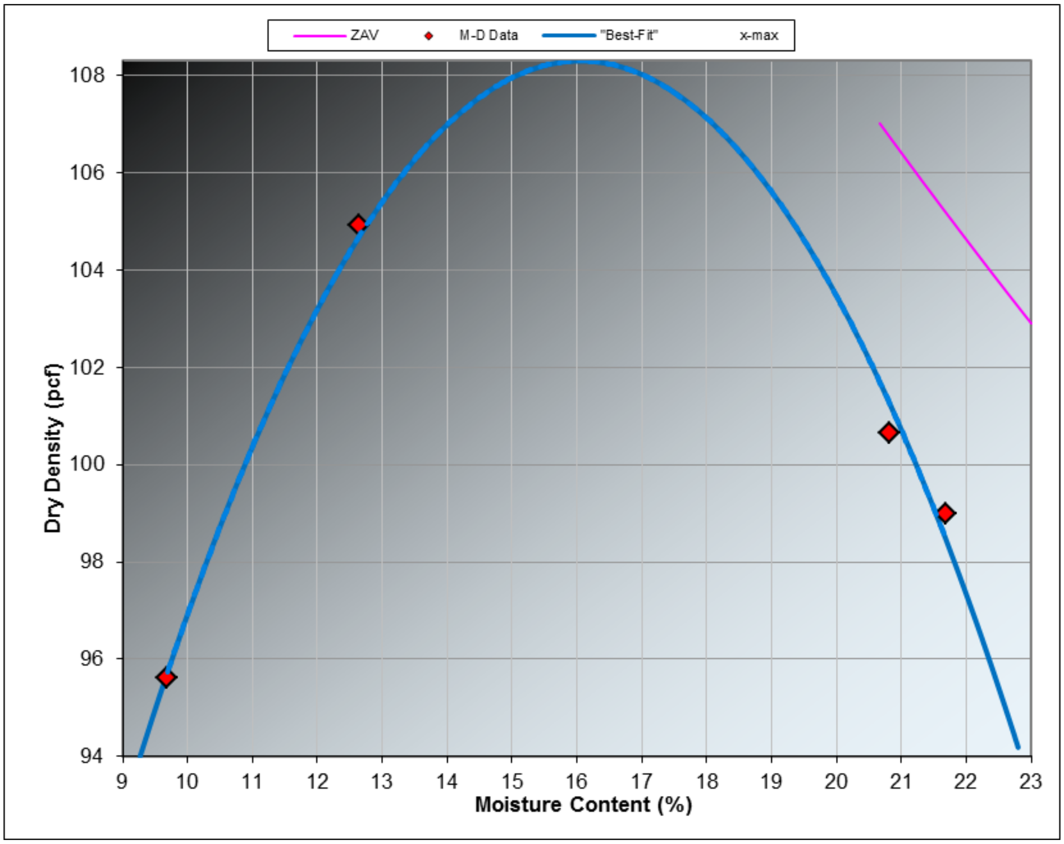

Figure 118. Moisture-Density Relation Subgrade Materials Only—Depth between 2 and 3 ft.

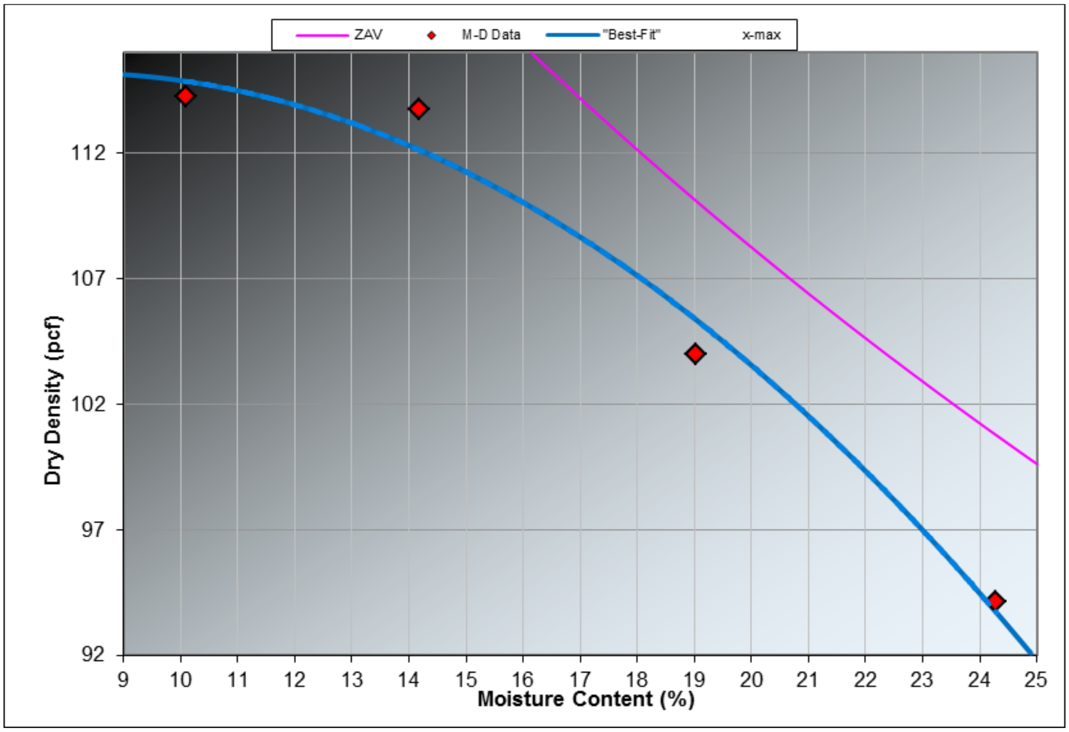

Figure 119. Moisture-Density Relation Subgrade Materials Only—Depth < 2 ft.

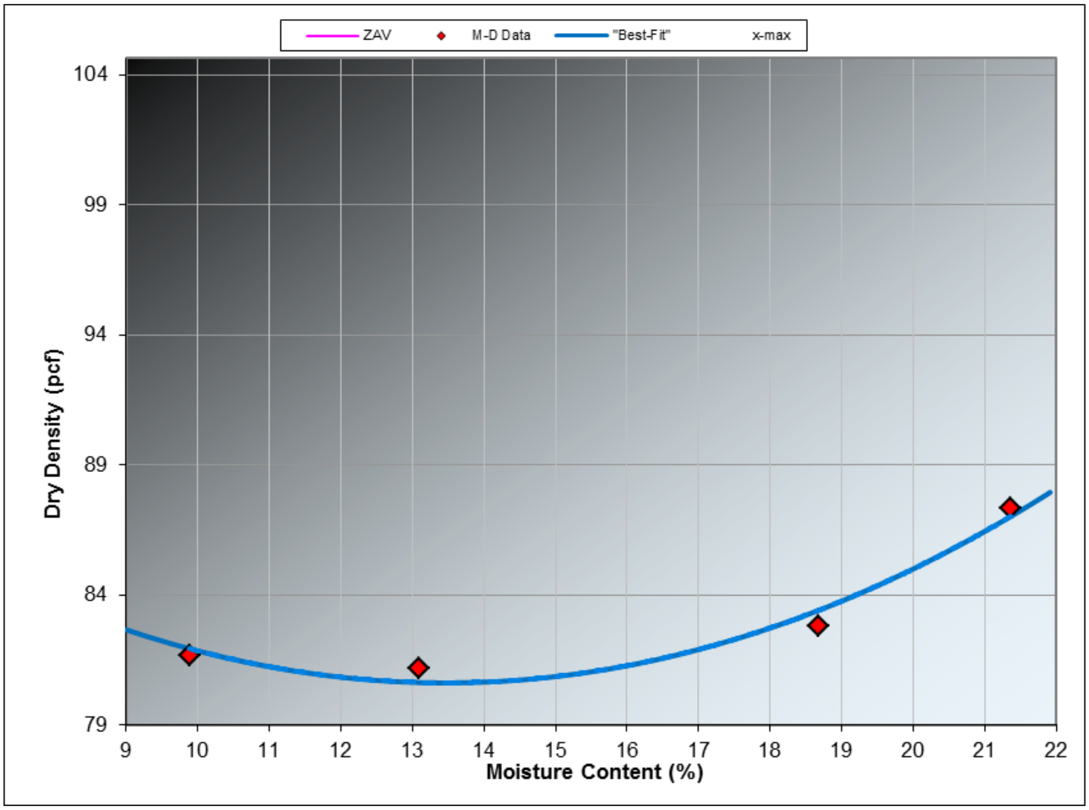

Figure 120. Moisture-Density Relation Subgrade Materials Only—Depth > 3 ft.

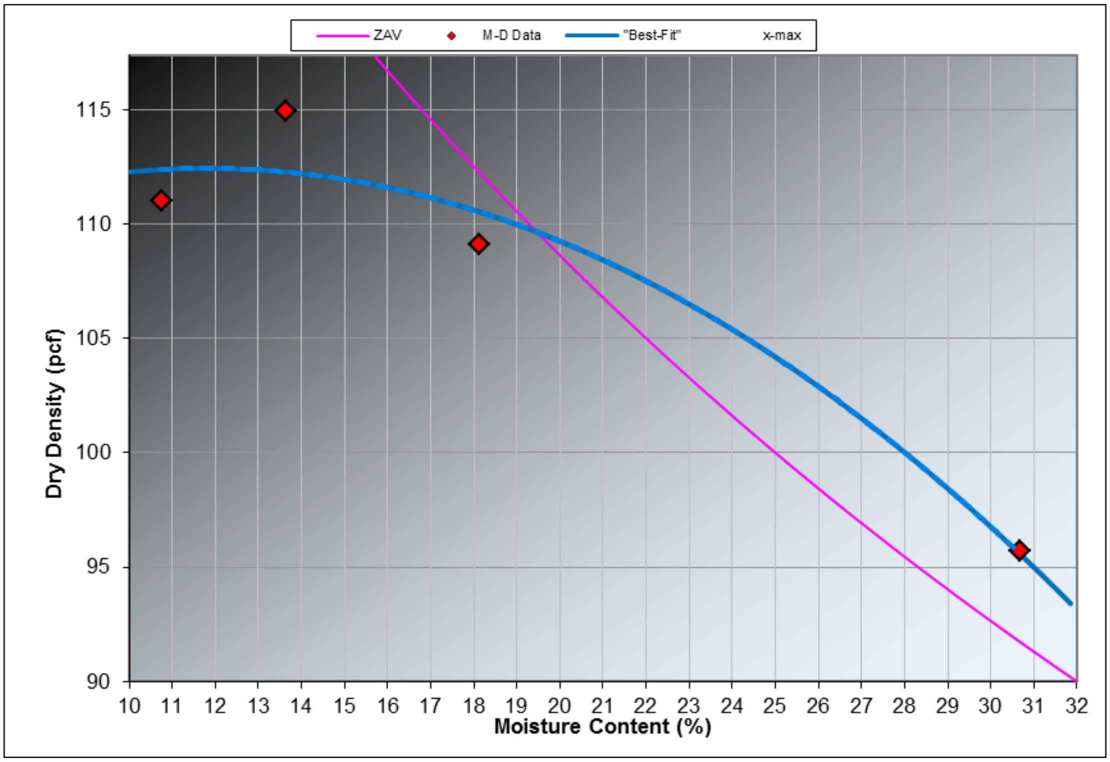

Figure 121. Moisture-Density Relation Subgrade+ 4 Percent Lime.

Measure pH for Subgrade

The subgrade materials are commonly stabilized using the lime. To determine the amount of lime required for subgrade material, pH values should be determined using Tex 121-E and Tex 114-E test procedures. pH testing is usually conducted by mixing different percent of lime (0, 2 percent, 4 percent, 6 percent, 8 percent, 10 percent) with subgrade samples and measuring the pH. The good percent of lime stabilization should meet 12.4 pH value. pH of 12.3 or 12.2, as a minimum value, can be used in case pH of 12.4 cannot be approached. The proper percent of stabilization is then taken as the minimum lime percent that satisfy the required pH value. Table 30 andTable 31 show the measured pH value for subgrade samples at depth less than 3 ft and more than 3 ft. Figure 122 shows the relationship between the lime percent and the pH values for different subgrade materials.

Table 30. pH Measurements for Subgrade Materials—at Depth < 3 ft.

Lime percent (%)	pH
0	7.7
2	12.2
4	12.3
6	12.3
8	12.3
10	12.4

Table 31. pH Measurements for Subgrade Materials—at Depth > 3 ft.

Lime Percent (%)	pH
0	7.62
2	12.1
4	12.2
6	12.2
8	12.2
10	12.2

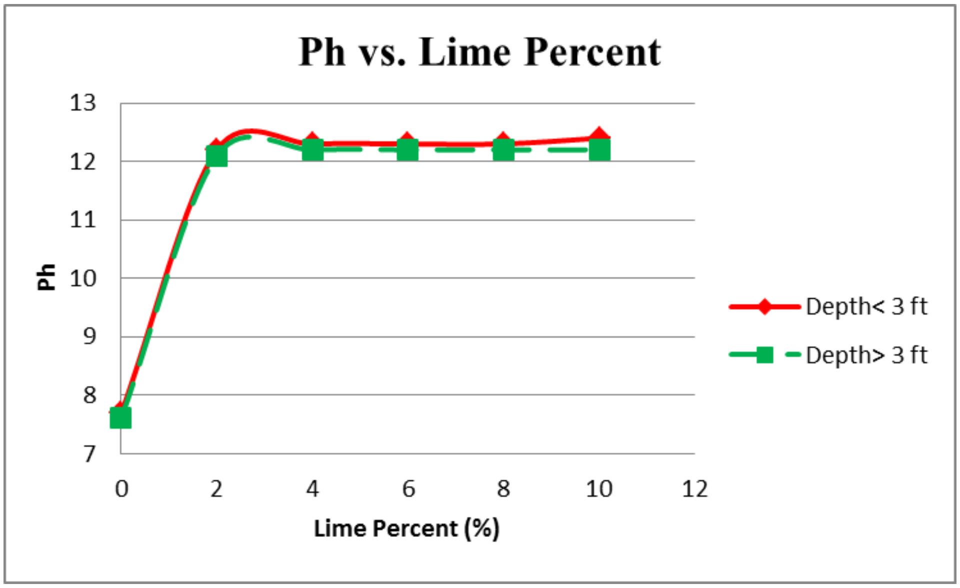

Figure 122. Relationship of pH with Lime Percent Change.

From the measured values of pH, the optimum amount of lime stabilization required for the subgrade materials at Karnes City is 4 percent of lime.

7-days Compressive Strength

Seven-days compressive strength was measured for stabilized base and subgrade materials. Compressive strength testing was conducted on base materials stabilized with 4 percent, 6 percent, 8 percent, and 10 percent cement as required by the Tex 120-E test procedure. For each cement percent, three samples were fabricated and tested after 7 days. An average corrected stress was then measured by the Tex 120-E excel sheet. Upon determining the average corrected stresses, the Tex 120-E excel sheet determined the best amount of cement stabilization based on the targeted stress of 500 psi. In the case of obtained base material, the targeted cement percent was 3.2 percent. Table 32 shows average corrected stresses obtained from the compressive strength testing on stabilized base materials. Additionally, compressive strength testing was conducted on subgrade samples stabilized by 4 percent of lime using Tex 114-E test procedure. Three samples were fabricated and tested as shown in Table 33.

Table 32. Average Corrected Stress Measurements Different Cement Percent.

Percent Cement, (%)	4	6	8	10
Avg. Corrected Stress, psi	**505.1**	**726.3**	**1360.5**	**1002**

Table 33. Average Compressive Strength Measurement for 4 Percent Lime Stabilized Subgrade Samples.

Specimen No.	1	2	3
Lime percent	4	4	4
Initial specimen height, in.	6	6	6
Average diameter, in	4	4	4
Cross sectional area, in^2	12.56	12.56	12.56
Lateral pressure	0	0	0
Max. load reading, div.	2012	3537	3281
Deformation at max. load, in.	0.2553	0.194	0.1975
Ultimate stress, psi	160.19	281.61	261.23
Average Compressive strength	**234.34**		

Capillarity Testing

Capillarity testing using Tex 117-E test procedure was conducted to determine the requirement of stabilization for subgrade or/and base materials. Capillarity testing, following the procedure in Tex 117-E, measures the amount of moisture ingress in a specific time. The amount of capillarity can be used then to judge whether the subgrade layer requires stabilization to perform well. Figure 123 shows the results of capillarity testing for base and subgrade samples. As seen in the figure, subgrade samples show higher moisture after capillarity test than base samples. These results are significant especially when comparing 4 in. × 6 in. subgrade samples with 6 in. × 8 in. base samples. As shown in the figure, subgrade specimens show that the results are within the same range and thus reasonable. Base specimens show some difference in moisture after capillarity. The first specimen seems more reasonable than the second one. The problem in the second specimen can be due to the lower compaction quality or the presence of surface cracks due to specimen fabrication.

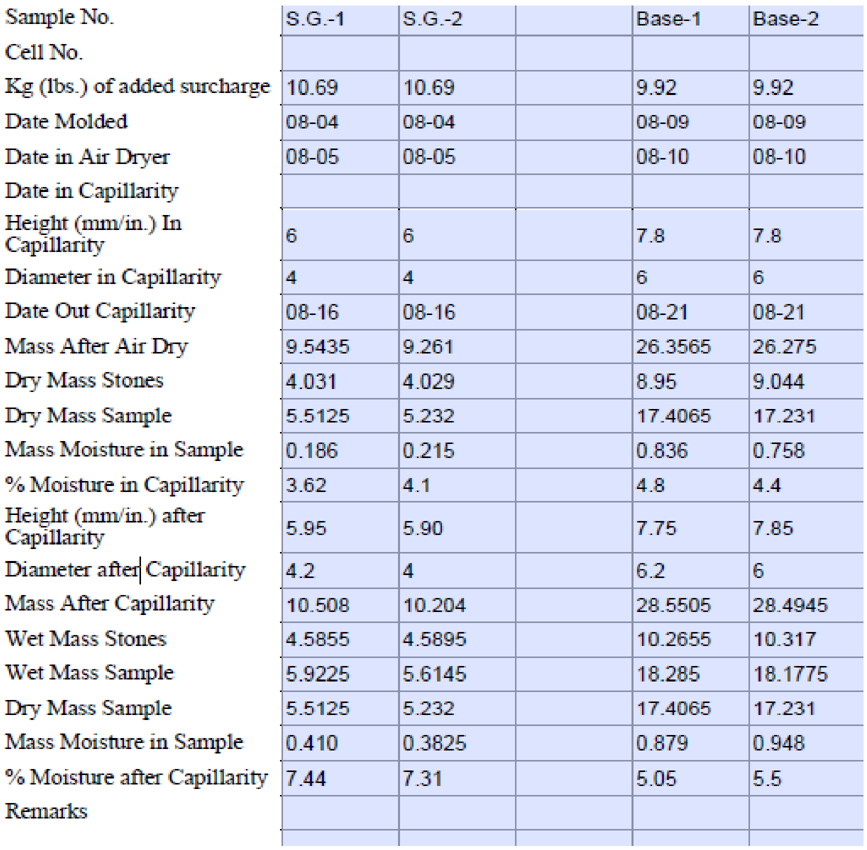

Sample No.	S.G.-1	S.G.-2		Base-1	Base-2
Cell No.					
Kg (lbs.) of added surcharge	10.69	10.69		9.92	9.92
Date Molded	08-04	08-04		08-09	08-09
Date in Air Dryer	08-05	08-05		08-10	08-10
Date in Capillarity					
Height (mm/in.) In Capillarity	6	6		7.8	7.8
Diameter in Capillarity	4	4		6	6
Date Out Capillarity	08-16	08-16		08-21	08-21
Mass After Air Dry	9.5435	9.261		26.3565	26.275
Dry Mass Stones	4.031	4.029		8.95	9.044
Dry Mass Sample	5.5125	5.232		17.4065	17.231
Mass Moisture in Sample	0.186	0.215		0.836	0.758
% Moisture in Capillarity	3.62	4.1		4.8	4.4
Height (mm/in.) after Capillarity	5.95	5.90		7.75	7.85
Diameter after Capillarity	4.2	4		6.2	6
Mass After Capillarity	10.508	10.204		28.5505	28.4945
Wet Mass Stones	4.5855	4.5895		10.2655	10.317
Wet Mass Sample	5.9225	5.6145		18.285	18.1775
Dry Mass Sample	5.5125	5.232		17.4065	17.231
Mass Moisture in Sample	0.410	0.3825		0.879	0.948
% Moisture after Capillarity	7.44	7.31		5.05	5.5
Remarks					

Figure 123. Capillarity Testing Results for Subgrade and Base Material Samples.

SUMMARY

Overall the condition of US 181 is currently within allowable distress limits. The SH 123 leg is experiencing severe failures in areas of patching, in full-depth repair areas, and original construction areas. The main distress on US 181 is the stripping of previous overlay layers. The heavy traffic turn lanes are the area of greatest distress and failure. The FWD data support the notion that the area in Run 5 (southeast-bound US 181 split lane) is failing in the asphalt layer and in the subgrade. The next step of the project will be coming up will viable designs for reconstruction. These data will be used in determining areas where base and subgrade repair will be required.

In the laboratory testing part, moisture-density curves were established for stabilized and non-stabilized subgrade and base materials. The required amount of lime stabilization for subgrade was determined through pH testing while the optimum percent of cement stabilization for base materials was measured along with the compressive strength testing procedure. To suggest the type of stabilization (subgrade or base stabilization) required for Karnes City case, the drainage factor (DF) was calculated. This can be calculated by dividing the volume of added moisture (through the capillarity test) by the number of testing hours (V/L). The number should be as close as possible to zero. The typical situation is to have higher DF value in subgrade than in base materials. In capillarity test results, DF for subgrade specimen was around 0.30 and DF for the base specimen was 0.08, which is reasonable. However, the DF value is considered high for subgrade materials specimen and that indicates the need for stabilization for the subgrade layer.

CHAPTER 3. DECISION TREE PROCEDURE FOR SUITABLE ALTERNATIVE SELECTION

INTRODUCTION

Pavement maintenance and rehabilitation plans require extensive information on the condition of the current pavements and facilities. Extra effort is also required to determine the suitable pavement selection. To achieve long-term pavement design, concrete pavement types are considered as the main alternatives for roadways in the energy sector. To install the newly designed concrete pavements properly, maintenance and rehabilitation of existing pavement surface is highly significant. Therefore, existing pavement condition, features of feasible pavement types and construction limitations should be merged to produce an effective decision-making process.

This chapter documents the development of guidelines for the selection of suitable alternatives from a list of feasible alternatives. Additionally, to guide the collection of needed additional pavement condition data to narrow the choices to a list of suitable alternatives. This step is referred to step 3 in the Task Report #4, Framework for Repair Alternative Selection. Step 3 in the mentioned document included the following six substeps:

1. Traffic and load information.
2. Select feasible alternatives.
3. Screen for acceptable alternatives.
4. Determine traffic level and time of construction.
5. Estimate first cost.
6. Identify suitable alternatives.

This chapter incorporates most of the previously mentioned substeps into summarized decision-making steps that can be easily used to identify the suitable alternatives that need further consideration and analysis. Due to use of concrete pavement systems, traffic and load information are important for the thickness design but not for the selection of the pavement material. The energy sector has a high traffic volume and concrete pavement systems are basically the initial solution of such cases. In addition, screening of feasible alternatives depends mainly on the life cycle of the pavement systems. In concrete pavement, the life cycles tend to be within the same range so it is not significant to consider this item in the decision tree process. Moreover, first cost is implicitly considered in the feasible concrete pavement options and is exchanged by the level of importance and the grade restriction of the roadway in the suitable concrete pavement selection. In case of overnight construction, as an example, precast concrete pavement options are selected without any consideration to the initial cost. Hence, the process was refined to consider the list of selection of feasible concrete pavement types and suitable concrete pavement types. So, the substeps are the following:

1. Select feasible concrete pavement types, which considers:
    - Heavy traffic level in the energy sector.
    - Pavement thickness.
    - Constructability in terms of time and contractor skill level.
2. Select suitable concrete pavement types.

SELECT FEASIBLE CONCRETE PAVEMENT TYPES

As mentioned before, the energy sector is suffering from the huge volume of truck traffic that requires using pavement types that can be constructed faster and last longer. Thus, using concrete pavements is the best potential solution for such case. To match concrete pavement options with the existing conditions, specifying the main features and limitations of each concrete pavement type is highly significant.

Table 34 lists PCC pavement types appropriate for the energy sector. The specific characteristics of each option allow engineers to tailor the design of concrete pavement type using key site conditions and design objectives associated with the use of a given pavement type. This will lead to reduce uncertainty in the design selection stage and effectively increase the durability of the selected pavement type.

Table 34. Types of Concrete Pavement.

Precast Concrete		Cast-In-Place Concrete	
Prestressed (Pretentioned)	Non-prestressed	Prestressed (Posttensioned)	Non-prestressed
o Precast-Prestressed Concrete pavement (PPCP)	o Precast Concrete Pavement	o Jointed Posttensioned Concrete Pavement (JPoCP) o Continuous Reinforced and Posttensioned Concrete Pavement (CRPoCP)	o Jointed Plain Concrete Pavement (JPCP) o Continuous reinforced Concrete Pavement (CRCP) o RCC

Initial cost is the driving force of using the cast-in-place pavement types such as the JPCP, CRCP, and RCC. However, other advantages can be obtained from these pavements as follows.

Jointed Plain Concrete Pavement

JPCP is placed at 15 ft, unreinforced with transverse joints between the slabs. The joints are close enough so that fatigue cracks do not occur until a late stage in the pavement service life. To handle the effect of heavy traffic presented in the energy sector, jointed system is doweled at the transverse joints. The other type of un-doweled jointed pavement is alternatively posttensioned. The 15-ft joint spacing is a significant component that will limit the environmental stress level to prevent premature cracking. The way that jointed system work is by developing the bottom-up cracking, which is considered a good feature of the long performance pavements. The selection of JCPC can be due to the following reasons:

- JPCP is the cheapest concrete pavement type due to the ease of placement and requirement of no special detailing. It is very economical because of the absence of financial burden to buying and installing steel dowelling.
- In regions where corrosion of steel is a major problem, using non-reinforced concrete yields less concern for corrosion. On the other side, in the case of using dowels at joint between slabs, epoxy coated dowels can provide a potential solution for steel corrosion.
- Compared to the CRCP, JPCP can typically be constructed at a lower initial cost that may not be substantiated on a life cycle basis. These features may allow adopting the JPCP to various pavement construction activities such as roadways with crosswalks or intersections with placements less than 500 ft.

Continuously Reinforced Concrete Pavement

CRCP is characterized by long paving distance using a layer of steel reinforcement with construction or isolation joints only. In CRCP, volumetric changes due to temperature and moisture are restrained by the steel reinforcement, which limits movement of transverse cracks that usually appear randomly in the pavement. A well designed and constructed CRCP can have the following advantages:

- Eliminate joints and their maintenance cost for the entire service life of the pavement. This will allow officials to allocate financial resources for other projects, helping meet the public’s desire in reducing maintenance zones and limiting user delay cost.
- Consistent performance is attained throughout the service life of CRCP. Such pavements can be expected to provide over 40 years of exceptional performance with minimal maintenance (*6*) as long as the longitudinal joints are well maintained. The purpose of the reinforcement is to limit movement at the cracks and hold them tight enough to limit the penetration of deterioration components such as chloride and water. By doing so, CRC pavement is more protective of the subgrade and most other forms of concrete pavement.
- Using steel reinforcement provides an adequate transfer of shear stresses from heavy wheel loads and enhances aggregate interlock, which significantly contributes into higher LTE. Thus, the use of CRCP is highly beneficial for urban and rural highways that experience high traffic volume with considerable number of trucks.

Roller Compacted Concrete

Due to many advantages of RCC pavements, its use has expanded to light industrial areas, arterial streets, local streets, maintenance, and replacement of street shoulders among other uses.

In high speed uses, RCC pavements have a shortcoming in terms of surface smoothness. Thus, diamond grinding or thin asphalt overlays are incorporated to provide an adequate surface finishing. However, using RCC should yield the following advantages:

- The main advantage of the RCC is the ability to be constructed in a short time period. RCC is placed and distributed using high-density asphalt paving equipment and is compacted using asphalt pavement rollers. Following this procedure eliminates the need for formwork and top surface finishing. For single lift RCC with thickness of 8 in., RCC pavement requires only a few roll passes to obtain an adequate density. These characteristics allow RCC to be a good candidate for limited construction time.
- The cost of the RCC is competitive with the cost of asphalt pavement. With the rising cost of oil and asphalt materials, RCC becomes a very good alternative. In addition, cost of RCC pavement is typically 25–30 percent less than conventional concrete systems (i.e., JPCP and CRCP). It does not require dowels, tie bars, or workers for texturing and finishing, which lowers initial construction cost. An additional cost benefit is obtained due to durability and resilience of RCC, which requires low maintenance cost during the service life of the pavement. Thus, RCC can be considered one of the most cost effective concrete pavement types.
- The use of low water content and high volume and dense aggregate gradation allow RCC to achieve higher level of compressive strength compared to the conventional concrete. Moreover, well-placed and compacted RCC pavements increase the density, which significantly increases the flexural strength. A good quality RCC pavement is able to evenly carry and distribute heavy traffic loading as long as the subbase layer is properly designed. Therefore, a well-designed and constructed form of RCC pavement can exhibit an excellent long-term performance without major maintenance.

Incorporating new systems to pavement construction is required to meet certain conditions. Construction time, heavy truck traffic, and grade restriction can be the major factors favoring the use of precast and/or prestressed concrete pavement. Moreover, important benefits can be obtained from using such systems.

Precast Concrete Pavement Systems

Advantages of using any type of precast concrete pavement are related to the concept of prefabrication beforehand, which will result in the following advantages:

- Short closure periods because concrete panels have been precast prior to installation. This means that their compressive strength has been developed under controlled condition and they are ready to bear traffic loading as soon as installation is complete. Thus, this benefit is extremely significant for overnight construction to reduce traffic disruption and reduce user delay cost.

- The quality of precast concrete is generally better than the cast-in-place concrete slabs. This is due to the ability to cast concrete without accounting for curing issues and the possibility of eliminating challenges associated with the cast-in-place pavement such as late or shallow joint saw cutting. Curling and warping behavior likely reduced as well, but this may eliminate any advantage that residue stresses might provide unless measures as noted below are taken.
- Controlled curing condition can assure the durability performance of precast pavements. Based on the expected weather curing conditions, the manufacturer can customize pavement panels with a negative built-in temperature gradient. This potentially increases the performance of concrete up to a certain point. On the other hand, a design curing regime could be applied during cast-in-place concrete pavement construction to achieve the same result.

Prestressed Concrete Pavement Systems

Using pretensioning or posttensioning in concrete pavement panels generates another level of performance advantages. These are:

- Pretensioned/posttensioned concrete pavement panels provide long lasting pavement systems. Pretensioning/posttensioning tendons induce pre-compression stresses throughout the pavement panel thickness. This allows the pavement to carry higher tensile stresses while reducing the occurrence of tensile cracking, which improves the overall performance of concrete under heavy traffic and increases its service life.
- Concrete prestressing reduces the design thickness of pavement panels. Compressive stresses induced by posttensiong/pretensioning in the concrete panels allows thinner slab to behave like a thicker slab resulting in an equivalent structural capacity, which can yield a comparable life-cycle cost.
- Adapting prestressing techniques enhance the LTE at joints due to the presented confining pressure.
- Prestressing can potentially reduce or eliminates the erosion at the base layer by maintaining the tightness of pavement joints for much longer period than conventional non-prestressed joints.

SELECT SUITABLE CONCRETE PAVEMENT TYPES

Based on the aforementioned advantages of the seven types of concrete pavements, decision trees for selection the appropriate pavement type were established in Figure 124 and Figure 125, respectively. As shown, the selection process has been divided into two decision trees, 1) rehabilitation treatment selection and 2) long-term pavement design selection. A third step of 3) verification of pavement design constructability is used to verify the applicability of the design options.

Rehabilitation Treatment Selection (Surface Preparation)

Development of initial decision tree for suitable strategies relates directly to the treatment strategy of the existing pavement surface. Based on the outcomes of field survey and field and laboratory testing, the causes of pavement deteriorations are determined and used to define the feasible treatment option. The most applicable treatment option is determined using the decision tree of the rehabilitation treatment selection. Figure 124 shows the decision tree for preparation selection for distresses found in the field survey.

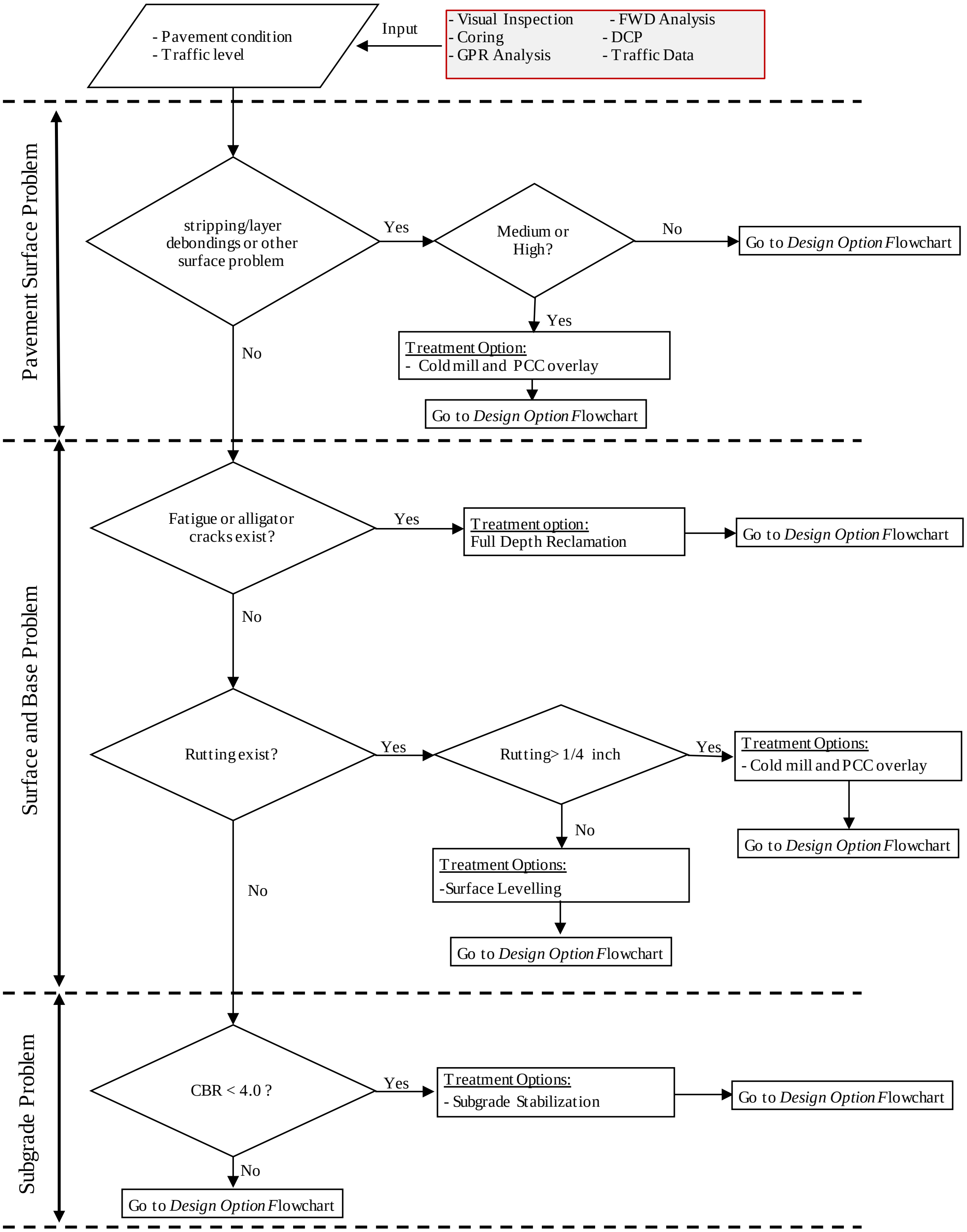
- Pavement condition
- Traffic level
Input
- Visual Inspection
- Coring
- GPR Analysis
- FWD Analysis
- DCP
- Traffic Data
Pavement Surface Problem
stripping/layer debondings or other surface problem
Yes
Medium or High?
No
Go to *Design Option* Flowchart
Yes
Treatment Option:
- Cold mill and PCC overlay
Go to *Design Option* Flowchart
No
Surface and Base Problem
Fatigue or alligator cracks exist?
Yes
Treatment option:
Full Depth Reclamation
Go to *Design Option* Flowchart
No
Rutting exist?
Yes
Rutting> 1/4 inch
Yes
Treatment Options:
- Cold mill and PCC overlay
Go to *Design Option* Flowchart
No
Treatment Options:
-Surface Levelling
Go to *Design Option* Flowchart
No
Subgrade Problem
CBR < 4.0 ?
Yes
Treatment Options:
- Subgrade Stabilization
Go to *Design Option* Flowchart
No
Go to *Design Option* Flowchart

Figure 124. Preconstruction or Pre-overlay Treatment Selection.

In Figure 124, distress types were categorized into:

- Pavement surface problems.
- Surface and base problems.
- Subgrade problems.

The above three categories were defined based on the field survey and relative testing inputs. In the first category, the direct criterion is existence of stripping layer, debonding, or other surface problems. The secondary criterion is the level of severity of related distresses. The surface problems are mainly a result of the materials malfunctioning so an improvement of the surface layer such as cold milling should be conducted before constructing the new concrete pavement. The second category considers the existing of fatigue, alligator cracking, or rutting as its direct criteria. A secondary criterion of rutting depth is also considered to determine best preparation or treatment option. In the surface and base problems category, the materials and load are expected to induce fatigue cracking and/or rutting. Thus, treatment process should include an improvement of the surface layer performance or a restoration of both surface and base layers. In case of fatigue/alligator cracking, FDR is necessary to rehabilitate the base material prior to placing concrete pavement panels. On the other hand, maintaining of existing rutting will depend on the depth of rutting. In case of rutting with depth of ¼ in. and more, cold mill should be conducted while surface leveling can be an adequate for rutting depth of less than ¼ in. The third category addresses the existence of subgrade problems. Based on the field testing analysis, the California Bearing Ratio value is considered the direct criterion to determine the need of subgrade treatment. The threshold value of 4 is used to consider subgrade stabilization. CBR is a way to evaluate the variability of the subgrade. Also, it is a good indicator of the soft areasthat require lime or cement treatment. As the design procedure depends on the erode-ability, number of wet days and traffic, it is significant to determine other parameters such as compressive strength and moisture content to verify the need of such major rehabilitation activity.

Long-Term Pavement Design Selection

After determining the preparation techniques for the existing pavement surface, the next step is to determine the long-term pavement design options. Figure 125 shows the decision tree for long-term pavement design selection.

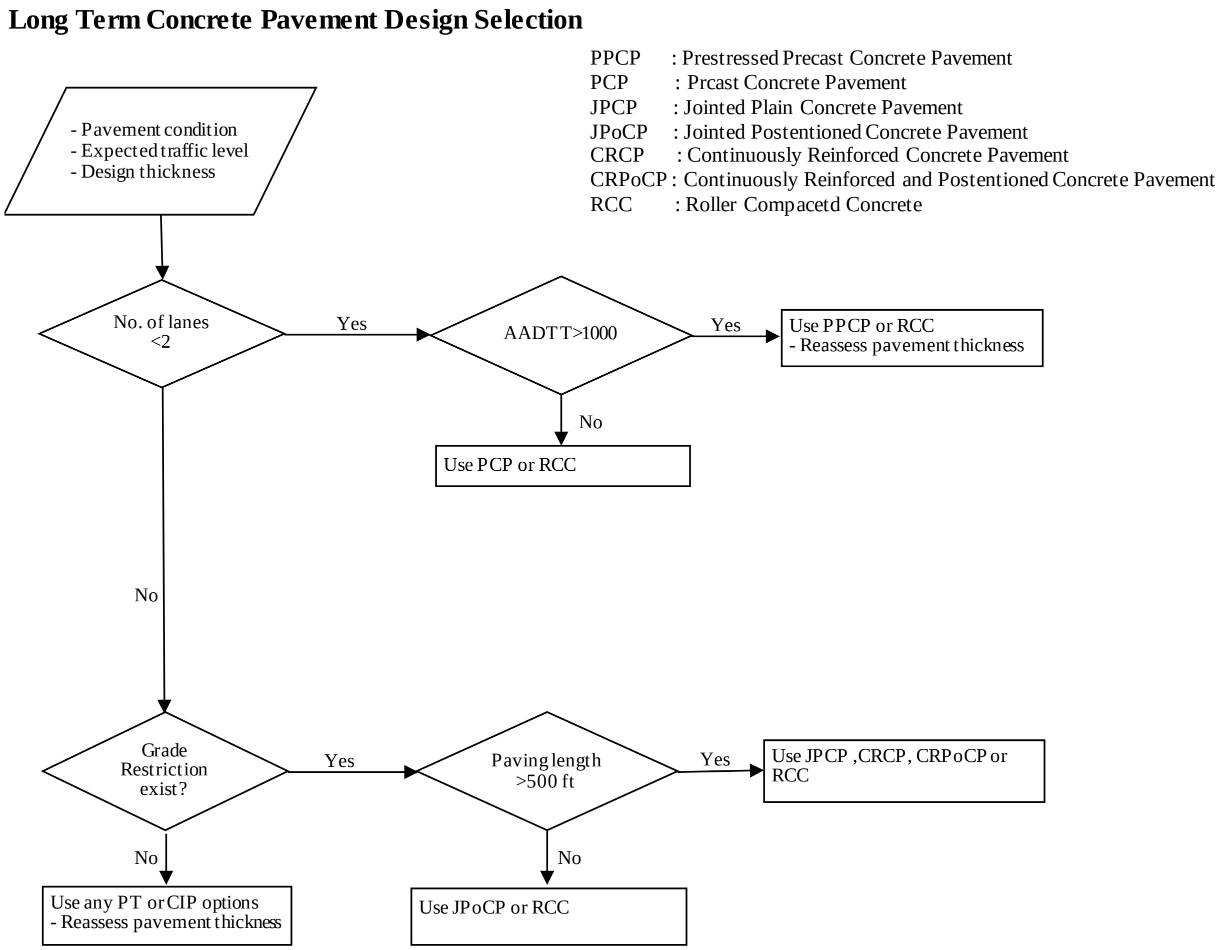
Long Term Concrete Pavement Design Selection
PPCP : Prestressed Precast Concrete Pavement
PCP : Prcast Concrete Pavement
JPCP : Jointed Plain Concrete Pavement
JPoCP : Jointed Postentioned Concrete Pavement
CRCP : Continuously Reinforced Concrete Pavement
CRPoCP : Continuously Reinforced and Postentioned Concrete Pavement
RCC : Roller Compacetd Concrete
- Pavement condition
- Expected traffic level
- Design thickness
No. of lanes <2
Yes
AADTT>1000
Yes
Use PPCP or RCC
- Reassess pavement thickness
No
Use PCP or RCC
No
Grade Restriction exist?
Yes
Paving length >500 ft
Yes
Use JPCP ,CRCP, CRPoCP or RCC
No
Use any PT or CIP options
- Reassess pavement thickness
No
Use JPoCP or RCC

Figure 125. Long-Term Concrete Pavement Design Selection.

In Figure 125, the following direct parameters were used to determine the design options:

- Number of lanes.
- Grade restriction.

Number of lanes was used to indicate the timeframe of the project. Existence of two lanes or less implies that the new pavement installation should be conducted overnight. This also means limited ways to conduct any detours and increase the pavement construction to a high priority. In that sense, the use of precast concrete pavement options is identical for this situation. Furthermore, AADTT was assigned as a secondary parameter to determine the need for pretensioning of precast pavement. In case of having two lanes or less with AADTT more than 1000 and limited work hours, PPCP is considered the best option. In case of AADTT less than 1000, the two precast options and the RCC are further analyzed to determine the best design option.

If number of lanes exceeds two, a construction detour can be managed and there is no need for overnight construction activity. Thus, the second primary criterion of grade restriction is considered to take into account the geometric constraints of the new pavement construction. Existing facilities elevations and bridges or tunnels clearances are a critical factor to determine the thickness of the new pavement. To determine existence of the grade restriction, geometric design should be conducted for the new pavement layout using the field and road surveying data and the new pavement thicknesses. In case of existence of grade restriction, paving length is the secondary parameter that determines the new pavement design options. If required paving length exceeds 500 ft, using of cast-in-place CRPoCP, nonprestressed concrete pavement options (CRCP and JPCP), and the RCC is typical. On the other hand, if paving length is less than 500 ft, the use of JPoCP and the RCC is recommended.

Verification of Pavement Design Constructability

Upon determining the new pavement design options based on the previous decision trees, additional verifications can be made through using secondary parameters to prioritize between the design options. Table 35 shows the secondary factors that, in addition to the existing pavement condition, can be used to weight a specific pavement design option over another. The listed secondary criteria provide only recommendations rather than requirements to the new pavement design type selection.

Table 35. Secondary Factors to Prioritize between Design Options.

Pavement Type	**Construction Factors**			**Base Material Factors**	
	Complex Road geometry	Limited Drainage space	Intermittent repair only	Shear Strength and Stiffness	
				Low	High
PPCP	○	○	√	√	○
PCP	○	√	√	○	○
JPoCP	√	○	○	○	√
CRPoCP	√	○	○	√	○
JPCP	√	√	○	○	√
CRCP	√	√	○	√	○
RCC	√	√	○	√	√

√ means that pavement type is recommended for the listed issue
○ means that pavement type is **not** recommended for the listed issue

RECOMMENDATIONS

The selection of the preferred alternative will be accomplished using step 4 from the Task Report: Framework for Repair Alternative Selection. Each of the suitable alternatives is evaluated for: 1) life cycle costs, 2) non-agency cost, 3) corridor impact, and 4) constructability. The rating value of each attribute component is user defined. The alternative with the greatest preferred rating is then selected as the preferred strategy.

The herein methodology was refined from the previous technical memorandum to provide a systematic and practical approach for selecting alternatives for rehabilitation of key energy sector pavements and can be computerized to facilitate its implementation. Pavement and non-pavement related components are considered to facilitate the alternative selection. Life cycle costs and corresponding user cost analysis for a given alternative can be arranged according to a preselected hierarchy for sequencing performance cycles, which provides greater user input flexibility in subsequent cycles for pavement rehabilitation.

CHAPTER 4. RIGID PAVEMENT DESIGN

INTRODUCTION

The majority of pavement design methods have elements that are done empirically. Empirical design is based on limited characteristics of a pavement's capability to withstand traffic over a given time frame (*7*). One of the most basic methods is AASHTO (*8*), which is based on analyzing test data obtained from the AASHTO road test that relate the present serviceability index with time and traffic levels. The main shortcoming in this methodology is its dependence on a specific subgrade types, strengths, slab properties, and one environment condition. Applying other material properties, subgrade types and/or different environmental conditions have usually yielded either conservative or unsafe pavement design sections.

To achieve a reliable design methodology of pavement, M-E design methodology provides the best approach. The M-E method depends on relationship between the material response and the empirical performance of the pavement. In this approach, material mechanics are used to compute the response of the pavement structure under different traffic levels and environmental conditions. This response will then be related to the deterioration rates. The relationship is usually developed by calculating the damage on the pavement due to traffic and environmental stresses. Miner's damage model is typically used to determine the level of damage due to different loading condition. Miner's hypothesis is defined by the sum of applied loads on the pavement structure divided by the allowable loads for a pavement to reach specific performance degradation level:

$$D = \sum_{i=1}^{k} \frac{n_i}{N_i} \tag{7}$$

Where,
D = the damage factor.
n_i = the expected number of load repetition during an identified time frame.
N_i = the allowable number of equivalent traffic (loading) repetitions required to reach performance limit of degradation calibrated to performance; that is usually calculated through a transfer function that incorporate pavement structure characteristics, environmental condition, pavement material properties…etc.

RIGID PAVEMENT DESIGN METHODOLOGY

The discussion below outlines key components of design for rigid pavement.

Key Parameters of Existing Rigid Pavement Design Methodologies

Design of pavement structures published by AASHTO provided AASHTO 1993 methodology was considered the most popular design procedures for rigid pavements for several years. As popular procedure developed by Portland Cement Association (PCA) had a mechanistic approach in determining the fatigue and erosion damages. Despite the differences in design approaches, key parameters for rigid pavement design remain for the most part constant in all design procedures. The main inputs for rigid pavement design are traffic, subgrade condition, environment factor, and concrete properties.

Traffic

Traffic is considered the main parameter of rigid pavement design. The number of heavy truck axles over the design life should be anticipated using the current traffic numbers, weights, volume, and projections. In the AASHTO methodologies, the ESAL of 18 kips single axle load is used to represent the number of the design loading (ESAL) after a specified design life. The concept of the ESALs represents the load equivalency factor between the damage produced by any axle type and weight to the damage produced by the 18 kips single axle. Since the release of the AASHTO 1993, the 18 kips equivalency of single axle concept have been widely accepted in the United States and around the world. PCA procedure, on the other hand, uses the traffic for load and axle groups to calculate the damage due to erosion and fatigue for single and tandem axles. AASHTO 2002 design guide relies on the load spectra to calculate the traffic and its projection over the design period. The load spectra depend on the weight distribution and axle configurations of different truck types. This concept has also been adopted by the mechanistic empirical design procedure instead of the ESALs.

Subgrade Condition

The modulus of subgrade reaction (k) is significant for rigid pavement design because it determines the properties of the subgrade and subbase foundation support. The modulus of subgrade is measured using the plate bearing test. The load is applied on a plate for a specific rate until the pressure reaches 10 psi. The 10 psi pressure is held until the deflection reaches 0.001 in. per minute for three minutes. The average of the readings is calculated to determine the average deflection. The modulus of the subgrade reaction can then be calculated using the following equation:

$$k = \frac{P}{\Delta} \tag{8}$$

Where,
k = the subgrade reaction in psi.
P = the pressure on the plate, which is usually 10 psi.
Δ = the deflection of the plate in inches.

The subgrade reaction value is usually determined from the field testing. Thus, it does not consider different moisture condition or densities for the worst condition during the service life of the pavement. Laboratory testing can be used to modify the k-value by simulating other conditions such as different moisture content and density. Detailed procedure for the plate bearing test and other laboratory testing can be found in Huang (*7*).

The plate loading test is time consuming and expensive so the k-value can be correlated to simpler tests such as CBR and R values tests (*7*). Figure 126 shows the approximate relationship between k-value and soil properties.

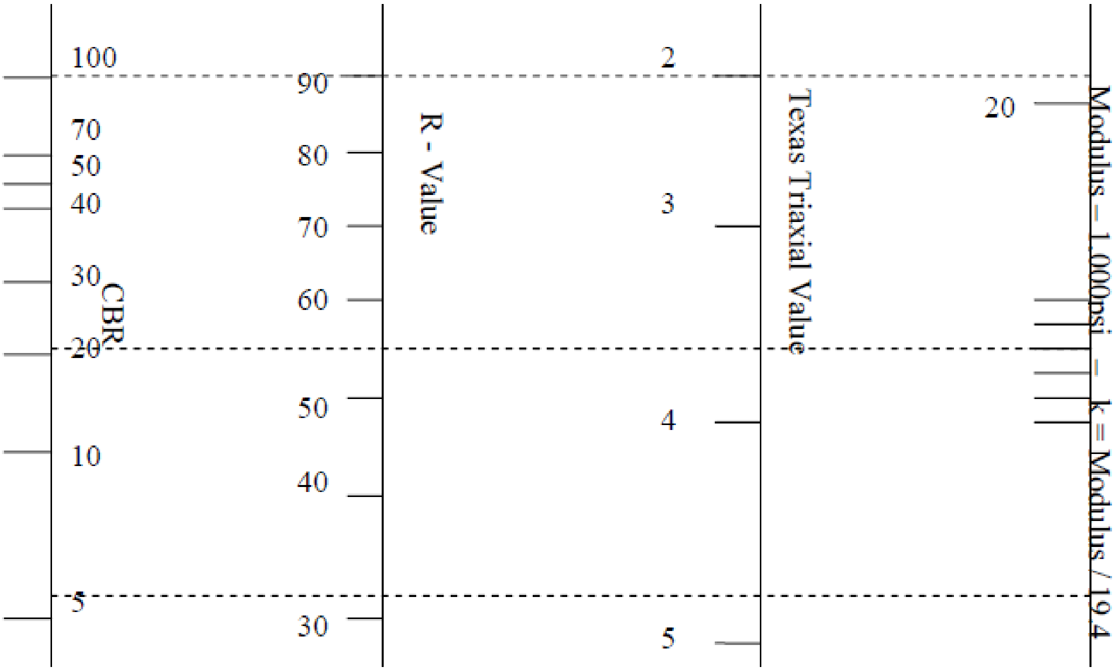

Figure 126. k-value Relationships with Other Soil Support Values (*8*).

As a result of different moisture content and densities of the subgrade and subbase, support strength varies over the year seasons and thus k-value varies accordingly. The k-value is high during the long freezing period and low during spring thaws periods. However, AASHTO 1993 thickness design equation is basically based on the ESALs and k-value has minor impact on the thickness. On the other design procedure such as PCA method, tedious method of determining the k-value was simplified by providing simple annual k-values as a design input (*9*).

Climate

The climatic variables, especially temperature gradient, significantly influence the concrete behavior. The following list of climate effects in rigid pavement is taken from a fall 2001 National Cooperative Highway Research Program 1-37A progress update on climatic data research for the 2002 Design Guide. This list displays the daily and seasonal variations of temperature and moisture affecting concrete pavement behavior:

1. Opening and closing of transverse joints in response to daily and seasonal variation in slab temperature, resulting in fluctuations in joint load transfer capability, which is the ability of each slab group to transfer wheel loads from one slab to the next.
2. Upward and downward curling of the slab caused by daily cycling of the temperature gradient through the slab thickness as pictured in Figure 127.
3. Upward warping of the slab due to early drying shrinkage and long-term shrinkage.
4. Erosion of base and foundation materials caused by abrasion and accumulation of excess water in the pavement structure, primarily from precipitation.

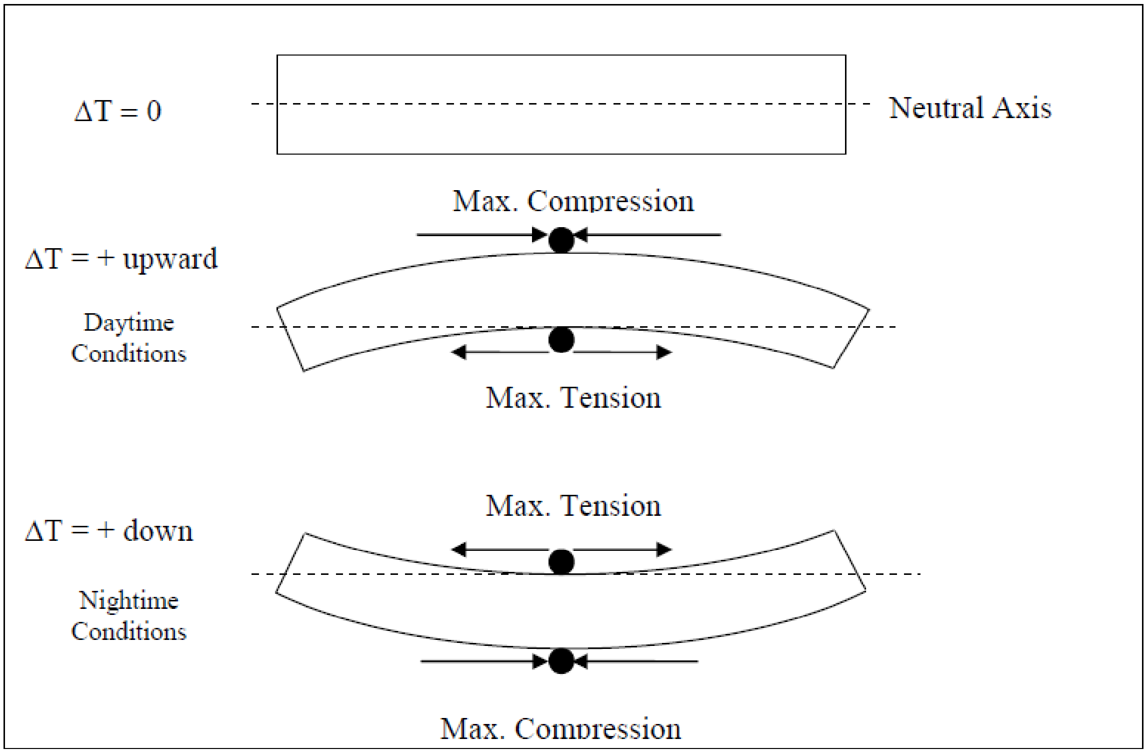

Figure 127. Maximum Stresses due to Curling and Warping.

Concrete Properties

The main concrete properties used in rigid pavement design are the flexural strength (Sc) and the modulus of elasticity. The flexural strength is usually determined using the by the 28-day modulus of rupture from third point beam loading tests ASTM C78-84 “Standard Test Method for Flexural Strength of Concrete using Simple Beam with Third Point Loading.” If testing beams is not possible, compressive strength can be used to estimate the flexural strength of concrete, as shown in Equation 9. The flexural strength or modulus of rupture is important to the concrete pavement design because it represent the resilient and durability of concrete. Hence, higher flexural strength usually yields into lower concrete slab thickness.

The modulus of elasticity can be also determined from the compressive strength for normal weight concrete using Equation 10:

$$Sc = 8\sqrt{f_c'} \ to \ 10\sqrt{f_c'} \ (7) \qquad 9$$

$$Ec = 57000 \sqrt{f_c'} \ (10) \qquad 10$$

Performance Indices

The pavement thickness design for all design procedures includes performance criteria that define the service life of the pavement. These criteria differ from one procedure to another. In AASHTO procedure, the performance criterion is the loss of serviceability that occurs due to the damage accumulation due to the traffic loading repetition throughout the design life. On the other hand, the PCA methodology adopted the idea of using fatigue and erosion damage as criteria of the performance level. As the total damage from fatigue and erosion are calculated, the user can define the permissible level of damage and select the design thickness that satisfies the performance requirements. For example, the thickness of slab required to limit the damage to 30 percent can be much larger than the thickness of slab to limit the damage to 80 percent under the same environment, subgrade condition, and ESALs.

Reliability

The reliability in rigid pavement design can be defined as the level of risk that agencies are willing to assume failure of the pavement. Thus, the reliability serves as the factor of safety in the design. As a consequence, a higher reliability means greater design thickness. Higher reliability design requirements usually is associated with higher functional class or importance and higher traffic volumes. In the AASHTO procedures, reliability is considered in the design by applying adjustment to the ESAL's calculation. The adjustment factor of reliability is based on the overall standard deviation of the AASHTO model, which represents the error in estimation of traffic and strength inputs and error associated with the fit quality between the model and the data obtained from AASHTO (*8*). As the reliability adjustment factor is applied to the ESALs, AASHTO recommends the use of the average values for the material inputs. On the other hand, PCA method does not account for reliability concept directly. However, it considers the safety factor in concrete pavement design by inducing a reduction in the measured or calculated modulus of rupture. PCA also accounts for uncertainty by increasing the traffic weight based on the roadway type.

CHAPTER 5. TRAFFIC ANALYSIS

INTRODUCTION

The traffic analysis in this design methodology is modeled based on load and category classification similar to that used by AASHTO. Just like the AASHTO procedures, this methodology uses the concept of distress-based equivalency, thus ESALs are calculated for the given traffic combination. The difference is in the way these ESALs are calculated. A simple but effective way to depict traffic input data for design that is often specified relative to three axle (single, tandem, and tridem), and Figure 128 shows load groups where axle loads are distributed. The legal loads range is defined between the lower and upper load limits. $\%ADT_L$ is the percentage of daily trucks with a loaded radius of R_L or less, and $\%ADT_U$ is the percentage of trucks with a loaded radius of R_U or less. The $\%F_L$ and $\%F_U$ parameters are used to determine the coefficients a, b, and c and the percentage of illegal truck loads. The following sections provide further explanation about calculation of coefficients and percentage of load groups.

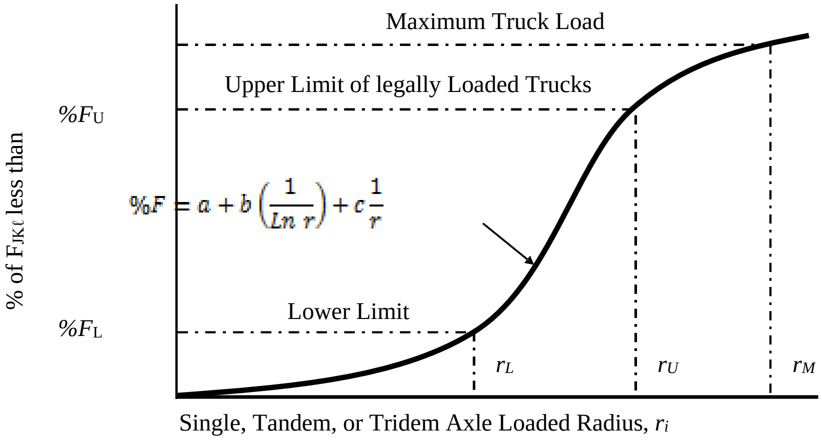

Figure 128. Load Distribution Model Used for a Given Axle Type.

TRAFFIC COMPUTATION MODEL

The traffic distribution model used in the design is illustrated in Figure 129by probability density (%*f*) and accumulative (%F) traffic loading; both of which are used to define relevant traffic factors and to establish useful relationships. The model computes the number of equivalent 18 kip single axles (ESALs) from inputs of ADT, LDF, and the %Trucks in the traffic mix. The equivalencies are computed with either respect to fatigue or erosion damage depending upon the failure mechanism being addressed in the design process. The limit ranges refer to the range of truck loads in the load distribution:

- Lower limit: lowest truck load.
- Upper limit: highest legal truck load.
- Maximum limit: maximum truck load.

Note also that the load distributions are defined for the loaded radius (r_{jkl}):

$$r_{Jk\ell} = \sqrt{\frac{P_{Jk\ell}}{p\pi}} \qquad 11$$

Where,

$P_{Jk\ell}$ = Axle load (lb) (l = 39).

P = Tire pressure (psi).

If the equation for the accumulative load distribution ($\%F_{Jk\ell}$) is defined as:

$$\%F_{Jk\ell} = a + b\frac{1}{Ln\left(r_{Jk\ell}\right)} + c\frac{1}{r_{Jk\ell}} \ for \ r_{Jk\ell} > r_L$$

And 12

$$\%F_{Jk\ell} = \left(\frac{P - P_{min}}{P_L - P_{min}}\right).\%F_L \ for \ r_{Jk\ell} \leq r_L$$

Where,

P_i = Axle load.

P_{min} = Minimum axle load.

P_L = Axle load lower limit of truck loading.

r_L = Loaded tire radius of the lower axle limit.

$\%F_L$ = % less than the lower axle limit.

The coefficients can be determined as a function of the load limits defined by the user as:

$$
\begin{aligned}
a_j &= \%F_{jL} - b_j \frac{1}{Ln\left(r_{iL}\right)} - c_j \frac{1}{r_{iL}} \\
b_j &= \frac{\%F_{j(M-L)} - c_{j0}\%F_{j(U-L)}}{a_{j0} - b_{j0}c_{j0}} \\
c_j &= \frac{\%F_{j(U-L)} - b_j b_{j0}}{\frac{1}{r_{jU}} - \frac{1}{r_{jL}}} \\
a_{j0} &= \frac{1}{Ln\left(r_{jM}\right)} - \frac{1}{Ln\left(r_{jL}\right)} \\
b_{j0} &= \frac{1}{Ln\left(r_{jU}\right)} - \frac{1}{Ln\left(r_{jL}\right)} \\
c_{j0} &= \frac{\frac{1}{\left(r_{jM}\right)} - \frac{1}{\left(r_{jL}\right)}}{\frac{1}{\left(r_{jU}\right)} - \frac{1}{\left(r_{jL}\right)}}
\end{aligned}
\tag{13}
$$

The shaded in area in the density diagram (Figure 128) is the incremental change in load distribution with loaded radius:

$$\Delta\%F_{Jk\ell} = \left(\%F_{Jk\ell+1} - \%F_{Jk\ell}\right) \tag{14}$$

The parameter $\%F_{Jk\ell}$ represents the cumulative fraction of the traffic as depicted in Figure 129; coefficients *b* and *c* are determined from regression of the load distribution data subsequently explained. Figure 128 shows the distributions for the PCA/ACI truck load distributions.

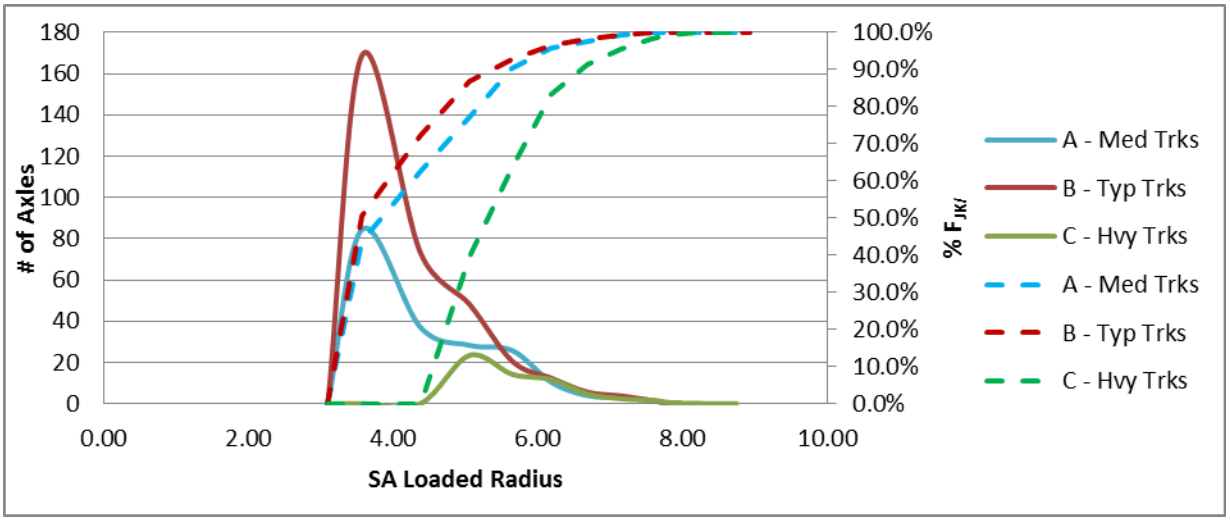

Figure 129. The Cumulative Fraction of the Traffic.

The indices *j* and *l* refer to axles and load categories, respectfully. The load parameters for the PCA/ACI truck load categories (A – C) are listed in Table 36.

Table 36. PCA/ACI Truck Load Categories (SA).

Coefficient	**Group A** (Med Trksl)	**Group B** (Typ Trks)	**Group C** (Hvy Trks)
P_L	4000	4000	8000
P_U	12000	14000	18000
P_M	16000	18000	20000
$\%F_L$	0.435	0.505	0.395
$\%F_U$	0.957	0.982	0.982
$\%F_M$	0.992	0.998	0.997

Note: $\left(\%F_{jkl+1} - \%F_{jkl}\right) = \Delta\%F$

The $\%AT_k$ represents the percentage of three axle types: single axle (SA), tandem axle (TA), and tridem axle (Trid) defined as:

$$\begin{aligned}
&\sum_{1}^{3} \%AT_j = 100\% \\
&\%SA = \%AT_{SA} \cdot \%Trucks \\
&\%TA = \%AT_{TA} \cdot \%Trucks \\
&\%Trid = \%AT_{Trid} \cdot \%Trucks
\end{aligned} \tag{15}$$

Table 37 lists the $\%AT_i$ values for the AASHTO truck classifications.

Table 37. Number and Percent (%AT) of Different Axles per Truck.

Truck Classification (TC)	Number of single axles per truck	Number of Tandem axles per truck	Number of Tridem axles per truck	$\%AT_{SA}$	$\%AT_{TA}$	$\%AT_{Trid}$
4	1.62	0.39	0.00	80.6%	19.4%	0.0%
5	2.00	0.00	0.00	100.0%	0.0%	0.0%
6	1.02	0.99	0.00	50.7%	49.3%	0.0%
7	1.00	0.26	0.83	47.8%	12.4%	39.7%
8	2.38	0.67	0.00	78.0%	22.0%	0.0%
9	1.13	1.93	0.00	36.9%	63.1%	0.0%
10	1.19	1.09	0.89	37.5%	34.4%	28.1%
11	4.29	0.26	0.06	93.1%	5.6%	1.3%
12	3.52	1.14	0.06	74.6%	24.2%	1.3%
13	2.15	2.13	0.35	46.4%	46.0%	7.6%

The average daily truck traffic is found from:

$$ADTT = ADT \cdot LDF \cdot \%Trucks \qquad 16$$

and ESAL:

$$ESAL_i = ADTT \cdot \sum_{l=1}^{4}\sum_{k=1}^{39}\sum_{j=1}^{3}\left(\left(\%F_{jkl+1} - \%F_{jkl}\right)\cdot \%AT_{jl} \cdot EAF_{jl}\right)\cdot ELF_{kl} \cdot SD_l \cdot EWF \cdot GF \cdot 365 \cdot LDF \qquad 17$$

Where,

TC_j = Truck Category (Table 37) (i = (4 to 13)).

$\%F_k$ = % Load Distribution (Table 36) (k = 39 loaded radius per AT).

$\%AT_{jl}$ = %Axle Type (j = 1 to 3) (Table 37).

EAF_{jl} = Equivalent Axle Factor

ELF_{kl} = Equivalent Load Factor for 18 kips SA

SD_l = Seasonal Distribution (l = 4).

EWF = Equivalent Wander Factor.Where,

$EWF = 0.8765\ln(\ell) - 3.0084$ for fatigue-based damage and

$EWF = e^{0.049 - \frac{25.207}{\ell} - \frac{0.775}{\ln(\%LTE)}}$ for erosion-based damage

GF $= \frac{(1+r)^n - 1}{r}$ (non-linear); $= n(1+r)$ linear.

LDF = Lane Distribution Factor.

ESTIMATING DESIGN ESALS

Equivalent Axle Factor

Equivalent axle factor (EAF) is defined as the factors required to transferring tandem or tridem axle into single axle. In this methodology, the EAF is determined using the stress ratios for the two main distress conditions: fatigue and erosion. Equations below are used to calculate the EAF:

Equivalency Factor	Fatigue-based Damage	Erosion-based Damage
EAF	SA: 1 TA: $10^{-17.61\,(R_{SA}-R_{TA})}$ TR: $10^{-17.61\,(R_{SA}-R_{TR})}$	SA: 1 TA: $10^{-17.61\,(R_{SA}-R_{TA})}$ TR: $10^{-17.61\,(R_{SA}-R_{TR})}$

Note for the determination of R_{TA} and R_{Trid} (see determination of τ in erosion model) RSA = the stress ratio for fatigue and erosion. In case of fatigue, the stress ratio can be defined as the ratio of the equivalent edge stress each load level of single axle to the modulus of rupture of concrete while for the stress ratio for erosion is defined as the shear stress induced by each load level of single axle to the shear strength of concrete.

R_{TA} = the stress ratio for fatigue and erosion. In case of fatigue the stress ratio can be defined as the ratio of the equivalent edge stress by each of load level of tandem axle to the modulus of rupture of concrete while for the stress ratio for erosion is defined as the shear stress induced by each of load level of tandem axle to the shear strength of concrete.

R_{TR} = the stress ratio for fatigue and erosion. In case of fatigue, the stress ratio can be defined as the ratio of the equivalent edge stress by each of load level of tridem axle to the modulus of rupture of concrete while for the stress ratio for erosion is defined as the shear stress induced by each of load level of tridem axle to the shear strength of concrete.

Fatigue and Erosion Load Equivalent Factors

Equivalent load factor (ELF) is defined as the equivalent of any load level in terms of 18 kips for single axle, 36 kips for tandem axles, and 54 kips for tridem axles. To pursue consistency in this design methodology, the ELF is determined using the stress ratios for the two main distress conditions: fatigue and erosion. Equations below are used to calculate the ELF:

Equivalency Factor	Fatigue-based Damage	Erosion-based Damage
ELF	SA: $10^{-17.61\left(R_{18kip\ load}-R_{load}\right)}$ TA: $10^{-17.61\left(R_{36kip\ load}-R_{load}\right)}$ TR: $10^{-17.61\left(R_{54kip\ load}-R_{load}\right)}$	SA: $10^{-17.61\left(R_{18kip\ load}-R_{load}\right)}$ TA: $10^{-17.61\left(R_{36kip\ load}-R_{load}\right)}$ TR: $10^{-17.61\left(R_{54kip\ load}-R_{load}\right)}$

In the previous equations, stress ratios for 18 kips for SA, 36 kips for tandem axle, and 54 kips for tridem axles are constant while the R_{load} indicates the stress ratio of each load level. The stress ratio of fatigue is simply calculated as the ratio of the equivalent stress at the wheel load stress divided by the modulus of rupture of concrete. On the other hand, the stress ratio for erosion is calculated by the ratio of the shear stresses induced by each wheel load level to the shear strength of concrete.

In calculation of stress ratio for erosion, the following equation should be followed:

$$r_i = \frac{\tau_i}{f_e} \qquad 18$$

Where,

r_i = Stress ratio of i load level.

τ_i = Interfacial shear stress.

f_e = Effective interfacial frictional resistance or bond strength.

$$f_e = \sigma_v \mu_e = x_b f_a + (1 - \%E) * f_F \qquad 19$$

$$f_a\ (adhesive\ bond\ strength) = \sigma_v (\mu_c - \mu_F) \qquad 20$$

Where,

σ_v = normal stress.

= $k_{eff}\,\Delta$.

k_{eff} = effective modulus of subgrade reaction.

Δ = loaded deflection.

μ_e = effective coefficient of friction.

L = Lift-off distance.

f_τ = cohesive shear strength of the weakest layer adjoining the interface = $\sigma_v \mu_c$.

K_I = fracture toughness of the weakest layer adjoining the slab interface.

f_F = frictional interfacial shear strength.

$= \left(\sigma_v - \theta f h_m\right) \tan\phi\ \sigma_v \mu_F$.

μ_F = interfacial coefficient of sliding friction (= tan φ).

f_t = tensile strength of the slab/base interface = $\frac{f_\tau}{tan\varphi}$.

Φ = friction angle.

K = $\frac{c6\sin\varphi}{\sqrt{3}\left(3-\sin\varphi\right)}$.

c = cohesion of the base layer.

Table 38. AASHTO-Typical Friction Coefficient of Stabilized Base/Subbase Materials.

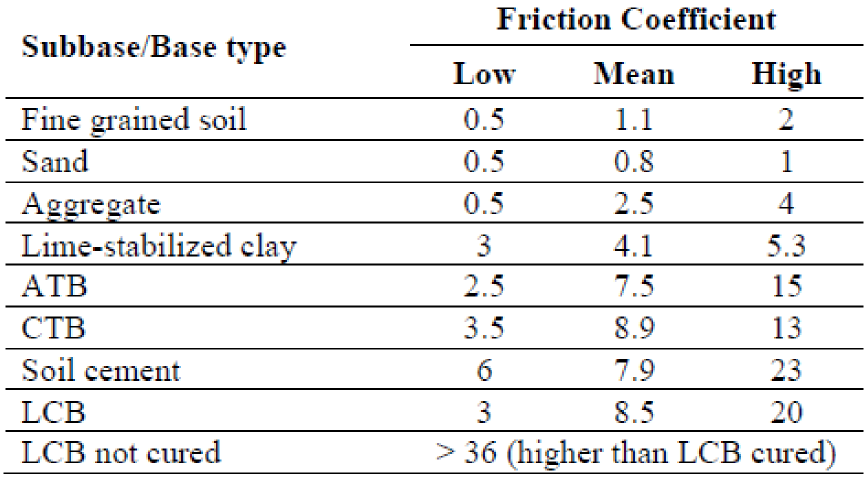

Subbase/Base type	Friction Coefficient		
	Low	Mean	High
Fine grained soil	0.5	1.1	2
Sand	0.5	0.8	1
Aggregate	0.5	2.5	4
Lime-stabilized clay	3	4.1	5.3
ATB	2.5	7.5	15
CTB	3.5	8.9	13
Soil cement	6	7.9	23
LCB	3	8.5	20
LCB not cured	> 36 (higher than LCB cured)		

Interfacial shear stress can be further broken down as follows:

$$\tau_i = \left(1-x_b\right)\frac{\partial DE}{\partial X}\frac{1}{k\delta_L}\frac{E_{sb}}{2\left(1+\upsilon\right)}\left(\frac{1}{\psi}\right) = \left(1-x_b\right)\frac{\partial\delta_{L_i}}{\partial X}\frac{E_{sb}}{2\left(1+\upsilon\right)}\left(\frac{1}{\psi}\right) \qquad 21$$

$$\frac{\partial\delta_{L_i}}{\partial X} = \frac{\partial\delta^*_{L_i}}{\partial x}\frac{P}{L^* k\ell^2} \qquad 22$$

$$\frac{\partial\delta^*_{L_i}}{\partial x} = 0.16\cdot\frac{h}{\ell} - 0.065 \qquad 23$$

Where,

x_b = degree of bond (specified by the user) = $\frac{h_p - h_u}{h_b - h_u}$.

h_p = partially bonded pavement thickness.

h_u = unbonded pavement thickness.

h_b = bonded pavement thickness.

DE = deformation energy = $\frac{k}{2}\delta_L^2$.

δ_{L_i} = loaded deflection $= \dfrac{\delta^*_{L_i} P}{k\ell^2}$.

$\delta^*_{L_i}$ = dimensionless deflection.

P = axle load.

ℓ = radius of relative stiffness.

k = modulus of subgrade reaction.

X = distance from the point of loading along the diagonal from the corner or from the edge of the slab.

E_{sb} = subbase modulus per base type.

υ = subbase Poisson's ratio per base type.

ψ = load transfer factor = $2.183 - 1.183\left(\dfrac{LTE}{100}\right)$ for edge loading.

= 1.00 for corner loading.

LTE = load transfer efficiency (%).

x = $\dfrac{X}{L^*}$.

L^* = $\dfrac{W}{2}$(for slab edge - CRC; or jointed in the wheel path).

= $\dfrac{W}{\sqrt{2}}$ (for slab corner – jointed concrete).

W = slab width.

h = slab thickness.

CHAPTER 6. DESIGN METHODOLOGY

The proposed design methodology is a simple and straight forward spread sheet design of jointed plain concrete pavement and continuously reinforced concrete pavement. The design method incorporates elements of AASHTO, PCA, and Mechanistic-Empirical Pavement Design Guidelines methods. The presented design procedure is different than AASHTO methods due to employment of performance models for fatigue and erosion to check the adequacy of pavement thickness design. In terms of traffic, ESALs are used to simplify the traffic input and calculation as a function of the AADTT. Truck traffic classification and distribution from AASHTO 2002 is used in the calculation of the ESALs. The JPCP design procedure includes using the fatigue and erosion models similar to those used in pavement M-E with some modifications in determining the faulting and erosion percentages. In CRCP design, the Pavement M-E guidelines in determining the punchout were modified to consider partial and full depth punchouts based on erosion potential. Erosion based-design is important for energy sector traffic.

BACKGROUND TO AASHTO AND PCA RIGID PAVEMENT DESIGN

As mentioned before, the design methodology incorporates elements from AASHTO, PCA, and MEPDG methods. The following discussion provides a background on the AASHTO and PCA procedures and point out their shortcomings that warn users from using them for energy sector pavement design.

AASHTO Methodology

The current AASHTO procedure is based on a regression equation that compiles the AASHTO road test data and research inputs. The empirical equation of the AASHTO rigid pavement design relates the allowable number of 18 kips ESALs as a function of slab thickness, axle type and weight, and terminal serviceability. The original model was developed to predict the performance of the JPCP and the jointed reinforced concrete pavementsections in the main loops of the AASHTO road test. Thus, the original relation is applicable to the traffic conditions, climate, subgrade, and materials properties of the AASHTO road test. This model was further developed to account for a given terminal serviceability for different concrete strength and modulus of elasticity and subgrade reaction than the ones in the AASHTO road test. Additionally, the design methodology was extended to cover the conversion of mixed axle load and types to 18 kips-ESALs through load equivalency factors as indicated in AASHTO 1993.

The main limitation in the developed AASHTO equation was basically in terms of design serviceability estimation. The extended AASHTO model considering axle load number, as the main source of degradation, does not account for the faulting in the overall roughness of the pavement. The reason is that, even though loss of support was existed in the doweled pavement types, tested samples did not fault. Thus, the loss of serviceability presented in the developed equation was presumed due to the slab cracking only (*11*). Moreover, as the main source of the empirical equation is field testing, it might be more accurate to apply it for prediction of performance of concrete pavement structures similar to those in the AASHTO road test. Therefore, it is an extrapolation to apply this equation for design of other pavement structures.

In general, AASHTO design guidelines, throughout development stages, have many limitations that can be yield into costly and sometime unsafe pavement design. Table 39 presents AASHTO guidelines development and their critical related limitations.

Table 39. AASHTO Guidelines Development and Limitations.

AASHTO Design Guide	Limitations
AASHTO Road test empirical Model, AASHTO 1986	• Design thickness to support the anticipated ESALs based on the loss of serviceability. In AASHTO design, the loss of serviceability depends only on the slab cracking. This will sometime lead to a design safety problem because as faulting is a controlling failure mode, the thickness design is not enough to accommodate the ESALs for the entire pavement's service life. • ELF is used to determine the damage obtained from different axle type and weight to the pavement surface relative to the 18 kips single axle type. This ELF is based on the AASHTO road test that considers failure of pavement is due to slab cracking only. However, many other failures can occur in rigid pavement due to erosion. The mode of failure depends on the concrete pavement type.
AASHTO 1993, supplement AASHTO 1998	• In addition to the above limitations, extended shortcomings can be noticed in the updated AASHTO guidelines. For example, the effects of tied concrete shoulder and widened lanes cannot be addressed in the AASHTO methodologies. • The AASHTO procedures also does not account for joint spacing and curling stresses in rigid pavements (*12*). • In AASHTO 1993, design procedure is limited in accounting for climate, subgrade, subgrade characterization and heavy vehicle types and different axle configurations.

PCA Methodology

The PCA rigid pavement design methodology was developed by PCA in 1984 replacing the one published in 1966. The PCA methodology depends mainly on finite element computer programming to evaluate the stresses and deflection at three critical locations on the concrete slab (edge, corner, joint). This procedure is considered the first M-E design methodology for rigid pavement because design tables and charts that incorporate stress calculations along with fatigue and erosion performance criteria. The PCA analysis method also took into account the LTE of dowels, aggregate interlock, and the degree of edge support provided by the concrete shoulder. Alike with AASHTO 1986–1993 procedure, PCA uses composite k concept where the design k is a function of the base thickness, base type, and the modulus of subgrade reaction.

The PCA method calculates separately the number of load repetitions of each load group and category during the design life of the pavement structure. Fatigue analysis assumes that 6 percent of truck loads should pass close to the edge of the slab to induce enough tensile stresses while erosion analysis considers the deflection of slab corner induced by the wheel load as a function of the slab thickness, k-value, and the estimation of the slab-foundation interface pressure (*11*).

For load levels associated with single and tandem axle types, the number of load repetition expected is presented as percentage of the allowable load repetitions to both fatigue and erosion. After calculation the damage using the Miner's hypothesis for both fatigue and erosion throughout the design life period, the total damage should be checked to not exceed 100 percent. The thickness of the pavement then can be the design thickness for that specific load repetition.

The main limitations of the PCA design method include the inability of analyzing the widened lanes or joint spacing. Also, it does not consider load transfer at the lane-shoulder location (*13*). The PCA does not account for joint spacing that has an important role in determining how short the fatigue cracking and/or faulting are going to occur in the pavement, thus a special consideration should be taken on increasing the joint spacing. Failure of PCA to deal with joint spacing, the complexity of traffic calculations and the complexity of charts in determining the level of damage limit applicability of PCA method in the energy sector pavement design.

TXDOT DESIGN PRACTICES

TxDOT lists two main commonly used types of concrete pavements, which are CRCP and jointed concrete pavement (JCP), which is also called concrete pavement contraction design (CPCD). The TxCRCP-ME program are usually used for the design of CRCP, while AASHTO 1993 or the automated version, AASHTO DARWin 3.1 program, is used for the design of CPCD or the JCP. The AASHTO guide is also used for designing of rehabilitation including concrete and asphalt overlays.

TxCRCP-ME Program for CRCP

The design method using TxCRCP-ME design was developed by the research project 0-5832 "Develop Mechanistic/Empirical Design for CRCP." The design methodology was developed using the finite element analysis to identify the mechanism and development of punchout distress. The main components causing punchout was determined and was represented mechanistically. Additionally, an empirical study was conducted on department's rigid pavement database to develop transfer function to convert mechanistic structural response to a pavement distress. The program was written using Microsoft Excel to determine the frequency of the punchout as the main distress in the CRCP pavement. The final results of the design procedure are presented by charts and tables.

AASHTO 1993—Rigid Pavement Design for CPCD

For the design of CPCD, TxDOT accept the results of the AASHTO 1993 design procedure. An automated version of the design procedure is provided in the AASHTO DARWin 3.1 program.

DESIGN INPUTS FOR JPCP

The design methodology relies on the use of an excel calculation sheet for thickness calculation of a JPCP overlay. The design parameters require interrelated design inputs to calculate the required thickness. The design inputs for this excel sheet can be categorized within the following parameters:

1. Traffic calculation.
2. Load equivalency.
3. Stress calculation.
4. Fatigue and erosion damage.
5. LTE.

Traffic Calculation

The traffic calculation is done similarly as done in pavement M-E traffic analysis. However, instead of using the load spectra to calculate the distresses damages for each load group and type, researchers adopted calculating the 18 kips-ESAL to simplify the design calculation process. The characteristics of traffic involve using the AASHTO TTC groups multiplied by the load equivalency factors for fatigue and erosion, the EAF, and the equivalent wander factor. The required inputs for traffic calculation can be summarized by the following list:

- **AADTT**: is the average annual daily truck traffic on the pavement, which can be obtained through various traffic monitoring techniques. The vehicle category is not required as design methodology uses the ESALs concept.
- **TTC group**: is the Truck Traffic Classification group. As reported by pavement M-E, there are 17 groups of truck traffic classifications. The user should specify one of the groups and the calculation sheet will generate the factor for truck type’s distribution. The truck considered in these factors is from 3 to 13. The appropriate group depends mainly on the description of the truck traffic classification presented in Table 40.

Table 40. Truck Traffic Classification Group Description and Distribution.

TTC Group	TTC Description	TC Distribution (percent)									
		4	5	6	7	8	9	10	11	12	13
1	Major single-trailer truck route (Type I)	1.3	8.5	2.8	0.3	7.6	74.0	1.2	3.4	0.6	0.3
2	Major single-trailer truck route (Type II)	2.4	14.1	4.5	0.7	7.9	66.3	1.4	2.2	0.3	0.2
3	Major single-and multitrailer truck route (Type I)	0.9	11.6	3.6	0.2	6.7	62.0	4.8	2.6	1.4	6.2
4	Major single-trailer truck route (Type III)	2.4	22.7	5.7	1.4	8.1	55.5	1.7	2.2	0.2	0.4
5	Major single-and multitrailer truck route (Type II)	0.9	14.2	3.5	0.6	6.9	54.0	5.0	2.7	1.2	11.0
6	Intermediate light and single-trailer truck route (I)	2.8	31.0	7.3	0.8	9.3	44.8	2.3	1.0	0.4	0.3
7	Major mixed truck route (Type I)	1.0	23.8	4.2	0.5	10.2	42.2	5.8	2.6	1.3	8.4
8	Major multitrailer truck route (Type I)	1.7	19.3	4.6	0.9	6.7	44.8	6.0	2.6	1.6	11.8
9	Intermediate light and single-trailer truck route (II)	3.3	34.0	11.7	1.6	9.9	36.2	1.0	1.8	0.2	0.3
10	Major mixed truck route (Type II)	0.8	30.8	6.9	0.1	7.8	37.5	3.7	1.2	4.5	6.7
11	Major multitrailer truck route (Type I)	1.8	24.6	7.6	0.5	5.0	31.3	9.8	0.8	3.3	15.3
12	Intermediate light and single-trailer truck route (III)	3.9	40.8	11.7	1.5	12.2	25.0	2.7	0.6	0.3	1.3
13	Major mixed truck route (Type III)	0.8	33.6	6.2	0.1	7.9	26.0	10.5	1.4	3.2	10.3
14	Major light truck route (Type I)	2.9	56.9	10.4	3.7	9.2	15.3	0.6	0.3	0.4	0.3
15	Major light truck route (Type II)	1.8	56.5	8.5	1.8	6.2	14.1	5.4	0.0	0.0	5.7
16	Major light and multitrailer truck route	1.3	48.4	10.8	1.9	6.7	13.4	4.3	0.5	0.1	12.6
17	Major bus route	36.2	14.6	13.4	0.5	14.6	17.8	0.5	0.8	0.1	1.5

- **Design Life:** is the number of years that the overlay lane should be designed for without exceeding the performance limitation.
- **Rate:** is the rate of traffic increase during the design life period.
- **ELF:** is the equivalent load factor is applied to the total number of ESALs to account for the applied bending and shear stresses, which are responsible for fatigue and erosion distresses. The ELF depends many factors including pavement thickness and stress ratio for fatigue and erosion. Inputs for ELF calculation are discussed later in this section.
- **Equivalent Wander Factor:** This factor is calculated and applied to the total ESALs to account for the vehicle wander during the design life of the pavement. Equivalent wander factor is expressed by the natural logarithm of the radius of relative stiffness (ℓ).

Load Equivalency

In this design methodology, the 18 kips ESAL concept is used to determine the load damage to the concrete pavement. The ESALs number over the design period is determined for erosion damage calculation and for fatigue damage calculations. Wander equivalency is applied in both ESALs as appropriate for the relevant distress type. The following are the inputs used to determine the equivalent axle load for fatigue and erosion damage:

- **Radius of relative stiffness (ℓ):** radius of relative stiffness is required to calculate the dimensionless stress for each axle load level. ℓ depends on slab thickness (h), modulus of subgrade/subbase reaction (k), modulus of elasticity of concrete (E), and Poisson's ratio of concrete (which usually assumed 0.35). In determining the mentioned inputs, ℓ can be calculated as follows:

$$\ell = \sqrt[4]{\frac{E_c * h^3}{12(1-\upsilon^2)k}} \tag{24}$$

Where,

h = thickness of the unbonded PCC layers.

E_c = Elastic modulus of the PCC layer = $33 \cdot \gamma^{1.5}\sqrt{f_c^{'}}$.

ν = Poisson's ratio (typically 0.35).

k = Modulus of subgrade reaction.

- **The dimensionless stress (S):** the dimensionless stress is used to determine the stresses of the wheel load for different load levels. S depends on the radius of relative stiffness divided by the contact area radius (ℓ/a) and the coefficient for free edge stresses. The dimensionless stresses can be calculated by the following equation:

$$s_i = a * \left(\frac{\ell}{a_i}\right)^2 + b * \left(\frac{\ell}{a_i}\right) + c \tag{25}$$

Where,

ℓ= the radius of relative stiffness as discussed earlier.

a_i = the radius of the pressure area and can be calculated as follows:

$$a_i = \sqrt{\frac{WL_i}{p * \pi}} \tag{26}$$

WL_i = wheel load which equal to the axle load divided by 2.

p = tire pressure which can be taken as 100 or 120.

a,b,c = coefficients used to calculate the free edge dimensionless stress, these coefficients are as follow.

Table 41. Dimensionless Stress Coefficients—Free Edge.

Coefficient	a	B	c
SA	-0.0171	0.652	-0.0032
TA	-0.009	0.5244	-0.0121
Tridem	-0.0104	0.46	0.0037

- **The edge stress (σ):** The free edge wheel load stresses are calculated for all axle load levels based on the dimensionless stresses. The following equation is used to obtain the stresses:

$$\sigma_i = \frac{wl * s_i}{{h_e}^2} \qquad 27$$

Where,

WL = wheel load which equal to the axle load divided by 2.

s = dimensionless stress (explained earlier).

h_e = equivalent thickness of the unbonded PCC layers.

- **Stress ratio for fatigue (r):** the stress ratio is used directly to calculate the load equivalency for each load level. The stress ratio for fatigue is defined as the equivalent edge stress divided by the modulus rupture of concrete:

$$r_i = \frac{\sigma_i}{MOR} \qquad 28$$

Where,

σ_i = the wheel load stress at the edge of the slab (explained earlier).

MOR = flexural strength or modulus of rupture of concrete, which can be calculated using $MR = 9.5 * (f_c')^{\frac{1}{2}}\ in\ psi$, where fc' is the compressive strength of concrete at 28 days.

- **Stress ratio for erosion (r):** the stress ratio is used directly to calculate the load equivalency for each load level. The stress ratio for erosion is defined as the interfacial shear stress divided by the effective interfacial resistance or bond strength.

$$r_i = \frac{\tau_i}{f_e} \qquad 29$$

Where,

r_i = Stress ratio of i load level.

τ_i = Interfacial shear stress.

f_e = Effective interfacial frictional resistance or bond strength.

The calculation used to calculate τ_i and f_e were discussed earlier.

Stress Calculation

For stress calculation, the design methodology requires calculating three types of stresses, which are: 1) the stress at the edge of the slab for calculating the fatigue ELF, 2) the shear stresses required to calculate the erosion ELF, and 3) total stresses, which is the sum of the stresses at the edge of the pavement and the net (climatic) stresses. The total stresses are usually used for calculation of the allowable number of traffic repetition for fatigue damage. Climatic factors affect the shear strength of slab-subbase interface and its resistance to erosion damage:

- **Edge stresses:** the edge stress is calculated as a function of the modulus of subgrade reaction and the slab thickness. In this methodology, the PCA tabular format was imitated where the stresses were calculated at the edge of the slab for slab thicknesses from 4 in. to 14 in. in 0.5-in. increment beside a k-values that vary from 50 to 700 psi. The equivalent edge stress (σ):

$$\sigma = \frac{wl * s_i}{h^2} \qquad 30$$

Where,

WL = wheel load, which equal to the axle load divided by 2. The axle load here is 18 kips for single axle.

s_i = dimensionless stress for different k and slab thickness (explained earlier).

h = thickness of the unbonded PCC layers.

- **Net (climatic stresses):** the net stresses are the accumulation of stresses due to moisture and temperature gradients (wrapping and curling stresses). The equation used to calculate the nest stresses are discussed earlier.
- **Shear stresses:** the shear stress is required along with the shear strength to calculate the load equivalency for erosion and the allowable of ESALs for erosion. Equations used to calculate the shear stresses and strength was discussed previously.

Fatigue and Erosion Damage

For fatigue and erosion damage, the cumulative increase of the ESALs over the design period should be calculated and plotted with the damage. To get the increase of ESALs overtime, the following inputs should be specified:

1. AADTT.
2. Growth rate.
3. Design life.

After determining the cumulative increase of the ESALs over the design period, the allowable ESALs should be calculated for fatigue and erosion.

- **Allowable ESALs for fatigue:** for this calculation the pavement M-E equation is used:

$$\log(N_f) = C_1 * \left(\frac{MR}{\sigma_i}\right)^{C_2} + 0.4371 \quad 31$$

Where,

N_f = the allowable load repetition for fatigue.

MR = Modulus of rupture or flexural strength of the PCC layer.

σ_i = the total stress (wheel load stress and net stress) of the 18 kips single axle.

C_1 = national calibration coefficient, which is usually taken as 2.0.

C_2 = national calibration coefficient, which is usually taken as 1.22.

- **Allowable ESALs for erosion:** for this calculation a calibrated model of erosion is used:

$$N_f = 10^{k_1 + k_2 * r_i} \quad 32$$

Where,

N_f = the allowable load repetition for erosion.

K_1 = first calibrated coefficient for Texas, which is taken as 6.348.

K_2 = second calibrated coefficient for Texas, which is taken as −2.47.

r_i = erosion stress ratio. For allowable load repetition calculation the load of 18 kips single axle load is considered.

Once the allowable ESALs for fatigue and erosion are calculated, the damage for each year is calculated and the percent of cracks and percent of erosion (faulting) is determined:

- **Damage for fatigue:** the calculation of fatigue damage can be estimated using miner's model:

$$D = \sum_{i=1}^{k} \frac{n_i}{N_i} \quad 33$$

Where,

D = the damage factor.

n_i = the cumulative number of ESALs for each year of the design period.

N_i = the allowable number of ESALs.

- **Damage for erosion:** the calculation of fatigue damage can be estimated using miner's model with additional modification on the value based on the percentage of wet days (NWD%):

$$D = \sum_{i=1}^{k} \frac{n_i}{N_i} * \%wet\ days \tag{34}$$

Where,
D = the damage factor.
n_i = the cumulative number of ESALs for each year of the design period.
N_i = the allowable number of ESALs.
% wet days = the percentage of wet days over the year (user input).

- **Percent of cracking:** %C of cracking versus damage is calculated for the fatigue damage. For calculating this parameter, the pavement M-E equation is used as follows. The national coefficients are also used in this equation:

$$\%C = \frac{1}{1+C_4 * FD^{C_5}} \tag{35}$$

Where,
C_4 and C_5 = the national calibration coefficients for fatigue cracking percentage calculation ($C_4 = 1.0$ and $C_5 = -1.68$).
FD = Fatigue distress damage, as calculated before.

- **Percent of erosion (%E):** %E is related to the level of faulting at the joints of the concrete pavement slab. The erosion parameter, a local calibration coefficient is used. The following relationship was used to determine the percent of erosion and the faulting level relative to a specific performance criteria (f_∞):

$$\%E = \frac{f_i}{f_\infty} = e^{-\left(\frac{\rho}{D_i}\right)^{\beta}} \tag{36}$$

Where,
%E = percent of erosion.
f_i = level of faulting.
f_∞ = ultimate faulting.
D_i = erosion damage function = $\frac{\sum n_i}{N_\infty} * (\%\text{Wet Days})$.
ρ, β = local calibration coefficients which can be taken as β = 1.147 and ρ = 8.025.

Load Transfer Efficiency

The proposed design methodology evaluates the use or nonuse of dowels at the joints. The evaluation of LTE is provided using three cases: 1) LTE by aggregate interlock only, 2) LTE by dowel only, and 3) LTE by dowel and aggregate interlock. The LTE for each case is measured for different crack widths so the designer can estimate the maximum (critical) allowable crack width in the design pavement and specify the joints spacing accordingly.

For this calculation, the following procedure is followed in the design sheet:

$$LTE = \frac{100}{1+\log^{-1}\left[\dfrac{0.214-0.183\left(\dfrac{a}{\ell}\right)-\log(J)}{1.18}\right]} \qquad 37$$

Aggregate Interlock

$$Log(J) = ae^{-e^{-\left(\frac{J_S-b}{c}\right)}} + de^{-e^{-\left(\frac{s_0-e}{f}\right)}} + ge^{-e^{-\left(\frac{J_S-b}{c}\right)}} \bullet e^{-e^{-\left(\frac{s_0-e}{f}\right)}} \qquad 38$$

Where,

a = −4.00 d = −28.85.

b = −11.26 e = 0.35.

c = 7.56 f = 0.38.

g = 56.25.

Js = load transfer on the shoulder/longitudinal joint.

$$s_{o_i} = \left\{s_0^*\right\}^{0.729} \cdot e^{-\left\{0.039\frac{cw_i}{D_N}\right\}} = \left\{\frac{77.38\cdot h^2}{9000}\right\}^{0.729} \cdot e^{-\left\{0.039\frac{cw_i}{D_N}\right\}} \qquad 39$$

Where,

so = Dimensionless seasonal shear capacity based on crack width.

s_o^* = Reference dimensionless shear capacity (based on a shear stress of 77.38 psi and a wheel load of 9000 lb).

hPCC = Thickness of the slab, (in.).

cwi = Crack width, joint opening, (mils); The width of the transverse crack is fundamental to many aspects of CRC pavement performance, since it plays a dominant role in controlling the degree of load transfer provided across the thickness as criteria for the required design steel content. Crack width is affected by several time-dependent design parameters, as shown in the following formula for a single layer of steel:

$$cw_{ki} = L_k\left(\varepsilon_{shri} + \alpha_{PCC}\Delta T_{\varsigma m}\right) - L_k\,\frac{c_{2ki}}{E_{PCCi}}\left(\frac{L_k U_m P_b}{c_{1ki} d_b} + C\sigma_0\left(1 - \frac{2h_s}{h_{PCC}}\right) + \frac{L_k}{2}\,f\right) \qquad 40$$

Where,

cw_{ki} = Average crack width at the depth of the steel for each time increment *i* and crack spacing *k*, mm (mils).

L_k = k^{th} crack spacing, mm.

$\varepsilon_{\text{shr i}}$ = Unrestrained concrete drying shrinkage at the depth of the steel for each time increment *i* and crack spacing *k*.

α_{PCC} = Concrete CTE, °C^{-1} (°F^{-1}).

$\Delta T_{\zeta m}$ = Seasonal drop in PCC temperature at the depth of the steel °C (°F).

$c_{1\,ki\,i}$ = First bond stress coefficient for time increment *i* and crack spacing *k*.

$c_{2\,ki\,i}$ = Second bond stress coefficient for each time increment *i* and crack spacing *k* (typical range = 0.7 to 0.9).

$= c_{2\,ki} = a_i + \frac{b_i}{k_1} + \frac{c_i}{L_k^{\,2}}$.

a_i = 0.7606 + 1772.5($\varepsilon_{tot-\varsigma i}$) – 2e06($\varepsilon_{tot-\varsigma i}$)^2.

b_i = 9e08($\varepsilon_{tot-\varsigma i}$) + 149486.

c_i = 3e09($\varepsilon_{tot-\varsigma i}$)^2 – 5e06($\varepsilon_{tot-\varsigma i}$) + 2020.4.

$\varepsilon_{tot-\varsigma i}$ = Total strain at the depth of the steel for the time increment (*i*) (typical range = 150 to 600 micro-strains).

$k_{1\,i}$ = Bond slip coefficient.

L_k = k^{th} Crack spacing, in.

$E_{PCC\,i}$ = Concrete modulus of elasticity for the time increment *i*, kPa (psi)

P_b = Percent steel, fraction.

d_b = Reinforcing steel bar diameter, mm (in.).

U_m = Peak Bond Stress, kPa (psi)

h_{PCC} = PCC slab thickness, mm (in.).

h_s = Depth to steel, mm (in.).

f = Subbase friction coefficient based on subbase type from test data or using AASHTO recommendations.

C = Bradbury’s correction factor for slab size *(*

$\sigma_{0\,ki}$ = Westergaard nominal environmental stress factor for slab curling and warping for each time increment *i*, kPa (psi).

$$\frac{E_{PCCi}\varepsilon_{tot-\Delta m}}{2(1-\mu_{PCC})} \qquad 41$$

Where,

μ_{ppc} = Poisson’s ratio.

$\varepsilon_{tot-\Delta m}$ = Equivalent total strain difference between the pavement surface and slab bottom.

For any given project, crack widths vary widely along the project from crack to crack. One may consider this variability to correlate with the variability in crack spacing.

The design calculation sheet objective is to provide the simplest way to determine the thickness based on specified performance criteria for fatigue cracking and erosion damage. The required LTE by designer is also evaluated through effect of crack width under using or not using dowels. Thus, the design calculation sheet requires the following inputs for each parameter.

Table 42. Design Calculation Inputs.

Parameter	Main Inputs	Source
Traffic calculation	Average daily truck traffic	User input. Estimate from field account data
	Design life	Built in as 20 years
	Tire pressure (p)	User input. Usually taken as 100 psi
	Yearly traffic increase rate (R)	User input
	AASHTO TTC group from 1-17	User Input
Load equivalency	Thickness of unbound PCC layer (h) from 4 to 14 in 0.5-in. increment	User Input
	Modulus of elasticity for PCC layer (Ec)	User input , $E_c = 33 \cdot \gamma^{1.5}\sqrt{f_c'}$
	Poisson’s ratio for concrete	User input. Usually taken as 0.35
	Modulus of subgrade/subbase reaction (k) from 50 psi to 700 psi in 50 psi increment	User input
	Tire pressure (p)	User input. Usually taken as 100 psi
	Modulus of rupture	User input. $MR = 9.5 * (f_c')^{\frac{1}{2}}$ in psi
	Friction Coefficient of Stabilized Base/Subbase Materials (μ_f)	User input. Use Typical Friction Coefficient of Stabilized Base/Subbase Materials suggested by AASHTO
Stress calculation	Thickness of unbound PCC layer (h) from 4 to 14 in 0.5-in. increment	User Input
	Modulus of elasticity for PCC layer (Ec)	User input , $E_c = 33 \cdot \gamma^{1.5}\sqrt{f_c'}$
	Poisson’s ratio for concrete	User input. Usually taken as 0.35
	Modulus of subgrade/subbase reaction (k) from 50 psi to 700 psi in 50 psi increment	User input
	Tire pressure (p)	User input. Usually taken as 100 psi
	Location of pavement. Four locations	User input

	are specified with different average temperature	
	Friction Coefficient of Stabilized Base/Subbase Materials (μ_f)	User input. Use Typical Friction Coefficient of Stabilized Base/Subbase Materials suggested by AASHTO
Fatigue and erosion damage	Thickness of unbound PCC layer (h) from 4 to 14 in 0.5-in. increment	User Input
	Modulus of subgrade/subbase reaction (k) from 50 psi to 700 psi in 50 psi increment	User input
	Friction Coefficient of Stabilized Base/Subbase Materials (μ_f)	User input. Use Typical Friction Coefficient of Stabilized Base/Subbase Materials suggested by AASHTO
	% wet days	User input. Historical records can be used
	Performance criteria of ultimate faulting allowed at the joint (f_{ult})	User input
	Performance criteria of percentage of cracks (%C) allowed during the design life	User input
LTE	Dowels	User input. Yes or No
	Dowels diameter if yes	User input
	Dowels spacing if yes	User input
	Performance criteria of required LTE	User input

DESIGN INPUTS FOR CRCP

The CRCP design procedure is concentrated on the potential for punchout and distresses related to it. The procedure involves modifications in determining the punchout distress as pointed out in pavement M-E. Design inputs are the same as for JPCP especially when it comes to estimating the traffic ESALs and prediction of fatigue and erosion distress. The following design methodology and modifications was taken from Jung et al.*(14)* .

Design Approach

Punchout and distress related to it are the most prevalent factors affecting the performance of CRC pavement. Therefore, appropriate prediction of punchout is the one of most important features in CRC pavement design. An important aspect of modeling the punchout process is the consideration of the effect of development of subbase erosion on performance. The CRC pavement design methodology introduces the formulation of a mechanistic approach that directly considers the erodibility potential of subbase layer and the potential for partial-depth punchouts as affected by deep delamination. This approach is important for energy sector traffic.

The potential for punchout distress is defined in terms of a combination of the probability associated with full-depth and partial-depth punchouts since performance databases have considered the distress types to be one in the same. The combined sum of probabilities can be weighted accordingly to the subbase erosion, vertical shear stress due to crack wear-out, loss of

LTE, loss of structural stiffness due to delamination at the level of the steel reinforcement, and fatigue cracking (Figure 130 and Figure 131). Furthermore, many design factors such as traffic level, effective slab thickness, subbase erodibility, effective radius of relative stiffness, and percent of wet days should be considered to calculate the number of distresses associated with each type of punchout.

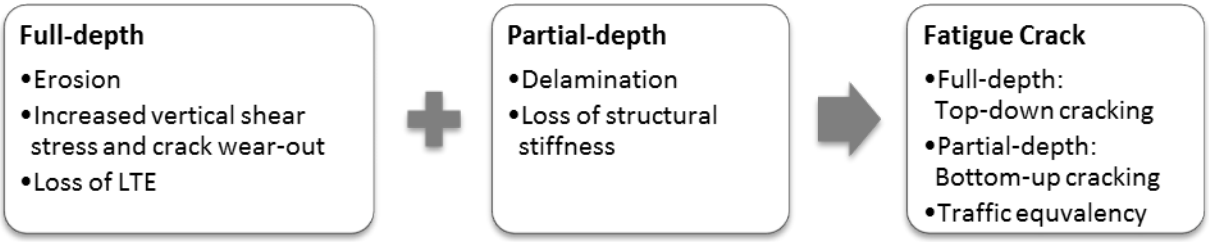
Full-depth
•Erosion
•Increased vertical shear stress and crack wear-out
•Loss of LTE
Partial-depth
•Delamination
•Loss of structural stiffness
Fatigue Crack
•Full-depth: Top-down cracking
•Partial-depth: Bottom-up cracking
•Traffic equvalency

Figure 130. Overview of Enhanced Punchout Model.

The factors listed in Figure 130 for the enhanced punchout model play a part in the potential for full-depth and partial-depth punchouts and affect the accumulated fatigue damage as well as the probability of deep delamination at the level of the steel reinforcement and erosion of the subbase, respectively, as illustrated in Figure 131. Coefficients in the punchout model are calibrated with field data to account for field conditions such as environmental and joint seal factors. The punchout probability mathematically shown in Equation 42 is used to predict the number of punchout relative to the traffic. Full-depth punchouts (Equation 43) are determined relative to the degree of erosion and fatigue cracking for crack spacings less than 3 ft apart. The potential for longitudinal fatigue cracking to form between two transverse cracks for both distress types is a function of traffic and the effect of curling stress increases as erosion progresses over the design period. Partial-depth punchout (Equation 44) is determined relative to the probability of deep delamination and fatigue cracking of delaminated slabs that have crack spacings larger than 8 ft.

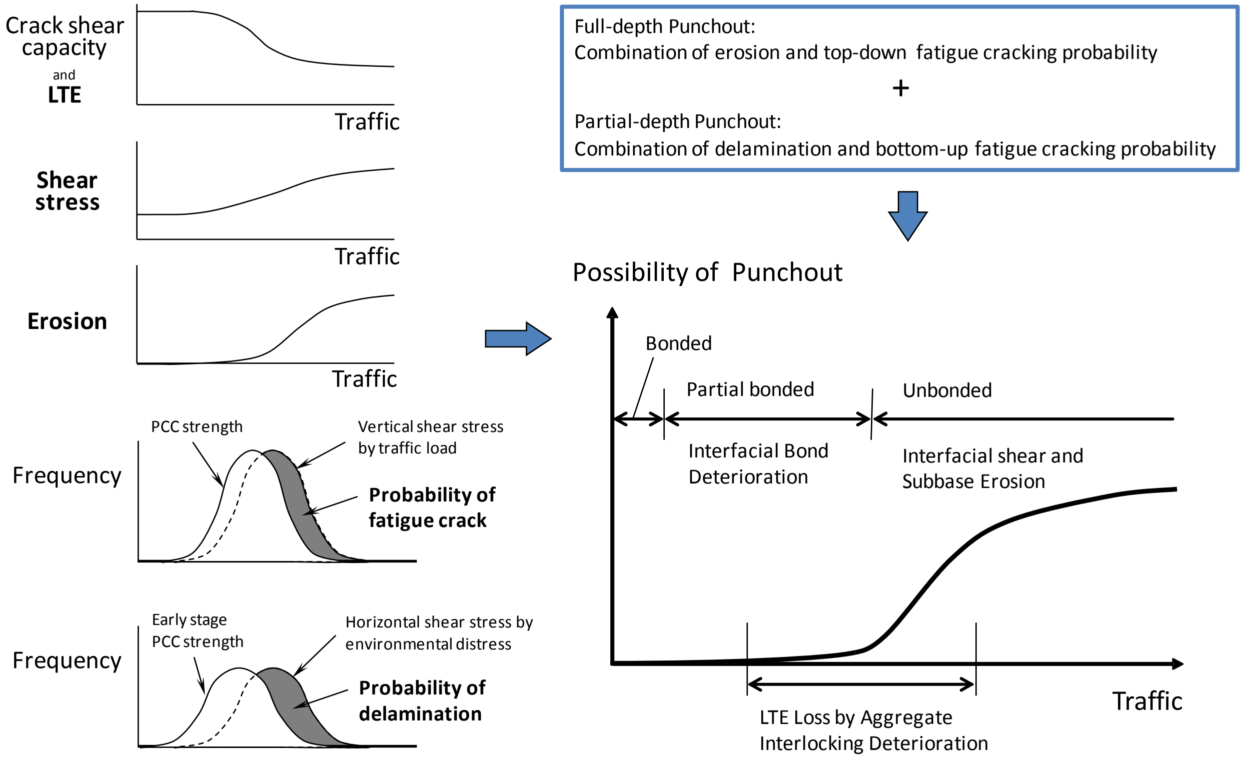

Crack shear capacity
and
LTE
Traffic
Shear stress
Traffic
Erosion
Traffic
PCC strength
Vertical shear stress by traffic load
Frequency
Probability of fatigue crack
Early stage PCC strength
Horizontal shear stress by environmental distress
Frequency
Probability of delamination
Full-depth Punchout:
Combination of erosion and top-down fatigue cracking probability
+
Partial-depth Punchout:
Combination of delamination and bottom-up fatigue cracking probability
Possibility of Punchout
Bonded
Partial bonded
Unbonded
Interfacial Bond Deterioration
Interfacial shear and Subbase Erosion
LTE Loss by Aggregate Interlocking Deterioration
Traffic

Figure 131. Schematic of Combination for Possibility of Punchouts.

$$PO = PO_{fd} + PO_{pd} \qquad 42$$

$$PO_{fd} = NC_{cw<3ft} \times P_{fc} \text{ (as affected by erosion damage)} \qquad 43$$

$$PO_{pd} = NC_{cw>8ft} \times P_{d} \times P_{fc} \qquad 44$$

Where,

PO = number of punchout.
PO_{fd} = number of full-depth punchouts per mile.
PO_{pd} = number of partial-depth punchouts per mile.
$NC_{cw<3ft}$ = number of cracks which has crack spacing smaller than 3 ft per mile.
P_{fc} = fatigue crack probability.
$NC_{cw>8ft}$ = number of cracks, which has crack spacing bigger than 8 ft per mile.
P_{d} = delamination potential.

Full Depth Punchout—Subbase Erosion Model

The erosion and interfacial shear strength model previously discussed and as calculated based on the erodibility test methodology using the Hamburg wheel-tracking device*(15,16)* . Mechanically induced horizontal shear stresses on the subbase surface are developed as a function of the up and down slab movement, which is simulated by deflection of a stiff plate. When interfacial debonding between PCC slab and subbase takes place, erosion will start and develop gradually with traffic, since LTE of crack will decrease due to wear-out of the aggregate interlocking under loading, which could result in greater slab deflection and greater transportation of fines by pumping of trapped water.

Full Depth Punchout—Vertical Shear Stress on the Transverse Crack

Vertical shear stress on a transverse crack face is related to wear out that occur under the effect of load transfer across the crack. The shear stress can be calculated by Equation 45 and will be increased to a maximum limit depending on the amount of traffic and erosion. Equation 46 explains initial shear capacity, which is a function of the transverse crack width and effective PCC slab thickness. Loss in shear capacity of a crack occurs as a result of wheel loads passing over the crack as shown in Equation 47. The amount of loss is a function of the width of the transverse crack and is important for accounting for the effect of aggregate wear-out. If crack width is smaller than 20 mils, little loss of shear capacity will take place. Equation 48 shows shear strength gain. The coefficients of this function may vary for different aggregate types, but preliminary test results indicate little difference in the shear wear-out behavior among mixes made with different coarse aggregate types:

$$\tau_i = \frac{Agg}{h_e}\left(\delta_L - \delta_{uL}\right) = \frac{Agg}{h}\delta_L\left(1 - LTE\right) = \frac{Agg}{h}\delta_{FE}\left(\frac{1-LTE}{1+LTE}\right) \tag{45}$$

$$s_0 = s_0^{*}\, e^{-0.039\frac{cw}{D_N}} = \left\{\frac{77.38\, h_e^2}{9000}\right\} e^{-0.039\,\frac{cw}{D_N}} \tag{46}$$

$$\Delta s = \left(0.069 - 1.5317 e^{-cw_i/h_{pcc}}\right)\left(\frac{n_i}{10^6}\right)\left(\frac{\tau_i}{f_\tau}\right) \tag{47}$$

$$f_{\tau_i} = \frac{s_0 P_i}{{h_{pcc}}^2} \tag{48}$$

Where,

τ_i = shear stress on a transverse crack face, (Pa or psi).

D_N = nominal coarse aggregate size, in.

P_i = traffic load level i, (N or lb).

h_e = effective slab thickness, (m or in.).

s_0 = initial dimensionless shear capacity (the range is 0 to 0.9).

s_0^{*} = reference dimensionless shear capacity; ranges from 0.55 to 1.3 as a function of slab thickness = $\left\{\frac{77.38\, h_e^2}{9000}\right\}$.

cw = crack width, (mil).

Δs = loss in shear capacity accumulated over shear capacity loss due to load applications in each weight/axle type group (i) ($\Delta s = 0$ if $cw < 0.0031\ h_{PCC}$).
n_i = number of axle load applications for current load level (i).

Full Depth Punchout—LTE

Equations 49 and 50 show transverse crack LTE due to aggregate interlock. The loss in shear capacity of a crack over the traffics will decrease transverse crack stiffness and result loss of LTE:

$$LTE_i = \frac{100}{1+\log^{-1}\left[\frac{0.214-0.183\frac{r}{l}-\log(J_{ci})}{1.18}\right]} \tag{49}$$

$$\log(J_{ci}) = ae^{-e^{-\left(\frac{J_s-b}{c}\right)}} + de^{-e^{-\left(\frac{S_i-e}{f}\right)}} + ge^{-e^{-\left(\frac{J_s-b}{c}\right)}}e^{-e^{-\left(\frac{S_i-e}{f}\right)}} \tag{50}$$

Where,
LTE_i = Load transfer efficiency on the transverse crack for current load level (i), (%).
r = loaded radius, (m or in.).
l = radius of relative stiffness, (m or in.).
J_{ci} = transverse crack stiffness for current load level (i) coefficients: $a = -4.0$, $b = -11.26$, $c = 7.56$, $d = -28.85$, $e = 0.35$, $f = 0.38$, $g = 56.25$.
J_s = stiffness of shoulder/longitudinal joint.
s_i = adjusted dimensionless shear capacity for current load level (i).

Partial Depth Punchout—Delamination Assessment

Analysis of partial-depth punchout is based on the potential of delamination. Deep delamination as shown in Figure 132 is dependent upon the shear stress at a certain depth below the pavement surface. Shear stress for deep delamination is created based on both plate theory and beam theory. Early age delaminations occur when shear stresses caused by slab curling and warping surpasses the concrete shear strength.

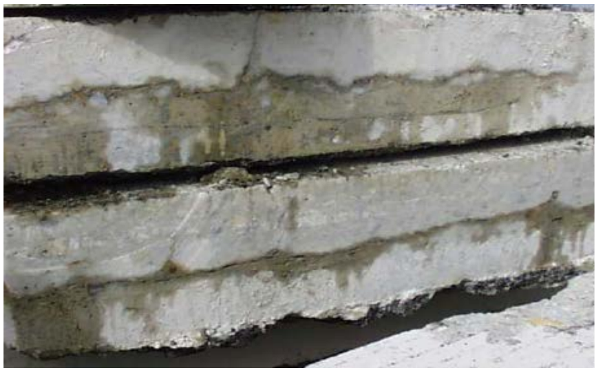

Figure 132. Formation of Deep Delamination.

Shear stress due to curling and warping behavior is also key to horizontal cracking at a greater depth coincidental with the plane of the reinforcing steel. The presence of the steel increases the stress levels due to modulus differences between the steel and the concrete. This deep delamination is a precursor to partial-depth punchouts where longitudinal fatigue cracking occurs. Deep delamination or shear stress at the level of the steel can be formulated following Vetter's (*14*) original analysis as:

$$\tau_{steel} = \frac{A_s n L}{b_{spc} \ell_d^2} \{E_c z - f_t\} \tag{51}$$

Where,

τ_{steel} = shear stress at the level of the steel mat (FL^{-2}).

A_s = area of reinforcing steel.

n = modular ratio = $\frac{E_s}{E_c}$.

E_s = steel modulus (FL^{-2}).

E_c = concrete modulus (FL^{-2}).

L = crack spacing (L).

b_{spc} = bar spacing (L).

ℓ_d = reinforcement development length (L).

z = drying shrinkage at the time of cracking.

f_t = tensile strength of the concrete at the time of cracking (FL^{-2}).

The degree that the concrete shear stress surpasses the concrete shear strength governs the degree or probability that delamination can occur. The probability that concrete shear stress exceeds in shear strength is represented by Equation 52. Specifically, the degree that concrete shear stress surpasses the concrete shear strength governs the degree that delamination can occur. Thus, the probability is based on the difference of means of two populations of shear strength and stress, which each have a standard deviation made up from the variances of the factors involved with the two populations:

$$\text{Prob}(\tau_{steel} - f_\tau > 0) \tag{52}$$

Where,

f_τ = shear strength, (Pa or psi) $(f_\tau \sim \frac{f_t}{2} \sim \frac{1}{4} \cdot MoR \sim \frac{1}{20} f_c)$.

f_t = tensile strength, (Pa or psi).

MoR = modulus of rupture, (Pa or psi).

f_c = compressive strength, (Pa or psi).

CHAPTER 7. ECONOMIC EVALUATION

INTRODUCTION

The cost of rehabilitation alternatives is often considered the most important decision criteria when determining a preferred pavement type or combination. Life cycle cost analysis (LCCA) requires inputs of both cost and time. Unfortunately, these elements are subject to some degree of uncertainty. For instance, the effective life of a rehabilitation technique is subject to such influences as quality of construction, environmental conditions, and traffic level. Too often, these factors are known in a subjective manner. To eliminate as much variability as possible, it is essential to collect information and data from standardized pavement management databases. Another important consideration in LCCA is that the same rehabilitation techniques, when applied to different pavements, may have variant effects. Furthermore, some methods may keep a pavement at a consistently high-condition level, while others may allow the condition of the same pavement to fluctuate. Thus, discrepancies of this nature are only accounted for by the cost analysis.

LCCA typically introduces risk analysis as a method to address uncertainty associated with LCCA inputs. It also includes a detailed, rational, highway capacity-based approach for determining work zone user costs associated with alternative pavement design strategies. Work zone user costs are the increased vehicle operating costs, delay, and crash costs to highway users resulting from MRR work zones. They are a function of the timing, duration, frequency, scope, and characteristics of the work zone; the volume and operating characteristics of the traffic affected; and the dollar cost rates assigned to vehicle operating, delay, and crashes. Risk analysis in LCCA is also accomplished, which helps quantify the uncertainty associated with data inputs. The LCCA is a key criterion for selecting the preferred strategy for MRR of rigid pavements. It makes use of the data developed in the pavement, traffic, and construction analyses.

Pavement maintenance and rehabilitation alternatives are often selected based on LCCA evaluations. To make consistent and cost effective decisions, the LCCA must take into account all costs. Unfortunately, due to limited traffic data on work zones, most agencies do not consider road user costs due to traffic delays in the work zone. Simple models are sufficient evaluate the additional road user costs in work zones, which are to be used to compute the life cycle costs of various MRR alternatives.

LCCA PROCEDURE

Life cycle cost is analyzed by using a few approaches. They are agency cost, user cost, deterministic approach, and risk analysis approach. LCCA process can be divided into several steps:

1. Establish strategies for analysis period.
2. Establish activity timing.
3. Estimate agency costs.
4. Estimate user costs.
5. Develop expenditure streams.
6. Compute net present value (NPV).
7. Risk analysis.
8. Reevaluate strategies.

Establish Strategies for Analysis Period

The primary purpose of an LCCA is to quantify the long-term implication of initial pavement design decisions on the future cost of maintenance and rehabilitation activities necessary to maintain some pre-established minimum acceptable level of service for some specified time. A pavement rehabilitation strategy is the combination of initial repair treatments and necessary supporting maintenance and rehabilitation activities. The analysis period is the time horizon over which future cost is evaluated. The first step in conducting an LCCA of alternative pavement designs is to identify the alternative pavement design strategies for the analysis period under consideration.

LCCA analysis period should be sufficiently long to reflect long-term cost differences associated with reasonable design strategies. The analysis period should generally always be longer than the pavement design period, except in the case of extremely long-lived pavements. As a rule of thumb, the analysis period should be long enough to incorporate at least one rehabilitation activity. Analysis period of at least 35 years for all pavement projects is recommended, including new or total reconstruction projects as well as rehabilitation, restoration, and resurfacing projects. At times, shorter analysis periods may be appropriate, particularly when pavement design alternatives are developed to buy time (say 10 years) until total reconstruction. It may be appropriate to deviate from the recommended minimum 35-year analysis period when slightly shorter periods could simplify salvage value computations. For example, if all alternative strategies would reach terminal serviceability at year 32, then a 32-year analysis would be quite appropriate. Regardless of the analysis period selected, the analysis period used should be the same for all alternatives. Figure 133 shows a typical analysis period for a pavement design alternative.

Typically, each design alternative will have an expected initial design life, periodic maintenance treatments, and possibly a series of rehabilitation activities. It is important to identify the scope, timing, and cost of these activities. Depending on the initial pavement design, State Highway Agencies employ various rehabilitation strategies to keep the highway facilities in functional condition. For example, Table 43 shows a typical supporting maintenance and rehabilitation strategy for new, reconstructed, and unbonded PCC pavements included. Note that user cost requirements are also identified.

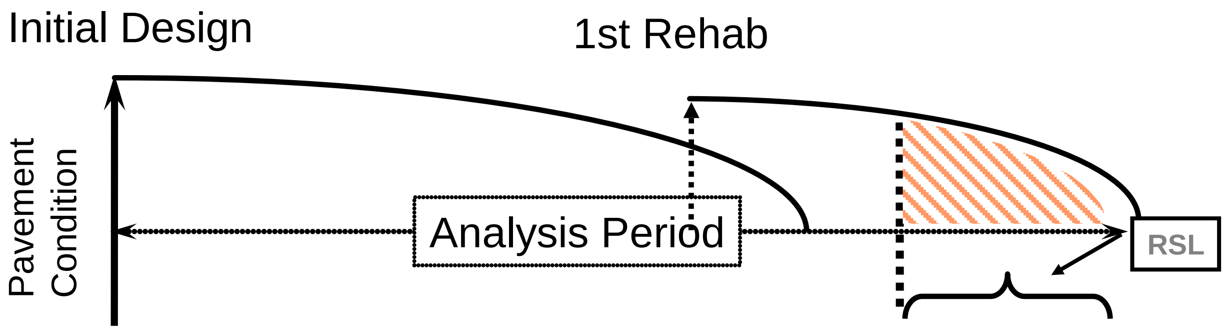

Figure 133. Establish Strategies and Activity Timing.

Establish Activity Timing

Performance life for the initial pavement design and subsequent rehabilitation activities has a major impact on LCCA results. It directly affects the frequency of agency intervention on the highway facility, which in turn affects agency cost and user costs during periods of construction and maintenance activities. SHA's can determine specific performance information for various pavement strategies through analysis of pavement management data and historical experience. Operational pavement management systems can provide the data and analysis techniques to evaluate pavement condition and performance and traffic volumes to identify cost-effective strategies for short-and long-term capital projects and maintenance programs. Some SHAs develop performance lives based on the collective experience of their senior engineers. Work zone requirements for initial construction, maintenance, and rehabilitation directly affect highway user costs and should be estimated along with pavement strategy development. The frequency, duration, severity, and year of work zone requirement are critical factors in developing user costs for the alternatives being considered.

Table 43. Framework of MRR Strategies.

Year	Treatment
5	Clean and seal 25% of longitudinal joints. Clean and seal 5% of transverse joints. 0% for neoprene seals. Seal coat shoulders if Type I paved shoulders.
10	Same as year 5.
15	Clean and seal 25% of longitudinal joints. Clean and seal 10% of transverse joints, 5% for neoprene seals. Seal coat shoulders, if Type I paved shoulders.
20	Concrete patch 5% of pavement area. Spall repair 1% of transverse joints (5sf/joint). Slab stabilization: minimum 25% of transverse joint. Diamond grind 100% of pavement area. Clean and seal all longitudinal joints, including shoulders. Clean and seal all transverse joints, 7% for neoprene seals. Seal coat shoulders, if Type I paved shoulders. Maintenance and protection of traffic. User delay.
25	Clean and seal 25% of longitudinal joints. Clean and seal 10% of transverse joints, 10% for neoprene seals. Seal coat shoulders, if Type I paved Shoulders.
30	Concrete patch 2% of pavement area. Clean and seal all joints with fiber asphalt membrane. 60-#/sy leveling course. 3.5-in ID-2 or 4-in ID-3/ID-2 overlay. Saw and seal joints. Type 7 paved shoulders. Adjust all guide rail and drainage structures. Maintenance and protection of traffic. User delay.
35	Seal coat shoulders.
Note: The CPR strategy slated for year 20 can be moved to year 15 at the district's discretion. However, when doing this, the overlay at year 30 must be moved to year 25, and another overlay added at year 33.	

Estimate Agency Costs

Construction quantities and costs are directly related to the initial design and subsequent rehabilitation strategy. The first step in estimating agency costs is to determine construction quantities/unit prices. Unit prices can be determined from SHA historical data on previously bid jobs of comparable scale.

LCCA comparisons are always made between mutually exclusive competing alternatives. LCCA need only consider differential costs between alternatives. Costs common to all alternatives cancels out; these cost factors are generally noted and excluded from LCCA calculations.

Agency costs include all costs incurred directly by the agency over the life of the project. They typically include initial preliminary engineering, contract administration, construction supervision and construction cost, and the associated administrative cost. Routine reactive-type maintenance cost data are normally not available except on a very general, area wide cost per lane mile. Fortunately, routine reactive-type maintenance costs generally are not very high, primarily because of the relatively high performance levels maintained on major highway facilities. Further, SHAs that do report routine reactive-type maintenance costs note little difference between most alternative pavement strategies. When discounted to the present, small reactive maintenance cost differences have negligible effect on NPV and can generally be ignored.

Agency costs also include maintenance of traffic cost and can include operating cost such as pump station energy costs, tunnel lighting, and ventilation. At times, the salvage value, the remaining value of the investment at the end of the analysis period, is included as a negative cost.

Salvage Value represents value of an investment alternative at the end of the analysis period. The two fundamental components associated with salvage value are residual value and serviceable life.

Residual Value refers to the net value form recycling the pavement. The differential residual value between pavement design strategies is generally not very large, and, when discounted over 35 years, tends to have little effect on LCCA results.

Serviceable life represents the more significant salvage value component and is the remaining life in a pavement alternative at the end of the analysis period. It is primarily used to account for differences in remaining pavement life between alternative pavement design strategies at the end of the analysis period. For example, over a 35-year analysis, Alternative A reaches terminal serviceability at year 35, while Alternative B requires a 10-year rehabilitation at year 30. In this case, the serviceable life of Alternative A at year 35 would be 0, as it has reached its terminal serviceability. Alternative B receives a 10-year rehabilitation at year 30 and will have 5 years of serviceable life at year 35, the year the analysis terminates conversely. The value of the serviceable life of Alternative B at year 35 could be calculated as a percent of design life remaining at the end of the analysis period (5 of 10 years or 50 percent) multiplied by the cost of Alternative B’s rehabilitation at year 30.

Sunk Costs represent a special category of costs that are irrelevant to the decision at hand. Analysts should be careful not to include them in LCCA. An example may serve best in understanding the concept. An individual places a $10 nonrefundable deposit on a $100 camera at Store A. Before picking up the camera, the individual finds an identical camera on sale at Store B for $80. From an economic efficiency perspective, from which store should the individual purchase the camera? What bearing does the $10 deposit have on the decision? The $10 deposits a sunk cost and is irrelevant to the decision. The decision comes down to paying Store A the $90 balance for the camera, or paying Store B $80 for an identical camera. Not all cases of sunk cost are this clear and, again, analysts need to take care to guard against including them in LCCA. An example more specific to pavement design might involve the reluctance of a designer to select an alternative with a much lower life-cycle cost because it would mean wasting the money previously spent on developing final plans for a clearly inferior alternative.

Estimate User Costs

In the simplest sense, user costs are costs incurred by the highway user over the life of the project. In LCCA, highway user costs of concern are the differential costs incurred by the motoring public between competing alternative highway improvements and associated maintenance and rehabilitation strategies over the analysis period. In the pavement design arena, the user costs of interest are further limited to the differences in user costs resulting from differences in long-term pavement design decisions and the supporting maintenance and rehabilitation implications. User costs, as previously noted, are an aggregation of three separate cost components: vehicle operating costsuser delay costs, and crash costs.

Develop Expenditure Streams

Expenditure stream diagrams are graphical representations of expenditures over time. They are generally developed for each pavement design strategy to help visualize the extent and timing of expenditures. Normally, costs are depicted as upward arrows at the appropriate time they occur during the analysis period, and benefits are represented as negative cost or downward arrows. In LCCA of pavement design alternatives, the basic benefits of providing and maintaining some pre-established pavement condition level on any given roadway are outside the scope of the analysis. The benefits of providing the specified level of pavement condition are considered to be the same for all pavement design strategies. As a result, the only concerns are the differential costs among alternatives. The only negative cost (i.e., the only downward arrow) would be the cost associated with any salvage value. Under these conditions, the LCCA objective becomes finding the alternative pavement design strategy that meets the performance requirement at the lowest life-cycle cost.

Compute NPV

In its broadest sense, LCCA is a form of economic analysis used to evaluate the long-term economic efficiency between alternative investment options. Economic analysis focuses on the relationship between costs, timings of costs, and discount rates employed. Once all costs and their timing have been developed, future costs must be discounted to the base year and added to the initial cost to determine the NPV for the LCCA alternative. As noted earlier, NPV is the amount at various points in time back to some base year is:

$$NPV = InitialCost + \sum_{k=1}^{N} FutureCost_k \times \left[\frac{1}{(1+i)^{n_k}} \right] \tag{53}$$

Where,
i = Discount rate.
n = Year of expenditure.

The $\left[\frac{1}{(1+i)^{n_k}}\right]$ component of the above formula is referred to as the present value (PV) factor for a single future amount. PV factors for various combinations of discount rates and future years are available in discount factor tables (more commonly referred to as interest rate tables). PV for a particular future amount is determined by multiplying the future amount by the appropriate PV factor. For example, if initial cost is $26 million, future cost is $9 million, discount rate is 4 percent, and year of expenditure is 20 years, then NPV will become $30.1 million by equation above. This can be depicted by Figure 134. NPV can be categorized by these two kinds of NPV. One is agency NPV. The other is user NPV. Since user costs may dominate total NPV, agency costs and user costs must be computed separately.

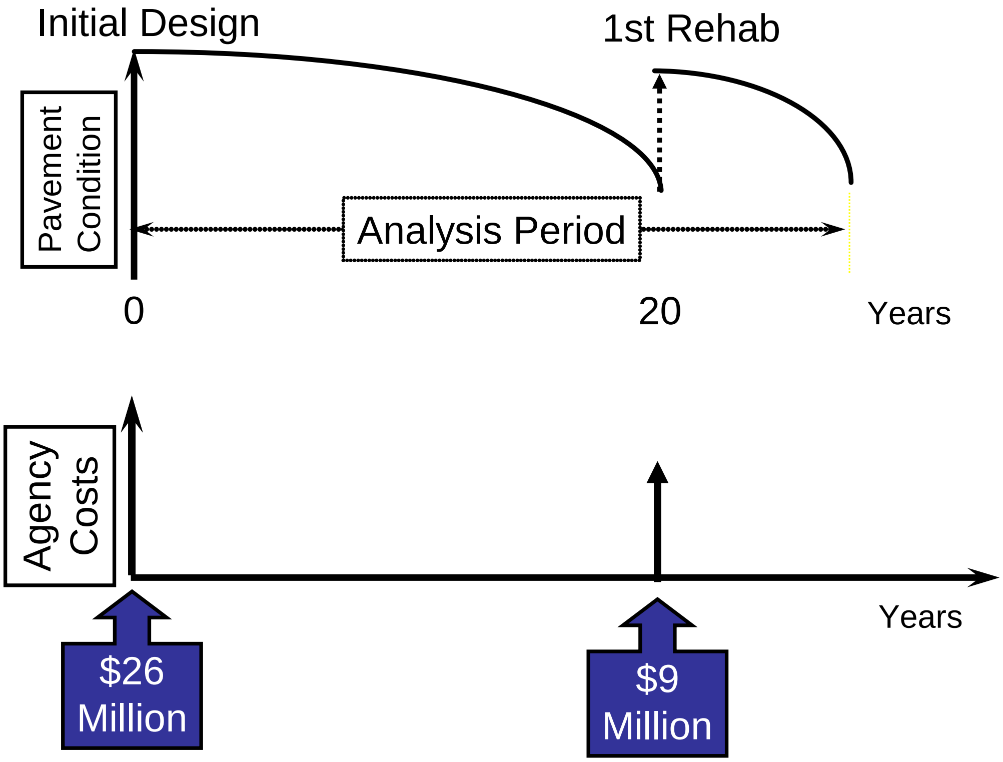
Initial Design
1st Rehab
Pavement Condition
Analysis Period
0
20
Years
Agency Costs
Years
$26 Million
$9 Million

Figure 134. Expenditures throughout the Analysis Period.

Risk Analysis

The concept of risk comes from the uncertainty associated with future events—the inability to know what the future will bring in response to a given action today. Risk can be subjective or objective. Subjective risk is based on personal perception, intuitively deciding how risky a situation may be. For example, many people may feel that flying is riskier than driving. This perception of risk may be related to the consequences of failureand the ability (or inability) to control the situation. Objective risk is based on theory, experiment, or observation.

Often the facts of the situation may dispute intuitive feelings. For example, for any given year there were 1,070 aviation fatalities; in the same year there were also 40,676 highway fatalities. Because individuals' perceptions of risk vary, decisions incorporating risk management concepts will depend to a large extent on the decision-maker's tolerance for risk.

Risk analysis is concerned with three basic questions about risk: 1) What can happen? 2) How likely is it to happen? 3) What are the consequences of its happening? Risk analysis answers these questions by combining probabilistic descriptions of uncertain input parameters with computer simulation to characterize the risk associated with future out comes. It exposes areas of uncertainty typically hidden in the traditional deterministic approach to LCCA, and it allows the decision-maker to weigh the probability of an outcome actually occurring.

Many analytical models treat input variables as discrete fixed values, as if the values were certain. In fact, the majority of input variables are uncertain. Economic models used in a typical LCCA are no exception. In conducting LCCA, it is important to be aware of the inherent uncertainty surrounding the variables used as inputs into the analysis. Uncertainty results from the assumptions, estimates, and projections made in conducting the analysis. Table 44 summarizes LCCA input variables and the general basis used to determine their values.

Traditionally, this uncertainty is often ignored in an LCCA. For example, the analyst may make a series of best guesses of the values for each input variable and compute a single deterministic result. The problem with this approach is that it often excludes information that could improve the decision.

In some cases, a limited sensitivity analysis may be conducted whereby various combinations of inputs are selected to qualify their effect on analysis results. However, even with a sensitivity analysis, this deterministic approach to LCCA often conceals areas of uncertainty that may be crucial to decision-making process. Often, stakeholders seize upon the uncertainty associated with LCCA inputs and vigorously debate the validity of the results. Traditional, deterministic-based LCCA results such as these generate endless debate over which alternative truly have the lowest life cycle cost. This process encourages division and unproductive debate.

The need to make strategic long-term investment decisions under short-term budget constraints is forcing SHAs to consider risk as a criterion for judging a course of action. Risk analysis exposes areas of uncertainty for the decision-maker. Based on this new information, the decision-maker has the opportunity to take mitigating action to decrease exposure to risk. With the emergence of user-friendly computer software, an SHA can easily integrate quantitative risk analysis concepts into the decision-making process (Figure 135).

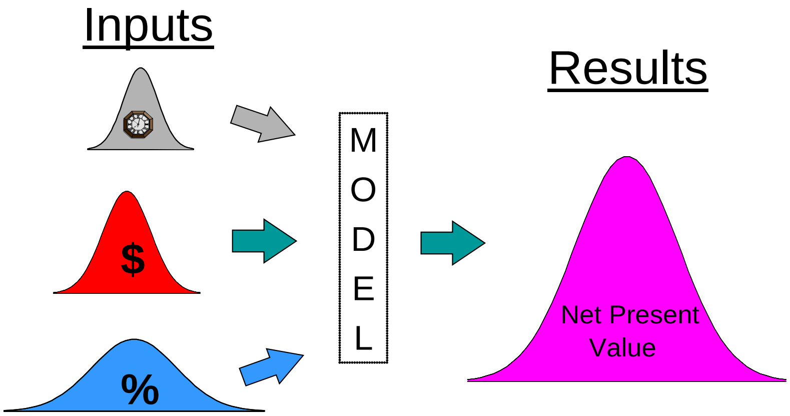

Figure 135. Risk Analysis Approach.

Reevaluate Strategies

Once the NPVs have been computed for each alternative and limited sensitivity analysis performed, the analyst needs to step back and reevaluate the competing design strategies. The overall benefit of conducting an LCCA is not necessarily the LCCA results themselves, but rather how the designer can use the information resulting from the analysis to modify the proposed alternatives and develop more cost-effective strategies.

For example, if user costs dwarf agency costs for all the alternatives, the analysis may indicate that none of the alternatives analyzed are viable. It could indicate that the designer needs to evaluate the current design strategies' impacts on future maintenance of traffic that the design strategies should reflect the need for additional capacity in the out-years to mitigate the impact on highway users. The solution to out-year pavement designs to allow for the use of the shoulder in subsequent rehabilitation traffic control plans. It also could include enhanced structural design of the mainline pavement to minimize the frequency of subsequent rehabilitation efforts and designing in features that will make future rehabilitation proceed more smoothly. Other options available include revising the maintenance of traffic plans, reducing the construction period, restricting the contractor's work hours or imposing lane rental fees, planning for additional lanes/routes, and even examining programs to temporarily shift traffic to alternative modes of travel. Restricting the contractor’s hours of operation or the number of work days allowed will more than likely increase agency cost.

LCCA results are just one of many factors that influence the ultimate selection of a pavement design strategy. The final decision may include a number of additional factors outside the LCCA process, such as local politics, availability of funding, industry capability to perform the required construction, and agency experience with a particular pavement type, as well as the accuracy of the pavement design and rehabilitation models. Chapter 3 of the 1993 AASHTO Pavement Design Guide further discusses such other factors. When such other factors weigh heavily in the final pavement design selection, it is imperative to document their influence on the final decision.

Many assumptions, estimates, and projections feed the LCCA process. The variability associated with these inputs can have a major influence on the confidence the analyst can place in LCCA results. It all depends on the accuracy of the inputs used. The accuracy of LCCA results depends directly on the analyst’s ability to accurately forecast such variables as future costs, pavement performance, and traffic for more than 30 years into the future. To effectively deal with the uncertainty associated with such forecasts, a probabilistic risk analysis approach (is increasingly essential to quantitatively capture the uncertainty associated with input parameters in LCCA results.

LCCA INPUTS FOR JPCP AND CRCP

In the development of LCCA process, each project level should include strategic alternatives to obtain the structural and performance objectives. Alternatives basically depend on the type of the pavement, performance level requirement and major rehabilitation intervals to achieve this performance level. After identifying the alternatives, the analyst should define the scheduled initial and future maintenance activities for each alternative during the analysis period. The time schedule of these activities, the amount of maintenance activity, and the estimated service life extension due to each activity depends on the performance level required for each alternative. Later, the costs of each activity should be estimated. To achieve close to accurate cost estimation, the direct agency expenditures (i.e., construction and maintenance costs) and the user’s cost due to agency work zone activity should be calculated.

Using the economic concept of discounting for each alternative, all agency’s and user’s costs are transformed into the present-time dollars and gathered for each alternative. This summation is called the present worth value, which can be used to compare the total expenditure of each alternative.

There are two computational approaches of LCCA. These are deterministic and probabilistic. The difference between the two is simply that the deterministic does not account for variability but fixed numbers while the probabilistic methodology account for the variability of LCCA inputs such as user's cost and service life of maintenance activities. To achieve reasonable of accuracy in the deterministic analysis, inputs should be obtained from historical data and professional personal judgment sources that have intensive experience in constructing and managing pavement construction within the specified project area. Deterministic method can be conducted using manual calculation or simple calculation sheets. Sensitivity analysis is possible in deterministic method; however, no more one input variation can be evaluated through deterministic simple calculation procedure. Varying many inputs can lead into much more complicated and/or inaccurate results.

In the case where different variables are required to be evaluated, probabilistic LCCA can be the best option to perform the analysis. Probabilistic LCCA analysis uses the computer utilities to simulate the simultaneous variations of parameter inputs. This approach requires defining inputs in the form of frequency or probability distribution that can be employed to perform risk analysis for the life cycle cost of each pre-established alternative.

In general, the deterministic and probabilistic methods are both used evaluate alternatives and prioritize the best alternative for any project. The FHWA's best practice LCCA process can be incorporated for any analysis. As mentioned before, different pavement types and performance levels can be analyzed. For the sake of accurate analysis, the following inputs should be established.

Table 44. LCCA Inputs.

FHWA LCCP steps	Input Data	Description	Notes
Establish Pavement Alternatives	Project details	Route, location, project name, and limits.	
	Analysis options	Contains analysis period, discount rate, the treatment of user costs in the LCCA, beginning of analysis period and number of alternatives.	Normal distribution for discount rate can be used
	Traffic Data	Includes the initial Average Annual Daily Traffic, percentage of single and combination trucks, annual growth, speed limit, free flow capacity, and flow in work zone, number of lanes and road type (urban, rural) for daily traffic distribution.	
	User cost	User costs associated with delay during work zone operations. The cost/hr is different based on the type of the vehicle.	Normal distribution can be used to consider variability in user cost
Determine Activity Timing	Alternatives construction and maintenance time	Determine the initial construction and maintenance intervals based on the required performance level of each alternative.	
Estimate Agency and User Costs	Alternatives cost	Determine the agency and user cost of each activity using the historical and current cost. Costs should include materials, engineering and inspection, traffic control, and incidental costs.	Agency and user cost can be taken as normal probability distribution to account for cost variability
Compute Life-Cycle Costs	Present worth value and area under the performance curve (AUPC)	Calculate the deterministic values of total cost at the present (initial construction) year and the AUPC. Additionally, variability of agency and user cost as well as discounting rate can be analyzed using probabilistic method.	
Analyze the Results	Graphical and tabular presentation for deterministic and probabilistic solutions of the LCCA	Show the graphical results of deterministic analysis at each maintenance time as well as show results of probabilistic, risk management, analysis.	

LCCA EXAMPLE FOR JPCP AND CRCP ALTERNATIVES

The project in this example is the intersection of US 181/SH 123 at Karnes City. The project involves construction of JPCP and CRCP of 4-lane undivided highway in a rural location. The length of the project is assumed to be 5 miles in length. The highway consists of four lanes with

12 ft width lane and 4 ft width shoulders. The two ways AADT over the four lanes was assumed to be 40,000 vehicle/day to reflect the high volume of traffic.

The two pavements are supposed to overlay an existing asphalt concrete pavement. The thickness of both concrete pavements is assumed to be 10 in. The two designs are to be evaluated based on deterministic and probabilistic LCCA for 60 years of analysis period. The normal distribution is applied for the discount rate with the mean of 3 percent and standard deviation of 0.75 percent. Also, normal distribution was used for service life of each activity as well as the agency costs and user costs. The uniform distribution was used for activity time by determining the minimum and maximum cost/hr for each vehicle type and the number of days to accomplish each activity. To simulate the heavy truck traffic, the automobiles percent was assumed 20 percent while the truck percent was assumed 80 percent.

The main objective of this example is to evaluate the use of different performance level simulated by using short-term and long-term maintenance regime. The higher performance level is associated with performing short-term maintenance plan (generally 10-year interval) while the lower performance level is associated in applying maintenance at the end of the designed service life of the pavement. Keeping this objective in mind, four alternatives were generated, which are:

1. Construction of 10 in. JPCP with short-term rehabilitation plan.
2. Construction of 10 in. JPCP with long-term rehabilitation plan.
3. Construction of 10 in. CRCP with short-term rehabilitation plan.
4. Construction of 10 in. CRCP with long-term rehabilitation plan.

Following the consistency in comparing different alternatives, the life-cycle cost calculations for each alternative were performed for 1-mile roadway section.

LCCA INPUTS

The RealCost 2.5 was used to perform the LCCA. The following summarize the key inputs for the traffic, alternative activities, timing, agency cost, and user cost.

Traffic

The list summarizes other traffic inputs were used in the simulation. They include the base year AADT, the traffic growth rate estimate, and the percent trucks and automobiles:

- Initial AADT (both directions): 40,000 vehicle/day.
- Traffic growth rate: 1.5 percent (deterministic).
- Percent automobiles: 20 percent.
- Percent trucks: 80 percent (20 percent single units, 60 percent combination units).

Alternatives and Activity Timing

Table 45 to Table 48 represent the alternatives simulated in the LCCA procedure. As discussed before, initiated alternatives were chosen to evaluate the effect of short-term and long-term rehabilitation plans for JPCP and CRCP overlays. As shown in the tables, the short-term rehabilitation plan alternatives show more frequent-small scale concrete pavement restoration CPR activities. On the other hand, long-term rehabilitation plan alternatives show large-scale rehabilitation using asphalt concrete overlays along with CPR activities. As probabilistic analysis results are preferable, the normal distribution was used in the service life of each activity by providing the mean and standard deviation of each activity.

Table 45. Alternative 1—Framework of MRR Activities for 60 Years.

Year	Treatment Activities	Service Life, years	
		Mean	Standard Deviation
0	- 10 in. JPCP pavement on existing 4 in. Asphalt concrete pavement	20	2
10	1. Reseal 25% of longitudinal joints. 2. Reseal 5% of transverse joints.	5	0.5
20	1. Partial depth repair 10% of pavement area 2. Reseal 25% of longitudinal joints. 3. Reseal 10% of transverse joints	10	1
30	1. Partial depth repair 10% of pavement area and 10 % of joints (5 sqf)	5	0.5
40	1. Joint retrofitting: minimum 25% of transverse joint. 2. Diamond grind: 100% of pavement area.	20	1.5
	Total number of structural life (Yrs)	60	

Table 46. Alternative 2—Framework of MRR Activities for 60 Years.

Year	Construction/Treatment Activities	Service Life, years	
		Mean	Standard Deviation
0	- 10 in. PCC pavement on existing 4 in. Asphalt concrete pavement	20	2
10–20	1. Preventive maintenance at 5 years interval	5	0.5
25	1. Clean and seal all longitudinal joints, including shoulders. 2. Clean and seal all transverse joints 3. 15% crack sealing 4. 2-in. Asphalt concrete overlay	15	1.5
40	1. 1-in. mill of concrete surface 2. 2 in. asphalt concrete overlay	20	2
	Total number of structural life (Yrs)	60	

Table 47. Alternative 3—Framework of MRR Activities for 60 Years.

Year	Treatment Activities	Service Life, years	
		Mean	Standard Deviation
0	- 10 in. CRCP pavement on existing 4 in. Asphalt concrete pavement	30	3
15	1. Reseal 25% of longitudinal joints. 2. Reseal 5% of transverse joints	5	0.5
30	4. Partial depth repair 10% of pavement area 5. Reseal 25% of longitudinal joints. 6. Reseal 5% of transverse joints	10	1
40	1. 1 in. mill of concrete surface 2. 3 in. Asphalt concrete overlay	20	2
Total number of structural life (Yrs)		60	

Table 48. Alternative 4—Framework of MRR Activities for 60 Years.

Year	Construction/Treatment Activities	Service Life, years	
		Mean	Standard Deviation
0	- 10 in. CRCP pavement on existing 4 in. Asphalt concrete pavement	30	3
5–25	1. Preventive maintenance at 5 years interval	10	1
30	1. Clean and seal all longitudinal joints, including shoulders. 2. Clean and seal all transverse joints 3. 15% crack sealing 4. 2 in. Asphalt concrete overlay	10	1
40	1. 1 in. mill of concrete surface 2. 4 in. Asphalt concrete overlay	20	2
Total number of structural life (Yrs)		60	

Agency Cost

Table 49 shows the estimate of each activity for all alternatives. The cost include price of materials and man force used for rehabilitation and maintenance activity along with traffic control costs, engineering costs, and all incidental costs for 1 mile of pavement section. These costs were expressed using normal distribution by providing the mean and standard deviation of each activity.

Table 49. Agency Cost Input Values.

Activity	Year	Cost (1 mi length) in US dollars	
		Mean	Standard Deviation
Alternative 1: 10" JPCP pavement over existing asphalt pavement with periodic (short-term) rehabilitation plan			
New overlay construction	0	1,386,690	138,669
Rehab No. 1	10	14,520	1,452
Rehab No. 2	20	199,210	19,921
Rehab No. 3	30	295,750	29,575
Rehab No. 4	40	423,330	42,33
Alternative 2: 10" JPCP pavement over existing asphalt pavement with long-term rehabilitation plan			
New overlay construction	0	1,386,690	138,669
Rehab. 1	25	315,060	315,06
Rehab. 2	40	820,850	82,085
Alternative 3: 10" CRCP pavement over existing asphalt pavement with short-term rehabilitation plan			
New overlay construction	0	2,975,540	297,554
Rehab No. 1	15	14,520	1452
Rehab No. 2	30	197,560	19,756
Rehab No. 3	40	316,630	31,663
Alternative 4: 10" CRCP pavement over existing asphalt pavement with long-term rehabilitation plan			
New overlay construction	0	2,975,540	297,554
Rehab No. 1	30	224,830	22,483
Rehab No. 2	40	417,320	41,732

Work Zone User Costs

The user cost is assessed for all activity including the newly installed overlays. For the new constructed overlays and rehabilitation activities, specific work zone hours and closure was assumed as follows for all activities. The difference between activities period was changed uniformly by specifying minimum and maximum number of days required to accomplish the activity during the below day times. PCC construction and rehabilitation work zone timing: 10 a.m. to 5 p.m. (inbound) and 6 a.m. to 3 p.m. (outbound).

Additionally, the following inputs are required to each activity to conduct analysis using RealCost 2.5. For the purpose of comparison, these inputs do not have significant impact on the LCCA analysis of alternative over another. Thus, all of them are assumed:

- Free flow capacity—720 vehicles per hour per lane (vphpl) (Assumed).
- Queue dissipation capacity—620 passenger cars per lane per hour (assumed).
- Maximum AADT (2-way)—250,000 vpd (assumed).
- Maximum queue length—10 mi (assumed based on distance to upstream detour exit).
- Work zone capacity—500 vphpl (assumed based on the queue dissipation capacity of each lane).

LCCA OUTPUTS

The LCCA results are represented using deterministic and probabilistic results. In the deterministic analysis, inputs such as discount rate, rehabilitation service life, agency cost, and user cost were taken as constant values. On the other side, probabilistic analysis was used to account for variability in the discount rate, agency and user's cost throughout the analysis period. To account for this variability, normal probability distribution was executed as an analysis output by assigning mean and standard deviation for different inputs such as discount rate and agency cost.

Deterministic Results

Table 50 and Figure 136 show the deterministic results of the LCCA. In this table, results are represented as the NPV and the equivalent uniform annual cost (EUAC). The table shows the JPCP and CRCP alternatives that agency can chose for concrete pavement overlay. As a reminder, the main parameter in this LCCA is the frequency of maintenance activities not the pavement type. Thus, the comparison should be made between alternatives of same pavement type overlay. As indicated in the table, alternative 1, which incorporates a short-term rehabilitation plan for JPCP has lower NPV in terms of agency cost than alternative 1. On the other side, user cost in alternative 1 is higher than alternative 2 due to the higher frequency of maintenance activities that affect user cost increase. However, the user cost can be reduced using other traffic solutions and techniques during maintenance activities. As the differences are not substantial, the benefit to cost (B/C) ratio can be the way to confirm the best option. The benefit can be defined as how long the pavement service life is extended after the application of the last rehabilitation. The B/C ratio can be calculated by dividing the benefit, which depends on AUPC, AADT, and roadway length over the NPV. As alternative 1 incorporates more maintenance activities, the AUPC can be significantly higher than AUPC in alternative 2. This might yield into a higher B/C ratio in alternative 1 than alternative 2 because the NPVs for both alternatives are almost the same. After all, available budgets dictate the best option for overlay design.

In case of CRCP, alternative 3 that uses a short-term maintenance plan shows lower NPV than alternative 4, which uses long-term maintenance plan. Due to the presence of no significant differences in NPV, the B/C ratio is also applicable in this case as well. However, as alternative 3 experiences more maintenance activities, the B/C ratio is most probably will confirm the decision of choosing alternative 3 for CRCP overlay.

Table 50. Summary of Deterministic Results.

Total Cost	Alternative 1		Alternative 2		Alternative 3		Alternative 4	
	Agency Cost ($1000)	User Cost ($1000)	Agency Cost ($1000)	User Cost ($1000)	Agency Cost ($1000)	User Cost ($1000)	Agency Cost ($1000)	User Cost ($1000)
Undiscounted Sum	$2,319.50	$29,803.34	$2,657.60	$28,220.63	$3,504.25	$29,815.99	$3,682.69	$28,220.63
Present Value	$1,759.41	$20,596.49	$1,852.69	$18,583.93	$3,163.32	$19,608.40	$3,213.55	$18,063.84
EUAC	$63.57	$744.21	$66.94	$671.49	$114.30	$708.51	$116.11	$652.70

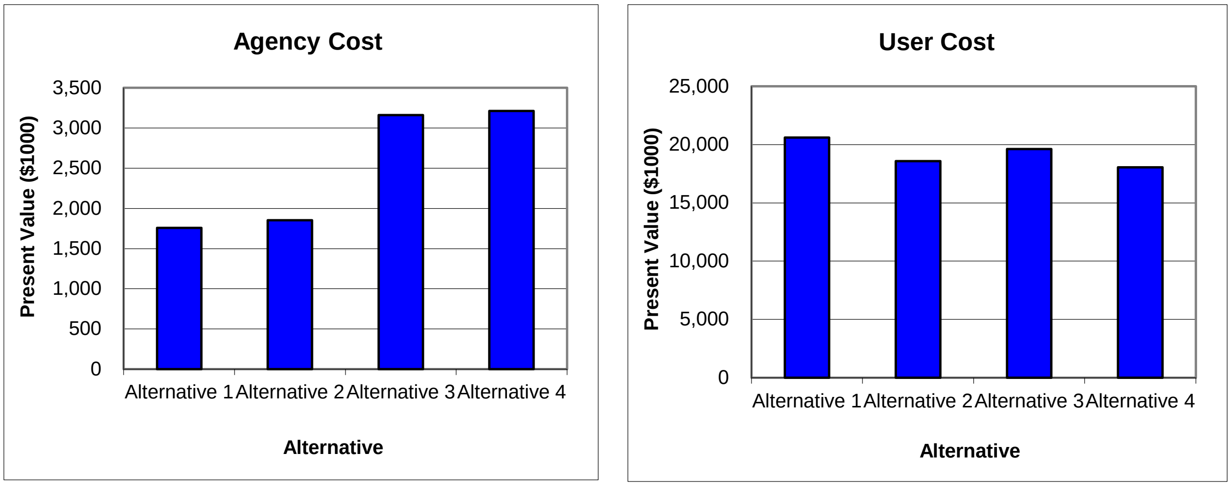

Figure 136. Agency and User Cost for All Alternatives.

Probabilistic Results

The probabilistic analysis considers the change in the discount rate, agency cost, and user cost. In addition, minimum and maximum timeframes were considered to determine work zone duration of the user's cost. Results of probabilistic analysis in terms of agency and user cost are presented in Table 51. As shown in the table, the NPV statistics are summarized by indicating the mean, standard deviation, maximum, and minimum for each alternative for agency and user cost. Figure 137 to Figure 140 summarize the probability distribution and cumulative probability distribution for agency and user cost for each alternative. As discussed before, the JPCP overlay alternatives (i.e., alternatives 1 and 2) should be compared separately as the initial cost of CRCP overlay alternatives 3,4 is much higher than JPCP overlay alternatives.

The probabilistic results show that the agency cost of alternative 1, which follow short-term maintenance procedure, is lower than agency cost of alternative 2 (long-term maintenance procedure). This means that alternative 1 can be a good potential to reduce the agency cost and increase the performance level of the applied overlays. User cost is much higher in alternative 1 than alternative 2. However, other traffic solutions can be applied to reduce the total user cost throughout the analysis period.

In the CRCP alternatives, the agency cost for alternative 3 (short-term maintenance procedure) is lower than alternative 4 (long-term maintenance procedure), which confirms the idea of that applying periodic CPR can increase the performance level of concrete overlay and reduce the agency cost of applied rehabilitation activities.

Table 51. Summary of Probabilistic Results.

Total Cost (Present Value)	**Alternative 1**		**Alternative 2**		**Alternative 3**		**Alternative 4**	
	Agency Cost ($1000)	User Cost ($1000)	Agency Cost ($1000)	User Cost ($1000)	Agency Cost ($1000)	User Cost ($1000)	Agency Cost ($1000)	User Cost ($1000)
Mean	$1,765.19	$20,678.04	$1,862.59	$18,697.98	$3,166.52	$19,646.77	$3,220.20	$18,151.29
Standard Deviation	$89.08	$2,351.49	$185.82	$2,186.57	$52.33	$2,335.99	$72.85	$2,197.99
Minimum	$1,538.68	$14,694.91	$1,240.19	$12,781.55	$3,052.18	$13,685.40	$3,057.27	$11,890.75
Maximum	$2,186.92	$31,001.54	$2,540.15	$27,905.29	$3,392.09	$28,172.54	$3,629.44	$27,024.97

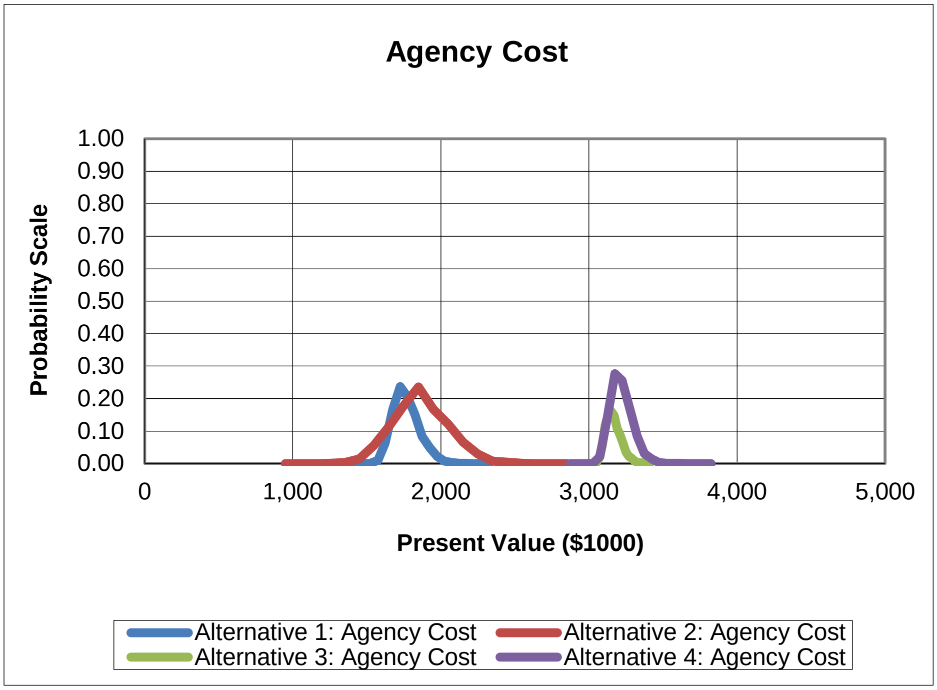

Figure 137. Probability Distribution of Agency Costs—Rural New Construction.

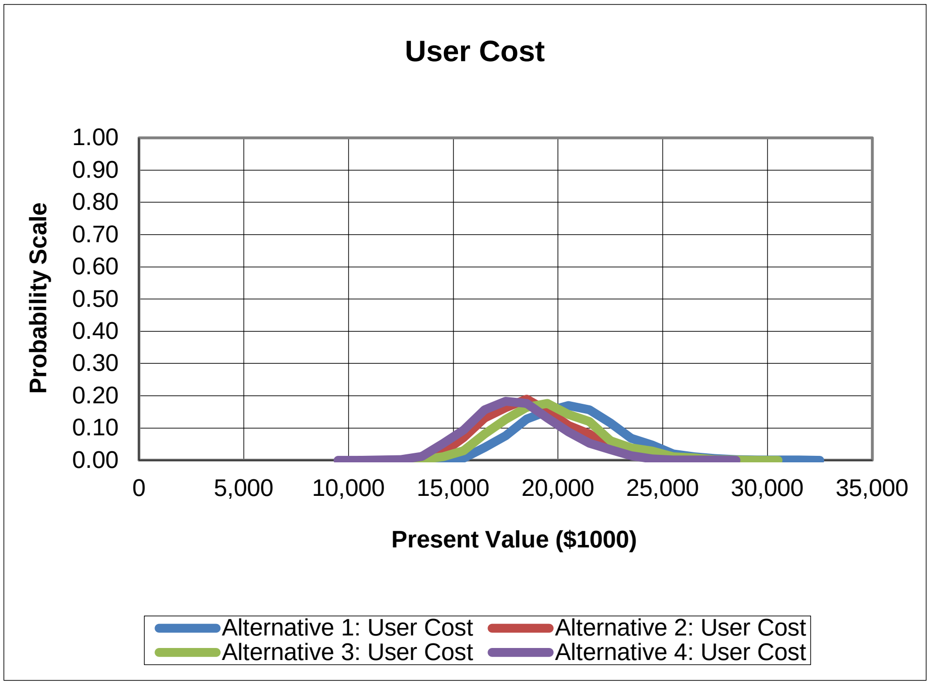

Figure 138. Probability Distribution of User Costs—Rural New Construction.

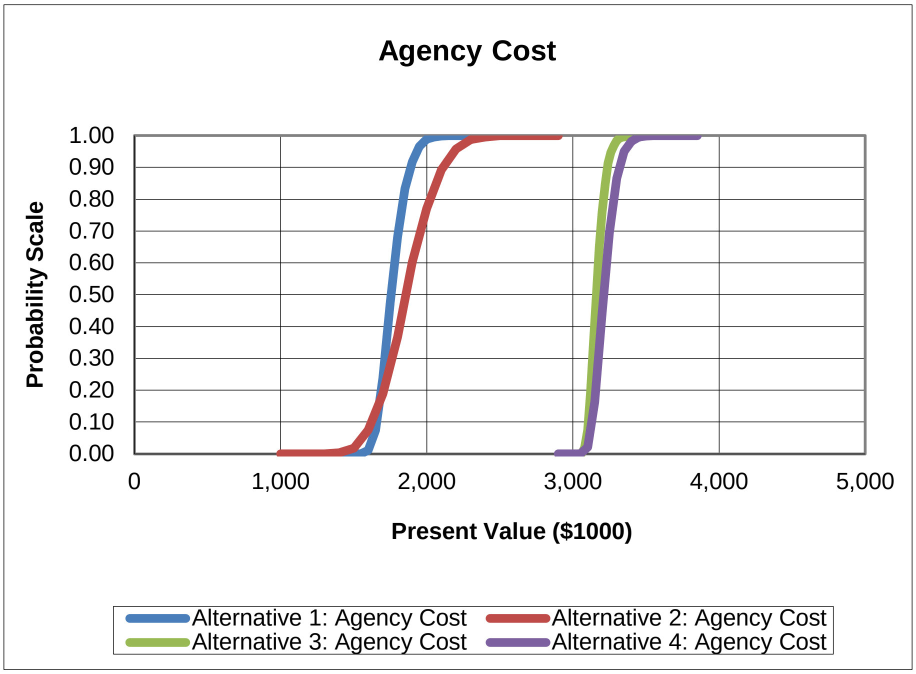

Figure 139. Cumulative Probability Distribution of Agency Costs—Rural New Overlay.

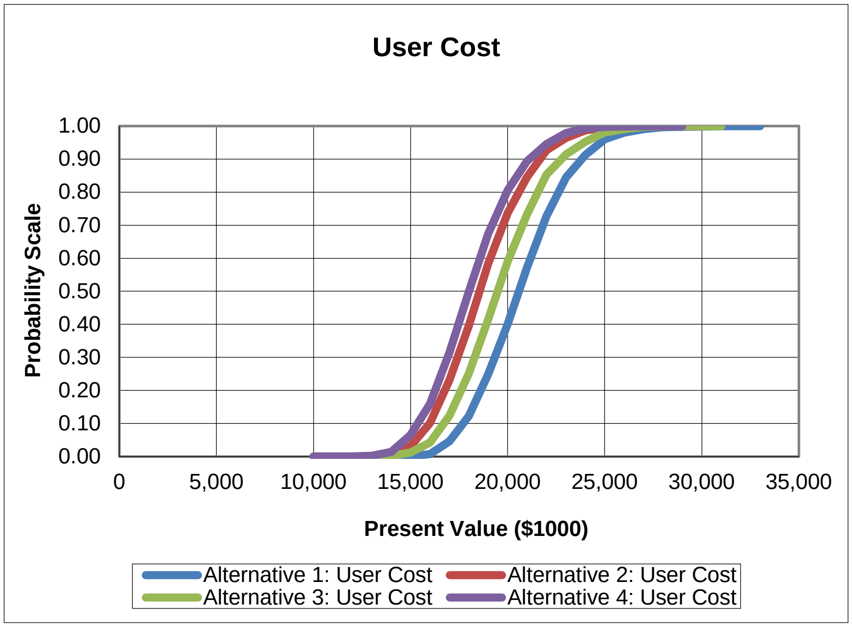

Figure 140. Cumulative Probability Distribution of User Costs—Rural New Overlay.

APPENDIX A. METHOD OF STRUCTURAL ASSESSMENT

Field evaluation of RCC pavement focuses on the behavior of the performance of the cracks in terms of slab deflections and deflection load transfer efficiency (LTE_{δ}). FWD test results provides a primary way of characterizing in-place conditions. Results of FWD testing may be described in part for the plate deflection (D_o) and the LTE. LTE may be defined as the deflection on the unloaded side of the crack divided by the deflection on the loaded side of the crack:

$$\text{LTE }\% = \frac{\delta_u}{\delta_L} * 100 \qquad 54$$

Where,

δ_u = unloaded deflection.

δ_L = loaded deflection.

The LTE of a joint or crack has an important effect on the composite stiffness manifested by a concrete pavement, and therefore on the level of stress developed in the pavement structure.

When a load is placed on a rigid pavement, particularly across a crack, the slabs on either side of the crack will deflect in the form of a basin. The deflected shape of the basin is a function of several variables, including the thickness and stiffness of the slab, the stiffness of the underlying materials (which is indirectly affected by the interlayer bond or frictional resistance), and the magnitude of the load. Other factors that affect the shape of the basin area are the thickness and types of subbase materials, nature of load transfer devices, the texture of the aggregate interlock, and the magnitude of joint openings.

Basin area gives an indication of the deflection profiles measured using FWD, and may be calculated from sensor deflections as (*15*):

$$\text{Area} = \left(\frac{12}{2 * D_o}\right)[D_o + 2\{D_1 + D_2 + \ldots\ldots.. D_{n-1}\} + D_n] \qquad 55$$

Where,

Area = basin area, in.

D_i = measured sensor deflection.

n = number of sensor (at 0.3m [12 in.] spacing) on one side of load plate minus one.

This area concept combines all measured deflections in the basin into a single parameter. The area being determined is essentially ½ of the cross sectional area of the deflection basin taken through the center of the load. Each deflection reading is normalized for the maximum deflection D_o. Thus the basin area has the units of length and is a function of the number and location of the sensors. For any given sensor arrangement, a relationship between the basin area and the radius of relative stiffness (P) exists in concept as illustrated in Figure 141.

A concrete pavement slab deforms under load depending upon the position, magnitude, and area of contact of the load on the pavement surface. The resistance to deformation depends upon the stiffness of the supporting medium, the pavement thickness, opening of the joint or crack, and the interlayer bond. One parameter that characterizes this combined resistance to deformation is called the radius of relative stiffness (P) and it depends upon the above characteristics. This relative stiffness is defined by the following equation:

$$\ell = \sqrt[4]{\frac{Eh_c^{\ 3}}{12(1-\nu^2)k}} = \sqrt[4]{\frac{D_c}{k}} \qquad 56$$

Where,

E_c = concrete modulus of elasticity (FL^{-2}).
h_c = slab thickness (L).
ν = poisson’s ratio.
k = foundation modulus (FL^{-3}).

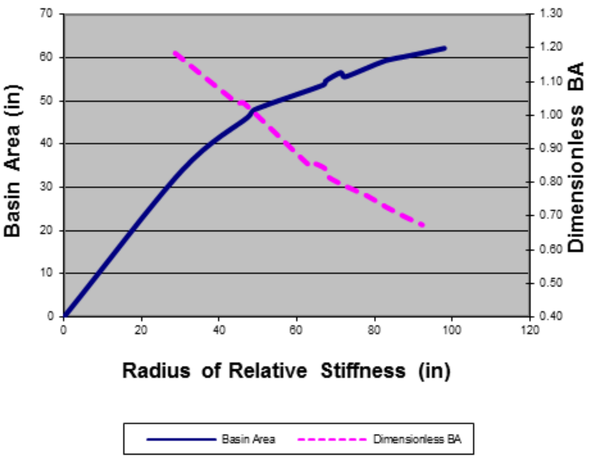

Figure 141. Variation of Deflection Basin Area with P (*16*).

SLAB THICKNESS AND INTERLAYER FRICTION STIFFNESS CONSIDERATIONS

Slab thickness and interlayer friction are components that have an indirect, yet important effect on slab stiffness particularly in the vicinity of a joint that can be demonstrated through consideration of slab bending behavior. This is accomplished through the application of theoretically sound, mechanistic structural evaluation concepts to slab behavior in the vicinity of a joint or crack. A rational characterization of this nature allows for consideration of the degree of bond or interlayer friction while under load on the overall joint stiffness.

There are two different extremes that will arise when considering friction effects on slab stiffness. The slab interface friction condition may range from bonded to unbonded. In the analysis of this range, the subbase is considered to be a part of the pavement system rather than part of the pavement support. Two-layer analysis may be used for an unbonded condition, whereas in a bonded slab each layer is combined as one equivalent layer. In both cases the layers are combined to form a composite, single layer thickness.

The composite bending moment (M_e) in a slab at the vicinity of a joint is the sum of the bending moment in the concrete layer (M_1) and the subbase layer (M_{base}). Medium-thick plate theory suggests that the maximum bending stress (σ_c) in the concrete layer is:

$$\sigma_c = 6\frac{M_e}{h^3{}_{e-p}} h_c \tag{57}$$

where

$$h^3{}_{e-p} = \ell_m^4 12(1-\upsilon^2)\frac{k}{E_c} \tag{58}$$

and
σ_m = radius of relative stiffness corresponding to the basin area measured at the slab edge or corner across the joint.

The parameter σ_m is obtained from the calculated basin area relation such as that shown in Figure 141. It is argued that P_m actually represents an in-place pavement stiffness at a crack as affected by the measured LTE and the effective interlayer bond exhibited by the pavement structural response. As such, the P_m term can represent a partially bonded, composite slab thickness (h_{e-p}) and may be determined or associated with P_m as noted above. The partially bonded condition between the slab and subbase is created by a certain amount of slippage due to frictional restraint that is allowed to occur under load, but still makes a contribution to the load transfer or the stiffness at a joint. This restraint is also formulated relative to the degree of bonding (x – a parameter that ranges between zero and 1.0) as:

$$h_{e-p} = \left(1-x\right)h_{e-u} + \left(x\right)h_{e-b} \tag{59}$$

Equation 56 can be rearranged to solve for the degree of bonding as:

$$x = \frac{h_{e-p} - h_{e-u}}{h_{e-b} - h_{e-u}} \tag{60}$$

The value of h_{e-p} will vary between the conditions of unbonded to bonded, depending of course upon the degree of bond. The composite or effective thickness for fully bonded layers is (*17*):

$$h_{e-b} = \left\{ h_1^3 + \frac{E_2}{E_1} h_2^3 + 12 \left[\begin{array}{l} \left(x_{na} - \frac{h_1}{2} \right)^2 h_1 \\ + \frac{E_2}{E_1} \left(h_1 - x_{na} + \frac{h_2}{2} \right)^2 h_2 \end{array} \right] \right\}^{1/3} \quad ; \; x_{na} = \frac{E_1 h_1 \frac{h_1}{2} + E_2 h_2 \left(h_1 + \frac{h_2}{2} \right)}{E_1 h_1 + E_2 h_2} \qquad 61$$

Effective thickness for unbonded layers: $h_{e-u} = \left[\left(h_1^3 + \frac{E_2}{E_1} h_2^3 \right) \right]^{1/3}$

Where,
E_c = Elastic modulus of the PCC layer (FL^{-2}).
h_{e-b} = Effective thickness of the bonded PCC layer (L).
h_{e-u} = Effective thickness of the unbonded PCC layer (L).
υ = Poisson’s ratio.
k = Foundation modulus (FL^{-2}/L).
E_1 or E_2 = Elastic modulus for layer 1 or 2 (FL^{-2}).
h_1 or h_2 = Thickness for layer 1 or 2 (L).
ℓ = Radius of relative stiffness (L).

Figure 142 depicts the relationships between the partially bonded and unbonded effective thicknesses and stresses; using simple proportioning, the effective partially bonded stress (σ_{e-p}) can be found as (*18*):

$$\sigma_{e-p} = \sigma_e \left[\frac{2h_{e-u}}{h_{e-p}} - 1 \right] \qquad 62$$

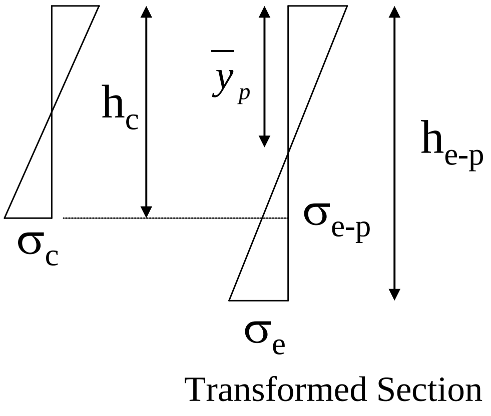

Figure 142. Stress Pattern of Unbonded and Partially Bonded Transformed Section of a Concrete Slab (*18*).

To formulate a relationship to the interlayer friction coefficient (μ), the effective partially bonded stress ($\sigma_{e\text{-}p}$) is equated to the difference between the unbonded stress ($\sigma_{e\text{-}u}$) and the frictional stress (τ) at the bottom of the slab as:

$$\sigma_{e-p} = \sigma_{e-u} - \tau = \frac{s_{e-u}P}{h_{e-u}} - \mu\left[\frac{h_c}{12} + \sigma_v\right] \qquad 63$$

Equations 62 and 63 can be rearranged to develop an expression for μ to be determined from FWD data as:

$$\mu = \frac{\sigma_{e-u} - \sigma_e\left[\dfrac{2h_{e-u}}{h_{e-p}} - 1\right]}{\dfrac{h_c}{12} + \sigma_v} \qquad 64$$

Where,

σ_e = $\frac{s_e P}{h_e^2}$; $s_e = a + b\ell_e + c\ell_e^2$ (for FWD plate loading) .

s_e = Dimensionless stress (for the composite pavement section).

P = Applied FWD load (F).

a, b, c = 0.0006, 0.0403, and −0.0002 (for FWD plate loading).

h_c = Concrete slab thickness (L).

σ_v = Load induced vertical pressure (FL^{-2}) (≈ 0.7 psi).

The interlayer frictional restraint is determined from the difference between the stress at the bottom of concrete layer ($\sigma_{e\text{-}u}$) and the interlayer bond stress (τ_f). The interlayer bond stress is related to the coefficient of friction (μ) between the subbase layer and the concrete layer (where the peak stress (ζ_f) is nominally $\frac{\mu h_c}{12}$ where h_c is in inches). Using the above expressions, the degree of bonding and the interlayer coefficient of friction can be calculated for each FWD testing location; sample results shown in Figure 143 suggesting functionally how the degree of bonding is related to the coefficient of friction (μ) through:

$$x = e^{-\left(\frac{A}{\mu}\right)^B} \qquad 65$$

Where,

A = $e^{\frac{1.232 - 0.065\mu}{B}}$; B = $-\left(0.039y^2\right)$; y = Ln(μ).

Actual test data indicate that the degree of bonding ranges from 0 to 0.83 but with a high degree of variability. In terms of design, the value of μ varies as of function of the subbase material type (for granular bases μ ≈ 1.5, asphalt concrete bases ≈ 3 to 6, and cement stabilized bases ≈ >15) (*19*). Consequently, since equation

$$\mu = \frac{\sigma_{e-u} - \sigma_e \left[\frac{2h_{e-u}}{h_{e-p}} - 1 \right]}{\frac{h_c}{12} + \sigma_v}$$

64 covers such a broad range of μ it can be used as a design tool to represents a wide range of subbase types.

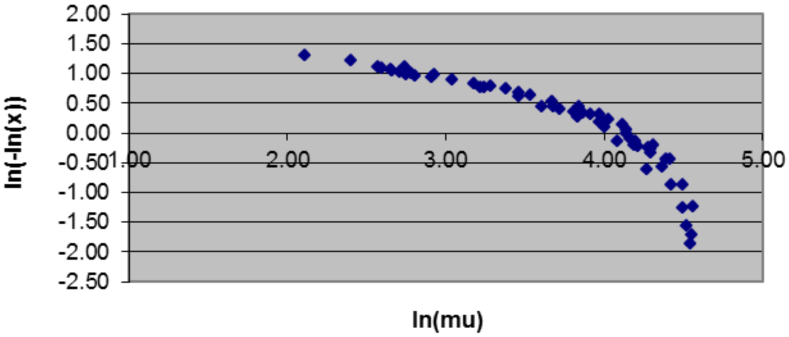

Figure 143. Relationship between Backcalculated Values of μ and Degree of Bond (*18*).

CLIMATIC STRESSES COMPUTATION

Climate stresses is considered one of the main factors of rigid pavement design. In the proposed methodology, unlike PCA method, the temperature and humidity gradients are taken into account to calculate the climatic stresses or the net stresses. These stresses, upon determination, will be added to the wheel load stresses calculated at the edge of the pavement. Note that total stresses will be used to calculate the allowable number of repetition until failure. Thus, the followed strategy ought to achieve safe but yet economic design thickness by considering all type of stresses. The temperature and humidity gradient in pavement can be explained by the following equation:

$$\text{grad}_x = - \left\{ \left(a_1 t + a_2 t^2 + a_3 t^3 \right) \cdot \left\{ \frac{z}{\sqrt{Dt_i}} \right\} - \left(a_1 + 2a_2 t + 3a_3 t^2 \right) \cdot \frac{p}{(1+pz)^2} \cdot \left\{ \frac{1}{2\sqrt{Dt_i}} \right\} \right\} \cdot e^{-z^2} \qquad 66$$

Where,

t = $\frac{1}{1+pz}$.

a_1 = 0.3480242.

a_2 = constant -0.0958798.

a_3 = constant 0.7478556.

p = constant 0.47047.
z = $\frac{h/3}{2\sqrt{Dt_i}}$.
h = slab thickness.
D = Thermal or humidity diffusion coefficient equal to 0.8 ft^2/day for thermal and 0.3 ft^2/day for humidity.
t_i = Cycle period.
a_1 = 0.3480242.
a_2 = −0.0958798.
a_3 = 0.7478556.
p = constant 0.47047.

Temperature Gradient

The following equations explain the calculation for the temperature gradient.

T_{g-x} = Daytime or nighttime temperature gradient per inch.
= $T_{\Delta-x}(grad_T)$.
Δ-x = Daytime or nighttime temperature change.
$T_{\Delta-day}$ = $T_{day} - T_{grd}$.
$T_{\Delta-night}$ = $T_{night} - T_{grd}$.
$T_{=day}$ = Seasonal daytime high temperature.
T_{night} = Seasonal nighttime low temperature.
T_{grd} = Seasonal ground temperature.

Humidity Gradient

The following equations explain the calculation for the temperature gradient.

h_{g-x} = Day or nighttime humidity coefficient gradient per inch.
= $h_{\Delta-x}(grad_h)$.
Δ-x = Daytime or nighttime humidity coefficient change.
$h_{\Delta-day}$ = $h_{day} - h_{grd}$.
$h_{\Delta-night}$ = $h_{night} - h_{grd}$.
h_{day} = Seasonal daytime low humidity coefficient.
= $1 - \left(\frac{rh_{day}}{100}\right)^3$.
rh_{day} = Seasonal daytime low humidity.
h_{night} = Seasonal nighttime high humidity coefficient.

$= 1 - \left(\frac{rh_{night}}{100}\right)^3 .$

rh_{night} = Seasonal nighttime high humidity.

h_{grd} = Seasonal ground humidity.

Net Strain Gradient

ε_{day} = Net daytime strain gradient.

$= \alpha\,(T_{g\text{-}day} - T_{set}) + \varepsilon_{ult\ shr}\, h_{g\text{-}day}$, in micro-strains.

T_{set} = Set temperature gradient.

ε_{night} = Net nighttime strain gradient.

$= \alpha\,(T_{g\text{-}night} - T_{set}) + \varepsilon_{ult\ shr}\, h_{g\text{-}night}$, microstrains.

$\varepsilon_{ult\ shr}$ = 1330 – 970y.

$y = \frac{1}{390 z_s^{-4} + 1}.$

$z_s = \left\{ 0.381\sqrt{f_c^{'}} \left[1.25\sqrt{\frac{a}{c}} + \frac{1}{2}\left(\frac{g}{s}\right)^2 \right] \sqrt[3]{\frac{1+\frac{S}{C}}{\frac{W}{CM}}} \right\} - 12 .$

y, z = Shrinkage parameters.

a/c = Total aggregate/cement ratio.

g/s = Coarse aggregate/cement ratio.

s/c = Fine aggregate/cement ratio (fraction, example about 1.8).

w/c = Water/cement ratio (fraction, example: around 0.42).

$f_c^{'}$ = Compressive strength at 28 days.

ε_{net} = Net climatic strain.

$= \{W_{day}\, \varepsilon_{day} + W_{night}\, \varepsilon_{night}\} h/1000000.$

W_{day} = Daytime weighting (typical value is 0.35).

W_{night} = Nighttime weighting (typical value is 0.30).

Net Climatic Stress

The net climatic stress can be calculated using the following equation:

$$\sigma_{net} = C\,\frac{E_c \varepsilon_{net}}{1-\nu^2} \qquad 67$$

$$C = 1 - \left(\frac{2 \cos \lambda \cos h \, \lambda}{\sin 2\lambda + \sin h \, 2\lambda} \right) \left[\begin{array}{l} (\tan \lambda + \tan h \, \lambda) \cos \frac{y}{\ell\sqrt{2}} \cos h \, \frac{y}{\ell\sqrt{2}} \\ \\ + (\tan \lambda - \tan h \, \lambda) \sin \frac{y}{\ell\sqrt{2}} \sin h \, \frac{y}{\ell\sqrt{2}} \end{array} \right]$$

Where: $y = 0$, $\lambda = \frac{b}{\ell\sqrt{8}}$ and $b = L/2$.

APPENDIX B. PIONEER SITE PHOTOS, PLOTS, AND DATA (JULY 2015)

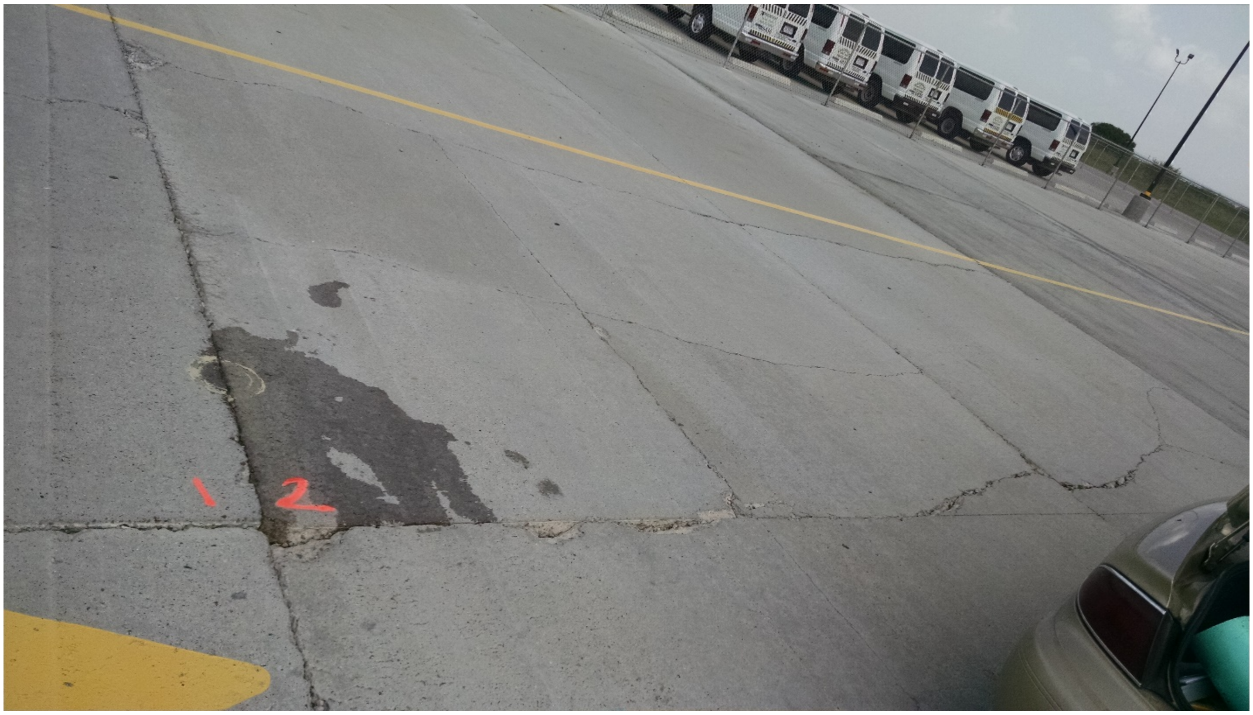

Figure 144. Pioneer Slab Tested.

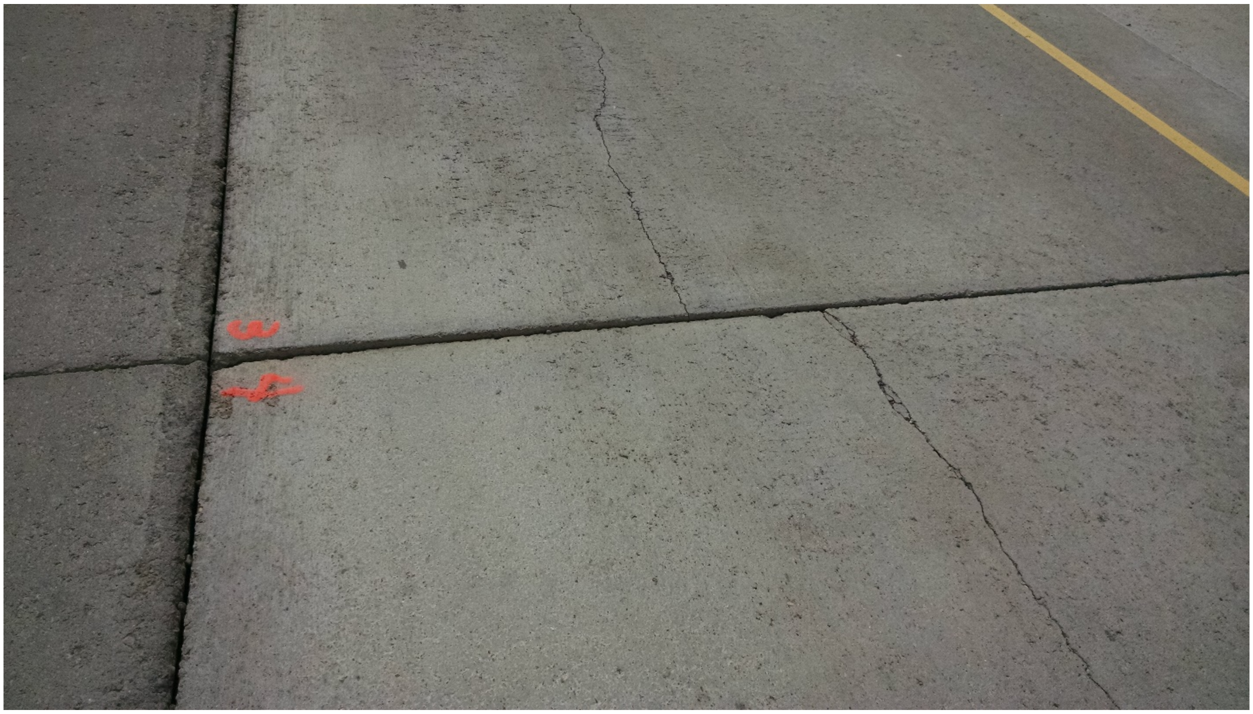

Figure 145. Location 3 and 4 (Joint Separation and Faulting).

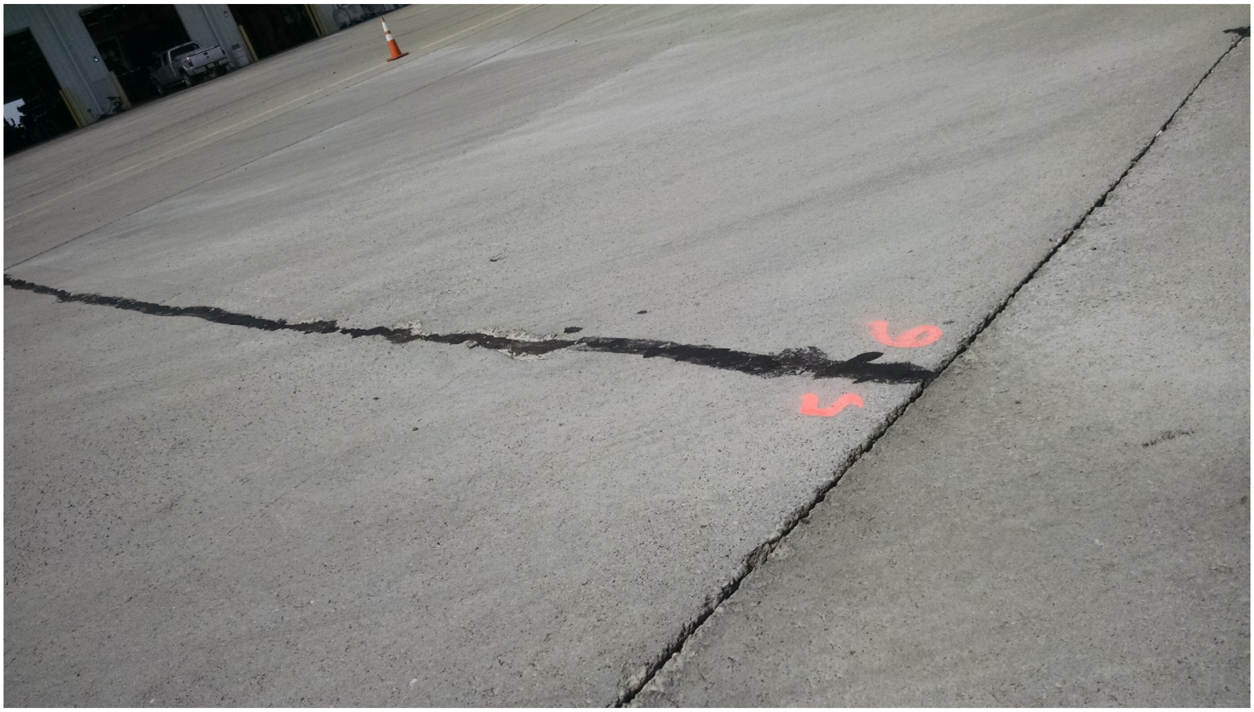

Figure 146. Pioneer Cracked Slab (Repair/Sealed with Asphalt).

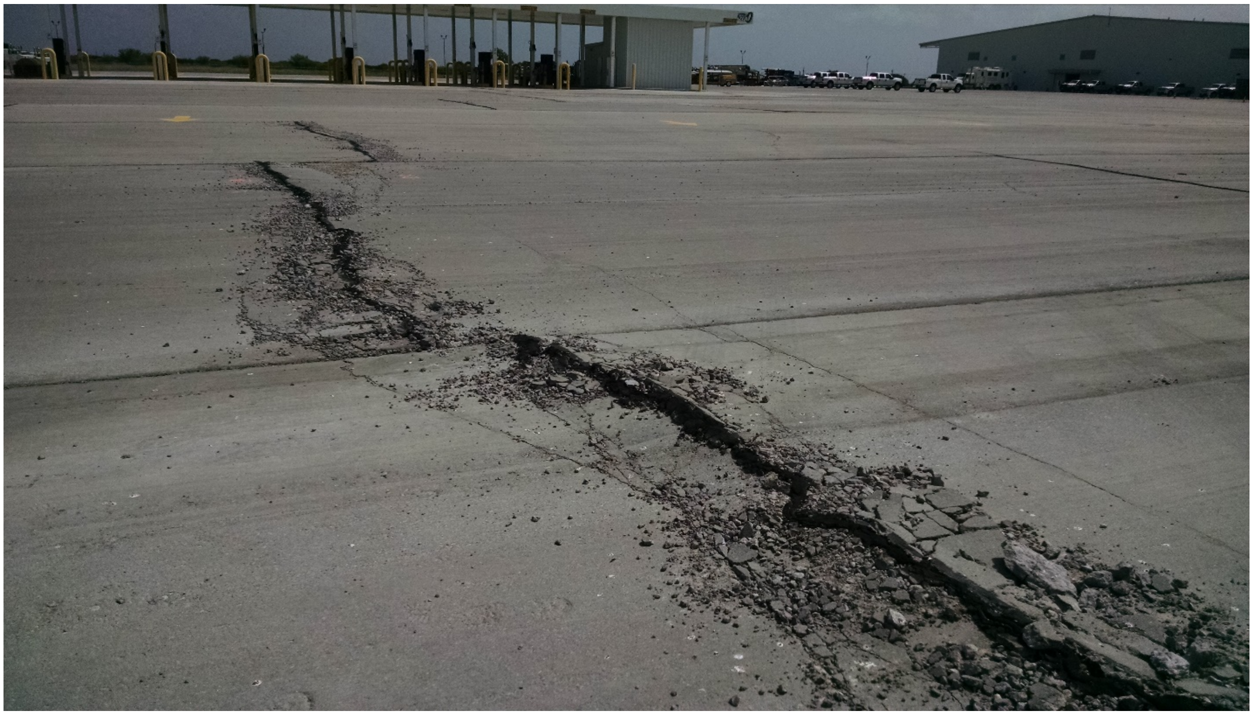

Figure 147. Major Blow-Up Located in the Center of the Property.

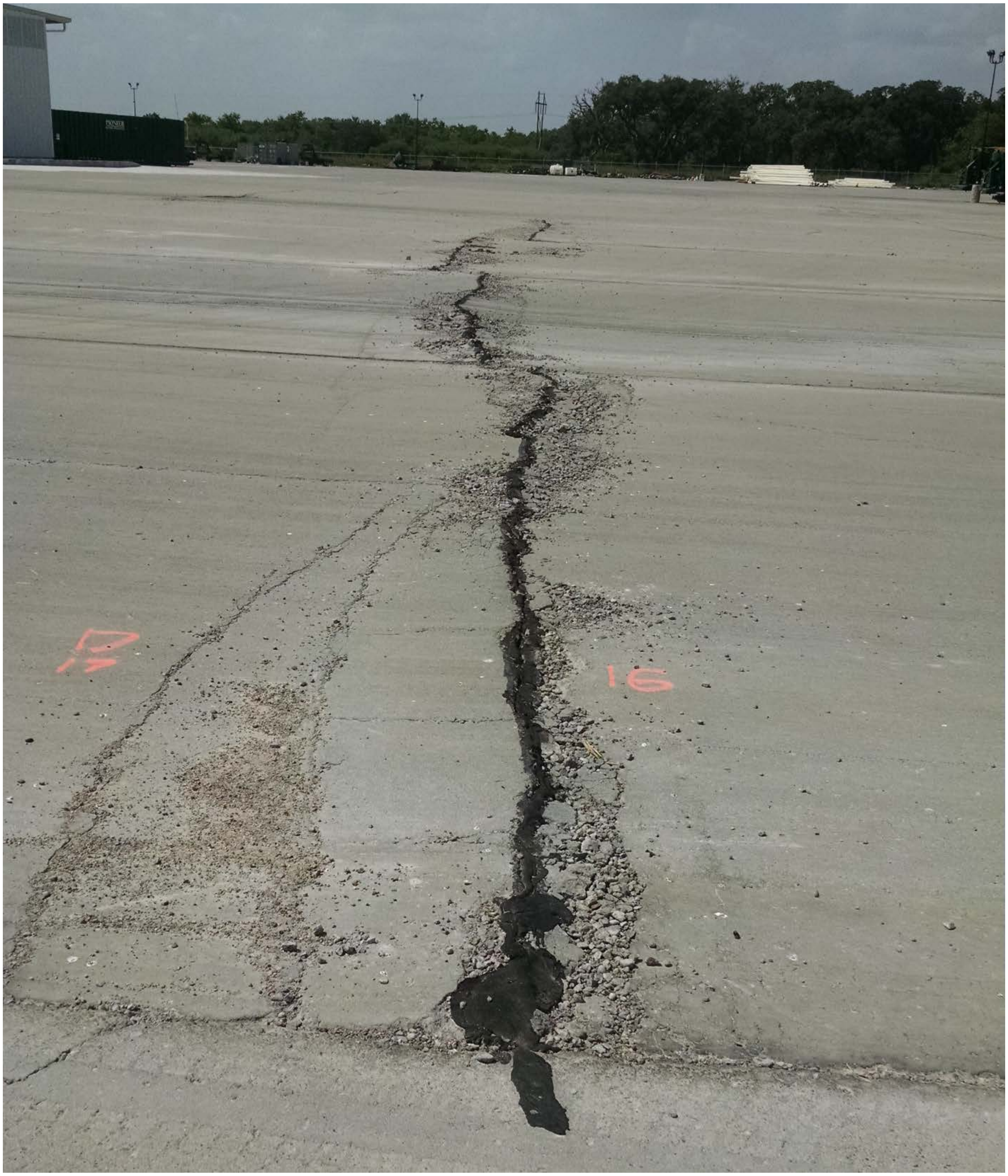

Figure 148. Pioneer Locations 16 and 17 (Major Blow-Up).

APPENDIX C. SEC SITE PHOTOS, PLOTS, AND DATA (JULY 2015)

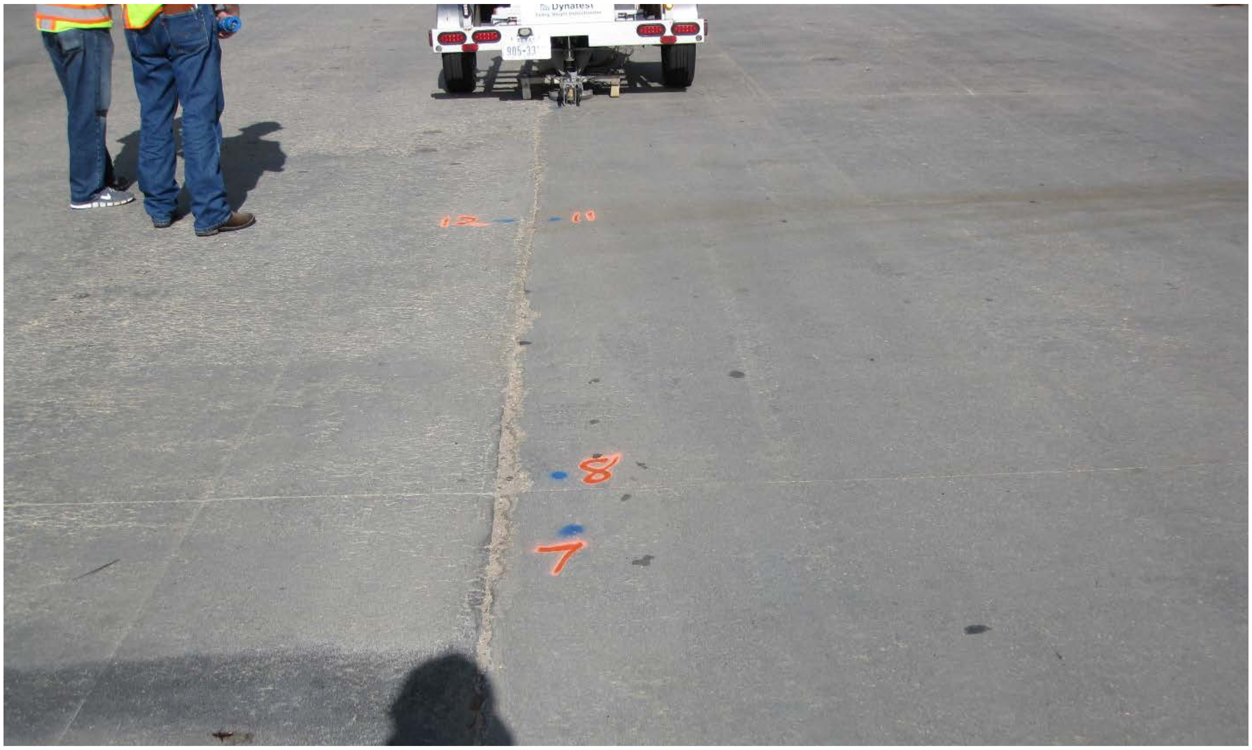

Figure 149. SEC Testing Location 7-12 (July 2015).

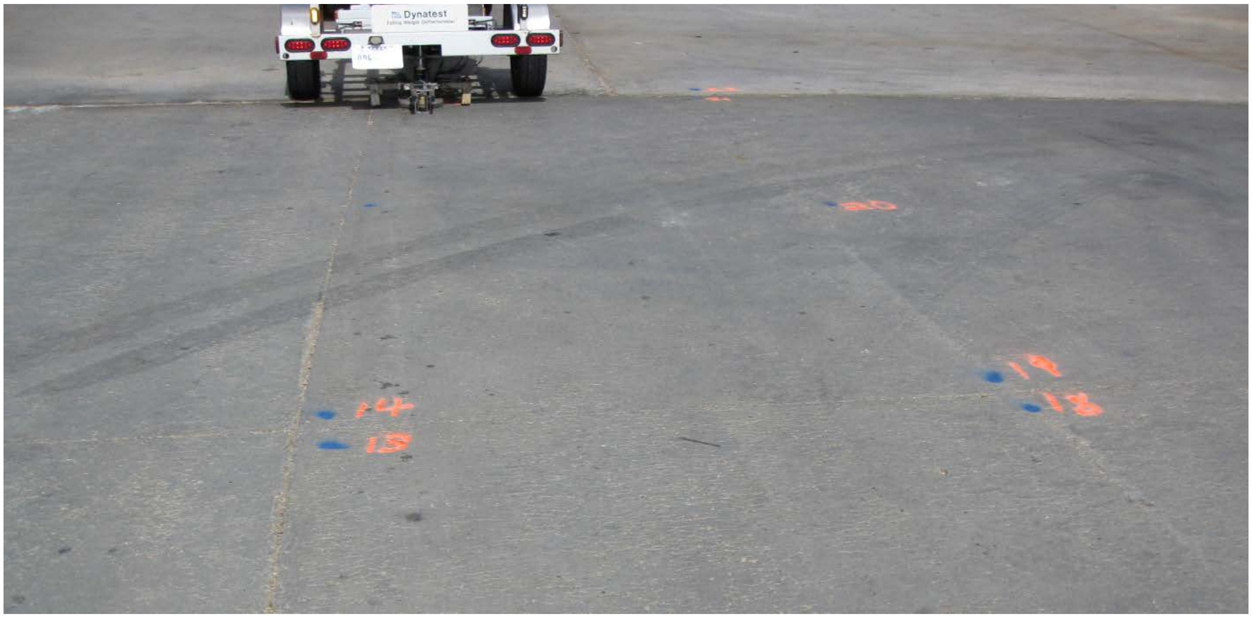
20
14
13
19
18

Figure 150. SEC Testing Locations 13-22 (July 2015).

APPENDIX D. SEC SITE PHOTOS, PLOTS, AND DATA (DECEMBER 2015)

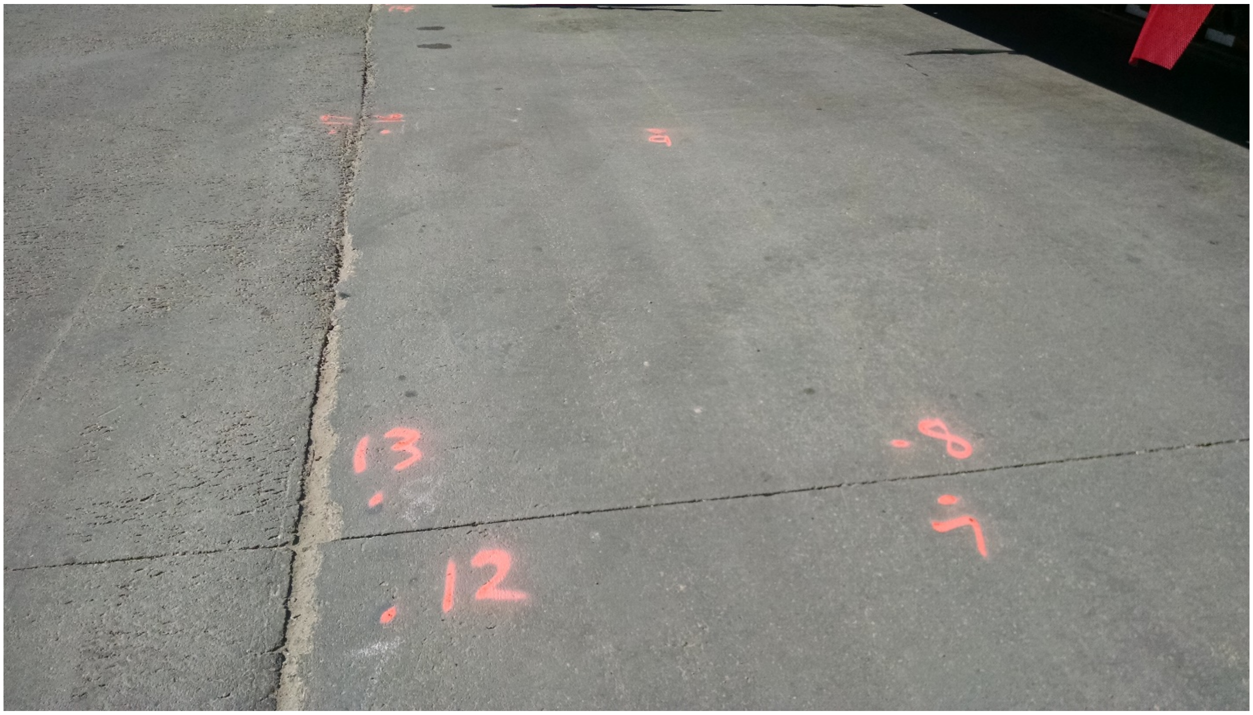

Figure 151. SEC Testing Locations 7-16 (December 2015).

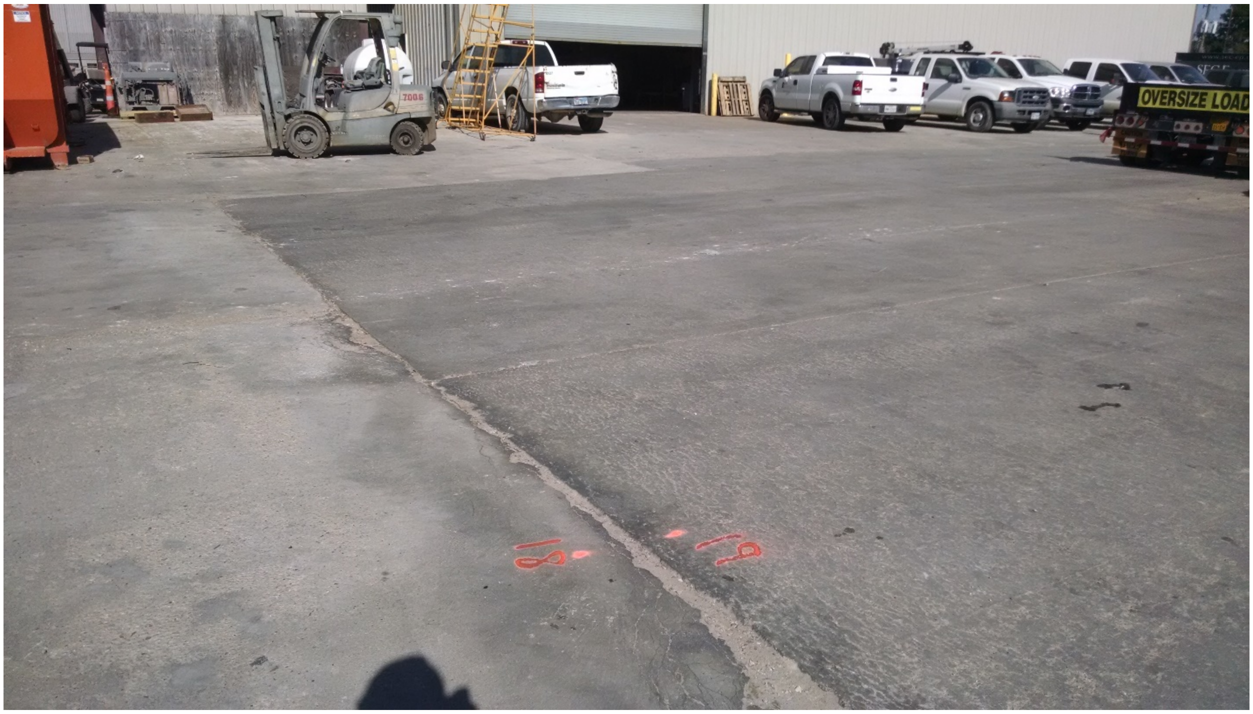

Figure 152. Construction Joint from Transverse to Longitudinal (December 2015).

APPENDIX E. BELLA VISTA SITE PHOTOS, PLOTS, AND DATA (JULY 2015)

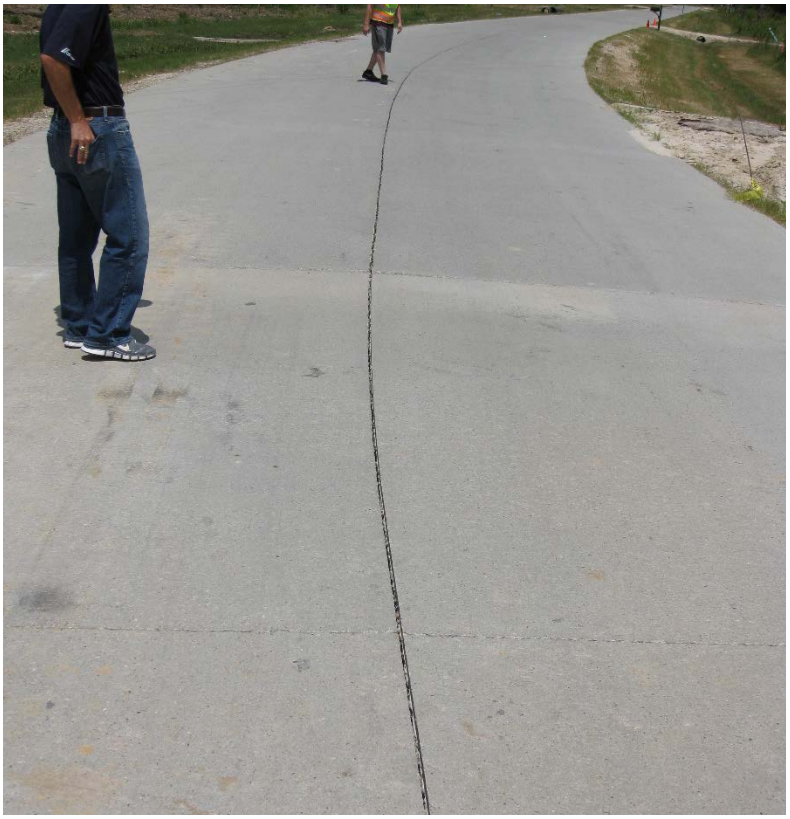

Figure 153. Longitudinal Joint Separation.

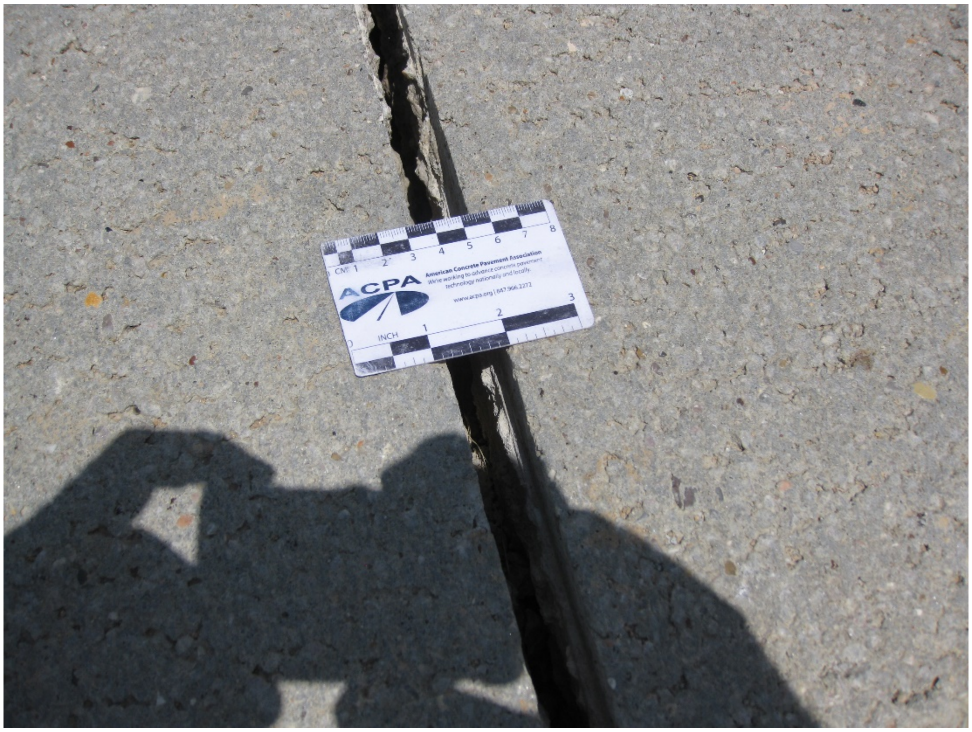
ACPA
American Concrete Pavement Association

Figure 154. Bella Vista Longitudinal Joint Separation (July 2015).

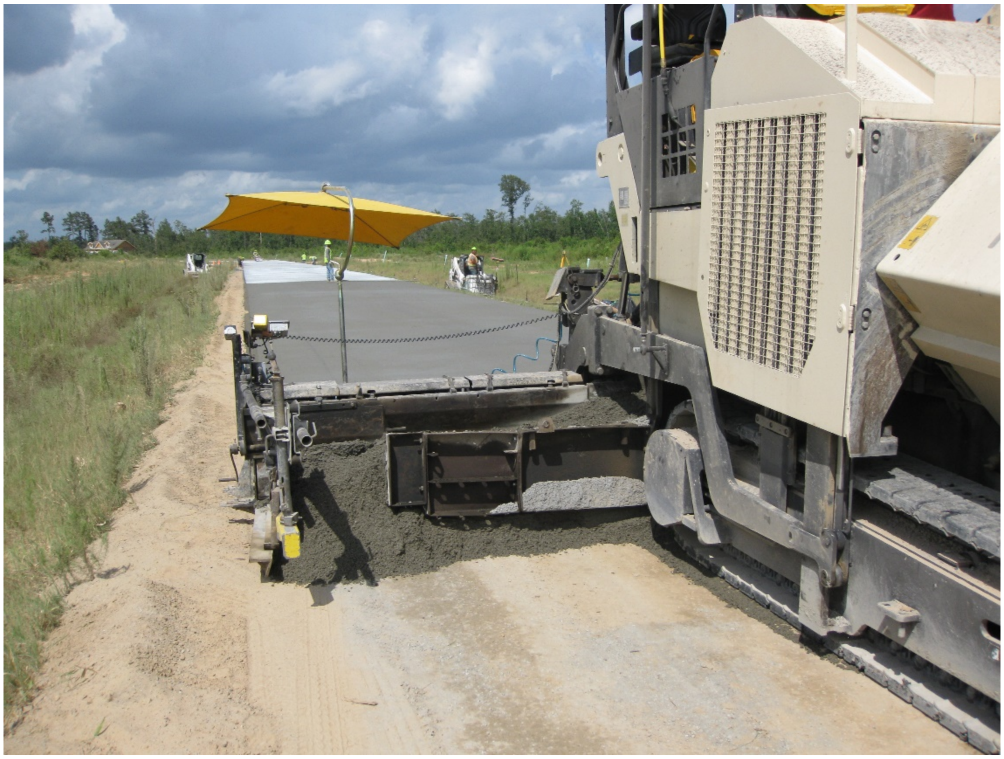

Figure 155. Bella Vista Paving Operation (July 2015).

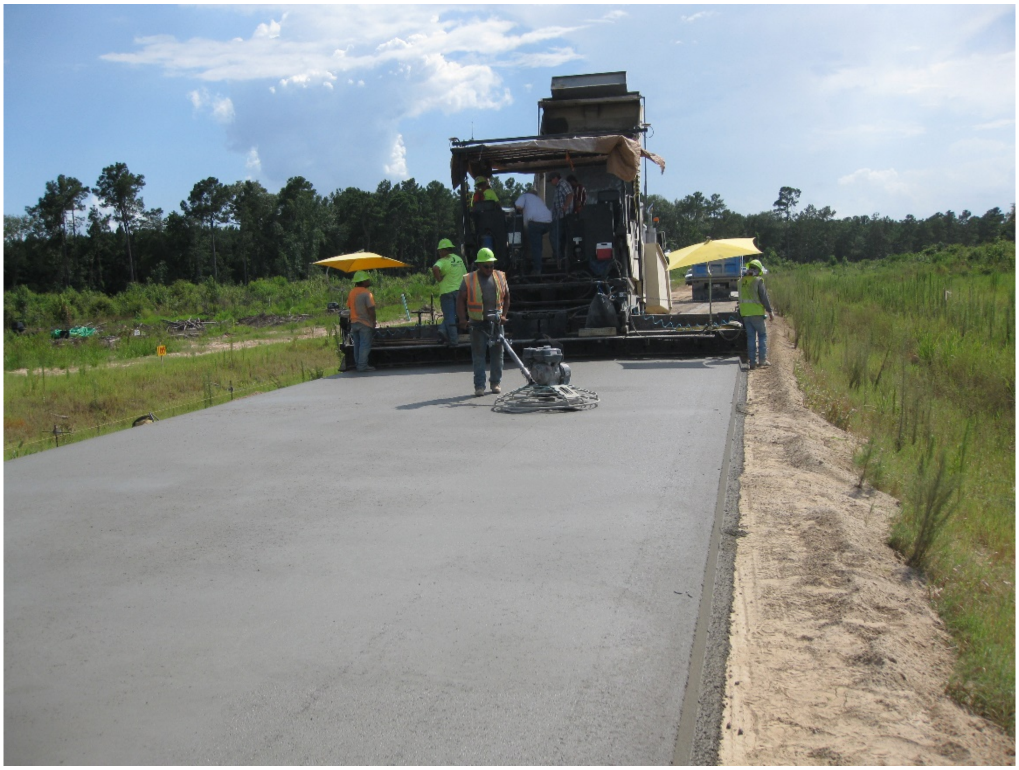

Figure 156. Bella Vista Finishing Operation.

APPENDIX F. BELLA VISTA SITE PHOTOS, PLOTS, AND DATA (DECEMBER 2015)

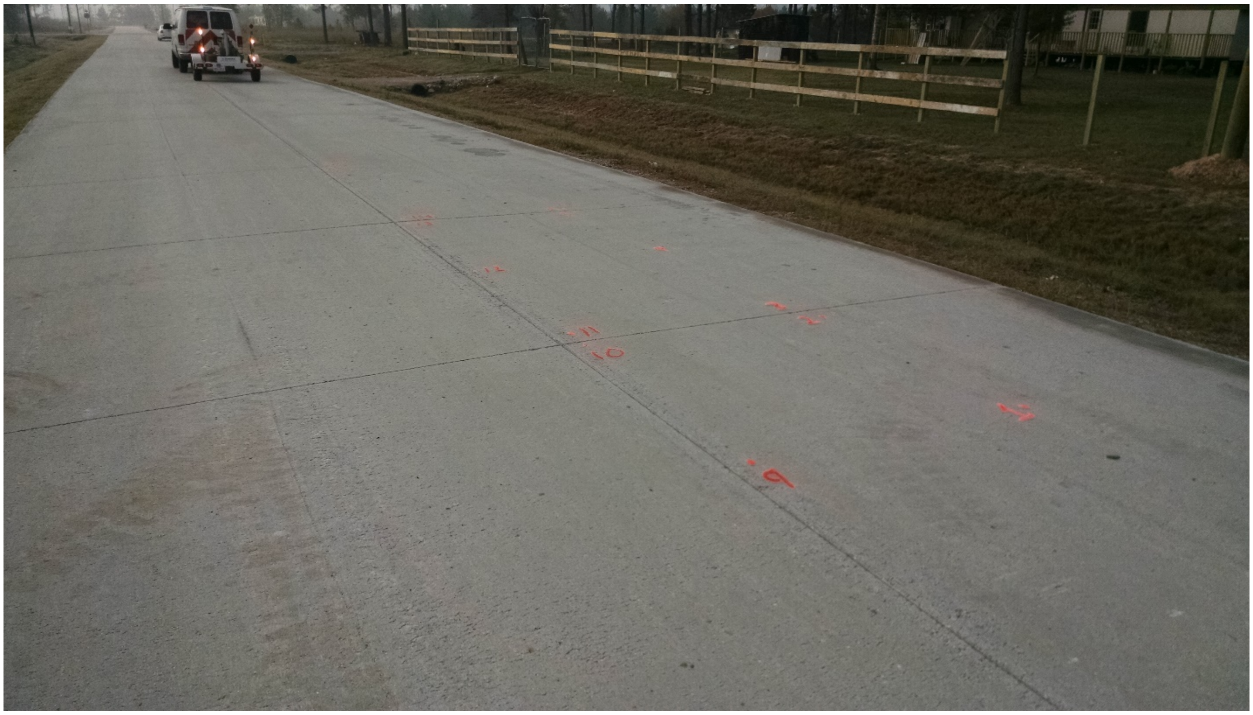

Figure 157. Bella Vista Testing Locations (1-16).

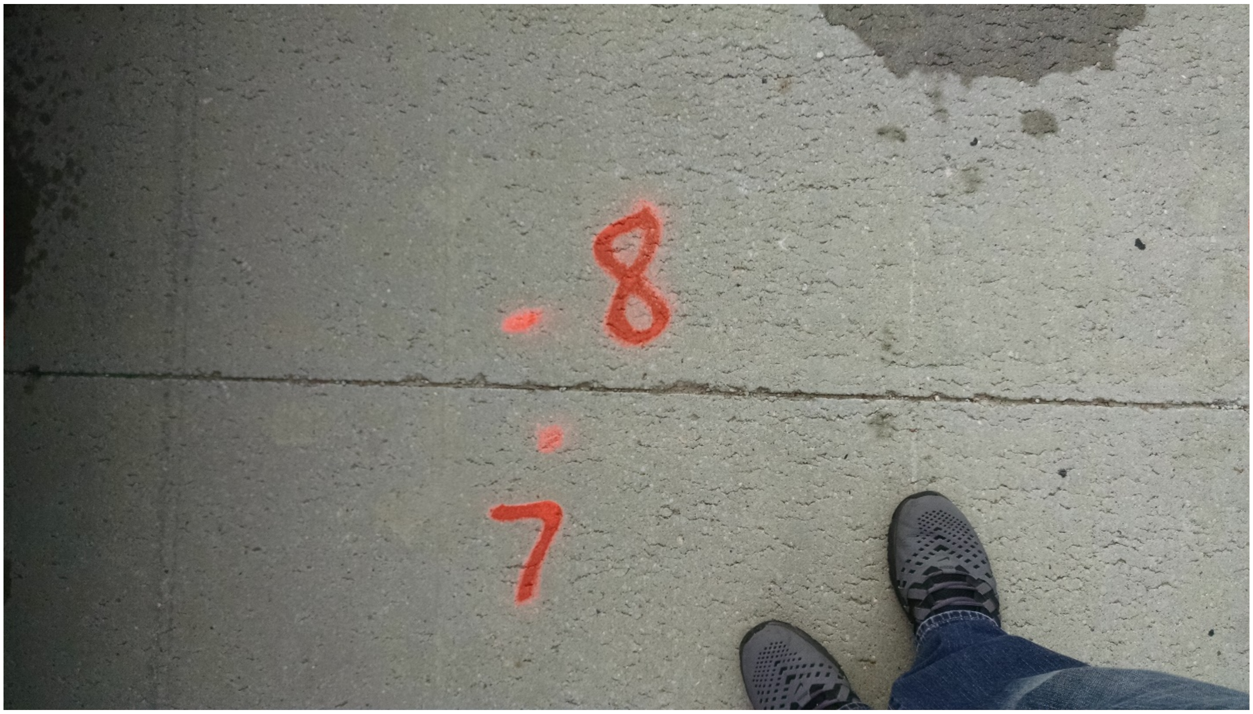

Figure 158. Bella Vista Transverse Joint Tested.

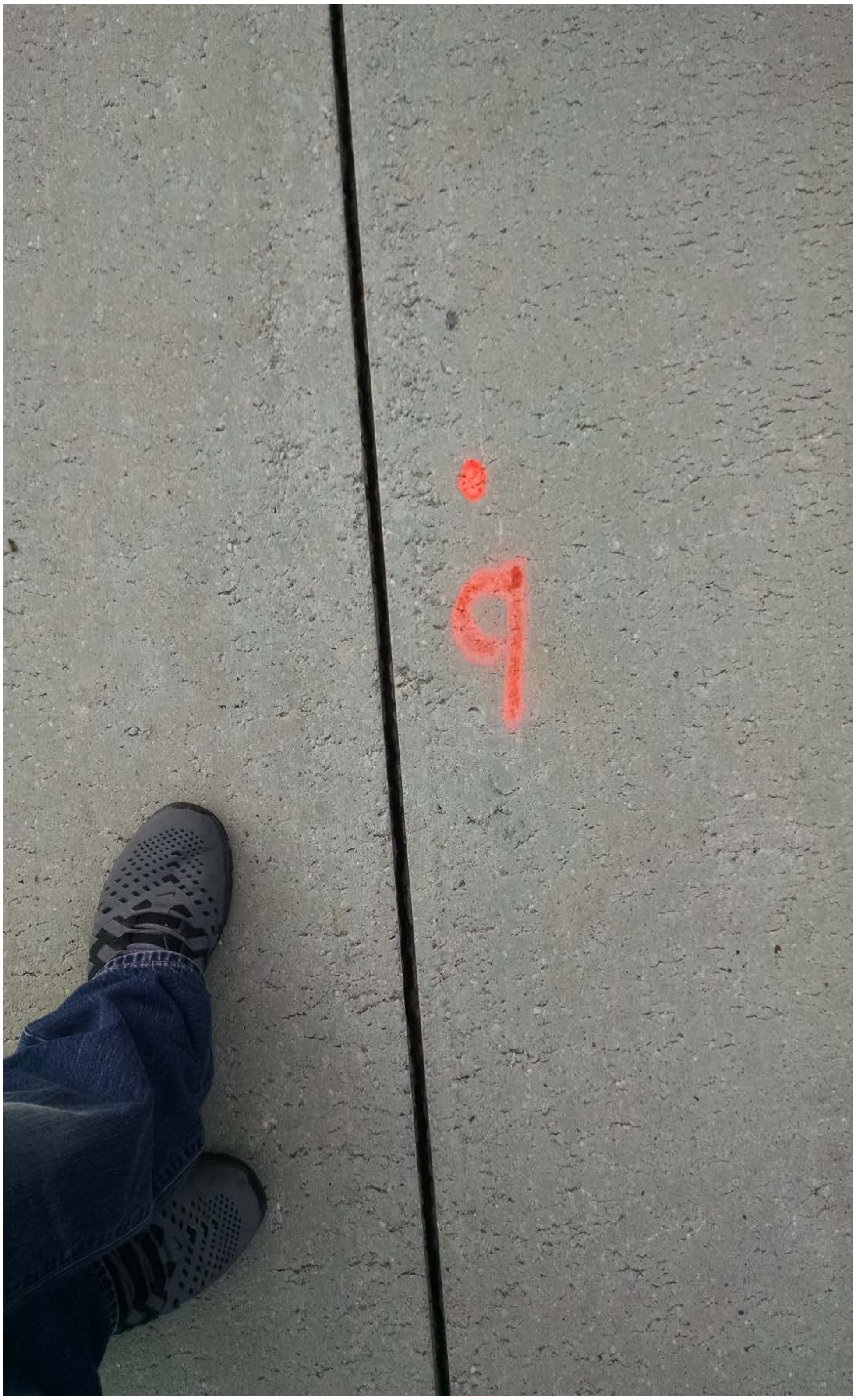

Figure 159. Bella Vista Longitudinal Joint (Separation Present) (December 2015).

Figure 160. Bella Vista Section—Stabilized Subgrade.

Figure 161. Bella Vista Site (Different Base Type).

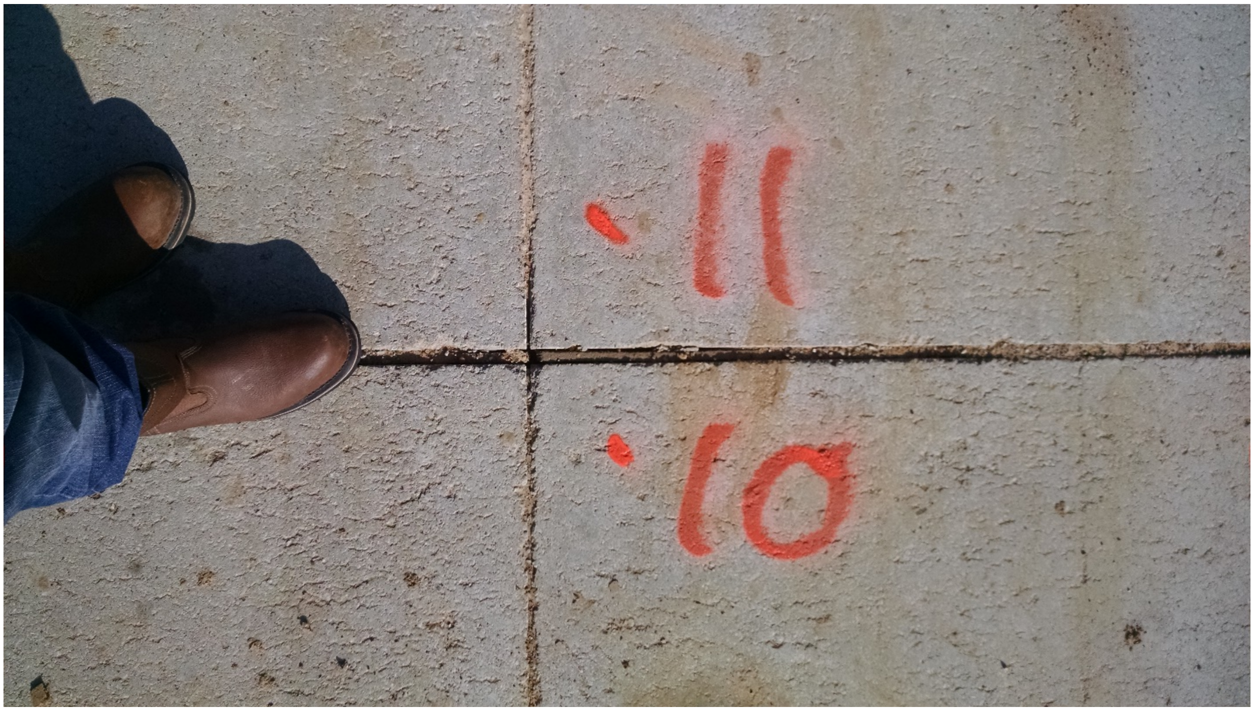

Figure 162. Bella Vista New Joint Filling with Dirt.

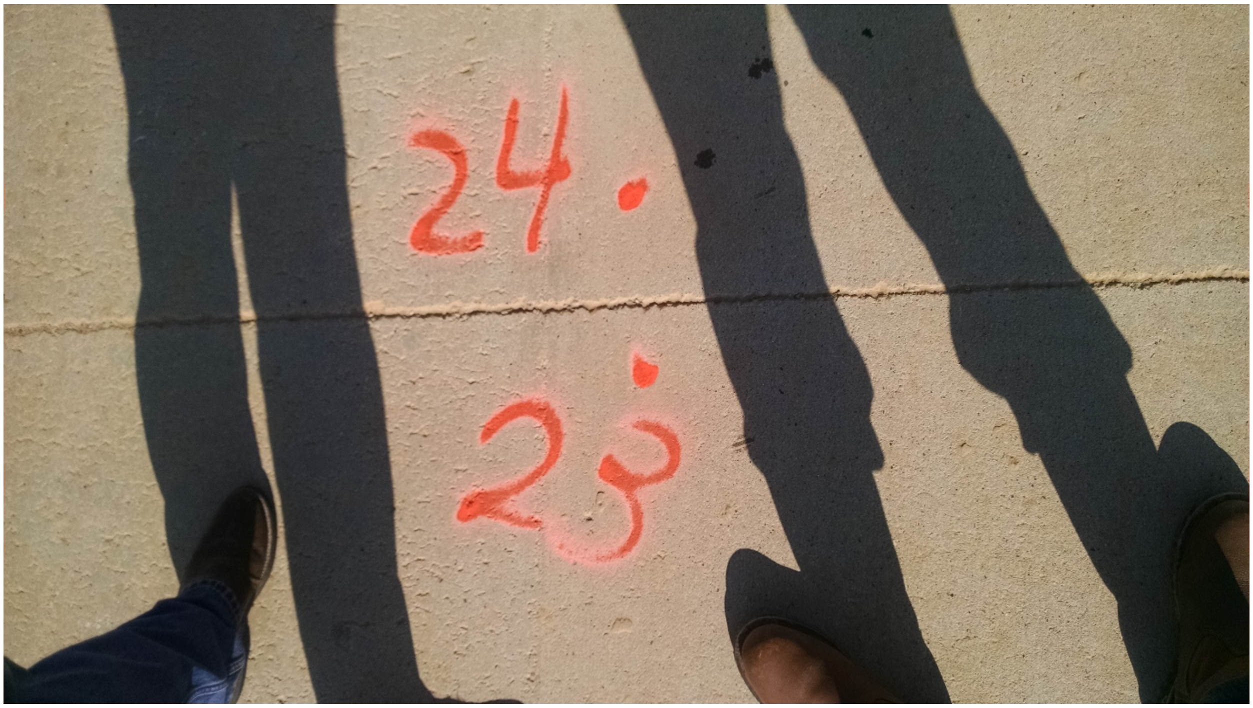

Figure 163. Bella Vista—Older Joint Already Compressed with Dirt Present.

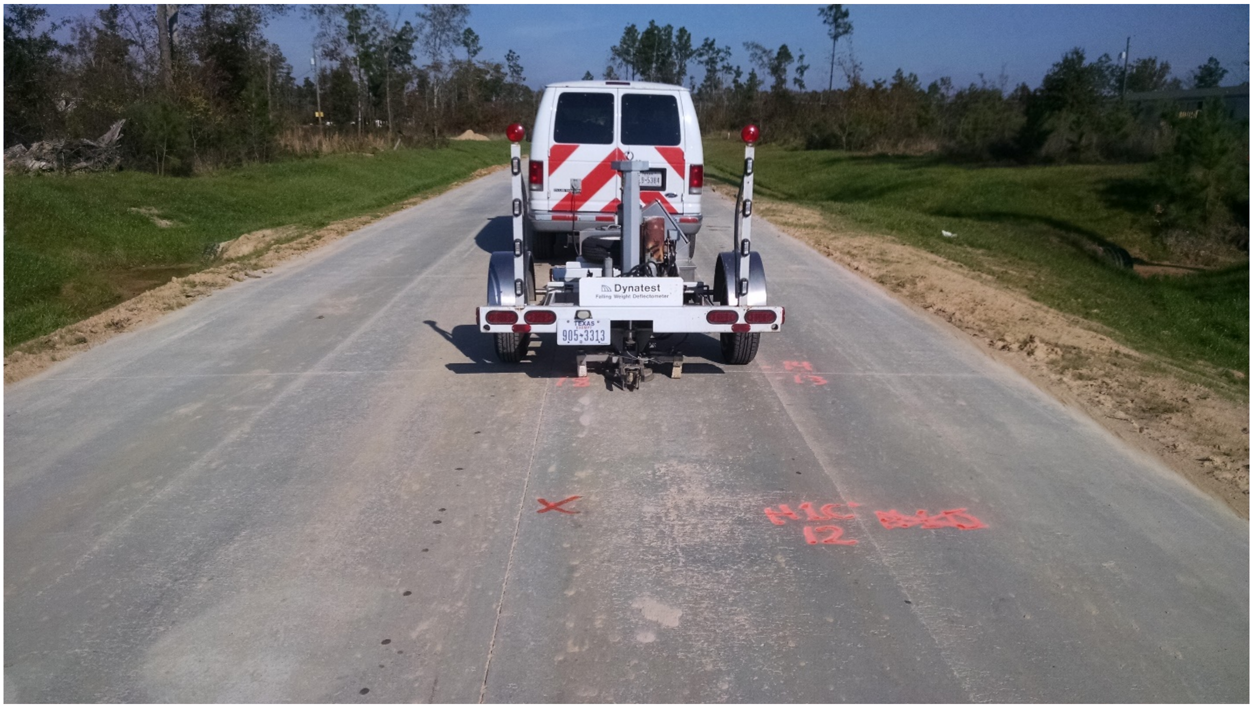
Figure 164. Bella Vista Natural Subgrade.

APPENDIX G. SOLMS RD. SITE PHOTOS, PLOTS, AND DATA (DECEMBER 2015)

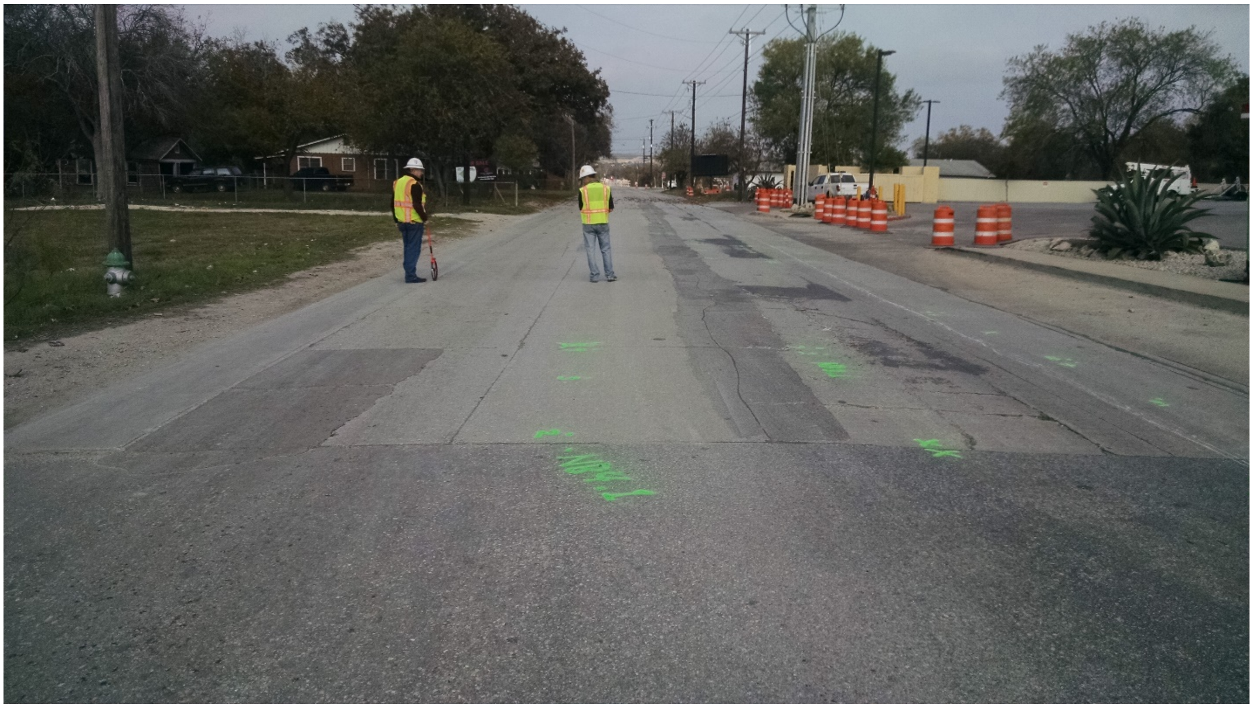

Figure 165. Solms Rd. Testing Paths/Lines Layout.

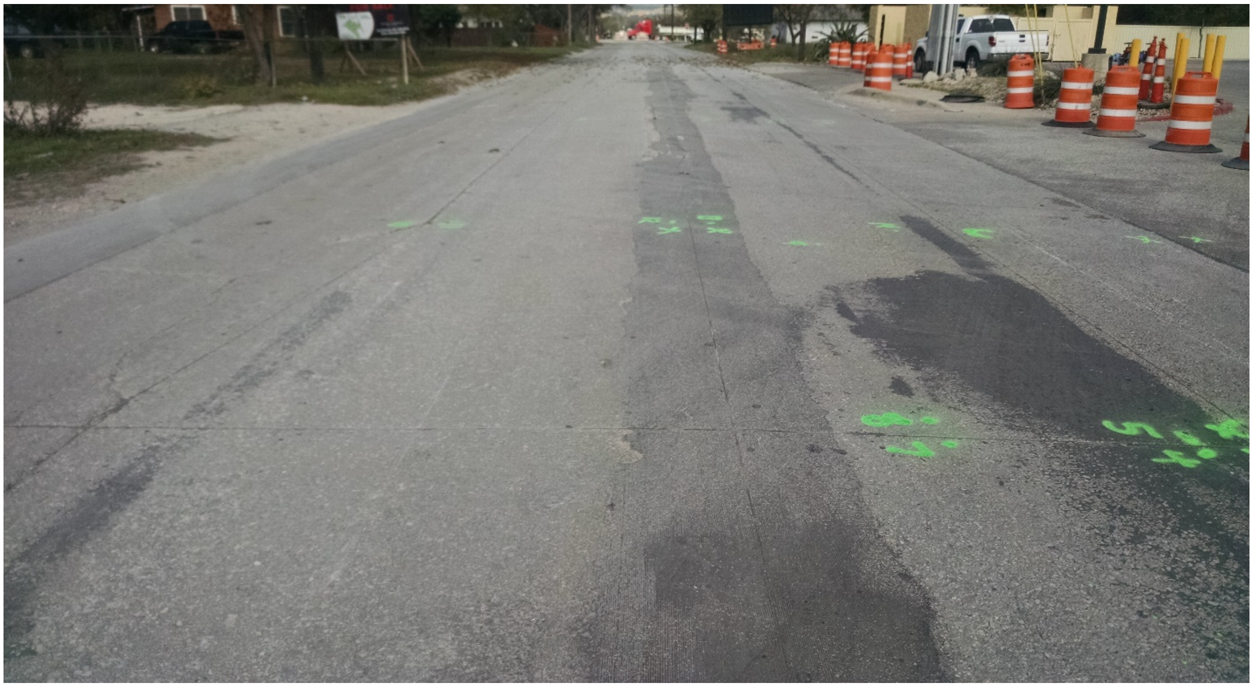

Figure 166. Solms Rd. Longitudinal Joint Spalling and Repair (along with Repair Material Failure).

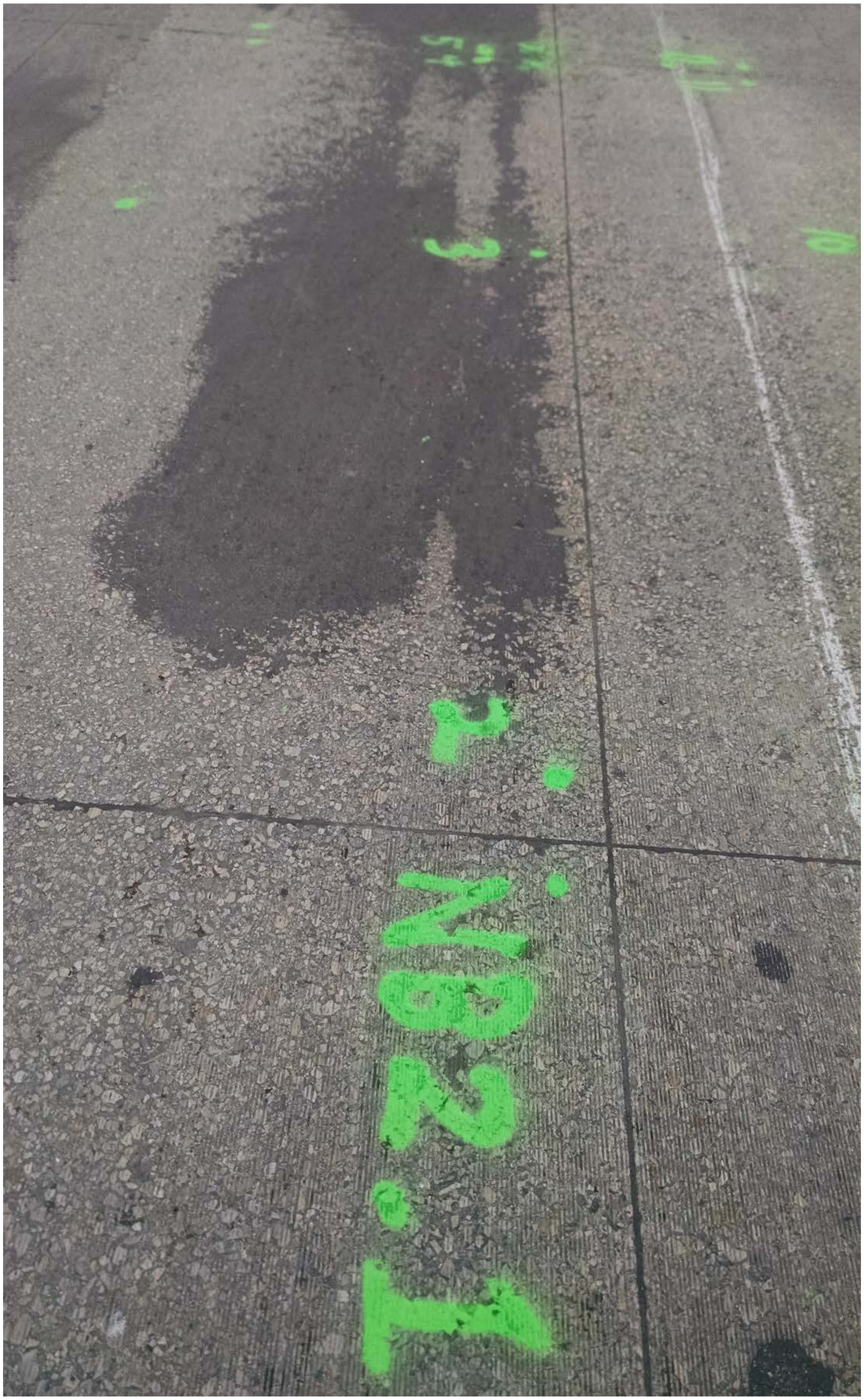

Figure 167. Solms Rd. (Run 2) Testing along Edges/Corners.

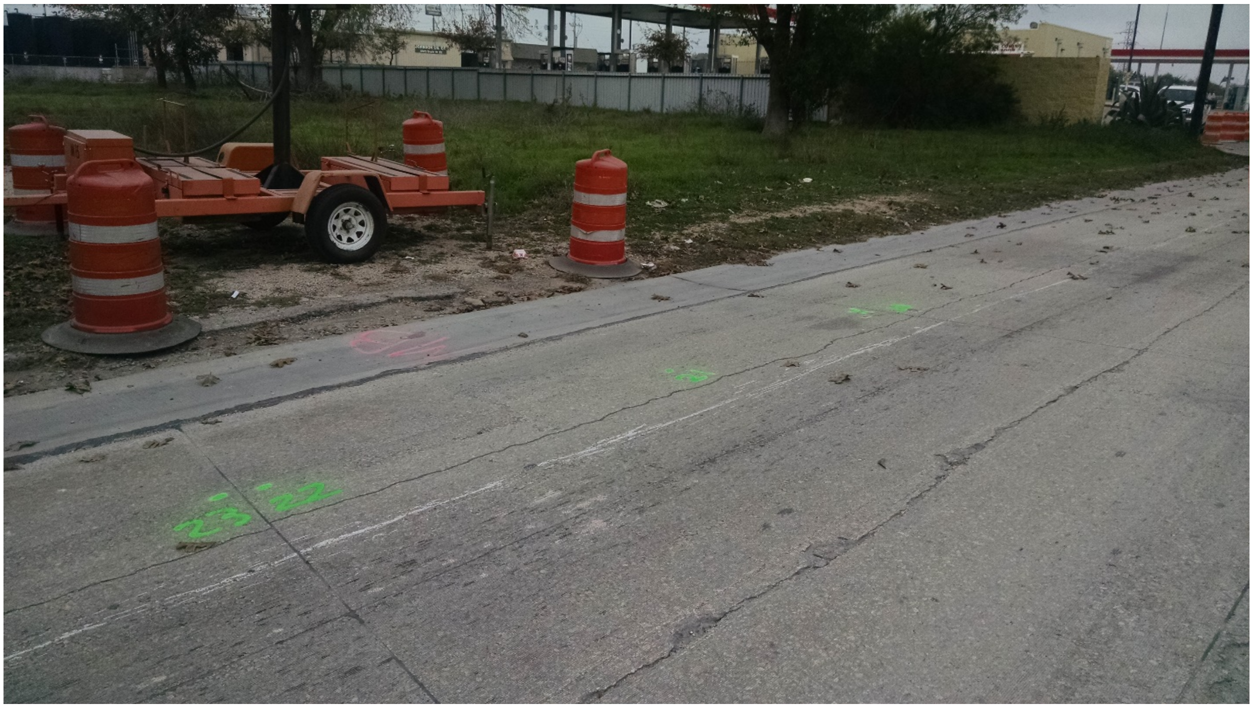

Figure 168. Solms Rd. Patching of Longitudinal Cracking.

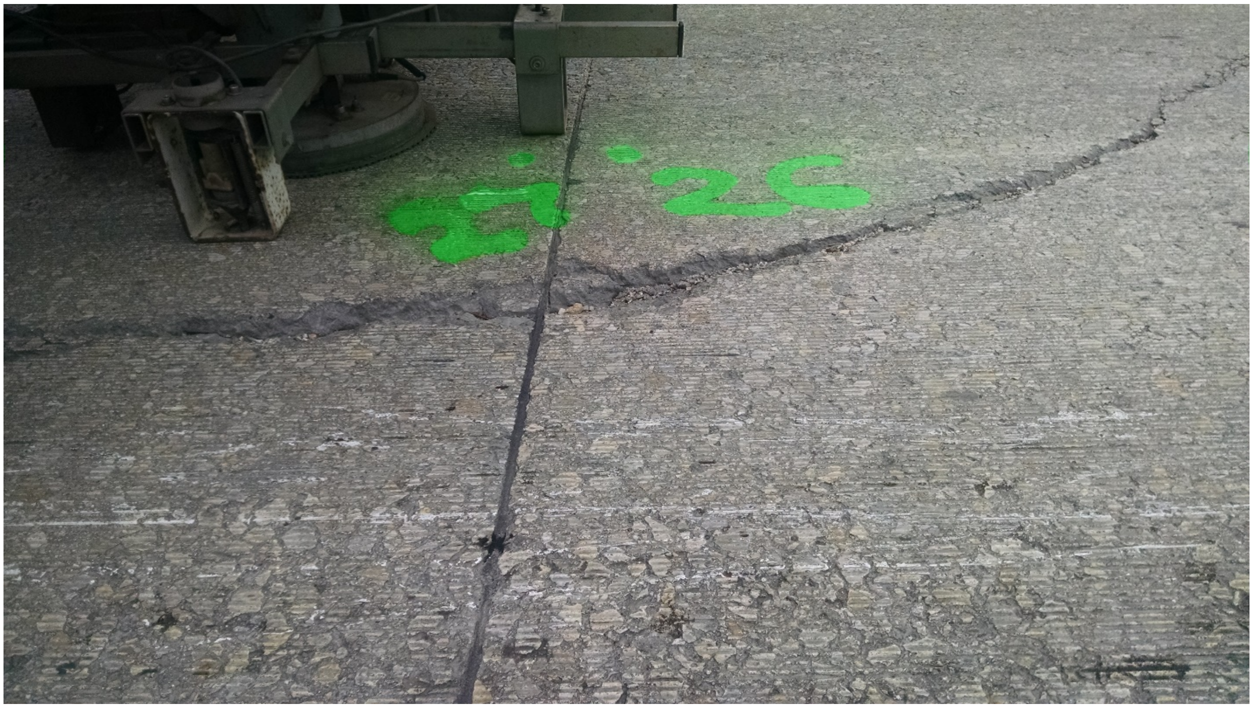

Figure 169. Solms Rd. Slab Heave and Failure/Crack Tested.

REFERENCES

1 Traffic Data and Analysis Manual. Texas Department of Transportation, Austin, Texas, September 2001. http://onlinemanuals.txdot.gov/txdotmanuals/tda/tda.pdf. Accessed 02/26/2014.

2 Huang, Y. H. *Pavement Analysis and Design*. Pearson Education, Inc. 2004.

3 Wirtgen. *Wirtgen Cold Recycling Technology,* 1st edition. Wirtgen GmbH. 2012.

4 Texas Department of Transportation. *Guidelines for Modification and Stabilization of Soils and Base for Use in Pavement Structures.* Construction Division. September 2005.

5 Quiroga, C., Kraus, E., Tsapakis, I., "Traffic Loads for Developing and Operating Individual Wells," Report No. IR-16-03, Texas A&M Transportation Institute, June 2016.

6 Rasmussen, R., Rogers, R., and Ferragut, T. *Continuously Reinforced Concrete Pavement: Design and Construction Guidelines*, Federal Highway Administration, 2011.

7 Huang, Y.H., *Pavement Analysis and Design*, Prentice Hall, New Jersey, 1993.

8 AASHTO. *AASHTO Guide for Design of Pavement Structures*. American Association of State Highway and Transportation Officials, 1993.

9 Portland Cement Association, *Thickness Design for Concrete Highway and Street Pavements*, Skokie, IL, 1984.

10 ACI Building Code Requirements for Structural Concrete and Commentary, American Concrete Institute, 2014.

11 Hall, K.T., "State of the Art and Practice in Rigid Pavement Design," AB202: Committee on Rigid Pavement Design, Transportation Research Board, Washington D.C., 2000.

12 Roesler, J.R., J.T. Harvey, J. Farver and F. Long, "Investigation of Design and Construction Issues for Long Life Concrete Pavement Strategies," California Department of Transportation, February, 2000.

13 Packard, R.G., *Thickness Design for Concrete Highway and Street Pavements*, Portland Cement Association, 1984.

14 Vetter, C.P., "Stresses in Reinforced Concrete Due to Volume Changes,' Transactions, ASCE, Vol. 98, 1933, pp. 1039–1053.

15 Ioannides, A.M. "Dimensional Analysis in NDT Rigid Pavement Evaluation." Journal of Transportation Engineering, Vol. 116, No. 1, pp. 23-26. 1990.

16 Zollinger, D.G., and E.J. Barenberg, *Continuously Reinforced Pavements: Punchouts and Other Distresses and Implications for Design*, Project IHR - 518, Illinois Cooperative Highway Research Program, University of Illinois at Urbana-Champaign, March 1990.

17 Ioannides, A.M., Khazanovich, L., and Becque, J.L. “Structural Evaluation of Base Layers in Concrete Pavement Systems.” Transportation Research Record 1370, Transportation Research Board, Washington, D.C., pp. 20-28. 1992.

18 Zollinger, Corey, Dan G. Zollinger, Dallas Little, and Adel Godiwalla, Innovative Approach to Pavement Rehabilitation Analysis and Design of Runway 15L-33R at George Bush Intercontinental Airport in Houston, Tx,” Proceedings, Eighth International Conference on Concrete Pavements, August 14-18th, 2005, Vol. 3, pp. 1101-1119, Colorado Springs, Colorado.

19 Wimsatt, A.W., McCullough, F.B., and Burns, N.H. *Methods of Analyzing and Factors Influencing Frictional Effects of Subbases*, Report 459-2F, Center For Transportation Research, Austin, TX. 1987.